

The University of Nottingham

UNITED KINGDOM · CHINA · MALAYSIA

PHARMACOLOGICAL CHARACTERIZATION OF ANNEXIN A2-S100A10 INTERACTION IN PANCREATIC CANCER USING 1,5-DIHYDRO-PYRROL-2-ONE COMPOUNDS

Khalid Elfsei

BPharm, MSc.

Thesis submitted to the University of Nottingham for the degree of Doctor of Philosophy

JANUARY 2016

Abstract

Pancreatic cancer is the eighth leading cause of cancer deaths in men and the ninth in women throughout the world. It remains an unfortunate disease with a 5-years survival rate of less than 3%. It is characterized by rapid progression, resistance to treatment and high rate of invasiveness. Annexin A2, a calcium dependent binding protein, has been found to be upregulated in pancreatic cancer cells. This upregulation is implicated in survival, chemo-resistance and invasion of pancreatic cancer cells. Annexin A2 exists in a soluble monomeric form inside the cells, however upon binding with S100A10, a member of calcium dependent S100 protein family and reported to be also upregulated in pancreatic cancer, it forms a stable complex (heterotetramer) composed of two subunits of each protein. These two proteins have been found to be involved in several phenotypic behaviours of pancreatic cancer cells such for instance, cell survival, chemo resistance and more significantly cell invasion through a plasminogen-dependent activation mechanism. It has been hypothesized that these proteins might affect pancreatic cancer by interacting with each other rather than as individual proteins. Dekker group has recently developed a first generation of small molecules that target complex formation between annexin A2 and S100A10 proteins. Therefore, the aim of this study was to investigate the implications of annexin A2-S100A10 complex disruption using these molecules on pancreatic cancer cells survival, chemo resistance and invasion.

In the first chapter, an overview of the effect of these molecules on the survival of pancreatic cancer cells was made using cell survival technique (MTT assay). These molecules have shown a wide range of anti-proliferative activity which has been correlated to the binding inhibitory activity of these molecules to the complex and intracellular expression of annexin A2. Measuring expression of annexin A2 after treatment with a potent annexin A2-S100A10 inhibitor (TRK317) revealed a downregulation in the expression of annexin A2 with significant decrease in pancreatic cell survival. Interestingly, there was no downregulation in annexin A2 expression or a decrease in the cell survival after treatment with a chemotype control compound (LW37) which showed no inhibition of annexin A2-S100A10 interaction. This has further reinforced the involvement of annexin A2 in pancreatic cell survival. Analysis of the physicochemical properties of these inhibitors using Crippen`s fragmentation method revealed a possible correlation of lipophilicity of these molecules with annexin A2-S100A10 complex inhibitory activity and the anti-proliferative activity against pancreatic cancer cells.

The second chapter focused on the involvement of the intracellular annexin A2-S100A10 complex in the chemo resistance developed during treatment of pancreatic cancer cells by gemcitabine. A model for gemcitabine-resistant pancreatic cancer cell was established by culturing wild pancreatic cancer cells in escalating dosages of gemcitabine over a period of five months.

Measuring the expression of annexin A2 and S100A10 revealed an upregulation of these proteins in gemcitabine-resistant cells as compared with wildtype cells. Treatment with TRK317 (Potent annexin A2-S100A10 inhibitor) resulted in downregulation of the expression of these proteins and an improvement in the anti-proliferative effect of gemcitabine. The synergy was confirmed by Chuo`s drug combination method. With further investigation, using annexin V apoptosis, cell cycle and immunoblotting assays annexin A2 dysregulation appeared to be correlated with p21 induced-cell cycle arrest.

In the third chapter, an investigation of the involvement of the extracellular annexin A2-S100A10 complex in pancreatic cancer cell invasion and endothelial cell adhesion was made. Annexin A2-S100A10 inhibitors as well as a peptide known to inhibit the complex formation on the cell surface inhibited the invasion of pancreatic cancer cells through a Matrigel coated membrane chamber. Interestingly, there was no inhibition to the cell invasion after treatment with the chemotype (LW37) or a scrambled peptide which further indicated an involvement of these two proteins in pancreatic cancer cells invasion. Using protease activation assays, this inhibition has been related to a plasminogen-dependent activation mechanism. Further analysis using immunoprecipitation, surface immuno-labeling and employing of an S100A10 fluorescent tracer the inhibitors were shown to cause a decrease in the binding of S100A10 to annexin A2 providing a molecular

mechanism of pancreatic cancer cell invasion inhibition by these molecules. Inhibition of surface protease activity also has been observed after employing these molecules to the surface of endothelial cells. This may implicate involvement of annexin A2-S100A10 complex formation in neoangiogenesis.

Expression of annexin A2 and S100A10 proteins on the surface of pancreatic cancer cells and endothelial cells was shown to mediate adhesion of pancreatic cancer cells to endothelial cells. Inhibition of the interaction between annexin A2 and S100A10 proteins using annexin A2-S100A10 inhibitors or the peptide also led to a decrease in the adhesion of pancreatic cancer cells to endothelial cells and further reinforced the involvement of annexin A2-S100A10 complex in the cell-cell adhesion of pancreatic cancer cells to endothelial cells.

In conclusion, in vitro inhibition of annexin A2-S100A10 interaction by these molecules attenuated pancreatic cancer cell chemo resistance to gemcitabine, invasiveness, progression and adhesion to endothelial cells.

Keywords: Pancreatic cancer, annexin A2-S100A10 complex, inhibitors (molecules), peptide, chemo- resistance, invasion, and adhesion.

Acknowledgements

First and foremost, I would like to express my totally inadequate thanks to **Allah (God)** for giving me the opportunity to pursue my passions and interests in cancer research in the UK. I should also thank him for giving me the strength to finish this study. This work could not have been done without his almighty.

My first supervisor **Dr. Lodewijk Dekker** you gave me the opportunity to work on such interesting and challenging project. Your encouragement, guidance, support and perseverance were helpful and appreciated. You taught me a lot. My second supervisor **Dr. Tracey Bradshaw** your smile, kindness, help and valuable advice were supportive in the hard times.

My parents, **brothers** and **sisters** your love, passionate encouragement and prayers made it possible for me to complete this project. My friends, **Ashraf Elfsei** and **Adel Alshiekhi** your phone calls and support during the PhD made me continue working. I will never forget your help.

Dr. Abdullahi Abbas your help at the beginning of the lab work made a huge difference. My lab colleagues; **Tiangong Lu, Anchala Kuruppu, Badraldin Hamad, Vijay Raja, Yidong Liu, Mohannad Qazzaz, Mohammed Al-Hayali**, you made years of the PhD such enjoyable and wonderful experience. **James Awford** your way of presentation was inspirational. **Lee Hibbett** your hard

work kept our lab running. To who has directly or indirectly helped to deliver this work, I express my thanks and gratitude.

Special thanks to my sponsor **Benghazi University**. Thanks to **Nottingham University**.

Finally, my deepest appreciation and thanks go to **my wife** and **my children (Mohamed, Mayar and Jinan)** who are such wonderful supporters throughout this journey. Without their support I would never have succeeded.

Dedication

This thesis is dedicated to **my beloved parents**, who have continued to make countless sacrifices and unconditioned love in my life, and **my country Libya,** who has suffered from disputes, people selfishness, desires and corruption; Yet, I believe in you. May Allah protect and bless you all.

Abbreviations

µl	Microlitre
µM	Micromolar
5-FU	5-Fluorouracil
Ac	Acetyl
ACA	6-aminocaproic acid
AMPS	Ammonium persulfate
ANOVA	Analysis of variance
ATCC	American Type Culture Collection
ATP	Adenosine triphosphate
Bak	Pro-apoptotic protein
Bax	Pro-apoptotic protein
BCECF-AM	2,7-bis-(2-carboxyethyl)-5,6 carboxyfluoresceinacetoxy methylester
Bcl-2	B-cell lymphoma 2
BNIP3	A pro-apoptotic member of the Bcl-2 family
BSA	Bovine serum albumin
C	Cys (Cysteine)
C.V	Cell survival
CDKs	Cyclin-dependent kinases

cm^2	Centimeter square
CPK	Chemistry colouring system
Cy5	Cyanine 5
DLC1	Rho GTPase activating protein
DMSO	Dimethyl sulfoxide
DNA	Deoxyribonucleic acid
DTT	Dithiothreitol
E	Glu (Glutamic acid)
E.coli	*Escherichia coli*
E2F	Transcription factor
EBM-2	Endothelial Basal Medium -2
E-cadherin	Epithelial cadherin
ECM	Extracellular matrix
EDTA	Ethylene diaminetetraacetic acid
EGF	Epidermal growth factor
F	Phe (Phenylalanine)
FACS	Fluoresence-activated cell sorting
FBS	Foetal bovine serum
FGF1	Fibroblast growth factor
FITC	Fluorescein isothiocyanate
FRET	Fluorescence resonance energy transfer

G1 phase	Gap 1 phase
G2/M phase	Gap2/Mitosis phase
GLUT1	Glucose transporter1
G-R	Gemcitabine-resistant
GTP	Guanosine 5’-triphosphate
H	His (Histidine)
h	Hour
HC	Hydrocortisone
HCT116	Colon cancer cells
HMEC-1	Microvascular endothelial cells
HT1080	Fibrosarcoma cells
I	Ile (Isoleucine)
IC_{50}	Concentration kills 50% of cells
IHC	Immunohistochemical
IMS	Industrial methylated spirit
IPTG	Isopropyl β-D-1-thiogalactopyranoside
K	Lys (Lysine)
L	Leu (Leucine)
L	Litre
LB	Luria-Bertani broth
LNCaP	Prostate adenocarcinoma cells

LogP	Logarithm partition coefficient
LogS	Logarithm aqueous solubility
M	Met (Methionine)
MDA-MB-231	Metastatic breast adenocarcinoma
MDCK II	Madin-Darby canine kidney cell lines,
mg	Milligram
MIA PACA-2	Pancreatic adenocarcinoma cell line
min	Minutes
ml	Millilitre
mM	Millimolar
MMP2	Matrix metalloproteinase 2
MMP9	Matrix metalloproteinase 9
MTT	3-(4, 5-dimethylthiazol-2-yl)-2,5-diphenyltetrazolium bromide
nm	Nanometer
nM	Nanomolar
OD600	Optical density 600 nm
P.IC_{50}	Target inhibitory activity in IC_{50} μM
p11	S100A10
p16	Cyclin-dependent kinase inhibitor 2A
p21	CDK-interacting protein 1
p36	Annexin A2

p53	Tumor protein 53
PANC-1	Pancreatic adenocarcinoma cell line
PanIN	Pancreatic intraductal neoplasia
PBS	Phosphate Buffer Saline
PI	Propidium iodide
Plg	Plasminogen
Plm	Plasmin
RAGE	Receptor for advanced glycation endproducts
RAW117	Lymphoma cells
RB/pRB	Retinoblastoma protein
ROS	Reactive oxygen species
rpm	Revolutions per minute
RPMI-1640	Roswell Park Memorial Institute
S phase	Synthesis phase
S	Ser (Serine)
SAR	Structural Activity Relationship
SDS-PAGE	Sodium dodecyl sulfate-polyacrylamide gel electrophoresis
SEM	Standard error of the mean
shRNA	Short hairpin RNA
siRNA	Small interfering RNA
T	Thr (Threonine)
TBST	Tris-Buffered Saline and Tween 20

TEMED	Tetramethylethylenediamine
TGF-β	Transforming growth factor beta
tPA	Tissue plasminogen activator
TSP-1	Thrombo-spondin-1
uPA	Urokinase plasminogen activator
uPAR	Urokinase plasminogen activator receptor
V	Val (Valine)
VEGF-A	Vascular endothelial growth factor-A
Y	Tyr (Tyrosine)

Content

Abstract **I**

Acknowledgements **V**

Dedication **VII**

Abbreviations **VIII**

List of Figures **XVIII**

List of Tables **XXVII**

1. INTRODUCTION **1**

1.1. Cancer 1

1.1.1. Hallmarks of cancer 2

1.2. Pancreatic cancer 14

1.2.1. Significance of pancreatic cancer 14

1.2.2. Morphological progression of pancreatic cancer 15

1.2.3. Molecular changes during pancreatic cancer developments 17

1.2.4. Proteomics of pancreatic cancer 21

1.3. Annexin proteins 23

1.3.1. Annexin A2 26

1.3.2. Annexin A2 in pancreatic cancer 30

1.4. S100 proteins 35

1.4.1. S100A10 37

1.4.2. S100A10 in cancer 38

1.5. Annexin A2-S100A10 interaction 42

1.6. Targeting S100A10 and annexin A2 47

1.7. Development of inhibitors targeting annexin A2-S100A10 interaction 50

1.7.1. The crystal structure of S100A10 with the annexin A2 N-terminal peptide 50

1.7.2. Designing of annexin A2-S100A10 interaction inhibitors 53

1.8. Aim and Objectives 62

2. DEPENDENCE OF PANCREATIC CANCER CELLS VIABILITY ON ANNEXIN A2 EXPRESSION AND THE SAR OF ANNEXIN A2-S100A10 INHIBITORS 64

2.1. Introduction 64

2.2. Aim and objectives 67

2.3. Results and discussion 68

2.3.1. Cell viability study of annexin A2-S100A10 inhibitors 68

2.3.2. Screening the effect of annexin A2-S100A10 inhibitors on the survival of PANC-1, MIA PACA-2 and HMEC-1 cell lines 68

2.3.3. Correlating annexin A2-S100A10 inhibitors target activity with anti-proliferative activity; dependence on annexin A2 expression levels 81

2.4. Relationship between annexin A2-S100A10 inhibitors structure and their cellular activity 94

2.4.1. Relationship between target inhibitory activity of annexin A2-S100A10 inhibitors and their lipophilicity and aqueous solubility 97

2.4.2. Relationship of the cellular activity of annexin A2-S100A10 inhibitors and their lipophilicity and aqueous solubility 100

2.5. Classification of annexin A2-S100A10 inhibitors 103

2.5.1. Target-potent intracellular active inhibitors 104

2.5.2. Target-potent intracellular inactive inhibitors 106

2.5.3. Target-potent intracellular moderately active inhibitors 108

2.5.4. Target-impotent intracellular inactive inhibitors 110

2.6. Conclusion and future plans 113

3. INHIBITION OF ANNEXIN A2-S100A10 INTERACTION IMPROVES THE ANTI-PROLIFERATIVE ACTIVITY OF GEMCITABINE IN RESISTANT PANCREATIC CANCER CELLS 114

3.1. Introduction 114

3.2. Aim and Objectives 118

3.3. Results and discussion 120

3.3.1. Development of gemcitabine-resistant pancreatic cancer cells 120

3.3.2. Determining the IC_{50} of gemcitabine on pancreatic cancer cells 120

3.3.3. Measuring the IC_{50} of PANC-1 G-R cells 122

3.3.4. Annexin A2 expression is upregulated in PANC-1 G-R cells 124

3.3.5. S100A10 expression concomitantly upregulated with annexin A2 expression in PANC-1 G-R cells 126

3.3.6. TRK317 inhibits the interaction of annexin A2 and S100A10 and downregulates their expressions 128

3.3.7. TRK317 synergizes with gemcitabine in PANC-1 G-R cells 133

3.3.8. Altered expression of annexin A2 and S100A10 in PANC-1 cells may affect cell cycle but not apoptotic pathway 139

3.3.9. Overexpression of annexin A2-S100A10 complex in PANC-1 G-R may mediate downregulation of p21 expression without significant change in p53 153

3.4. Conclusion and Future work 157

4. INHIBITION OF ANNEXIN A2-S100A10 INTERACTION REVEALS INVOLVEMENT IN INVASION AND ADHESION OF PANCREATIC CANCER CELLS **158**

4.1. Introduction 158

4.2. Aim and objectives 163

4.3. Results and discussion 165

4.3.1. Inhibition of pancreatic cancer cell invasion by peptide and annexin A2-S100A10 inhibitors 165

4.3.2. Protease cascade is involved in pancreatic cancer invasion 168

4.3.3. Establishment of annexin A2 and S100A10 expression on the surface of pancreatic cancer cells and flow cytometry 172

4.3.4. Annexin A2 and S100A10 antibodies inhibit protease cascade on the surface of PANC-1 cells 175

4.3.5. Inhibition of protease cascade by N-terminal peptide and annexin A2-S100A10 inhibitors 179

4.3.6. Annexin A2 and S100A10 are colocalized in PANC-1 cells 184

4.3.7. Annexin A2-S100A10 inhibitors and N-terminal peptide inhibit surface interaction of annexin A2 and S100A10 188

4.3.8. Annexin A2-S100A10 inhibitors increase binding of Cy5-S100A10 to the surface of pancreatic cancer cells 193

4.3.9. N-terminal peptide and annexin A2-S100A10 inhibitors may be involved in endothelial blood vessel formation 204

4.3.10. Pancreatic cancer cells adhere to endothelial cells 210

4.4. Conclusion and Future work 216

5. GENERAL CONCLUSION AND DISCUSSION **218**

6. MATERIALS AND METHODS **227**

6.1. Material list 227
6.1.1. Cell culture conditions 227
6.1.2. Viability assay (MTT) 227
6.1.3. Resistant cell line developments 228
6.1.4. Adhesion assay 228
6.1.5. Plasminogen Activation Assay 228
6.1.6. Invasion assay 229
6.1.7. Cell cycle analysis 229
6.1.8. Apoptosis Assay 230
6.1.9. Surface expression of proteins 230
6.1.10. Electrophoresis and immunoblot analysis 231
6.1.11. Immunoprecipitation Assay 237
6.1.12. Cell Surface Protein Biotinylation 237
6.1.13. Cytoplasmic and nuclear proteins extraction 237
6.1.14. Recombinant protein expression and purification 238
6.2. Methods 241
6.2.1. Cell lines and culture conditions 241
6.2.2. Cell passage and freezing 242
6.2.3. Cell counting 242
6.2.4. Viability assay (MTT) 243
6.2.5. Resistant cell line developments 244
6.2.6. Adhesion assay 245
6.2.7. Plasminogen Activation Assay 246
6.2.8. Plasminogen Activation on the surface of the cells 246

6.2.9. Invasion assay 247
6.2.10. Flow Cytometry 248
6.2.11. Cell cycle analysis 249
6.2.12. Apoptosis Assay (Annexin V - FITC and propidium iodide) 250
6.2.13. Surface expression of proteins 251
6.2.14. Electrophoresis and immunoblot analysis 252
6.2.15. Immunoprecipitation Assay 255
6.2.16. Cell Surface Protein Biotinylation 256
6.2.17. Cytoplasmic and nuclear proteins extraction 257
6.2.18. Recombinant protein expression and purification 258
6.2.19. S100A10 Cy5 labelling 262
6.2.20. S100A10 tracer binding assay 262
6.2.21. Statistical analyses 263
7. REFERENCES **264**

List of Figures

Figure 1.1: Hallmarks of cancer. 3

Figure 1.2: The cancer survival rates for a group of metastatic pancreatic cancer patients who were diagnosed between 2000 and 2011. 15

Figure 1.3: Morphological changes happening during pancreatic cancer progression. 16

Figure 1.4: Molecular and pathological progressions accompanied pancreatic ductal adenocarcinoma. 17

Figure 1.5: Cell cycle phases with cyclin-dependent kinases (CDKs) and their cyclin regulatory subunits. G1, S, G2 and M represent Gap1, synthesis, Gap2 and mitosis phases respectively; G0 is the Gap 0 or resting. 18

Figure 1.6: Ribbon presentation showing the three-dimensional structure of annexin A2 in a calcium free state. 24

Figure 1.7: Immunohistochemical analysis of annexin A2 in pancreatic ductal adenocarcinoma. 31

Figure 1.8: Domain structure of S100 proteins showing the two EF hands. 35

Figure 1.9: Structural organization of S100 protein. (A) Apo-S100 protein is shown with blue and yellow subunits. Ca^{+2} binding, grey circles, induces a conformational change in S100 protein results in exposure of hydrophobic cleft and binding to its binding partner (green triangle). (B) Ribbon and surface diagrams of apo-S100, Ca^{+2} bound S100 and the Ca^{+2} bound S100–

peptide complex. Individual subunits are shown in blue and yellow, the Ca^{+2} ions shown in grey spheres, and the peptide is shown in green. 36

Figure 1.10: Complex structure of S100A10 dimer (blue and yellow) with the annexin A2 N-terminal peptide (green). 51

Figure 1.11: Close-up view of the interaction between the N-terminal peptide (green) and S100A10 dimer (yellow and blue). (A) The residues involved in the binding after refinement. (B) The critical points required for the interaction. 52

Figure 1.12: Structural formula of TRK5. Chemical formula of TRK5 is 3-hydroxy-1-(2-hydroxypropyl)-5-(4-isopropylphenyl)-4-(4-methylbenzoyl)-1H-pyrrol-2(5H)-one). 55

Figure 1.13: The template structural formula of the 1, 4 and 5 substituted pyrrol-2-one molecules. 56

Figure 1.14: Structure-based design of annexin A2-S100A10 inhibitors. A, the hydrophobic H1 (cyan), H2 (yellow) and hydrophilic H3 (magenta) are subsites of the S100A10 binding pocket. B, the interaction between the N-terminal annexin A2 peptide (grey CPK stick models) and the binding pocket of S100A10 (green CPK surface). C, the predicted binding poses of verified virtual screening hits of TRK5 (grey CPK stick models) with binding pocket of S100A10 (green CPK surface). 61

Figure 2.1: Effects of DMSO serial concentrations on the survival of PANC-1 and MIA PACA-2 cancer cells. 69

Figure 2.2: The effect of annexin A2-S100A10 inhibitors at 50 μM 1% DMSO on the survival percentage of PANC-1 cells as measured using an MTT assay. 72

Figure 2.3: The effect of annexin A2-S100A10 inhibitors at 50 μM 1% DMSO on the survival percentage of MIA PACA-2 cells as measured using an MTT assay. 73

Figure 2.4: The effect of annexin A2-S100A10 inhibitors at 50 μM 1% DMSO on the survival percentage of HMEC-1 cells as measured using an MTT assay. 74

Figure 2.5: The effect of potent annexin A2-S100A10 inhibitors serial concentrations on the survival of PANC-1 cells as measured using an MTT assay. 77

Figure 2.6: The effect of potent annexin A2-S100A10 inhibitors serial concentrations on the survival of MIA PACA-2 cells as measured using an MTT assay. 78

Figure 2.7: Correlation between cell survival percentage (anti-proliferative effect) and the target inhibitory activity of annexin A2-S100A10 inhibitors in PANC-1, MIA PACA-2 and HMEC-1 cells. 82

Figure 2.8: Annexin A2 expression in PANC-1 cells. (A) Annexin A2 levels in non-treated control, pretreatment with LW37 50 μM or with TRK317 50 μM. (B) Quantification of annexin A2 expression in non-treated control, treatment with LW37 50 μM or with TRK317 50 μM in PANC-1. 86

Figure 2.9: Correlation between cell survival percentage (anti-proliferative activity) and the target inhibitory activity of annexin A2-S100A10 inhibitors in PANC-1 cells. 88

Figure 2.10: Correlation between cell survival percentage (anti-proliferative activity) and the target inhibitory activity of potent and impotent annexin A2-S100A10 inhibitors in PANC-1 cells. 90

Figure 2.11: Annexin A2 expressions in PANC-1 cells. (A) Annexin A2 levels in non-treated control, pre-treatment with TRK342 50 μM. (B) Quantification of annexin A2 expression in non-treated control, treatment with TRK342 50 μM in PANC-1. 92

Figure 2.12: The relationship between lipophilicity (A) and aqueous solubility (B) of annexin A2-S100A10 inhibitors and their target activity. 97

Figure 2.13: The relationship between lipophilicity (A) and aqueous solubility (B) of annexin A2-S100A10 inhibitors and their anti-proliferative activity in PANC-1 cells. 100

Figure 2.14: Chemical structures of 1, 4-Substituted-3-hydroxy-5-(4-isopropylphenyl)-1Hpyrrol-2(5H)-ones (II) and 1, 4-Substituted-3-hydroxy-5-(3,5-bis(trifluoromethyl)phenyl)-1Hpyrrol-2(5H)-ones (I). 103

Figure 2.15: Diagrammatic representation of annexin A2-S100A10 inhibitors targeting extracellular and intracellular annexin A2-S100A10 complex formation in PANC-1 cells. 112

Figure 3.1: The effect of serial gemcitabine concentrations on the viability of MIA PACA-2 cells and PANC-1 cells. 121

Figure 3.2: Dose response curves of gemcitabine in PANC-1 wildtype cells (close circle) as compared to PANC-1 G-R cells (open circle). 123

Figure 3.3: Western blot analysis of annexin A2 expression in PANC-1 wildtype and G-R cells. β-actin was used as a loading control. 125

Figure 3.4: Western blot analysis of annexin A2 and S100A10 expressions in PANC-1 wildtype and G-R cells. 127

Figure 3.5: Analysis of the interaction between S100A10 and annexin A2. 129

Figure 3.6: Western blot analysis of annexin A2 and S100A10 expressions after TRK317 treatment in PANC-1 G-R cells. 130

Figure 3.7: (A) TRK317 improves the anti-proliferative effect of gemcitabine in PANC-1 G-R cells. (B) Fractional effect-combination index (Fa-CI) plot of combination index analysis in PANC-1 G-R cells. 136

Figure 3.8: Annexin V assay showing a comparison between PANC-1 wildtype and G-R cells treated with gemcitabine 10 μM or irinotecan 10 μM. 142

Figure 3.9: A comparison between PANC-1 wildtype and G-R cells treated with gemcitabine 10 μM or irinotecan 10 μM. 143

Figure 3.10: A dose response curve of PANC-1 wildtype (close circle) and G-R (open circle) cells treated with serial concentrations of irinotecan. 144

Figure 3.11: Cell cycle phases showing a comparison between PANC-1 wildtype and G-R cells responses to gemcitabine 1 μM, irinotecan 10 μM and TRK317 50 μM. 147

Figure 3.12: A comparison in cell cycle phases between PANC-1 wildtype and G-R cells. 148

Figure 3.13: A comparison in cell cycle phases between PANC-1 wildtype and G-R cells treated with gemcitabine 1 μM, irinotecan 50 μM and TRK317 50 μM. 149

Figure 3.14: (A) Western blot analysis of annexin A2, p21 and p53 in PANC-1 wildtype and G-R cells. (B) Multiple immunoblots show a significant ($P < 0.05$) increase in annexin A2 expression and a decrease in p21 expression without marked change in p53 ($P > 0.05$) in PANC-1 G-R cells as compared with PANC-1 wildtype cells. 153

Figure 3.15: Western blot analysis of annexin A2, p21 PANC-1 G-R cells treated with a combination of gemcitabine 10 μM and TRK317 50 μM as compared with non-treated control. 155

Figure 3.16: Diagrammatic representation of reversion of gemcitabine resistance by TRK317 (An annexin A2-S100A10 inhibitor) in PANC-1 G-R cells. 156

Figure 4.1: The effect of annexin A2-S100A10 inhibitors (A) and peptides (B) on the invasion of PANC-1 cells. 166

Figure 4.2: (A) Plasmin generation signal. (B) Rate of plasmin generation in PANC-1 cells. 169

Figure 4.3: Rate percentage of plasmin generation (protease activity percentage) in PANC-1 cells pre-incubated with (A) benzamidine and (B) uPA inhibitor II. 171

Figure 4.4: Expression of annexin A2 and S100A10 on the surface of PANC-1 cells using flowcytometry and biotinylation techniques. 173

Figure 4.5: Effect of antibodies treatment on the rate of plasmin generation (protease activity percentage) on the surface of PANC-1 cells. 176

Figure 4.6: Effect of ACA and glycine on the rate percentage of plasmin generation (protease activity percentage). 178

Figure 4.7: Effect of (A) N-terminal peptide, (B), (C) and (D) annexin A2-S100A10 inhibitors on the rate of plasmin generation (protease activity) in PANC-1 cells. 180

Figure 4.8: Effect of 1 h pre-incubation with moderately cellular active and cellular active annexin A2-S100A10 inhibitors on PANC-1 cells viability. 183

Figure 4.9: Analysis of the interaction between S100A10 and annexin A2. S100A10 was immunoprecipitated then annexin A2 in the immunoprecipitate was analyzed by western blotting using an annexin A2 antibody. 186

Figure 4.10: Effect of N-terminal peptide treatment on the surface S100A10 signal of PANC-1 cells. 189

Figure 4.11: Effect of annexin A2-S100A10 inhibitors treatment on the surface S100A10 signal of PANC-1 cells. 191

Figure 4.12: Multiple purified S100A10 fractions stained with Coomassie blue. 194

Figure 4.13: Nano drop absorbance of a purified S100A10 at 280 nm with 10 mm path length. 195

Figure 4.14: Nano drop absorbance of a purified labelled S100A10 at 650 and 280 nm with 10 mm path length. 196

Figure 4.15: Cy5-labelled S100A10 dependent-annexin A2 binding to PANC-1 cells surface. 198

Figure 4.16: Measuring Cy5-S100A10 binding after pre-incubation with annexin A2-S100A10 inhibitors. 200

Figure 4.17: Mechanistic representation of annexin A2-S100A10 inhibitors effect on PANC-1 cells invasion. (A) Plg dependent tPA activation on annexin A2-S100A10 complex leads to generation of plasmin (Plm) and PANC-1 cells invasion. (B) Inhibition of annexin A2 and S100A10 interaction by annexin A2-S100A10 inhibitors releases S100A10 with Plg leading to inhibition of plasmin (Plm) generation and PANC-1 cells invasion. 203

Figure 4.18: (A) Plasmin generation signal. (B) Rate of plasmin generation in HMEC-1 cells. 205

Figure 4.19: Effect of (A) N-terminal peptide, (B), (C) and (D) annexin A2-S100A10 inhibitors on the rate percentage of plasmin generation (protease activity percentage) in HMEC-1 cells. 208

Figure 4.20: Interaction between pancreatic cancer cells and endothelial cells. 211

Figure 4.21: Inhibition of pancreatic cancer cells adhesion to endothelial cells by (A) N-terminal peptide and (B) Annexin A2-S100A10 inhibitors. 213

Figure 4.22: Diagrammatic representation showing inhibition of pancreatic cancer cells adhesion to endothelial cells by N-terminal peptide and annexin A2-S100A10 inhibitors. 215

List of Tables

Table 1.1: Summary of the effects of annexin A2 on cancer cells. 27

Table 1.2: Summary of the effects of annexin A2 in pancreatic cancer. 32

Table 1.3: Summary of the roles of S100A10 in cancer cells. 40

Table 1.4: Summary of annexin A2-S100A10 interactions roles with relevant inhibition mechanism. 44

Table 1.5: List of the inhibitors with their chemical formula and the IC_{50} of annexin A2-S100A10 inhibitory potency expressed in μM. 56

Table 2.1: The IC_{50}s of potent annexin A2-S100A10 inhibitors in PANC-1 and MIA PACA-2 cells as measured using an MTT assay. 79

Table 2.2: Correlation coefficient values for interpreting the strength and direction of a relationship between two variables according (Cohen, 1992).84

Table 2.3: List of target-potent intracellular active annexin A2-S100A10 inhibitors with their chemical structures. 104

Table 2.4: List of target-potent intracellular inactive annexin A2-S100A10 inhibitors with their chemical structures. 106

Table 2.5: List of target-potent intracellular moderately active annexin A2-S100A10 inhibitors with their chemical structures. 108

Table 2.6: List of target-impotent intracellular inactive annexin A2-S100A10 inhibitors with their chemical structures. 110

Table 3.1: Dose dependent inhibition of PANC-1 G-R survival by gemcitabine or TRK317. 134

Table 3.2: Combination treatment of gemcitabine serial concentrations with TRK317 50 μM in PANC-1 G-R cells show a synergistic effect as indicated by combination index (CI < 1). 135

CHAPTER 1

1. INTRODUCTION

1.1. Cancer

Cancer is defined as a disease in which a group of cells grow abnormally and uncontrollably by disobeying the normal rules of cell division. Normal cells are constantly subjected to signals that control growth, differentiation and apoptosis. Cancer cells develop a degree of independence to these signals, resulting in uncontrolled growth, proliferation and resistance to death. If this continues, it might lead to tumour spreading in a process called metastasis. Actually, nearly 90% of cancer-related deaths are due to tumour metastasis (Hejmadi, 2010).

Cancer biology foundation rests on a simple concept. Almost all mammalian cells share similar molecular networks that control cell growth, differentiation and apoptosis. The principle that has led to genesis and treatment of cancer is that normal cells are transformed into cancers as a result of changes in these networks at the molecular and cellular level. Therefore, cancer is being defined now as a disease which involves mutations in the normal cell genome. These changes (DNA mutations) lead to change in proteins level and disruption of the delicate cellular balance resulting in cells dividing out of body control (Hejmadi, 2010).

Therefore, differentiating between cancer cells and normal cells is essential in cancer research in order to target the cancer cells with minimum effects on the normal cells.

1.1.1. Hallmarks of cancer

Despite several decades of intense research, our understanding of how cancer develops and progresses is still limited. A major goal of cancer research is to understand how to counteract mechanisms that determine the ability of cancer cell to become malignant and metastasize. Hanahan and Weinberg have proposed ten essential alterations in cell physiology that collectively make a tumour cell becomes malignant: mutation and genomic instability, self-sufficiency in growth signals, insensitivity to growth-inhibitory (antigrowth) signals, evasion of programmed cell death (apoptosis), limitless replicative potential, sustained angiogenesis, reprogramming of cellular metabolism, avoiding immune response, promoting inflammation, tissue invasion and metastasis (Hanahan and Weinberg, 2011) as shown in Figure 1.1.

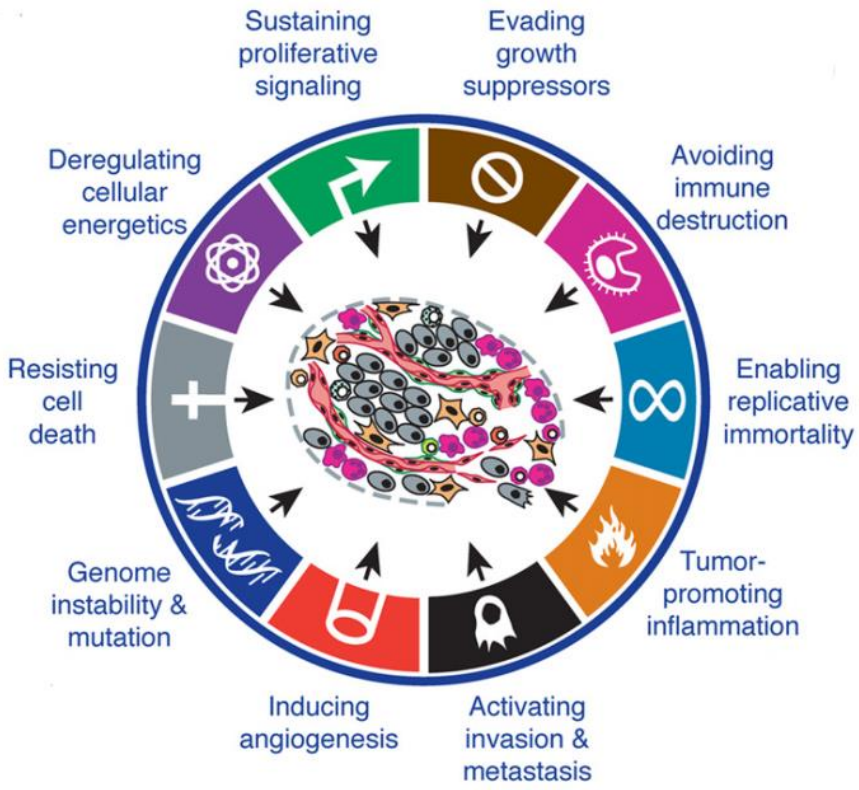


Figure 1.1: Hallmarks of cancer. Copied and modified from (Hanahan and Weinberg, 2011).

1.1.1.1. Sustaining proliferative signalling

Normal cells control the production and release of growth-promoting signals and thereby determine when and where cell growth and division occur and thus maintenance of normal tissue structure and function. In cancer cells, these signals are deregulated thus they become masters of their own destinies (Hanahan and Weinberg, 2011).

Cancer cells maintain and control growth-promoting signals in a number of ways: production of growth factor ligands which result in an autocrine proliferative stimulation; sending signals to stimulate the surrounding normal cells which react by supplying the cancer cells with various growth factors (Cheng et al., 2008); overexpressing or altering cell surface receptors therefore cells become less responsive to such limited amounts of growth factor ligand; constitutively activating the downstream pathways of these receptors thus hindering their ability to be stimulated by ligand-mediated receptor activation; disrupting negative-feedback mechanisms that inhibit proliferative pathways, for instance PTEN phosphatase which dephosphorylates PIP_3 leading to inhibition of the proliferative PI3K and Akt signalling pathways. PTEN mutations lead to amplification in the PI3K signalling pathway and promote tumorigenesis in various cancer models (Jiang and Liu, 2009, Yuan and Cantley, 2008).

1.1.1.2. Evading (avoiding) growth suppressors

Beside their ability to maintain and control growth-promoting signals, cancer cells also bypass the action of tumour suppressor genes which negatively regulate cell proliferation.

Two tumour suppressor proteins, RB and p53 govern the decisions of cells to proliferate by inhibiting cell cycle progression, activating senescence (stop division) and promoting programmed cell death (apoptosis). The RB protein receives signals from extracellular or intracellular sources and, in response, decides whether a cell should proceed through division cycle or not (Burkhart and Sage, 2008). Hypo-phosphorylation of RB stops progression of cells from the Gap 1 (G1) phase to the DNA synthesis (S) phase of the cell cycle. RB in association with the E2F transcription factor prevents damaged DNA from replicating and progressing through the cell cycle. This regulatory mechanism is missing in cancer cells which have defective RB proteins thereby they do not have the gatekeeper of the cell cycle progression.

p53 serves as a genome policeman. It is negatively regulated by MDM2 and concentrations of the protein remain relatively low. Various stresses including DNA damage can increase the level of p53 by disrupting its association with MDM2 triggering a cell cycle halt if a little damage in the DNA has occurred until the genome is repaired and normalized. If the damage is severe and irreversible, p53 would direct the cell to apoptosis. Therefore cancer cells with un-functional p53 are unable to manage DNA

damage and may progress through the cell cycle with mutated genomes (Hanahan and Weinberg, 2011).

1.1.1.3. Resisting cell death

The natural ability of cells to evade cancer development by triggering apoptosis has been established and confirmed over the last 20 years (Adams and Cory, 2007).

Programmed cell death or apoptosis comprises regulators and effectors (Adams and Cory, 2007). Regulators are divided into two pathways, one for receiving extracellular death signals and the other sensing intracellular signals. Both activate normally latent proteases (caspase 8 and 9 respectively) that initiate a cascade of proteolysis by activation of executor caspase 3, leading eventually to cell been disassembled and consumed by phagocytic cells. TP53 induces apoptosis by upregulating expression of some pro-apoptotic proteins (Bax and Bak), as a result of DNA damage. These pro-apoptotic proteins disrupt the mitochondrial membrane leading to the release of cytochrome c which activates caspase 9 resulting in cell death. Tumour cells overcome the apoptosis by impairing p53 function resulting in insensitivity to DNA damage (Hanahan and Weinberg, 2011).

1.1.1.4. Enabling replicative immortality

Normal cells in the body are only able to pass through limited number of successive cell growth and division cycles. It is widely accepted that cancer cells are able to replicate to unlimited numbers of cell division cycles. The ability of cells to replicate for unlimited proliferations has been linked to telomeres that protect the ends of chromosome (Blasco, 2005). Telomeres are formed from multiple hexa-nucleotide repeats that shorten progressively in non-immortalized cells leading eventually to the loss of their ability to protect the ends of chromosomal DNA (Artandi and DePinho, 2010). As a result, cell viability will be affected. Therefore, the length of telomeric DNA in a cell determines how many successive generations will pass through before telomeres eroded and lost their protective functions. Thus, telomere shortening is considered as a clocking device that determines the lifespan of a cell. Cancer cells significantly increase the level of telomerase, a special DNA polymerase that add telomere repeats to the end of telomeric DNA and prevent its shortening, thereby protecting the end of chromosomal DNA and making the cell immortalized (Hanahan and Weinberg, 2011). This process can be partially regulated by p53-mediated surveillance of genomic integrity. However, the realization that impaired telomere function can promote tumour progression has come from a study of mutant mice lacking both p53 and telomerase function (Artandi and DePinho, 2010).

1.1.1.5. Inducing angiogenesis

As normal cells, cancer cells require to sustain and supply themselves with oxygen and nutrients and to evacuate wastes and CO_2.

Endothelial cells are the major and key regulator for developing new vasculatures (vasculogenesis) and sprouting of new vessels from the existing vessels (angiogenesis) during embryogenesis. Following this morphogenesis, the new vasculature becomes largely quiescent (dormant). However, in the adult as a part of healing process, angiogenesis is turned back until the healing is finished. The latter effects are governed by regulatory factors that either induce (vascular endothelial growth factor-A (VEGF-A)) or oppose (thrombo-spondin-1 (TSP-1)) angiogenesis (Baeriswyl and Christofori, 2009). This angiogenic switch remains on during cancer development causing normally quiescent vasculature to continually sprout new vessels that help sustain tumour growth (Hanahan and Folkman, 1996).

1.1.1.6. Activating invasion and metastasis

Our understandings of the mechanisms which make the cancer cell invade and metastasize are still enigmatic.

As the cancer cells progress to a higher grade of malignancy they develop changes in their shape and their attachments to other cells as well as to the

extracellular matrix (ECM). The best example of these changes is the alteration in E-cadherin, a key cell-to-cell adhesion molecule, which helps to assemble epithelial cell sheets and maintain the quiescence of the cells within these sheets. Overexpression of E-cadherin was always correlated with decreased possibility of invasion and metastasis whereas reduction of its expression was known to potentiate these phenotypes (Cavallaro and Christofori, 2004). Matrix metalloproteinases (MMPs) have been identified as important regulators of tumour invasion and metastasis (Curran and Murray, 1999). Association of MMPs with tumour metastasis can be related to their proteolytic activity against collagen IV which forms most of extracellular matrix components (Stamenkovic, 2000).

The sequence of invasion and metastasis has been organized stepwise in an 'invasion-metastasis cascade' by Talmadge and Fidler (Talmadge and Fidler, 2010). This cascade begins with local invasion, then intravasation by cancer cells into nearby blood and lymphatic vessels. This is followed by transit of cancer cells through the lymphatic and blood vessels, and escape of cancer cells from the lumina of such vessels into the parenchyma of distant tissues (extravasation) leading to the formation of small nodules of cancer cells (micro metastases), and finally the growth of micro metastatic lesions into macroscopic tumours in a process called colonization.

1.1.1.7. An enabling characteristic: genome instability and mutation

During generation of cells, the rate of spontaneous mutation is very low due to the remarkable ability of genomic system to maintain and repair defects in DNA.

Cancer cells initiate tumourigenesis by increasing the rates of mutation (Negrini et al., 2010). This mutability is often achieved by increased sensitivity to mutagenic agents and/or by damaging the components of the genomic maintenance machinery. An increased rate of mutation can also be accomplished by inhibiting the surveillance systems that normally monitor genomic stability and directed genetically damaged cells into either senescence or apoptosis (Jackson and Bartek, 2009). The role of TP53 is very essential here, leading to it being called the ‘‘guardian of the genome’’ (Hanahan and Weinberg, 2011).

1.1.1.8. An enabling characteristic: tumour-promoting inflammation

There is a strong line of evidence that some tumours are attacked by cells of the immune system and thereby mirror inflammatory conditions arising in non-neoplastic tissues (Dvorak, 1986). Nowadays, it is clear that almost every neoplastic lesion contains immune cells presented at different densities (Pages et al., 2010).

Response of the immune system to cancer cells was always correlated with an attempt of the body to eradicate tumours. However, there were many clues that tumour-associated inflammation had a paradoxical effect of enhancing tumour growth and progression. Inflammatory response to cancer cells believed to supply the microenvironment of tumour with bioactive molecules such as growth factors, survival factors, proangiogenic factors as well as enzymes that facilitate angiogenesis, invasion, and metastasis (Hanahan and Weinberg, 2011). Moreover, inflammatory cells may use cytokines such as TNF-α to stimulate ROS accumulation in neighboring epithelial cells, which act as mutagen for these cells, enhancing their genetic mutations toward states of heightened malignancy (Grivennikov et al., 2010).

1.1.1.9. An emerging hallmark: reprogramming energy metabolism

In normal cells, glucose is metabolized under aerobic condition to pyruvate via glycolysis in the cytosol and thereafter to carbon dioxide in the mitochondria; under anaerobic conditions, glycolysis is favoured and less pyruvate is dispatched to the mitochondria. Otto Warburg first observed (Warburg, 1956a, Warburg, 1956b) that, even in the presence of oxygen, cancer cells reprogram their glucose metabolism toward lactic acid fermentation in the cytosol and avoid energy production by mitochondria a characteristic of cancer cell which has been known later on as Warburg

effect. By doing this cancer cells must compensate for a nearly 18-fold decrease in ATP production afforded by glycolysis relative to mitochondrial oxidative phosphorylation. This is achieved by upregulation of glucose transporter GLUT1, which dramatically increases glucose import into the cytoplasm (DeBerardinis et al., 2008). Indeed, a significant increase in glucose uptake and utilization has been documented in many human tumour types. Activation of either Akt or c-Myc has been found to enhance the Warburg effect as indicated by increased cellular glucose uptake (Fan et al., 2010).

1.1.1.10. An emerging hallmark: evading immune destruction

The long-lasting hypothesis of immune surveillance suggests that cells and tissues are constantly under monitoring of an ever-alert immune system, and such immune surveillance is responsible for detecting and eradicating cancer cells and thus preventing the formation of tumours. Cancer cells may counteract immune responses by secreting TGF-β or other immunosuppressive factors (Yang et al., 2010). Moreover, they can recruit immunosuppressive inflammatory cells such for instance, regulatory T cells (Tregs) and myeloid-derived suppressor cells (MDSCs) leading to inhibition of the cytotoxic lymphocytes (Mougiakakos et al., 2010). Therefore, solid tumours have somehow managed to get round and avoid detection and destruction by immune system, thereby evading eradication. This notion has

been strengthened by an observation noted an increase in the number of tumours in immunodeficient mice as compared with immunocompetent controls (Teng et al., 2008). Also it has been supported by a remarkable increase in the cases of cancers in immunocompromised patients (Vajdic and van Leeuwen, 2009). However in the latter, a vast majority of these cases are virus-induced cancers. Therefore, it is still required to be fully characterized and resolved how the cancer cells evade the immune system and progress to form tumours.

1.2. Pancreatic cancer

Pancreatic cancer, 90% of which manifests as pancreatic ductal adenocarcinoma (Muniraj et al., 2013), is an aggressive and destructive disease characterized by rapid progression, resistance to treatment and high rate of invasiveness. It remains an unfortunate disease with an overall 5-years survival rate of less than 3% (Bardeesy and DePinho, 2002). This has been related to the late diagnosis in the absence of early symptoms, resulting in identification of the disease at advanced stages (Zavoral et al., 2011).

1.2.1. Significance of pancreatic cancer

Pancreatic cancer is the eighth cause of cancer deaths in men and the ninth in women throughout the world (Ryan et al., 2014). In the US, it is the fourth leading cause of cancer death, and expected to become the second by 2020 (Muniraj et al., 2013). This has been attributed to the very low survival rate as shown in Figure 1.2.

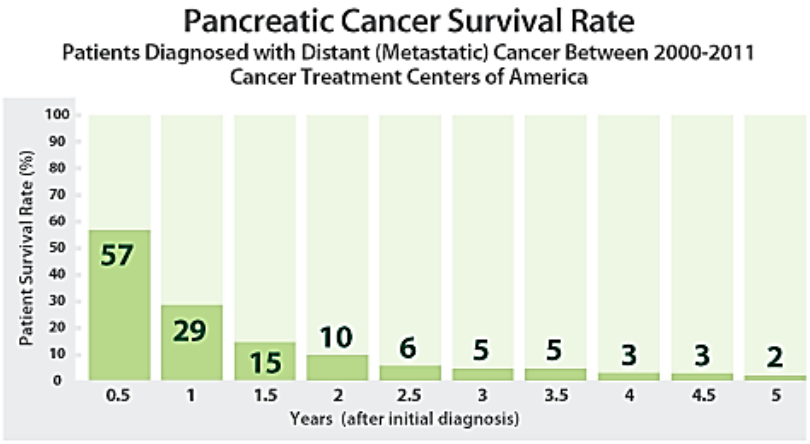


Figure 1.2: The cancer survival rates for a group of metastatic pancreatic cancer patients who were diagnosed between 2000 and 2011. Copied from (Cancercenter.com, 2015).

1.2.2. Morphological progression of pancreatic cancer

In normal ducts, epithelial cells appeared as cuboidal with single layer. However, when the cells have been mutated, they start showing morphological changes that lead to invasion of the surrounding stroma and metastasis to distant organs. As shown in Figure 1.3, these morphological alterations can be classified as following:

- Pancreatic intraductal neoplasia 1A and B (PanIN-1A and B); show elongated cells, mucin production, and papillary architecture.
- Pancreatic intraductal neoplasia 2 (PanIN-2); shows enlargement in nuclei and loss of cell polarity.

- Pancreatic intraductal neoplasia 3 (PanIN-3); cells show budding into lumen and severe nuclear atypia.
- Adeno-carcinoma stage; there is invasive growth and significant stromal reaction (Bardeesy and DePinho, 2002).

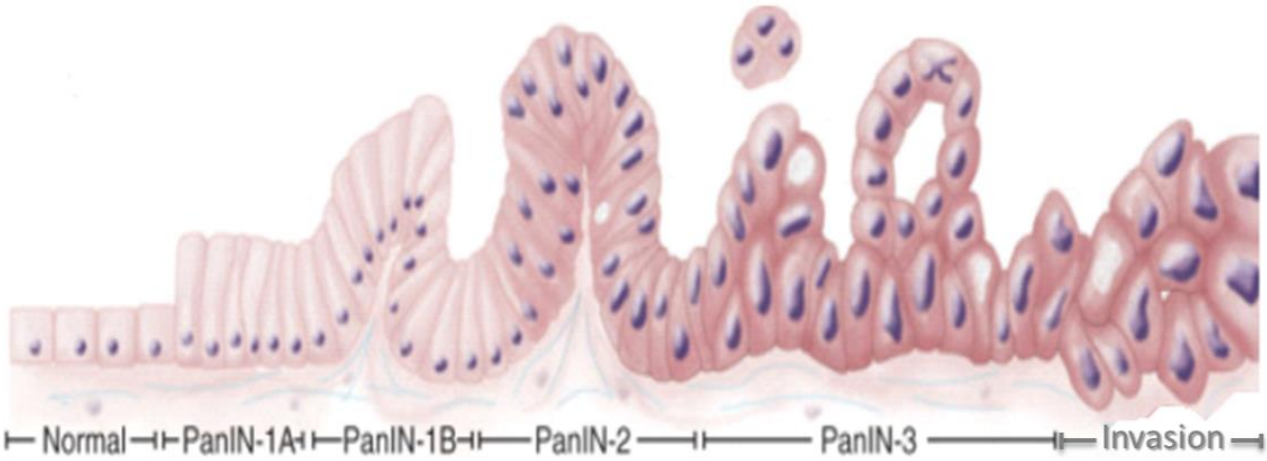


Figure 1.3: Morphological changes happening during pancreatic cancer progression. Reproduced from (Maitra et al., 2003).

1.2.3. Molecular changes during pancreatic cancer developments

Recent advances in molecular biology have given us a better understanding of the molecular and genetic changes that occur during pancreatic cancer progression. Most importantly, the changes occur in cell cycle in which serial stages occur for generation of a faithful copy of the cell itself as shown in Figure 1.5 (Vermeulen et al., 2003). There are several gene mutations accompanying histological and morphological changes of pancreatic cancer (Figure 1.4) and attributed to the alterations and disruptions in cell cycle phases. These mutations are summarized in the next sub-sections,

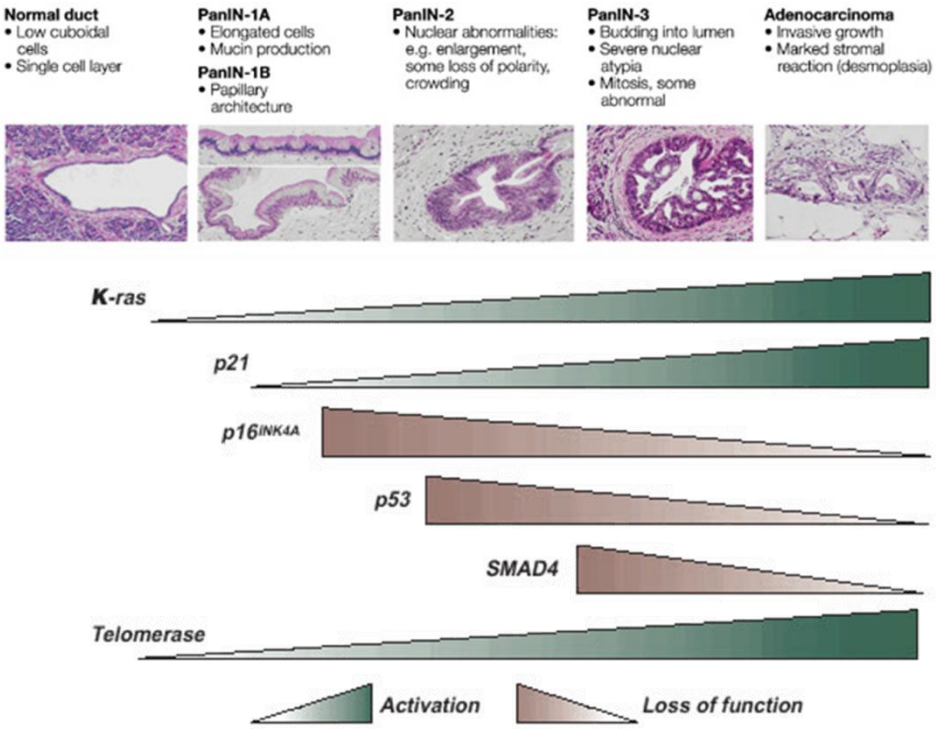


Figure 1.4: Molecular and pathological progressions accompanied pancreatic ductal adenocarcinoma. Modified from (Hruban et al., 2006, Bardeesy and DePinho, 2002).

1.2.3.1. Alterations in tumour suppressor genes

It is important to mention the steps or phases of the cell cycle before discussing the changes that happen in the genes that regulate it. These phases are; DNA replication phase (S) and chromosomal segregation and division phase (M). Between these two phases there are Gap1 (G1) and Gap2 (G2) phases during which the cell continues to grow and monitoring of S and M phases occurs to ensure accurate transmission of the genetic material (Suryadinata et al., 2010) (Figure 1.5).

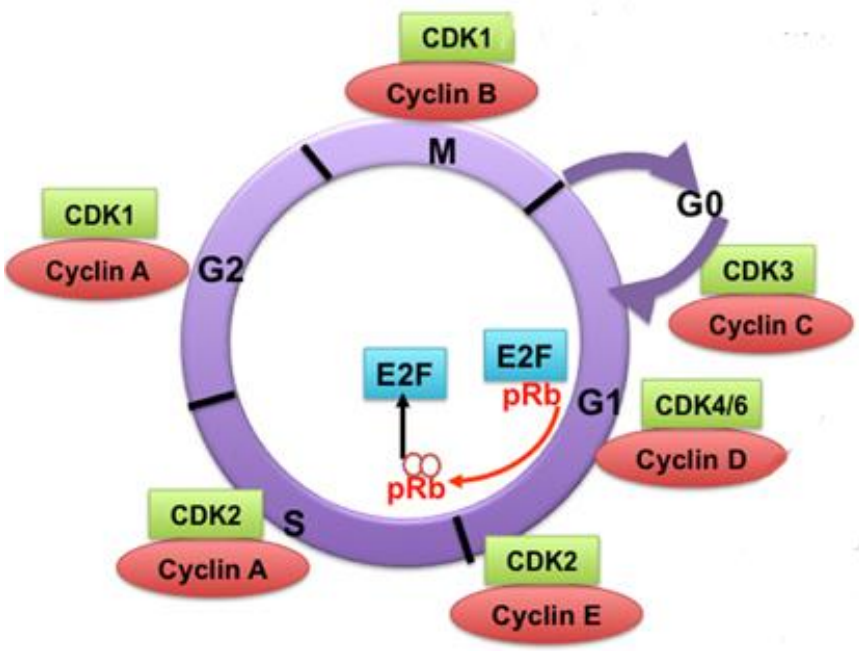


Figure 1.5: Cell cycle phases with cyclin-dependent kinases (CDKs) and their cyclin regulatory subunits. G1, S, G2 and M represent Gap1, synthesis, Gap2 and mitosis phases respectively; G0 is the Gap 0 or resting. Copied from (Aleem and Arceci, 2015).

Regulation of the cell cycle involves mechanisms crucial to the survival of a cell, including the sensing and repairing of DNA damage as well as preventing uncontrolled cell division. This is achieved by cyclins and cyclin-dependent kinases (CDKs), the main regulators of the cell cycle, which form complexes that control cell cycle progression. These complexes can be inactivated by specific endogenous inhibitors.

An important inhibitor is tumour suppressor gene retinoblastoma (pRB), a regulator of progression through G1 that binds to E2F (a transcription factor required for DNA synthesis). Phosphorylation of pRB by the cyclin D and E complexes leads to the release of E2F and progression of the cycle (Chellappan et al., 1991). p53, another tumour suppressor gene activates transcription of a cyclin dependent kinase inhibitor p21. Following DNA damage, increased expression of p53 and p21 results in inactivation of specific CDK4/6 cyclin complexes (Xiong et al., 1993) and halting the cell cycle until the DNA repair or apoptosis have occurred. The p16 gene is also a tumour suppressor gene which regulates cell cycle progression by inhibiting cyclin D/CDK4/6 complexes and thus inhibition of RB phosphorylation (Serrano et al., 1996). SMAD4, a gene responsible for coding of transforming growth factor beta TGF-β protein which mediates growth inhibitory signal pathway and induces G1 arrest (Wrana, 2000).

Most of the above tumour suppressor genes are significantly changed in pancreatic cancer.

p53 gene alterations have been reported to occur in more than 50% of pancreatic cancers (Nakamori et al., 1995). p21 is also reported to be mutated in more than 70 % of pancreatic cancers (Kawesha et al., 2000). More than 80% of pancreatic cancers show mutations of p16 (Kawesha et al., 2000) and SMAD4 (Biankin et al., 2001).

1.2.3.2. Changes in oncogenes

Oncogenes encode proteins that regulate cellular growth, differentiation and survival. Most important, is the K-ras which encodes small guanosine 5'-triphosphate (GTP)-binding cytoplasmic proteins that are involved in signal transduction of growth factors on the surface of the cell. K-ras is found to be mutated in more than 50% of pancreatic cancer (Hruban et al., 1993).

1.2.3.3. Chromosomal instability

Pancreatic cancer is no exception from other cancers in that it exhibits complex chromosomal rearrangements during its progression. Each end of a chromosome is composed of a telomere which serves as a cap to maintain DNA stability and integrity. As mentioned before, telomere stability is maintained by the enzyme telomerase. Increased expression of telomerase

has been reported in more than 90% of pancreatic cancer (Hiyama et al., 1997).

1.2.4. Proteomics of pancreatic cancer

The study of protein expression profiles of pancreatic cancer tissues is currently a very active field of research. The purpose of these studies is to search for biomarkers that could be used for early diagnosis, to determine responsiveness to treatment, and most significantly to understand the molecular mechanisms of its invasiveness. Several changes in protein expressions have been found in many pancreatic cancer cell lines. A study conducted by (Qi et al., 2008) has found 30 potential biomarkers differentially expressed in pancreatic cancer tissues. Proteins, such as anterior gradient homolog 2, syncollin, olfactomedin-4, polymeric immunoglobulin receptor, and collagen alpha-1(VI) chain were all upregulated in pancreatic cancer (Makawita et al., 2011). Immunohistochemistry analysis of pancreatic cancer tissue revealed overexpression of fascin and cathepsin (Lu et al., 2004).

Several studies have also confirmed that, S100 proteins are upregulated in pancreatic cancer tissue (Fritz et al., 2010). Expressions of S100A4, S100A6 and S100A10 are higher in pancreatic cancer tissues than in normal tissues (Chen et al., 2009, Nedjadi et al., 2009, Sekine et al., 2012).

Increased expression of annexin A2 was observed in pancreatic cancer by (Vishwanatha et al., 1993) and (Esposito et al., 2006). Takano et al also reported upregulation of annexin A2 in pancreatic cancer cells which was correlated with a resistance to chemotherapy (Takano et al., 2008).

A change in the expressions of annexin A2 and S100A10 has led to alterations in behaviours of pancreatic cancer cells in terms of chemo-resistance, adhesion and invasion (Hedhli et al., 2012). Therefore, it is important to have an idea about these proteins and to know how exactly they contribute in pancreatic cancer progression. In fact, investigation of a complex formation between these two proteins is the main topic of this thesis.

1.3. Annexin proteins

Annexins are family of proteins that bind phospholipid in a calcium dependent manner (Bharadwaj et al., 2013). The name annexin is derived from a Greek word annex which means link or bring together. A word describes the principal function of annexins. (i.e holding biological structures together especially membranes) (Gerke and Moss, 2002).

Annexins are composed of two domains; the variable N-terminal head and the conserved 33 kDa C-terminal tail domains.

The N-terminal domains show a high diversity among annexins; these domains differ in length and sequence. According to the length, they can be classified into; short N-terminal domains (20-21 residues) present in annexin A3, 4, 5, 6, 8, 10 and 13a, intermediate N-terminal domains (up to 55 residues) present in annexins A1, 2, 9 and 13b and long N-terminal domains (more than 100 amino acids) present in annexin A7 and A11.The N-terminal is responsible for functional peculiarities of each member. Its extension is crucial for the stability of the structure and mediates the interaction with other proteins like for example, S100 proteins (Lizarbe et al., 2013).

The C-terminal domains (Annexin core) share a highly conserved core which is composed of four homologous domains of about 70 residues. Each domain comprises a four alpha-helix bundle arranged in a cylindrical way covered by a fifth alpha-helix (Rescher and Gerke, 2004) as shown in Figure 1.6.



Figure 1.6: Ribbon presentation showing the three-dimensional structure of annexin A2 in a calcium free state. Modified from (Rosengarth and Luecke, 2004).

Annexins have several cellular functions and may be involved in cancer in many ways. For instance annexin A1 was found to enhance the activity of anti-inflammatory drugs leading to an increase in apoptosis of pancreatic and colon cancers cells (Zhang et al., 2010b). Upregulation of annexin A4 was found to promote the progression and chemoresistance of colorectal cancer, esophageal squamous cell carcinoma, gastric cancer, lung cancer,

and breast cancer (Wei et al., 2015). Downregulation of Annexin A6 was found to enhance breast cancer progression and invasion by promoting the loss of functional cell-cell adhesion (Sakwe et al., 2011). In pancreatic cancer cells, inhibition of annexin A8 expression resulted in elevated caspase-3 and -7 activities and a consequent cell death (Hata et al., 2014).

An important member of the annexin family is annexin A2 which has diverse cellular functions and has been implicated in cancer progression. As previously mentioned, the aim of this study was to determine the implications of annexin A2 expression in pancreatic cancer.

1.3.1. Annexin A2

Annexin A2 (also known as p36) is a Ca^{+2}-dependent phospholipid binding protein, which was formerly described as a substrate for pp60 src tyrosine kinase (Flood and Hajjar, 2011).

Several reports have mentioned involvement of annexin A2 in cancer progression (Table 1.1). Upregulation of annexin A2 in pancreatic, colorectal, and brain tumours was correlated with poor outcome and metastatic potential of these cancers (Lokman et al., 2011). A higher expression of annexin A2 was also observed in highly metastatic breast cancer cells compared with non-metastatic cells (Lokman et al., 2011). Another study conducted by Wu et al. (2002) using 2D-gel electrophoresis of two head and neck squamous carcinoma cell lines derived from primary and metastatic tumours reported annexin A2 upregulation in cell line derived from metastatic tumour (Wu et al., 2002). Annexin A2 interacts with tenascin C, an ECM molecule overexpressed in tumour microenvironment which has a role in tumourigenesis (Orend and Chiquet-Ehrismann, 2006). This interaction regulates cell migration and enhances cell proliferation of endothelial cells (Chung et al., 1996). Colocalization of annexin A2-S100A10 complex with cathepsin B has been reported to be involved in degradation of endothelial cells ECM during in vitro tube formation (Cavallo-Medved et al., 2009). Zhang et al. (2010) demonstrated a reduced ability of annexin A2 silenced breast cancer cells to proliferate, invade and metastasize (Zhang et

al., 2010a). Deceased levels of MMP2 and MMP9 have been reported in hepatocellular carcinoma cells after silencing of annexin A2 expression. This reduction resulted in a decreased ability of these cells to invade the surrounding (Zhao et al., 2010). Silencing of annexin A2 expression resulted in a reduced migration ability of glioma cells (Tatenhorst et al., 2006) as well as in multiple myeloma cells (Bao et al., 2009). These effects have been summarized in table 1.1.

Table 1.1: Summary of the effects of annexin A2 on cancer cells.

Function	Observations	Ref
Motility	Annexin A2 interaction with HAb18G/CD187 enhanced migration of hepatocellular carcinoma.	(Zhao et al., 2010)
	Annexin A2 interaction with S100A6 protein enhanced migration of pancreatic cancer cells.	(Nedjadi et al., 2009)
	Annexin A2 and t-PA induced migration of breast cancer cell line.	(Sharma et al., 2010)
	Annexin A2 overexpression inhibited migration of prostate cancer cell.	(Liu et al., 2003b)
	Annexin A2 knockdown by siRNA or neutralizing antibodies inhibited the motility of ovarian cancer cells.	(Lokman et al., 2013)
	Annexin A2 silencing by shRNA inhibited the motility of hepatoma cells.	(Zhang et al., 2013)
Invasion	Annexin A2 mediated invasion of breast cancer cells	(Sharma et al.,

	through a plasmin dependent generation mechanism.	2006)
	Annexin A2 interaction with t-PA promoted invasion of pancreatic cancer cell.	(Diaz, 2004)
	Annexin A2 siRNA or shRNA silencing inhibited invasion of pancreatic cancer cells.	(Zheng et al., 2011)
	Annexin A2 interaction with HAb18G/CD187 promoted invasion of hepatocellular carcinoma.	(Zhao et al., 2010)
	Annexin A2 enhanced invasiveness of multidrug resistant breast cancer cell lines.	(Zhang et al., 2009)
	Annexin A2 knockdown by siRNA or neutralizing antibodies inhibited the invasion of ovarian cancer cells.	(Lokman et al., 2013)
	Annexin A2 silencing by shRNA inhibited the invasion of hepatoma cells.	(Zhang et al., 2013)
Adhesion	Annexin A2 regulated the adhesion of prostate cancer cells.	(Shiozawa et al., 2008)
	Annexin A2 regulated cell adhesion of RAW 117 cells to the endothelial cells.	(Tressler et al., 1993)
	Annexin A2 mediated adhesion of breast cancer cells to endothelial cells.	(Myrvang et al., 2013)
	Annexin A2 tyrosine phosphorylation mediated baby hamster kidney cell adhesion.	(Rescher et al., 2008)
Apoptosis	Annexin A2 plays a role in p53 induced apoptosis in lung cancer cells, Annexin A2 knockdown increased the levels of p53 and its downstream gene expression, and caused p53 translocation from the cytoplasm to the nucleus.	(Huang et al., 2008)
	Annexin A2 induced cleavage by glycogen synthase kinase-	(Wang et al.,

	3 has led to cell cycle inhibition and apoptosis of human lung carcinoma cells.	2009)
	Annexin A2 mediated anti-apoptotic effects of progastrin in pancreatic cancer cells.	(Rengifo-Cam et al., 2007)
Proliferation	Annexin A2 siRNA knockdown resulted in a decreased proliferation of multiple myeloma cells.	(Bao et al., 2009)
	Annexin A2 siRNA Knockdown decreased proliferation of invasive breast cancer cell lines.	(Zhang et al., 2010a)
	Annexin A2 enhanced the proliferation of proliferative hepatocytes.	(Masaki et al., 1994)
	Annexin A2 shRNA down-regulation decreased the proliferative capacity of human lung adencarcinoma cells A549.	(Wang et al., 2012b)
	Annexin A2 suppression by RNA interference (RNAi) in breast cancer cells has led to accumulation of the cells in G1 phase with a decrease in G2/M phase and a reduction in cell proliferation.	(Zhang et al., 2010a)

1.3.2. Annexin A2 in pancreatic cancer

Immunohistochemical (IHC) analysis of pancreatic cancer sections revealed that, annexin A2 exists in 36% of PanIN-1A (Pancreatic intraepithelial neoplasia) and 19% of PanIN-1B non-invasive lesions. Conversely, annexin A2 was expressed in higher than 80% of the more invasive lesions (PanIN-2 and PanIN-3) suggesting that annexin A2 might have a role in invasiveness of pancreatic cancer progression (Esposito et al., 2006) as shown in Figure 1.7.

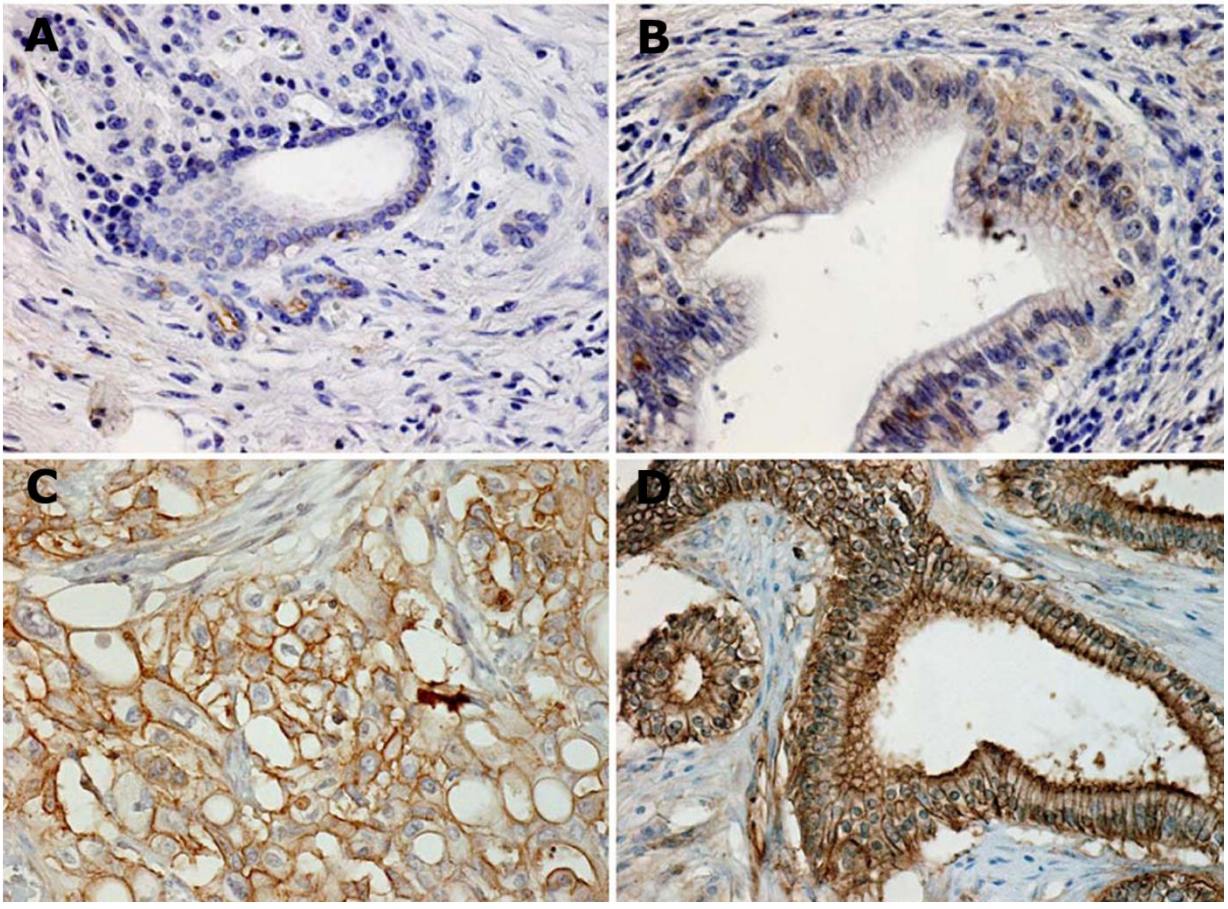


Figure 1.7: Immunohistochemical analysis of annexin A2 in pancreatic ductal adenocarcinoma. Increased membrane localization of annexin A2 with the progression of pancreatic cancer; A, and B represent PanIN-1A and PanIN-1B respectively; C and D show the more invasive PanIN-2 and PanIN-3. Copied and modified from (Takano et al., 2008).

Zheng et al reported that, annexin A2 is a tumour associated antigen in pancreatic ductal adenocarcinoma and once its expression on the cell surface is inhibited by shRNA or annexin A2 antibodies, there was a marked reduction in pancreatic cancer invasion both in vivo and in vitro (Zheng et al., 2011). Overexpression of tPA in pancreatic cancer cells enhances tumour growth, angiogenesis, and invasion (Takano et al., 2008, Diaz et al., 2002), the latter effect might involve an interaction with pancreatic cell surface annexin A2 and subsequent production of plasmin (Takano et al., 2008, Diaz et al., 2004). A summary of annexin A2 involvement in pancreatic cancer is shown table 1.2.

Table 1.2: Summary of the effects of annexin A2 in pancreatic cancer.

System	Effect	Reference
In vivo	Mediated invasion of mouse pancreatic ductal adenocarcinoma cells through a semaphorin 3D dependent mechanism.	(Foley et al., 2015)
In vitro	Mediated resistance to gemcitabine by increasing the activity of NF-κB.	(Jung et al., 2015)
In vitro	Knock-down by siRNA, blockade by anti-annexin A2 antibodies, suppressed invasion pancreatic cancer cells.	(Zheng et al., 2011)
In vivo	shRNA knockdown, a mutation at tyrosine23 or anti- annexin A2 antibodies, inhibited metastases in a mouse model.	(Zheng et al., 2011)
In vitro	Interaction between annexin A2 and alternatively spliced segment of tenascin-C (TNfnA-D) mediated gemcitabine resistance.	(Gong et al., 2010)
In vitro	Co-localization of tPA and annexin A2 mediated pancreatic cancer cells proliferation.	(Ortiz-Zapater et al., 2007)
Western blot analysis	Annexin A2 is upregulated in gemcitabine MIA PACA2 resistant cells as compared wild type.	(Takano et al., 2008)
Western blot analysis	Annexin A2 level is increased in pancreatic carcinoma cells of Syrian Hamsters.	(Kumble et al., 1992)
Western blot analysis	Annexin A2 is upregulated in pancreatic tumorous tissues as compared with non-tumorous.	(Tian et al., 2008)
Northern blotting	Annexin A2 is overexpressed in pancreatic cancer	(Vishwanatha et al.,

	cells.	1993)
Immunohistochemistry	Annexin A2 overexpression mainly at the surface of pancreatic cancer cells.	(Takano et al., 2008)
Immunohistochemistry	Annexin A2 is overexpressed concomitantly with tPA ductal tumours in mice model.	(Aguilar et al., 2004)
Immunohistochemistry	Annexin A2 is overexpressed concomitantly with tenascin C in the process of pancreatic carcinogenesis.	(Esposito et al., 2006)
Immunohistochemistry	Annexin A2 is expressed strongly in cancer areas but weakly in normal pancreatic areas.	(Tian et al., 2008)
Proteomic analysis	Annexin A2 is overexpressed in pancreatic cancer.	(Chen et al., 2007)
Proteomic analysis	Annexin A2 is overexpression in 93% of 127 pancreatic ductal adenocarcinoma samples.	(Chen et al., 2005)
Proteomic analysis	Annexin A2 expression is changed more than 10 folds in pancreatic ductal adenocarcinoma versus normal pancreas.	(Crnogorac-Jurcevic et al., 2005)
Proteomic analysis	Annexin A2 expression is increased more than 3 folds comparing with normal epithelial cells.	(Sitek et al., 2009)
Proteomic analysis	Affinity capture tPA-Sepharose followed by 2-DE and MALDI-MS PMF identified annexin A2 as a tPA receptor in pancreatic cancer cells.	(Roda et al., 2006)
Radioimmunoassay	Annexin A2 is secreted in the cell media and detectable intracellularly in pancreatic cancer cells.	(Davis and Vishwanatha, 1995)
In vitro	Inhibition of annexin A2 expression in GEM-MIA	(Takano et al.,

	PaCa-2 resistant cells significantly increased the chemocytotoxic efficacy of gemcitabine.	2008)
In vitro	Supplementation of r-annexin A2 in the medium increased resistance to anticancer drugs in pancreatic cancer cells.	(Sato et al., 2012)
In vitro	Increased surface expression of annexin A2 promotes pancreatic cancer cells growth.	(Ptak-Belowska et al., 2009)
In vitro	Annexin A2 interaction with t-PA promotes invasion of pancreatic cancer cell.	(Diaz et al., 2004)
In vitro	Annexin A2 has been reported to mediate anti-apoptotic effects of progastrin in pancreatic cancer cell.	(Rengifo-Cam et al., 2007)

1.4. S100 proteins

The S100 protein family belongs to the group of EF hand calcium binding proteins which has been described of having extracellular and/or intracellular functions (Pathuri et al., 2008). There are 24 S100 proteins which are classed by their distribution as extracellular, intracellular or a combination of both (Donato et al., 2013). Moore group discovered the first member of this family in brain tissues. They were called S100 because they were soluble in 100% saturated ammonium sulphate (Moore, 1965). They are 10-12 kDa acidic proteins existing as a homodimer composed of two monomers stabilized by non-covalent interaction. Each monomer contains two EF hands (helix-loop-helix motif). The N-terminal EF hand (also termed pseudo EF hand) is composed of 14 amino acids and has a low binding affinity to calcium. The C-terminal EF hand (also named canonical EF hand) encompasses 12 amino acids, and has a higher binding affinity to calcium via side chain carboxylate oxygen (Pathuri et al., 2008) as seen in Figure 1.8.

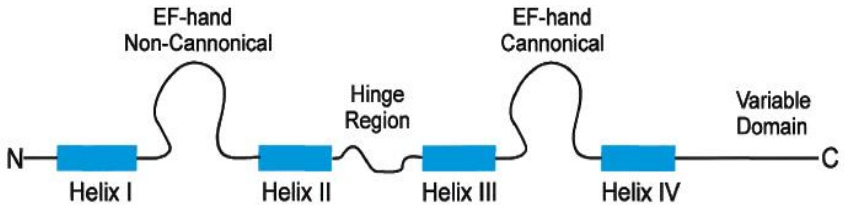


Figure 1.8: Domain structure of S100 proteins showing the two EF hands. Adapted from (Eckert et al., 2004).

Nearly all S100 proteins (except S100A10) have two conformations: the apo or inactive closed conformation in the absence of calcium and the active or calcium bound conformation in which the monomer is capable to bind its binding partners (Pathuri et al., 2008) as exhibited in Figure 1.9.

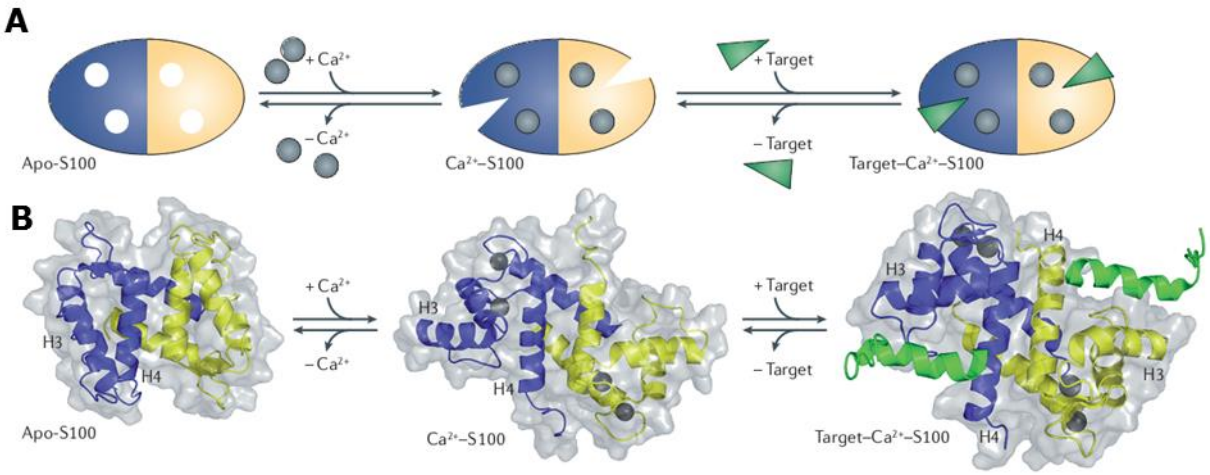


Figure 1.9: Structural organization of S100 protein. (A) Apo-S100 protein is shown with blue and yellow subunits. Ca^{+2} binding, grey circles, induces a conformational change in S100 protein results in exposure of hydrophobic cleft and binding to its binding partner (green triangle). (B) Ribbon and surface diagrams of apo-S100, Ca^{+2} bound S100 and the Ca^{+2} bound S100–peptide complex. Individual subunits are shown in blue and yellow, the Ca^{+2} ions shown in grey spheres, and the peptide is shown in green. Reproduced from (Bresnick et al., 2015).

S100 proteins are expressed in a cell specific manner, suggesting that they have a variety of functions and roles. To name a few S100A1 is found to be expressed in cardiac muscle and some neurons and believed to improve

calcium handling and contractile performance of the heart (Donato et al., 2013). S100A2 is considered as a tumour suppressing protein due to its potentiating effect on p53 and its downregulation in several cancers is associated with poor prognosis (Wolf et al., 2011, van Dieck et al., 2009). S100A4 expression is associated with poor outcome in many cancer patients due to stimulation of survival motility and invasion (Garrett et al., 2006). S100A6 is involved in cell proliferation, cytoskeletal dynamics and tumour development (Lesniak et al., 2009). S100A7 is believed to stimulate Akt and NF-kB, thereby promotes aggressiveness of breast cancer (Emberley et al., 2005).

1.4.1. S100A10

S100A10. Also termed p11 or annexin A2 light chain, is an S100 family member. In contrast to all other S100 proteins, S100A10 is incapable of binding calcium due to mutations and deletions in its EF hands. However it is still able to bind its binding partners irrespective of calcium and considered as constitutively active (Pathuri et al., 2008). S100A10 tethers some membrane proteins including, the small GTPase of the Rho family cdc42, acid sensing ion channel ASIC1a, actin-binding protein AHNAK, tissue plasminogen activator tPA and serotonin 1B receptor to annexin A2 (Svenningsson and Greengard, 2007, Rescher and Gerke, 2008). Therefore

it helps in transferring these proteins to the cell membrane or anchoring them on the surface (Donato et al., 2013). Inside the cells, most of S100A10 exists in a heterotetrameric complex with annexin A2 that directs the complex toward the plasma membrane (Rescher and Gerke, 2008).

1.4.2. S100A10 in cancer

S100A10 is found to be overexpressed in breast, stomach, gallbladder and kidney cancers (Chen et al., 2014). It has been proposed as a tumour biomarker in aggressive anaplastic carcinoma (Rust et al., 2005), renal cell carcinoma (Domoto et al., 2007), advanced diffuse large B-cell lymphoma (Nishiu et al., 2002), colorectal cancer (Shang et al., 2013), and most importantly pancreatic adenocarcinoma (Crnogorac-Jurcevic et al., 2003, Sitek et al., 2009).

Expression of S100A10 on the surface of HT1080 fibrosarcoma cells has been found to activate plasmin production through a uPA dependent mechanism (uPA is the main plasminogen activator secreted by cancer cells) (Choi et al., 2003). The authors noted that transfection of HT1080 cells with S100A10 antisense results in loss of S100A10 expression with concomitant decrease in plasmin production and invasion capacity. Conversely, transfection of these cells with S100A10 sense results in increased level of S100A10 with subsequent increase in plasmin generation and invasion

capability (Choi et al., 2003). A reduced level of S100A10 has also been correlated with a decrease in cell proliferation, plasmin production, and invasion of breast cancer cells (Zhang et al., 2010a).

Another study conducted on lung carcinoma cells reported that DLC1, a Rho GTPase activating protein and a known tumour suppressor protein, can inhibit the interaction of S100A10 and annexin A2 by occupying and interacting with the S100A10 binding site for annexin A2. This interaction resulted in decreased level of S100A10 and led to a decrease in migration and invasion of these cells through a Matrigel extracellular matrix barrier (Yang et al., 2011). The tumour suppressor protein DLC1 functions by preventing transformation of normal cells to tumour cells.

S100A10 was also found to inhibit Bcl-2-associated death promoter (BAD) protein, leading to a decreased level of BAD-induced apoptosis (Hsu et al., 1997). S100A10 expression has a negative correlation with BNIP3 expression, a proapoptotic member of the Bcl-2 family known to induce cell death (Mahon et al., 2007). Therefore, dysregulated S100A10 protein levels may have a link with the process of tumour growth and metastasis. A summary of the involvement of S100A10 in cancer is given in table 1.3.

Table 1.3: Summary of the roles of S100A10 in cancer cells.

Function	Observations	Ref
Motility	S100A10 is essential for migration of tumor-promoting macrophages into tumor sites.	(Phipps et al., 2011)
	S100A10 siRNA knockdown reduces the cell spreading of cervical and breast cancer cells via Rac1 related mechanism.	(Sayeed et al., 2013)
Invasion	S100A10 interaction with DLC1 inhibited in vitro invasion of lung cancer cells through a Rho gap-independent mechanism.	(Yang et al., 2011)
	S100A10 downregulation inhibited breast cancer cell invasion.	(Zhang et al., 2010a)
	S100A10 siRNA silencing reduced plasmin dependent invasion of colorectal cancer cells.	(Zhang et al., 2004)
	S100A10 siRNA knockdown inhibits pancreatic cancer cell dependent plasmin invasion.	(Bydoun et al., 2015)
	S100A10 loss from the surface of human fibrosarcoma cells resulted in a decrease in cellular plasmin production, ECM degradation, and cellular invasiveness.	(Choi et al., 2003)
Adhesion	S100A10 interaction with annexin A2 mediates adhesion of breast cancer cells to endothelial cells.	(Myrvang et al., 2013)
	S100A10 interaction with annexin A2 mediated adhesion of acute lymphoblastic leukemia cells to osteoblasts.	(Gopalakrishnapillai et al., 2015)

	S100A10 interaction with annexin A2 mediated tight junction formation between kidney cells.	(Lee et al., 2004)
Proliferation	S100A10 promoted growth of murine lung carcinoma through a macrophage dependent mechanism.	(Phipps et al., 2011)
	S100A10 downregulation inhibited the growth of hepatocellular carcinoma.	(Shan et al., 2013)
	S100A10 interaction with DLC1 Inhibits tumorigenicity of lung cancer cells through a Rho GAP-Independent Mechanism	(Yang et al., 2011)
	S100A10 downregulation inhibited breast cancer cell proliferation.	(Zhang et al., 2010a)
	S100A10 increased pancreatic cancer cell resistance to gemcitabine treatment by the inhibition of autophagy-related protein (VMP1-Mediated Autophagy).	(Pardo et al., 2010)

1.5. Annexin A2-S100A10 interaction

Annexins have been known to form a heterotetramer with many S100 proteins including annexin A1 with S100A11, annexin A11 with S100A6, as well as annexin A2 with S100A10. The latter interaction is one of the best characterized biochemically and has been suggested to be involved in many cellular functions (Pathuri et al., 2008, Liu et al., 2015).

Annexin A2 exists in a soluble monomeric form inside the cells, however upon binding with S100A10, it forms a stable complex (heterotetramer) composed of two subunits of each protein (annexin A2.S100A10)^2 (Flood and Hajjar, 2011). The complex is thought to be involved in several phenotypic behaviours of cancer cells.

Co-expression of annexin A2 with S100A10 has been established by many reports. Puisreux et al. (1996) reported co-expression of annexin A2 and S100A10 in colon, renal and hepatocellular carcinoma cell lines (Puisieux et al., 1996). Zhang et al. (2010) also noted an overexpression of annexin A2 and S100A10 in invasive breast cancer cells (Zhang et al., 2010a). Sitek et al. also reported upregulation of both proteins in pancreatic carcinoma (Sitek et al., 2009).

S100A10 anchored by annexin A2 or alone is thought to serve as a receptor for plasminogen, thereby facilitating the production of plasmin. This is thought to contribute to the fibrinolysis seen in the clinical haemorrhagic

phenotype of acute promyelocytic leukemia (O'Connell et al., 2011). Plasmin is a serine proteinase with a broad proteolytic activity against ECM, that is formed from a precursor zymogen plasminogen (Plg) by plasminogen activators, tPA and uPA. In addition to its ability to activate matrix metalloproteinases facilitating migration and invasion, plasmin is also able to degrade some ECM proteins such as laminin and fibrenoctin leading eventually to invasion of macrophage cells (O'Connell et al., 2010).

In RAW117 cells, a cell line known to express annexin A2-S100A10 complex on their surface (Yeatman et al., 1993), the rate of plasmin generation has been dramatically decreased after annexinA2-S100A10 complex silencing and this significant decrease has been reversed by addition of exogenous annexin A2-S100A10 complex to the system (Kang et al., 1999).

Annexin A2-S100A10 complex has been found to have a role in the formation of tight junction between MDCK II cells, (Madin-Darby canine kidney cells) (Lee et al., 2004). Myrvang et al. have shown that a labelled Cy5-S100A10 can bind to the surface of MDA-MB-231 cells via an annexin A2 receptor, proving that the complex might exist on the surface of these cells. It was suggested in this study that annexin A2-S100A10 interaction is involved in cell-cell interaction (Myrvang et al., 2013). A summary of the roles of annexin A2-S100A10 interactions with relevant inhibitory mechanism is shown in table 1.4.

Table 1.4: Summary of annexin A2-S100A10 interactions roles with relevant inhibition mechanism.

Annexin A2-S100A10 interaction	Inhibition mechanism	Ref
Pancreatic cancer cells.	None to date	None to date
Mediated adhesion of breast cancer cells to endothelial cells.	Adhesion has been inhibited by N-terminal (Ac-1-14) annexin A2 peptide.	(Myrvang et al., 2013)
Mediated intracellular trafficking of Human papillomaviruses into Human Keratinocytes.	Annexin A2 N-terminal antibody inhibited Human papillomaviruses internalization.	(Dziduszko and Ozbun, 2013)
Mediated stability of S100A10 and prevent its polyubiquitination and degradation.	N-terminal deletion of annexin A2 enhanced polyubiquitination of S100A10.	(He et al., 2008)
Involved in the Formation of E-cadherin-based adherens junctions in Madin-Darby Canine Kidney cells.	Annexin A2 siRNA knockdown inhibited E-cadherin recruitments at cell-cell contact site.	(Yamada et al., 2005)
Mediated adhesion of acute lymphoblastic leukemia to osteoblasts.	Adhesion inhibited by an annexin A2-S100A10 inhibitor and annexin A2 antibodies.	(Gopalakrishnapillai et al., 2015)
Mediated resistance of acute lymphoblastic leukemia to	An annexin A2-S100A10 inhibitor improved the sensitivity of acute	(Gopalakrishnapillai et al., 2015)

chemotherapy.	lymphoblastic leukemia to dexamethasone and vincristine.	
Annexin A2 –S100A10 interaction regulated liposomal exocytosis in endothelial cells.	Acetylated N-terminal annexin A2 peptide inhibited binding to liposomes.	(Konig et al., 1998)
Annexin A2–S100A10 interaction mediated the formation of tight junction between kidney cells.	Acetylated N-terminal annexin A2 peptide disrupted the tight junction formation between kidney cells.	(Lee et al., 2004)
Annexin A2 and/or S100A10 interaction mediated homing of bone marrow progenitor cells to the bone marrow of irradiated mice.	The survival of mice that received transplants was lower in the group treated with Annexin A2 antibody and S100A10 antibody or N-terminal peptide as compared with control.	(Jung et al., 2007)
Annexin A2-S100A10 interaction might mediate in vitro cell invasion and tumourigenicity of lung cancer cells.	DLC1, a tumour suppressor protein, inhibited the invasion and the proliferation of lung cancer cells by competing with annexin A2 for interaction with S100A10.	(Yang et al., 2011)
Annexin A2 binding to S100A10 sequestered annexin A2 in the cytoplasm and prevented its nuclear transport in human	Nuclear accumulation of annexin A2 has been enhanced by nuclear export inhibitor leptomycin B (LmB).	(Eberhard et al., 2001)

astrocytoma cells.		
Annexin 2A binding to S100A10 with heat stress and tyrosine 23 phosphorylation mediates translocation of the complex to the cell surface of endothelial cells.	Annexin A2 translocation inhibited upon depletion of p11, inactivation of tyrosine kinase, or mutation of tyrosine 23.	(Deora et al., 2004)

1.6. Targeting S100A10 and annexin A2

Several approaches have been used to modulate S100A10 and annexin A2 in cancer progression.

siRNA silencing of annexin A2 expression in gemcitabine-resistant pancreatic cancer cells, significantly improved the cytotoxic efficacy of the drug on the resistant cells (Takano et al., 2008). Zheng et al reported a marked suppression of pancreatic cancer cell invasion both in vivo and in vitro as a result of annexin A2 surface inhibition by siRNA or annexin A2 antibodies (Zheng et al., 2011). Annexin A2 silencing has also been associated with reduced invasion, migration, and proliferation of hepatoma cells (Zhang et al., 2013). A significant decrease in plasminogen activation, migration, and invasion has been observed in macrophage cells recovered from S100A10 null mice (O'Connell et al., 2010). Silencing of the S100A10 also reduced plasmin generation and invasive capacity of colorectal cancer cells (Zhang et al., 2004). Endothelial cells recovered from S100A10-null mice showed a marked reduction in plasminogen binding and plasmin generation in vitro (Surette et al., 2011). This approach reversed many phenotypic behaviours of cancer however, due to the long half live of S100 proteins (Bresnick et al., 2015), it might be difficult to achieve a low-steady state level to elicit a therapeutic effect. Moreover, there is a possibility of modulating expression of other proteins that are regulated under same transcriptional regulator leading eventually to off-target responses.

A different strategy involves the inhibition of the interaction between the two proteins. A peptide known to block the interaction between annexin A2 and S100A10 inhibits the invasion of prostatic cancer cells into bone marrow in animal model, while a scrambled peptide, having same number of amino acids but different sequence did not (Shiozawa et al., 2008). Similar peptide was found to decrease pancreatic cancer cell invasion in vitro (Diaz, 2004). As well as inhibited endothelial cell invasion into Matrigel plugs in a mouse model system (Ling et al., 2004). In the Madin-Darby canine kidney cell lines, (MDCK) II cells, expression of annexin A2 and S100A10 is the cause of tight junction formation between these cells. This tight junction has been disrupted by a synthetic peptide known to inhibit the interaction between annexin A2 and S100A10 (Lee et al., 2004). Adhesion of breast cancer cells to endothelial cells has been blocked significantly by N-terminal annexin A2 peptide (Ac-1-14) (Myrvang et al., 2013). This approach is more specific and could reduce the off-target effect however; its efficiency is limited to the extracellular annexin A2 and S100A10 proteins.

An important strategy to inhibit S100 proteins is by using small molecules that block the site required for binding of S100 proteins with their partners (Yap et al., 1999). For example; cromolyn, a mast cell stabilised, disrupts the interaction of S100P with RAGE resulting in decreased pancreatic tumour growth and increased sensitivity to gemcitabine treatment (Arumugam et al., 2013). Amlexanox, an anti-inflammatory drug, inhibits interaction of

S100A13 with fibroblast growth factor (FGF1) resulting in a reduction of mitogenic and angiogenic effects of FGF1 (Rani et al., 2010). Phenothiazine interacts with S100A4 resulting in oligomerization and sequestering of the protein away from its binding partners (Malashkevich et al., 2010).

Therefore, development of small molecules inhibitors targeting the interaction between S100A10 and annexin A2 is the key for eliciting the in vivo functions of the complex and to differentiate between intracellular and extracellular activity of these proteins.

1.7. Development of inhibitors targeting annexin A2-S100A10 interaction

Our group has discovered a first generation of compounds targeting the annexin A2-S100A10 interaction (Reddy et al., 2011, Reddy et al., 2012, Reddy et al., 2014). However, before describing the discovery of these compounds, it is important to investigate the binding pocket responsible for the interaction of S100A10 with the N-terminal peptide of annexin A2.

1.7.1. The crystal structure of S100A10 with the annexin A2 N-terminal peptide

Structure of S100A10 is composed of a pair of helix-loop-helix EF-hand motifs linked together by a flexible loop. The two EF hands (H1-L1-H2) and (H3-L3-H4) lie close to each other, with a short antiparallel β-strand forming between loops L1 and L3. Both EF hand loops are on the same side of the molecule, opposite the N- and C termini (Figure 1.10) (Rety et al., 1999).

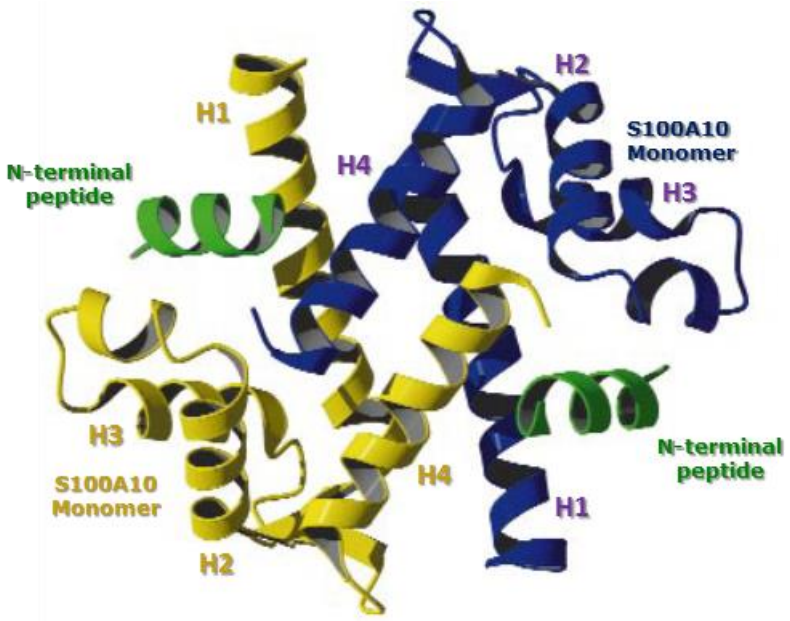


Figure 1.10: Complex structure of S100A10 dimer (blue and yellow) with the annexin A2 N-terminal peptide (green). Copied and modified from (Rety et al., 1999).

S100A10 dimerizes through the H1 and H4 helices. The four helices (two from each monomer) are arranged in an antiparallel manner and interact on their hydrophobic sides (Rety et al., 1999). Annexin A2 interacts with its ligand S100A10 via the short stretch of 12 amino acids (Ac-S-T-V-H-E-I-L-C-K-L-S-L) situated at the N-terminus (Becker et al., 1990). Although the peptide corresponds to the first 12 amino acids of annexin A2 found to be involved in the interaction, Rety et al have shown in the crystal structure that, only the first 10 amino acids have a well-defined electron density after refinement (Figure 1.11A). These form an alpha-helix as predicted, which lies

in a hydrophobic cleft formed by loop L2 and helix H4 of one monomer and helix H1 of the other. The N-acetyl nestles at the bottom of the hydrophobic cleft and is essential for binding affinity of N-terminal annexin A2 to S100A10 (Nazmi et al., 2012, Becker et al., 1990). A few hydrogen bonds complete the interaction, in particular His4 of the peptide with the carboxyl group of Glu5 of S100A10. The hydrophobic cleft is closed by Glu9 of S100A10 whose carbonyl group makes hydrogen bonds with the amides of the peptide bonds of Thr2 and Val3 of the N-terminal peptide (Figure 1.11B) (Rety et al., 1999).

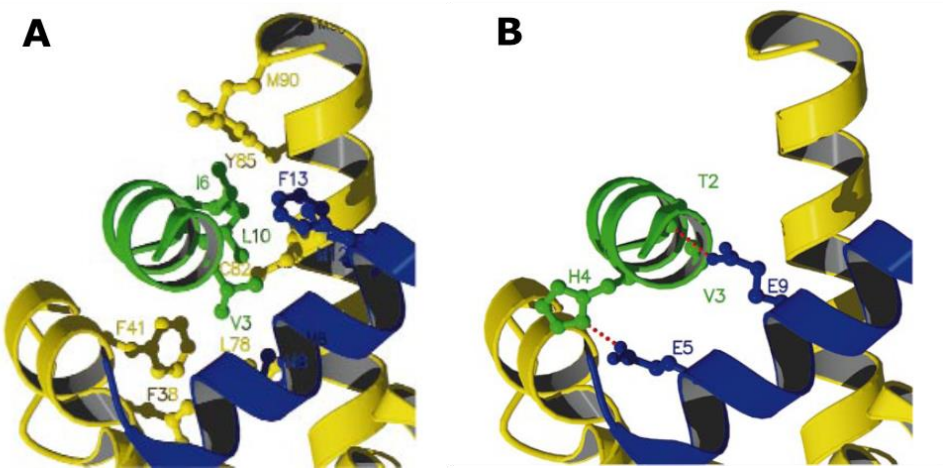


Figure 1.11: Close-up view of the interaction between the N-terminal peptide (green) and S100A10 dimer (yellow and blue). (A) The residues involved in the binding after refinement. (B) The critical points required for the interaction. Copied from (Rety et al., 1999).

1.7.2. Designing of annexin A2-S100A10 interaction inhibitors

The binding pocket of S100A10 has been used as template to perform in silico virtual screening of more than 700000 molecules. The molecules have been selected on the basis of drug like properties (Reddy et al., 2011).

GOLD (genetic optimization for ligand docking) has been used to perform screening of these compounds. Then the docked compounds (ligands) were ranked according the fitness scores generated from the virtual screening and the top scoring 1% of the hit compounds has been chosen for further analysis. The 1% hit compounds were then rescored using GOLD in standard parameter mode and as a result, the conformational search efficiency of the compounds was increased. After rescoring, 775 compounds were reselected again for binding analysis (Reddy et al., 2011).

The binding poses were subjected to visual inspection and ranked based on the ability of hit compounds to

1. Occupy the binding pocket.

2. Donate and accept hydrogen bonds.

3. Form electrostatic interactions with the binding pocket.

Based on these criteria, a subset of 394 compounds was selected and classified into 27 different clusters according to the similarity in their chemical structures. Then all the compounds were evaluated and screened

using a competitive binding assay based on fluorescence resonance energy transfer (FRET) between a Cy5 labelled S100A10 and a Cy3 labelled N-terminal annexin A2 peptide (Li et al., 2010). This has resulted in 29 compounds, belonging to 10 different clusters, possessed measurable activity against the complex. Based on the inhibitory activity, drug likeness properties, and capability to synthesize, a compound (TRK5), belongs to cluster 9, was chosen as a medicinal chemistry starting point for designing and developing candidates that target the annexin A2-S100A10 interaction (Figure 1.12). Thus the 1-substituted 4-aroyl-3-hydroxy-5-phenyl-1H-pyrrol-2(5H)-one was the initial template to make multiple compounds that target complex formation (Reddy et al., 2011).

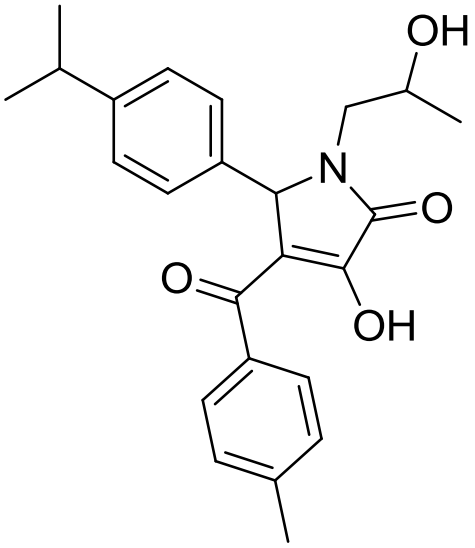


Figure 1.12: Structural formula of TRK5. Chemical formula of TRK5 is 3-hydroxy-1-(2-hydroxypropyl)-5-(4-isopropylphenyl)-4-(4-methylbenzoyl)-1H-pyrrol-2(5H)-one). The structure of TRK5 has been drawn by ChemBioDraw Ultra 12.0 software available at Nottingham University.

Measuring the inhibitory activity of TRK5 by FRET assay showed a potency of 14 μM against annexin A2-S100A10 interaction (Reddy et al., 2011). This finding has led to the synthesis of several novel analogues that were having a wide micro-molar range of inhibitory activity. All the compounds shared a common structural formula as seen in Figure 1.13 and differ accordingly to the substitution at R1, R2 and R3 and target inhibitory activity as shown in Table 1.5.

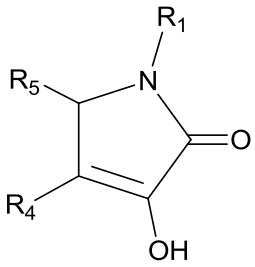


Figure 1.13: The template structural formula of the 1, 4 and 5 substituted pyrrol-2-one molecules.

Table 1.5: List of the inhibitors with their chemical formula and the IC_{50} of annexin A2-S100A10 inhibitory potency expressed in μM.

ID	IC_{50}(μM)	R1	R4	R5
TRK342	1.2	3-(1H-imidazol-1-yl)propyl	4-methylbenzoyl	3,5-bis(trifluoromethyl)phenyl
TRK370	2	2-methoxyethyl	4-methoxybenzoyl	3,5-bis(trifluoromethyl)phenyl
TRK371	2	2-methoxyethyl	4-methoxybenzoyl	3,5-bis(trifluoromethyl)phenyl
TRK330	2.4	2,3-dihydroxypropyl	4-methylbenzoyl	4-isopropylphenyl
TRK330	2.4	2,3-dihydroxypropyl	4-methylbenzoyl	4-isopropylphenyl
TRK407	2.5	2-hydroxypropyl	furan-2-carbonyl	3,5-bis(trifluoromethyl)phenyl
TRK355	2.6	4-(trifluoromethyl)phenyl	4-methylbenzoyl	4-isopropylphenyl
TRK416	2.8	2-hydroxypropyl	furan-2-carbonyl	4-isopropylphenyl
LW71	3	2-hydroxypropyl	4-chlorobenzoyl	4-isopropylphenyl
TRK106	3	3-methoxypropyl	4-methylbenzoyl	4-isopropylphenyl
TRK380	3	2-hydroxypropyl	4-methoxybenzoyl	3,5-bis(trifluoromethyl)phenyl
TRK412	3	butyl	furan-2-carbonyl	3,5-bis(trifluoromethyl)phenyl
TRK348	3.1	4-isopropylphenyl	4-methylbenzoyl	3,5-bis(trifluoromethyl)phenyl
TRK406	3.5	butyl	4-methylbenzoyl	3,5-bis(trifluoromethyl)phenyl
TRK347	3.7	4-(trifluoromethyl)phenyl	4-methylbenzoyl	3,5-bis(trifluoromethyl)phenyl

TRK381	3.9	3-(1H-imidazol-1-yl)propyl	4-methoxybenzoyl	3,5-bis(trifluoromethyl)phenyl
TRK317	4	2-hydroxypropyl	4-methylbenzoyl	3,5-bis(trifluoromethyl)phenyl
TRK336S	4	(S)-2-hydroxypropyl	4-methylbenzoyl	3,5-bis(trifluoromethyl)phenyl
TRK337R	4	(R)-2-hydroxypropyl	4-methylbenzoyl	3,5-bis(trifluoromethyl)phenyl
TRK60	4	2-hydroxypropyl	4-methylbenzoyl	3,5-bis(trifluoromethyl)phenyl
TRK372	4.6	allyl	4-methoxybenzoyl	3,5-bis(trifluoromethyl)phenyl
LW83	5	3-methoxypropyl	2-ethoxybenzoyl	3-fluoro-4-(trifluoromethyl)phenyl
TRK340	5	2,3-dihydroxypropyl	4-methylbenzoyl	3,5-bis(trifluoromethyl)phenyl
TRK340	5	2,3-dihydroxypropyl	4-methylbenzoyl	3,5-bis(trifluoromethyl)phenyl
TRK369	5	propyl	4-methoxybenzoyl	3,5-bis(trifluoromethyl)phenyl
TRK397	5.5	2-hydroxybutyl	4-methylbenzoyl	3,5-bis(trifluoromethyl)phenyl
TRK343	5.7	2-(piperazin-1-yl)ethyl	4-methylbenzoyl	3,5-bis(trifluoromethyl)phenyl
AA32	6	2-hydroxypropyl	4-methylbenzoyl	4-(trifluoromethyl)phenyl
LW53	6	allyl	4-chlorobenzoyl	4-(trifluoromethyl)phenyl
TRK100	6	allyl	4-methylbenzoyl	4-isopropylphenyl
TRK345	6.3	phenyl	4-methylbenzoyl	3,5-bis(trifluoromethyl)phenyl
TRK368	6.4	propyl	4-methoxybenzoyl	4-isopropylphenyl
TRK388	6.5	2-(1H-imidazol-1-yl)ethyl	4-methylbenzoyl	3,5-bis(trifluoromethyl)phenyl
TRK354	6.8	phenyl	4-methylbenzoyl	4-isopropylphenyl
TRK394	6.8	cyclopropylmethy	4-methylbenzoyl	3,5-bis(trifluoromethyl)phenyl
AA50	7	2-hydroxypropyl	3-methoxybenzoyl	4-isopropylphenyl
TRK61	7	2-hydroxypropyl	4-methylbenzoyl	3,5-dichlorophenyl
TRK86	7	2-hydroxypropyl	2-ethoxybenzoyl	4-isopropylphenyl
TRK404	7.8	2-hydroxypropyl	1-naphthoyl	3,5-bis(trifluoromethyl)phenyl
TRK103	8	2-methoxyethyl	4-methylbenzoyl	4-isopropylphenyl
TRK79	8	2-hydroxypropyl	4-methylbenzoyl	2,4-bis(trifluoromethyl)phenyl
TRK85	8	2-hydroxypropyl	4-methylbenzoyl	4-chloro-3-(trifluoromethyl)phenyl
TRK87	8	2-hydroxypropyl	4-methylbenzoyl	3-(trifluoromethyl)phenyl
TRK87RS	8	2-hydroxypropyl	4-methylbenzoyl	3-(trifluoromethyl)phenyl
TRK402	8.1	2-hydroxy-3-methylbutyl	4-methylbenzoyl	3,5-bis(trifluoromethyl)phenyl
TRK395	8.3	3-hydroxybutyl	4-methylbenzoyl	3,5-bis(trifluoromethyl)phenyl
TRK80	9	2-hydroxypropyl	4-methylbenzoyl	4-(trifluoromethoxy)phenyl
TRK405	10	2-methylpropanoic acid	4-methylbenzoyl	3,5-bis(trifluoromethyl)phenyl
LW85	11	3-methoxypropyl	2-ethoxybenzoyl	4-(trifluoromethyl)phenyl

TRK389	11	3-(1H-imidazol-1-yl)propyl	4-methylbenzoy	4-isopropylphenyl
TRK399	11	3-acetyl-4-hydroxyphenyl	4-methylbenzoyl	3,5-bis(trifluoromethyl)phenyl
TRK84	11	2-hydroxypropyl	4-methylbenzoyl	3-isopropylphenyl
TRK384	12	3-methoxypropyl	4-methylbenzoyl	3,5-bis(trifluoromethyl)phenyl
TRK387	12	allyl	4-methylbenzoyl	3,5-bis(trifluoromethyl)phenyl
TRK97	12	2-hydroxyethyl	4-methylbenzoyl	4-isopropylphenyl
TRK363	13	propyl	furan-2-carbonyl	4-ethylphenyl
AA16	14	2-hydroxypropyl	benzoyl	4-isopropylphenyl
TRK322	14	2-hydroxypropyl	4-methylbenzoyl	4-isopropylphenyl
TRK324S	14	(S)-2-hydroxypropyl	4-methylbenzoyl	4-isopropylphenyl
TRK325R	14	(R)-2-hydroxypropyl	4-methylbenzoyl	4-isopropylphenyl
TRK5	14	2-hydroxypropyl	4-methylbenzoyl	4-isopropylphenyl
AA30	16	2-hydroxypropyl	4-methylbenzoyl	4-ethylphenyl
TRK321	16	2-hydroxypropyl	acetyl	4-isopropylphenyl
TRK385	17	2-methoxyethyl	4-methylbenzoyl	3,5-bis(trifluoromethyl)phenyl
TRK81	18	2-hydroxypropyl	4-methylbenzoyl	4-propylphenyl
TRK373	21	2-hydroxyethyl	4-methoxybenzoyl	3,5-bis(trifluoromethyl)phenyl
LW13	28	allyl	6-methylnicotinoyl	4-(trifluoromethyl)phenyl
TRK62	28	2-hydroxypropyl	4-methylbenzoyl	4-(tert-butyl)phenyl
TRK359	30	propyl	furan-2-carbonyl	3,5-bis(trifluoromethyl)phenyl
TRK92	56	2-hydroxypropyl	4-cyanobenzoyl	4-isopropylphenyl
TRK362	67	propyl	furan-2-carbonyl	p-tolyl
TRK351	69	propyl	furan-2-carbonyl	4-isopropylphenyl
TRK353	69	propyl	furan-2-carbonyl	4-isopropylphenyl
TRK335	75	2-(piperazin-1-yl)ethyl	acetyl	4-isopropylphenyl
TRK57	79	2-hydroxypropyl	3-methylbenzoyl	4-isopropylphenyl
AA28	85	2-hydroxypropyl	4-methylbenzoyl	p-tolyl
TRK339	93	3-(1H-imidazol-1-yl)propyl	acetyl	4-isopropylphenyl
TRK65	105	2-hydroxypropyl	4-methylbenzoyl	3-chlorophenyl
TRK333	111	2-morpholinoethyl	acetyl	4-isopropylphenyl
TRK63	117	2-hydroxypropyl	4-methylbenzoyl	4-chlorophenyl
TRK64	128	2-hydroxypropyl	4-methylbenzoyl	naphthalen-2-yl
LW31	182	3-methoxypropyl	6-methylnicotinoyl	3-fluoro-4-(trifluoromethyl)phenyl

LW79	186	3-methoxypropyl	4-chlorobenzoyl	3-fluoro-4-(trifluoromethyl)phenyl
LW15	269	3-methoxypropyl	6-methylnicotinoyl)	4-(trifluoromethyl)phenyl
AA34	275	2-hydroxypropyl	4-methylbenzoyl	4-(dimethylamino)phenyl
TRK59	616	2-hydroxypropyl	4-methoxybenzoyl	4-isopropylphenyl
LW37	794	2-hydroxypropyl	6-methylnicotinoyl	4-isopropylphenyl
AA26	1000	2-hydroxypropyl	4-methylbenzoyl	phenyl
AA38	1000	2-hydroxypropyl	4-methylbenzoyl	4-hydroxyphenyl
LW73	1000	allyl	nicotinoyl	4-(trifluoromethyl)phenyl
LW75	1000	3-methoxypropyl	nicotinoyl	4-(trifluoromethyl)phenyl
TRK319	1000	2-hydroxypropyl	acetyl	3,5-bis(trifluoromethyl)phenyl
TRK334	1000	3-morpholinopropyl	acetyl	4-isopropylphenyl
TRK338	1000	2,3-dihydroxypropyl	acetyl	3,5-bis(trifluoromethyl)phenyl
TRK341	1000	2,3-dihydroxypropyl	acetyl	3,5-bis(trifluoromethyl)phenyl
TRK390	1000	2-(1H-imidazol-1-yl)ethyl	4-methylbenzoy	4-isopropylphenyl
TRK392	1000	2-(dimethylamino)ethyl	4-methylbenzoyl	3,5-bis(trifluoromethyl)phenyl
TRK413	1000	2-hydroxybutyl	furan-2-carbonyl	3,5-bis(trifluoromethyl)phenyl
TRK414	1000	2-(1H-imidazol-1-yl)ethyl	furan-2-carbonyl	3,5-bis(trifluoromethyl)phenyl
TRK415	1000	3-(1H-imidazol-1-yl)propyl	furan-2-carbonyl	3,5-bis(trifluoromethyl)phenyl
TRK82	1000	2-hydroxypropyl	4-methylbenzoyl	isopropyl

Analysis of the interaction between annexin A2 N-terminus and S100A10 protein shows that the annexin A2 recognition site of S100A10 is a comparatively compact, hydrophobic, and concave binding pocket composed of residues from both S100A10 molecules of dimer. The pocket can be classified into three sites (two hydrophobic regions H1, H2, and one somewhat hydrophilic H3) (Figure 1.14A). As shown in (Figure 1.14C), the 4-isopropylphenyl moiety occupies the H1 site and possibly forms hydrophobic interaction, whereas the 2-hydroxypropyl group binds to the H2

site. The methyl group of the 2-hydroxypropyl substituent undergoes a CH-π stacking interaction with the phenyl ring of Phe41. The hydroxyl moiety donates a strong hydrogen bond to the carboxylate oxygen of Glu5. In addition, the 4-methylbenzoyl group is positioned in the H3 site. From the above analysis of the binding poses, it appears that the two hydrophobic regions (H1 and H2) play a dominant role in the binding affinity of all of the inhibitors. The proposed hydrogen bond formation of either or both of the Glu5 and the Glu9 receptor residues with the inhibitors TRK5 appear to mimic the hydrogen bond interaction of Glu5 and Glu9 residues with the annexin A2 N-terminal peptide in the crystal structure (Figure 1.14B). Overall, in view of the chemical nature of the inhibitor compounds analysed and the nature of the interactions with the binding pocket, it appears that the hydrogen bond acceptor sites of Glu5 and Glu9 and the two hydrophobic regions (H1 and H2) of the receptor could be considered as the key pharmacophoric features as shown in Figure 1.14.

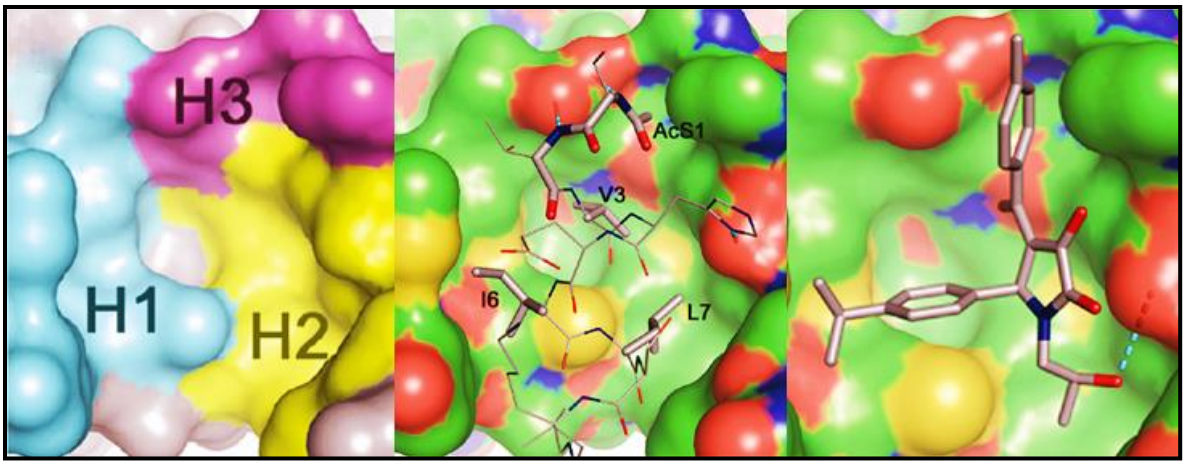


Figure 1.14: Structure-based design of annexin A2-S100A10 inhibitors. A, the hydrophobic H1 (cyan), H2 (yellow) and hydrophilic H3 (magenta) are subsites of the S100A10 binding pocket. B, the interaction between the N-terminal annexin A2 peptide (grey CPK stick models) and the binding pocket of S100A10 (green CPK surface). C, the predicted binding poses of verified virtual screening hits of TRK5 (grey CPK stick models) with binding pocket of S100A10 (green CPK surface). Copied and modified from (Reddy et al., 2011).

Thus, above work identified a novel class of chemical probes (inhibitors) suitable for functional exploration of annexin A2-S100A10 interaction and could be used as potential lead molecules for further development as pancreatic cancer drugs. Ultimately these molecules might provide us with the information to initiate a lead optimization programme for the generation of new classes of drugs that targeting pancreatic cancer development and progression.

1.8. Aim and Objectives

The major goal of this study is to investigate the functional properties of annexin A2-S100A10 complex in pancreatic cancer cells using annexin A2-S100A10 inhibitors that have been recently developed.

As indicated above, several studies have linked the progression of pancreatic cancer, chemo-resistance to gemcitabine and most importantly migration, adhesion and metastasis to the expression of annexin A2 and/or S100A10. Moreover silencing of annexin A2 or S100A10 expression appeared to be effective in reversing many of these phenotypic behaviours. However, nearly all of these studies were done on individual proteins and very little is known about the effect of annexin A2-S100A10 complex formation on these behaviours. In fact, hardly anything is known about the impact of the annexin A2-S10010 complex formation on oncogenesis and metastasis of pancreatic cancer cells.

A hypothesis has been made that S100A10 protein affects pancreatic cancer by interacting with its binding partner annexin A2 protein. The pyrrol-2-ones molecules (annexin A2-S100A10 inhibitors) represent unique tools to address this hypothesis. This would validate the importance of annexin A2-S100A10 interaction as a potential therapeutic target and provide useful information for further development of second generation inhibitors for the treatment of pancreatic cancer.

Therefore, the general aim of this PhD was to study the contribution of annexin A2-S100A10 complex inhibition on the following:

1. Pancreatic cancer cells survival and apoptosis.
2. Pancreatic cancer cells resistant to gemcitabine treatment.
3. Pancreatic cancer cells invasion into cellular matrix; assess surface protease activity.
4. Pancreatic cancer cells adhesion to endothelial cells.

CHAPTER 2

2. DEPENDENCE OF PANCREATIC CANCER CELLS VIABILITY ON ANNEXIN A2 EXPRESSION AND THE SAR OF ANNEXIN A2-S100A10 INHIBITORS

2.1. Introduction

Annexin A2 overexpression was found to be linked to cell proliferation and growth of pancreatic cancer cells (Vishwanatha et al., 1993). In a recent report, annexin A2 upregulation was correlated with survival of pancreatic cancer cells (Wang and Lin, 2014). Annexin A2 has been found to act as an anti-oxidant protecting a cell from reactive oxygen species (Madureira et al., 2011a). Increased level of ROS leads to DNA damage, lipid peroxidation and irreversible protein damage that eventually result in apoptosis and cell death (Brandes et al., 2009). Indeed protein oxidation of liver and lung tissue was elevated in annexin A2–null mice compared to wild-type mice (Madureira et al., 2011a). Recent data suggested that annexin A2 promotes the cell cycle and cell proliferation of lung cancer cells partly through a p53 dependent mechanism (Wang et al., 2012a). These data imply that the relative amount of intracellular annexin A2 may determine the ability of the cells to survive or undergo apoptosis.

Silencing of annexin A2 expression causes parallel decrease in the levels of S100A10 proteins and it was associated with reduced proliferation of breast

cancer cells (Zhang et al., 2010a). Moreover, there is an autostability balance between annexin A2 and S100A10 and once this balance is altered by tumour suppressor protein DLC1, which competes with annexin A2 for S100A10 binding, there was a decrease in tumourigenicity of lung cancer cells (Yang et al., 2011). Therefore, a dysregulated S100A10 protein level is also linked with the process of oncogenesis.

The relative amount of annexin A2 monomer to the heterotetramer (annexin A2 and S100A10 complex) varies according to the cell type from an estimated 100% heterotetramer in intestinal epithelial cells to about 50% in cultured fibroblasts (Eberhard et al., 2001). This suggested that, a significant amount of the annexin A2 may exist in the form of the heterotetramer (annexin A2-S100A10 complex) which if disrupted could lead to a change in annexin A2 protein levels and interference with its pathway eventually resulting in cell survival modulation.

Taken together all these observations, it might be hypothesized that inhibiting intracellular interaction between annexin A2 and S100A10 would affect pancreatic cancer cells survival by modulating the relative amount of annexin A2 and/or S100A10 inside pancreatic cancer cells.

Annexin A2-S100A10 inhibitors that have been recently developed showed a wide range of activity against annexin A2-S100A10 complex formation as seen in Table 1.5. Therefore, it was assessed if there is a correlation

between the capability of these inhibitors to disrupt the annexin A2-S100A10 complex and their cellular activity against pancreatic cancer cells.

2.2. Aim and objectives

Based on the observations mentioned earlier, it has been hypothesized that inhibiting the intracellular annexin A2-S100A10 interaction in pancreatic cancer cells might affect cell viability and would help understanding the involvement of the annexin A2-S100A10 complex in the oncogenesis of pancreatic cancer cells. It would also allow rationalizing and classifying annexin A2-S100A10 inhibitors according to their target inhibitory activity and intracellular activity. Therefore, the aim was to study the effect of annexin A2-S100A10 inhibitors on pancreatic cancer cell viability in correlation with their target inhibitory activity and chemical structures.

The main objectives of this chapter were to address the following:

1. How do pancreatic cancer cells behave when treated with annexin A2-S100A10 inhibitors?
2. Is the cellular activity of annexin A2-S100A10 inhibitors correlated with the target inhibitory activity?
3. Are the intracellular annexin A2 protein levels involved in the cellular activity of annexin A2-S100A10 inhibitors?
4. Are the chemical structures of annexin A2-S100A10 inhibitors related to the target activity and intracellular activity?

2.3. Results and discussion

2.3.1. Cell viability study of annexin A2-S100A10 inhibitors

2.3.2. Screening the effect of annexin A2-S100A10 inhibitors on the survival of PANC-1, MIA PACA-2 and HMEC-1 cell lines

In this section the aim was to have a full overview of the activity of annexin A2-S100A10 inhibitors against PANC-1, MIA PACA-2 and HMEC-1 cells. PANC-1 and MIA PACA-2 cells were chosen because they are pancreatic cancer cell lines and they have been shown to express annexin A2 at different levels (Takano et al., 2008). HMEC-1 cells were chosen to assess the effect of annexin A2-S100A10 inhibitors on normal non-cancer cells and unpublished data from Dekker group noted a higher expression of annexin A2 than in MIA PACA-2 cells. Thus it would be possible to correlate the expression of annexin A2 with the cellular activity of these molecules in PANC-1, MIA PACA-2 and HMEC-1 cells.

2.3.2.1. Measuring the effect of dimethyl sulfoxide (DMSO) on pancreatic cancer cell viability

The top stock concentration of annexin A2-S100A10 inhibitors was 5 mM in 99.9% DMSO. It was necessary to estimate whether the DMSO has an anti-proliferative effect on pancreatic cancer cells and to measure the maximum tolerated dose to exclude any effect other than that of the inhibitors themselves.

Cells were plated at a density of 3×10^3 cell per well. The following day, the cells were treated with serial concentrations of DMSO ranging from 9.99 to 1% (1.27 to 0.127 M). 72 h later, the cells were subjected to an MTT survival assay (refer to 6.2.4 for more details).

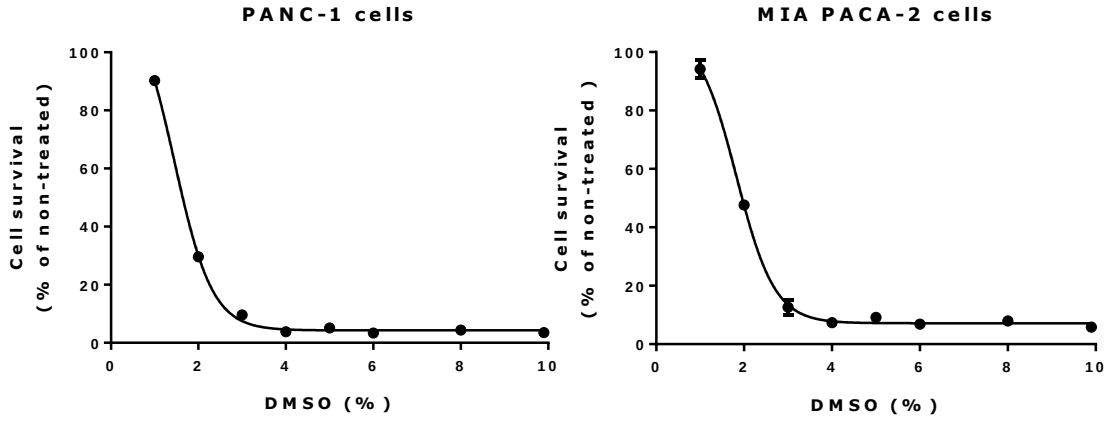


Figure 2.1: Effects of DMSO serial concentrations on the survival of PANC-1 and MIA PACA-2 cancer cells. Data are expressed as mean ± SEM (n = 3).

As seen in Figure 2.1, there is a dose dependent anti-proliferative activity of DMSO on PANC-1 cells and MIA PACA-2 cells. In PANC-1 cells, 1% DMSO causes a reduction in cell viability up to 9% (90.2 ± 0.96% cell survival) whereas in MIA PACA-2 cells, it causes a reduction up to 5% (94.2 ± 1.8% cell survival). Therefore the DMSO percentage in annexin A2-S100A10 inhibitors solutions should be taken into account.

Other studies also refer to DMSO as affecting cell survival. For example DMSO at 2.5% induced apoptosis in mouse lymphoma cells due to decrease in Bcl-2, decline in mitochondrial membrane potential, release of cytochrome c and subsequently activation of caspases 9 and 3 (Liu et al., 2001). DMSO at concentrations of 2.5-7.5 mol% is able to decrease the membrane thickness and at 10-20 mol% it induces formation of transient water pores and it destroys lipid bilayer at higher concentrations (Gurtovenko and Anwar, 2007).

2.3.2.2. Measuring the effect of annexin A2-S100A10 inhibitors on cell viability

Based on the previous result, the top maximum concentration of DMSO that could be tolerated to some extent by the cells was 1% which (given the stock concentration of annexin A2-S100A10 inhibitors 5 mM 100% DMSO) is corresponding to a 50 µM concentration of annexin A2-S100A10 inhibitors. Therefore treatment of the cells with annexin A2-S100A10 inhibitors has been done at 50 µM 1% DMSO.

Cells were plated at a density of 3×10^3 cell per well. The following day, the cells were treated with annexin A2-S100A10 inhibitors at 50 µM 1% DMSO concentration. 72 h later, the cells were subjected to an MTT assay (refer to 6.2.4 for more details).

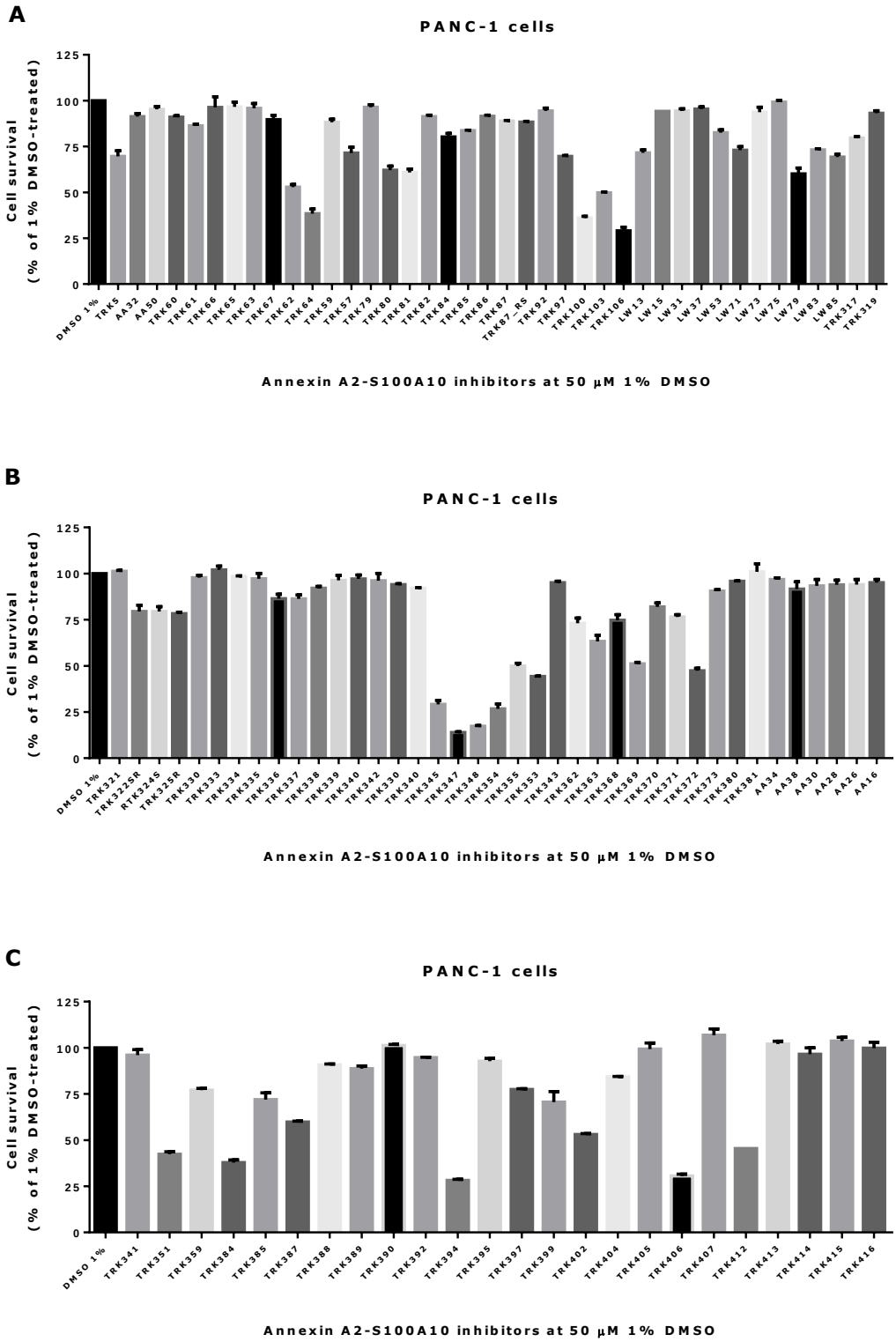


Figure 2.2: The effect of annexin A2-S100A10 inhibitors at 50 µM 1% DMSO on the survival percentage of PANC-1 cells as measured using an MTT assay. A representation of single experiment is shown. Data are expressed as mean ± SEM (n = 4).

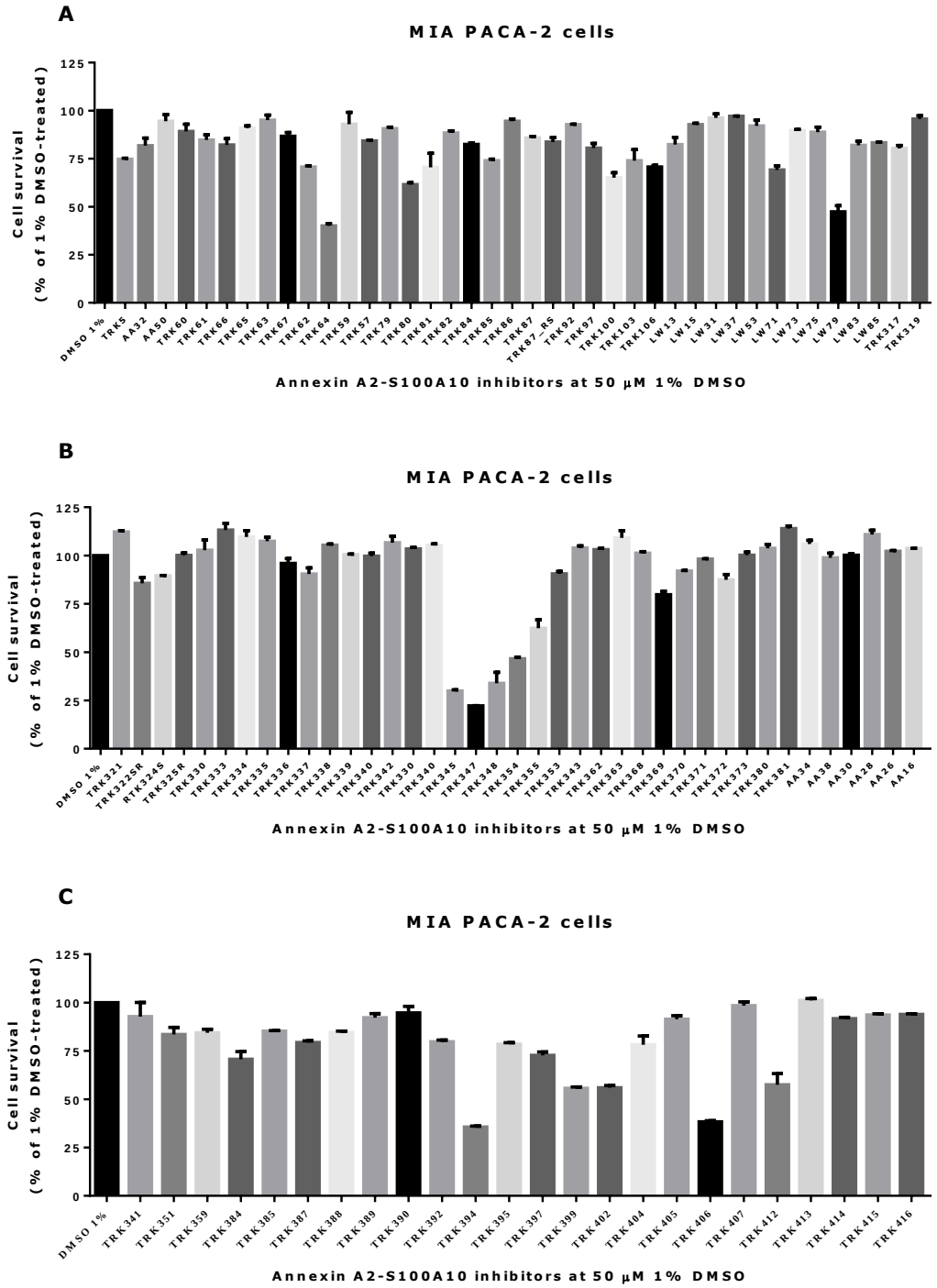


Figure 2.3: The effect of annexin A2-S100A10 inhibitors at 50 µM 1% DMSO on the survival percentage of MIA PACA-2 cells as measured using an MTT assay. A representation of single experiment is shown. Data are expressed as mean ± SEM (n = 4).

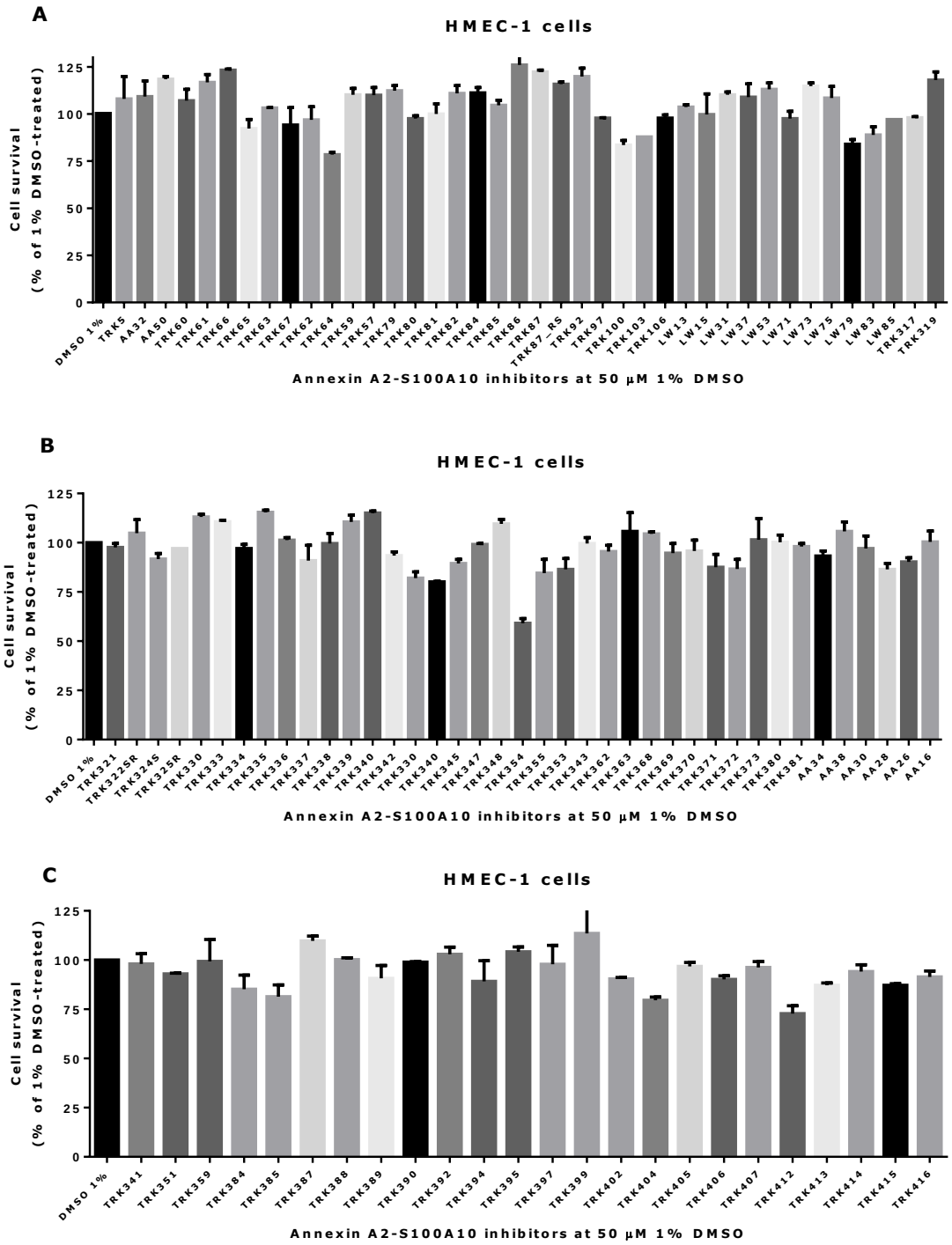


Figure 2.4: The effect of annexin A2-S100A10 inhibitors at 50 µM 1% DMSO on the survival percentage of HMEC-1 cells as measured using an MTT assay. A representation of single experiment is shown. Data are expressed as mean ± SEM (n = 2).

As shown in Figures 2.2, 2.3 and 2.4, there was a wide range of responses to annexin A2-S100A10 inhibitors treatment, both within a cell line and between the cell lines. These results revealed a difference in the target activity of annexin A2-S100A10 inhibitors and maybe in the annexin A2 protein levels between the three cell lines.

Annexin A2-S100A10 inhibitors that inhibited cell survival by more than 50% (measured using MTT assay) were rescreened to obtain their IC_{50}s. Since there were no inhibitors inhibited more than 50% in HMEC-1 cells IC_{50}s were obtained from PANC-1 and MIA PACA-2 cells only.

2.3.2.3. IC_{50}s of annexin A2-S100A10 inhibitors in PANC-1 and MIA PACA-2 cells

In this section the aim was to assess the effect of serial concentrations of the more potent anti-proliferative annexin A2-S100A10 inhibitors on the viability of PANC-1 and MIA PACA-2 cells. Thus the IC_{50}s of TRK64, LW79, TRK345, TRK347, TRK348, TRK354, TRK394, and TRK406 in PANC-1 and MIA PACA-2 cells were obtained.

Cells were plated at a density of 3×10^3 cell per well. The following day, the cells were treated with the potent anti-proliferative annexin A2-S100A10 inhibitors at serial concentrations ranging from (50 to 0.0005 μM 1% DMSO). 72 h later, the cells were subjected to an MTT assay (refer to 6.2.4 for more details) as seen in Figures 2.5 and 2.6 and Table 2.1.

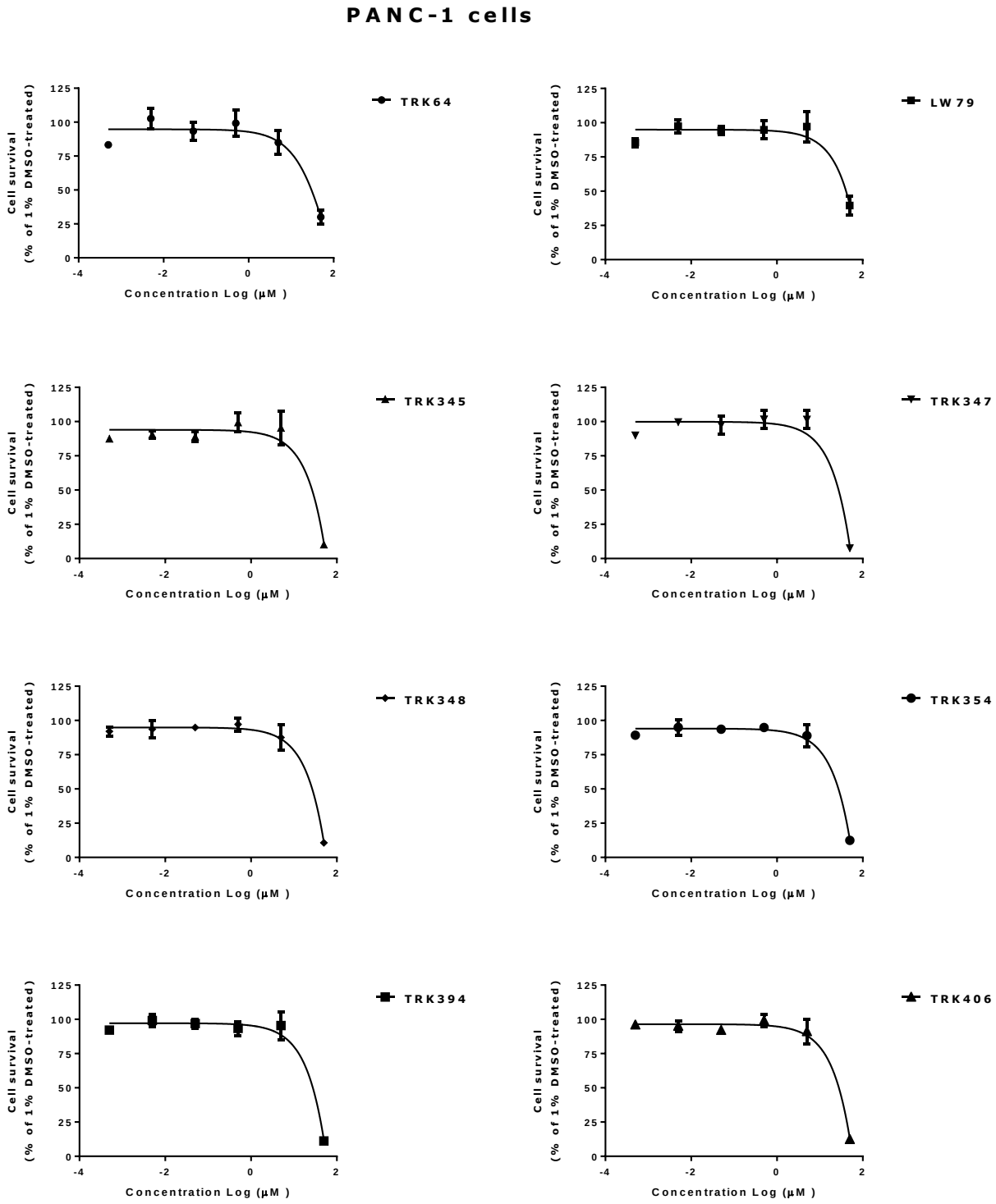


Figure 2.5: The effect of potent annexin A2-S100A10 inhibitors serial concentrations on the survival of PANC-1 cells as measured using an MTT assay. Data are expressed as mean ± SEM (n = 4).

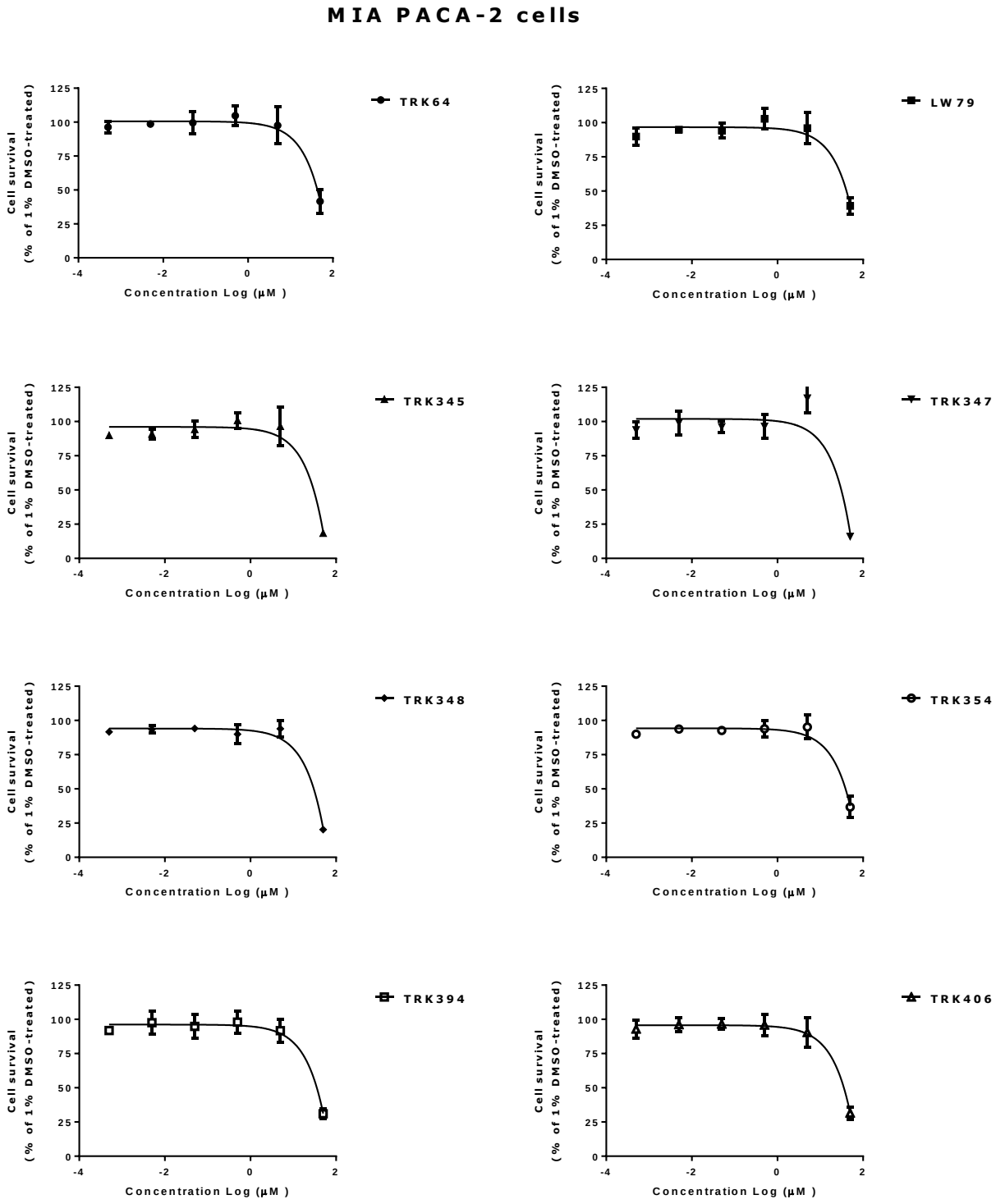


Figure 2.6: The effect of potent annexin A2-S100A10 inhibitors serial concentrations on the survival of MIA PACA-2 cells as measured using an MTT assay. Data are expressed as mean ± SEM (n = 4).

Table 2.1: The IC_{50}s of potent annexin A2-S100A10 inhibitors in PANC-1 and MIA PACA-2 cells as measured using an MTT assay.

IC_{50} of potent annexin A2-S100A10 inhibitors expressed in µM		
ID	**PANC-1 cells**	**MIA PACA-2 cells**
TRK64	23.36	41.23
LW79	37.69	37.18
TRK345	17.57	21.46
TRK347	18.64	26.81
TRK348	15.23	20.80
TRK354	16.12	33.65
TRK394	17.69	27.08
TRK406	16.97	26.76

Figures 2.5 and 2.6 show that, concentrations from 0.0005 to 5 µM the chosen inhibitors did not inhibit PANC-1 and MIA PACA-2 cell survival. However at 50 µM concentration these inhibitors inhibited the survival of PANC-1 and MIA PACA-2 cells by more than 50%. Thus 50 µM might be the optimal concentration for these inhibitors to inhibit the interaction between annexin A2-S100A10 complex in a cell system.

Comparing the IC_{50}s of these inhibitors in PANC-1 and MIA PACA-2 cells indicated a higher anti-proliferative activity of these inhibitors (all but LW79) in PANC-1 cells than in MIA PACA-2 cells as shown in Table 2.1. This might

implicate a difference in the relative amount of the annexin A2 in these two cell lines. Indeed Takano et al., have shown a higher expression of annexin A2 in MIA PACA-2 cells than in PANC-1 cells (Takano et al., 2008). HMEC-1 cells as mentioned in section 2.3.2 showed a higher expression of annexin A2 than MIA PACA-2 cells (unpublished data from Dekker group) and in Figure 2.4 they did not show a significant response to annexin A2-S100A10 inhibitors. This further reinforces the hypothesis that annexin A2 expression levels are somehow related to the anti-proliferative activity of these inhibitors.

Therefore, the next aim was to compare the relation between the anti-proliferative activity of these inhibitors with the expression of annexin A2 and target inhibitory activity of annexin A2-S100A10 inhibitors in the three cell lines (PANC-1, MIA PACA-2 and HMEC-1 cells). All annexin A2-S100A10 inhibitors have been screened before for inhibition of the primary target using a competitive binding assay based on fluorescence resonance energy transfer (FRET) between a Cy5 labelled S100A10 and a Cy3 labelled N-terminal annexin A2 peptide. This has yielded the IC_{50} values of the inhibitory activity against annexin A2-S100A10 complex as mentioned before and shown in Table 1.5.

2.3.3. Correlating annexin A2-S100A10 inhibitors target activity with anti-proliferative activity; dependence on annexin A2 expression levels

Measuring the expressions of annexin A2 in PANC-1, MIA PACA-2 and HMEC-1 cells was done by seeding these cells in 10 cm^2 dishes. The following day, media was aspirated and fresh media was added to the attached cells. Two days later, cells were harvested and proteins extracted from the cells were subjected to electrophoresis and immunoblotting (refer to 6.2.14 for more details).

For each cell line (PANC-1, MIA PACA-2 and HMEC-1 cells), the observed annexin A2-S100A10 inhibitor anti-proliferative effect measured using MTT assay was plotted against the known target inhibitory activity measured by FRET assay (Table 1.5) and correlated with annexin A2 expression as shown in Figure 2.7A, B, and C.

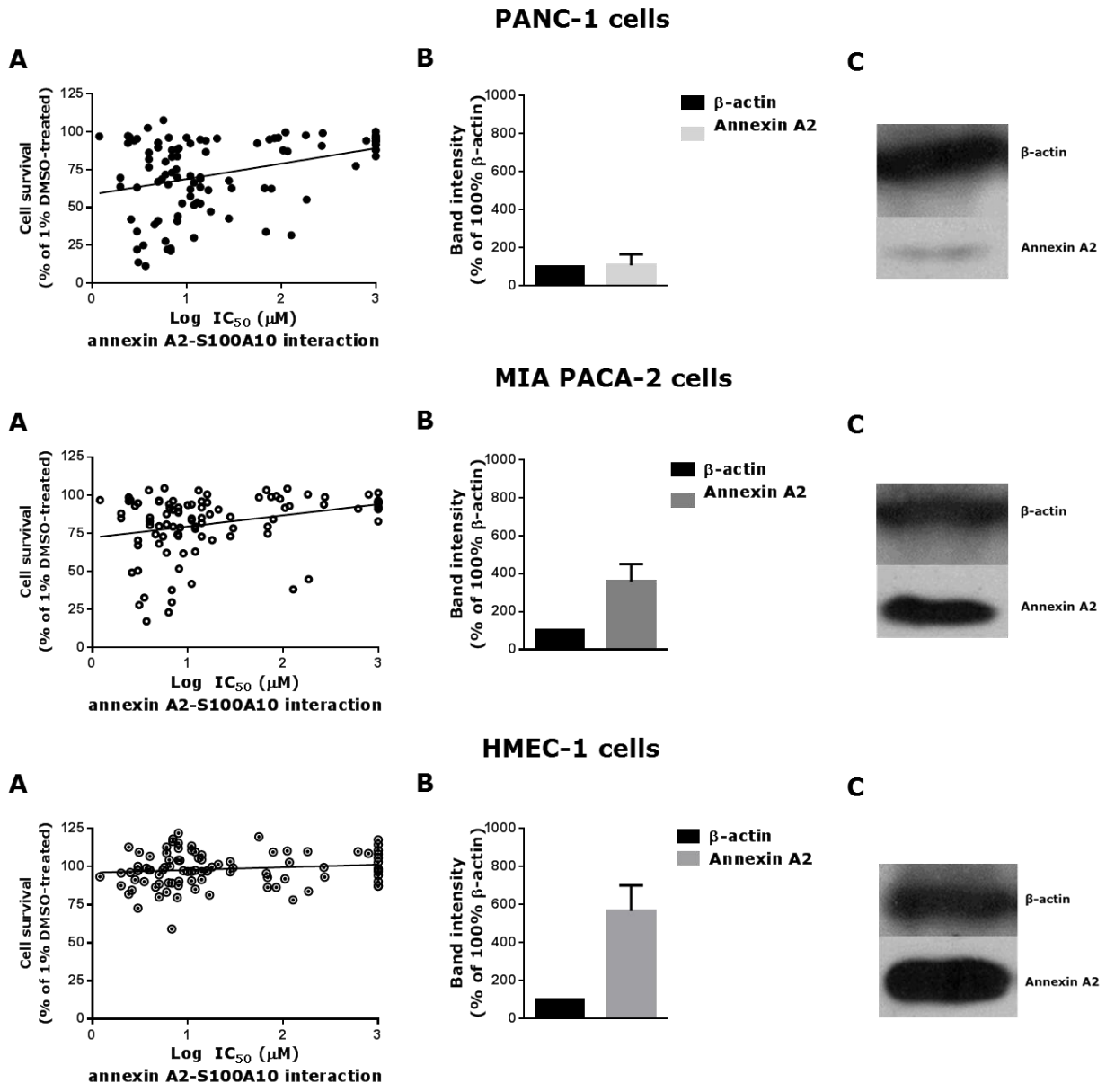


Figure 2.7: (A) Correlation between cell survival percentage (anti-proliferative effect) and the target inhibitory activity of annexin A2-S100A10 inhibitors in PANC-1, MIA PACA-2 and HMEC-1 cells. A correlation plot was obtained by linear regression. (B) Quantification of annexin A2 expression in PANC-1, MIA PACA-2 and HMEC-1 cells. The bands were corrected to 100% β-actin. (C) Western blot analysis

of annexin A2 expression in PANC-1, MIA PACA-2 and HMEC-1 cells. β-actin has been used as a loading control.

In order to estimate if there is a relationship between the anti-proliferative activity and target potency of annexin A2-S100A10 inhibitors, a linear regression analysis was done on the three cell lines (PANC-1, MIA PACA-2 and HMEC-1 cells). This has revealed a significant relationship (the slop of the linear regression was significantly deviated from zero) between the anti-proliferative activity and target inhibitory activity of annexin A2-S100A10 inhibitors in PANC-1 (P = 0.0002) and MIA PACA-2 (P = 0.001) but not in HMEC-1 (P = 0.2) cells. This result indicates that the anti-proliferative activity of annexin A2-S100A10 inhibitors might be explained by their target inhibitory activity in PANC-1 and MIA PACA-2 cells but not in HMEC-1 cells.

The strength and the direction of the correlations between the anti-proliferative activity and target inhibitory activity of annexin A2-S100A10 inhibitors in PANC-1 and MIA PACA-2 cells was done using correlation coefficient (Pearson r). The strength and direction of correlation (Pearson r) was assessed according to Cohen (1992) guidelines for the interpretation of a correlation coefficient as shown in table 2.2.

Table 2.2: Correlation coefficient values for interpreting the strength and direction of a relationship between two variables according (Cohen, 1992).

Size of correlation	interpretation
0.90 to 1.0 (-0.90 to -1.00)	Very strong positive (negative) correlation
0.50 to 0.90 (-0.50 to -0.90)	Strong positive (negative) correlation
0.30 to 0.50 (-0.30 to -0.50)	Moderate positive (negative) correlation
0.10 to 0.30 (-0.10 to -0.30)	Weak positive (negative) correlation
0.00 to 0.10 (0.00 to -0.10)	Negligible correlation

Measurement of the correlation coefficient in PANC-1 and MIA PACA-2 cells yielded a Pearson r of 0.36 and 0.32 respectively. Thus according to the above table a positive moderate correlation between the anti-proliferative activity and the target inhibitory activity of annexin A2-S100A10 inhibitors existed in PANC-1 and MIA PACA-2 cells. As the target inhibitory activity of annexin A2-S100A10 inhibitors increases, there is a probability that their anti-proliferative activity also increases.

As shown before (Figure 2.7), PANC-1 cells showed the lowest expression of annexin A2 followed by MIA PACA-2 then HMEC-1 cells. Linking these results with the anti-proliferative activity of annexin A2-S100A10 inhibitors in the three cell lines suggested that the expression levels of annexin A2 may be a factor for these inhibitors to inhibit the cell survival rate. And as the relative amount of annexin A2 (monomeric or tetrameric form) in a cell increases,

the ability of these inhibitors to inhibit the annexin A2-S100A10 complex appears to decrease therefore their anti-proliferative activity decreases. A decreased ability of pancreatic cancer cells to proliferate after blocking of the interaction between annexin A2 and S100A10 appears to be in line with published data mentioning that blocking of the interaction between annexin A2 and S100A10 inhibited the proliferation of lung cancer cells (Yang et al., 2011).

In this section a conclusion could thus be drawn that these inhibitors affect the cell survival of PANC-1 and MIA PACA-2 cells through an annexin A2 dependent mechanism.

In PANC-1 cells there was a significant relationship between the anti-proliferative activity and the target activity of annexin A2-S100A10 inhibitors with Pearson r of 0.36 which has been related to the lowest expression of annexin A2 levels among the three cell lines. Therefore the next step was to compare the effect of a potent annexin A2-S100A10 inhibitor and a non-potent annexin A2-S100A10 inhibitor on the expression of annexin A2 in PANC-1 cells.

2.3.3.1. Effect of an active (TRK317) and inactive (LW37) target inhibitors on the expression of annexin A2 in PANC-1 cells

Based on the result in Figure 2.7, it was hypothesized that annexin A2-S100A10 inhibitors might have affected the cell survival by modulating expression of annexin A2 as a result of interfering with annexin A2-S100A10 interaction inside the cell. Therefore, TRK317, an active annexin A2-S100A10 inhibitor (Table 1.5) with a moderate anti-proliferative activity (Figure 2.2), and LW37, an inactive chemotype annexin A2-S100A10 inhibitor (Table 1.5) with insignificant anti-proliferative activity (Figure 2.2), were selected to assess their effects on PANC-1 cells annexin A2 expression (refer to 6.2.14 for experimental methodology) as shown in Figure 2.8.

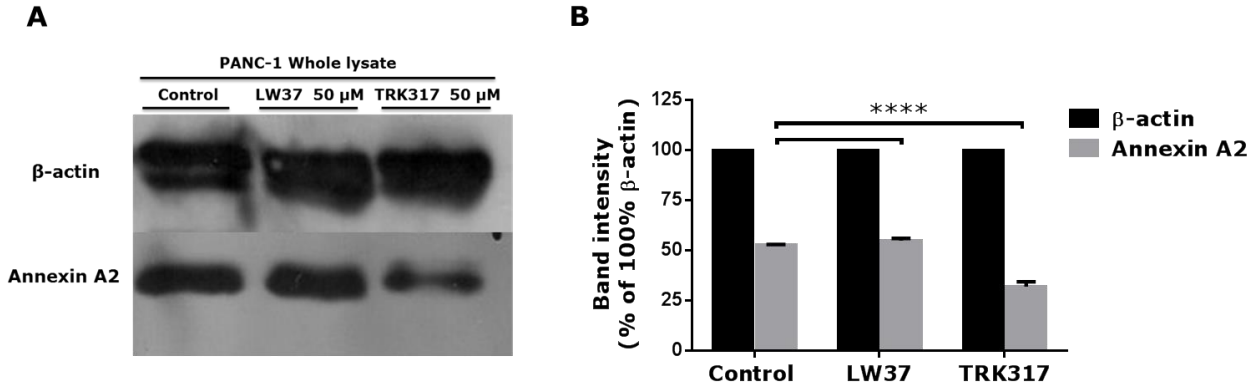


Figure 2.8: Annexin A2 expression in PANC-1 cells. (A) Annexin A2 levels in non-treated control, pretreatment with LW37 50 µM or with TRK317 50 µM. (B) Quantification of annexin A2 expression in non-treated control, treatment with

LW37 50 μM or with TRK317 50 μM in PANC-1. The bands were corrected to 100% β-actin. β-actin has been used as a loading control.

As seen in Figure 2.8, annexin A2 expression in PANC-1 cells was significantly ($P < 0.05$) downregulated after treatment with TRK317 50 μM, but not ($P > 0.05$) when the cells pre-treated with LW37 50 μM, both as compared with non-treated control. This might explain the possible mechanism by which annexin A2-S100A10 inhibitors inhibited PANC-1 cells survival. Potent (TRK317) but not impotent (LW37) annexin A2-S100A10 inhibitors interfered with annexin A2-S100A10 complex formation that could have led to a change in the expression levels of annexin A2 and maybe S100A10 inside the cells. Therefore their relative amount might have been altered resulting in modulation of PANC-1 cells viability.

A reduced PANC-1 cells viability after treatment with annexin A2-S100A10 inhibitor (TRK317) as a result of downregulation of annexin A2 expression appears to be in line with the observations noted a decrease in cell proliferation after silencing of annexin A2 expression (Zhang et al., 2013, Takano et al., 2008, Zhang et al., 2010a). It is also consistent with published data mentioning an inhibition in lung cancer cell proliferation due to blockade of annexin A2-S100A10 interaction by a tumour suppressor protein DLC1, though the authors related this inhibition to a downregulation in S100A10 expression (Yang et al., 2011).

This section has further reinforced the hypothesis that inhibiting the interaction between annexin A2 and S100A10 would modulate the relative amount of annexin A2 leading to a change in the survival of the PANC-1 cells as seen in Figure 2.9.

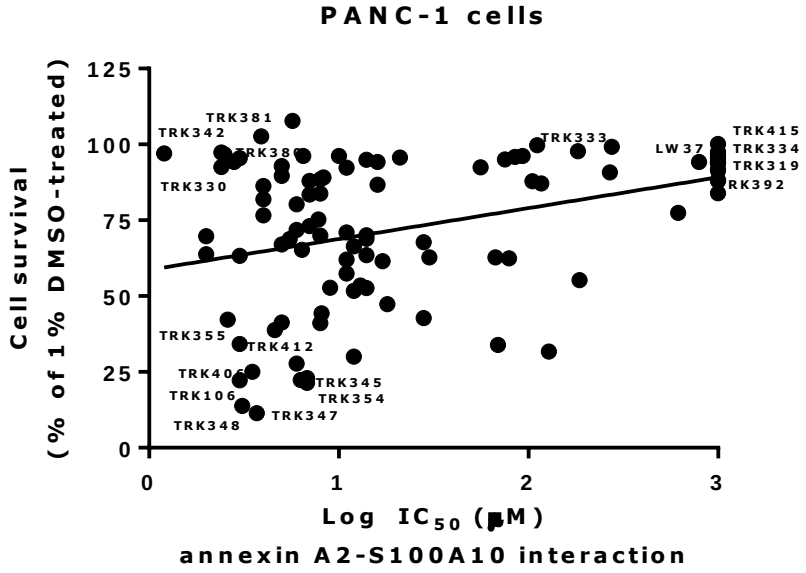


Figure 2.9: Correlation between cell survival percentage (anti-proliferative activity) and the target inhibitory activity of annexin A2-S100A10 inhibitors in PANC-1 cells.

Applying this hypothesis on Figure 2.9 reveals a consistency in correlating the anti-proliferative activity with target inhibitory activity of annexin A2-S100A10 inhibitors. For instance TRK347, TRK345, TRK354 and TRK406 all had target inhibitory activity of 3.7, 6.3, 6.8 and 3.5 μM (Table 1.5) respectively and at the same time they inhibited more than 75% of PANC-1 cell viability (Figure 2.9 lower left side). Moreover, LW37, TRK333, TRK334 and TRK319 all were inactive in terms of target inhibitory activity (Table 1.5)

and they showed insignificant anti-proliferative activity (less than 5%) to PANC-1 cells (Figure 2.9 upper right side). However, a number of annexin A2-S100A10 inhibitors did not follow this pattern. Amongst these inhibitors was TRK342. This inhibitor had the most potent target inhibitory activity (1.2 μM) (Table 1.5), but it had insignificant anti-proliferative activity against PANC-1 cells (less than 3%; Figure 2.9 upper left side). In fact, when this inhibitor and its analogues (TRK389, TRK380, TRK381 and TRK388 inhibitors) (Potent target inhibitory but insignificant anti-proliferative activity) have been removed from the scatterplot of PANC-1 cells (Figure 2.9 upper right side), the strength of correlation (Pearson r) between the anti-proliferative activity and target inhibitory activity of annexin A2-S100A10 inhibitors increased from 0.36 to 0.61 (moderate positive to strong positive correlation) as seen in Figure 2.10.

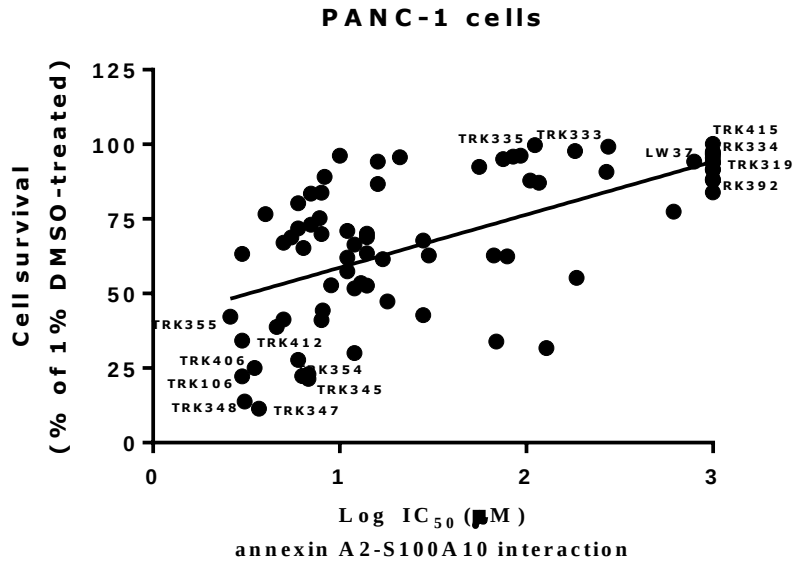


Figure 2.10: Correlation between cell survival percentage (anti-proliferative activity) and the target inhibitory activity of potent and impotent annexin A2-S100A10 inhibitors in PANC-1 cells.

Figure 2.10, shows that the strength of correlation coefficient increased from moderate positive to strong positive correlation as shown in Table 2.2 after removal of annexin A2-S100A10 inhibitors with potent target inhibitory but insignificant anti-proliferative activity. Therefore a further investigation was required to understand the reasons for this observation.

It has been shown in Figure 2.8 that pre-treatment of PANC-1 cells with a potent annexin A2-S100A10 inhibitor resulted in a downregulation of annexin A2 expression as compared with non-treated control. Thus it was predicted that pre-treatment of PANC-1 cells with more potent annexin A2-S100A10 inhibitor (TRK342) would result in a downregulation in annexin A2

expression as compared with non-treated control. Therefore the aim was next to assess the expression of annexin A2 in PANC-1 cells pre-treated with TRK342.

2.3.3.2. Effect of TRK342 treatment on the expression of annexin A2 in PANC-1 cells

It has been shown in the last section that inhibiting annexin A2-S100A10 interaction would result in a downregulation of annexin A2 that might have led eventually to a decrease in the survival of PANC-1 cells. However, there were potent inhibitors that did not follow this pattern (not showing anti-proliferative activity). Therefore, the aim was in this section to assess the effect of TRK342 pre-treatment on the expression of annexin A2 in PANC-1 cells.

Measuring the expressions of annexin A2 after treatment with TRK342 was done by seeding PANC-1 cells in 10 cm^2 dishes. The following day, media was aspirated and fresh media containing TRK342 50 μM was added to the attached cells. Two days later, cells were harvested and proteins extracted from the cells were subjected to electrophoresis and immunoblotting (refer to 6.2.14 for more details) as seen in Figure 2.11.

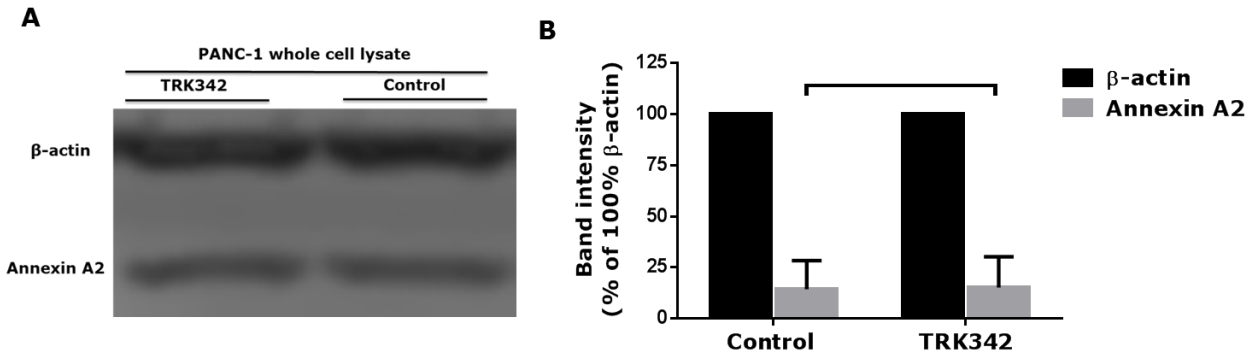


Figure 2.11: Annexin A2 expressions in PANC-1 cells. (A) Annexin A2 levels in non-treated control, pre-treatment with TRK342 50 μM. (B) Quantification of annexin A2 expression in non-treated control, treatment with TRK342 50 μM in PANC-1. The bands were corrected to 100% β-actin. β-actin has been used as a loading control.

Figure 2.11 shows that pre-treatment of PANC-1 cells with the most potent annexin A2-S100A10 inhibitor (TRK342) did not change the expression of annexin A2 as compared with non-treated control ($P > 0.05$) (two-way ANOVA). This result was not in agreement with the result in Figure 2.8 as there was a downregulation in annexin A2 expression after treatment with the inhibitor TRK317. Therefore it was hypothesized that TRK342 may not be able to pass through the cell membrane and inhibit the intracellular annexin A2-S100A10 complex. Unpublished data from our group using co-immunoprecipitation assays suggested this as well. TRK342 could not inhibit the protein interaction between S100A10 and annexin A2 when the inhibitor was incubated with intact cells prior to extraction for immunoprecipitation, but it could inhibit the protein interaction when it was incubated directly with an extracted complex prior to immunoprecipitation. This observation with

the result in Figure 2.11 indicates that TRK342 and its structural analogues might have not inhibited the proliferation of PANC-1 cells because they were not able to pass through the cell membrane. However, further analysis of these inhibitors in terms of physiochemical properties would be required to support this conclusion.

2.4. Relationship between annexin A2-S100A10 inhibitors structure and their cellular activity

As mentioned in the previous section, a number of annexin A2-S100A10 inhibitors possessed good target inhibitory activity while at the same time showing a slight or insignificant anti-proliferative activity. Therefore, a hypothesis has been made that these inhibitors could not penetrate through the biological membrane in order to inhibit the intracellular annexin A2-S100A10 interaction and modulate proteins expressions. Obviously, they might be still able to inhibit extracellular annexin A2-S100A10 complex formation (see chapter 4).

According to Lipinski rule of 5, a drug-like molecule is most likely to have poor absorption or permeation when there are more than 5 H-bond donors, 10 H-bond acceptors, the molecular weight (MWT) is greater than 500 and the calculated LogP (CLogP) is greater than 5 (Lipinski et al., 2012). However, complying with the rule of 5 is not a guarantee that a molecule is drug-like and vice versa. In fact, several molecules that are used as drugs do not comply with the rule of 5 such for instance CNS drugs (Lipinski, 2004).

Since annexin A2-S100A10 inhibitors were relatively small molecules (molecular weight around 500) (Reddy et al., 2011), it may be predicted that these molecules might have good permeation ability through the

biological membranes. It is known that LogP (logarithm partition coefficient), the ratio of concentration of a compound in two immiscible phases, is proportional to the ability of a drug to pass through biological systems (Beig et al., 2013). Furthermore, it is widely accepted that there is a correlation between drugs lipophilicity and their protein binding ability (Laznicek and Laznickova, 1995, Laznicek et al., 1987). Thus an indication of lipophilicity (LogP) of annexin A2-S100A10 inhibitors would help to understand their ability to pass through the biological membrane and inhibit the intracellular annexin A2-S100A10 complex.

LogP can be determined experimentally or theoretically. The most reliable method of LogP determination is the shake-flask method using n-octanol and water as two separation solvents however, for a large set of compounds it may be material consuming (Benfenati et al., 2003) and in this study, an estimation of the lipophilicity of these inhibitors was required. Many theoretical approaches for calculation of LogP involve fragment descriptors have been used (Varnek, 2011). Herein this section Crippen fragmentation method applied in ChemBioDraw Ultra software available at Nottingham University was used. Fragmentation method is an approach which breaks a molecule into fragments and assumes that the LogP of a molecule is the sum of all contributions of each fragment (Wildman and Crippen, 1999). The correlation coefficient (r) between predictable and experimental values of LogP in a set of 131 organic compounds was more than 0.97 (Souza et al.,

2011). This indicates that Crippen fragmentation is a reliable method in predicting the lipophilicity of annexin A2-S100A10 inhibitors.

In addition to lipophilicity, the water solubility of a molecule is also a significant parameter that determines uptake and transport of a drug (Hou et al., 2004). Therefore, the theoretical solubility LogS of these inhibitors has also been estimated using ChemBioDraw Ultra software available at Nottingham University.

Therefore the aim was to correlate annexin A2-S100A10 inhibitors target activity and anti-proliferative activity with their estimated lipophilicity and aqueous solubility.

2.4.1. Relationship between target inhibitory activity of annexin A2-S100A10 inhibitors and their lipophilicity and aqueous solubility

Herein this section the intention was to assess the relationship between the ability of annexin A2-S100A10 inhibitors to block the annexin A2-S100A10 interaction with LogP and LogS.

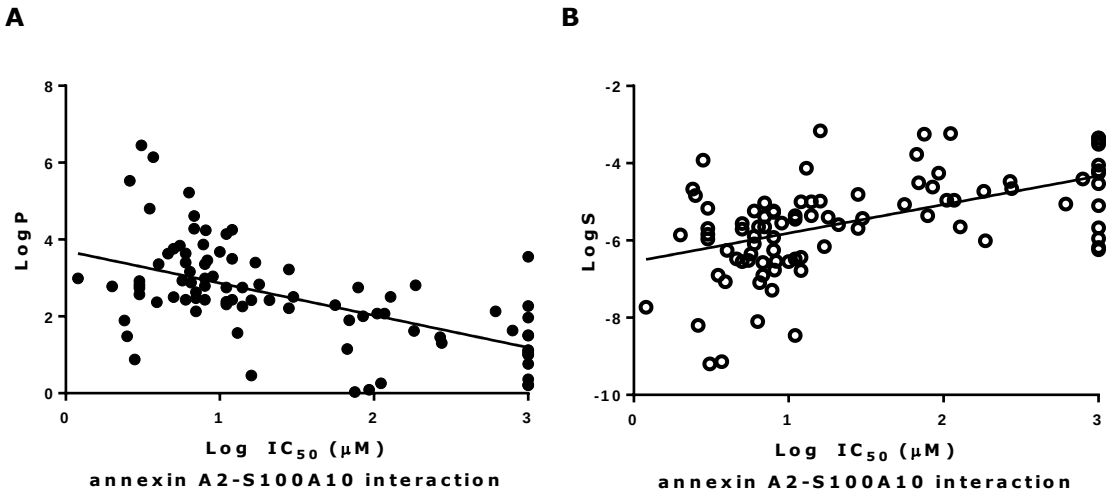


Figure 2.12: The relationship between lipophilicity (A) and aqueous solubility (B) of annexin A2-S100A10 inhibitors and their target activity. The lipophilicity (LogP) and aqueous solubility (LogS) were calculated using ChemBioDraw Ultra software available at Nottingham University.

In Figure 2.12A, linear regression analysis revealed a significant relation between target potency and LogP of annexin A2-S100A10 inhibitors (P < 0.0001) (the slop of the linear regression was significantly deviated from zero). The strength and the direction of this relation were strong and negative with Pearson r of -0.60. Thus as the lipophilicity of annexin A2-S100A10 inhibitors decreases their target inhibitory activity appears to decrease.

Similarly in Figure 2.12B, linear regression analysis revealed a significant relation between target potency and LogS of annexin A2-S100A10 inhibitors (P < 0.0001) (the slop of the linear regression was significantly deviated from zero). The strength and the direction of this relation were strong and positive with Pearson r of 0.53. Thus as the aqueous solubility of annexin A2-S100A10 inhibitors increases their target inhibitory activity appears to decrease.

Laznicek group also noted a relation between protein binding of some drugs with their lipophilicity (Laznicek et al., 1987). Thus this data suggests an involvement of annexin A2-S100A10 inhibitors structures in terms of lipophilicity and aqueous solubility in their target inhibitory activity. However, a consideration should be taken as the criteria used to develop these inhibitors were dependent on the ability of these inhibitors to accommodate the binding pocket with formation of hydrogen bonds as well as electrostatic interaction with S100A10 (Reddy et al., 2011). Moreover,

drugs with very high lipophilicity are not always favourable and most likely fail to proceed to advanced stages of research because they characterized by low oral bioavailability (Beig et al., 2013). Therefore, a balance between lipophilicity and aqueous solubility of these inhibitors should be taken into account.

2.4.2. Relationship of the cellular activity of annexin A2-S100A10 inhibitors and their lipophilicity and aqueous solubility

Herein this section the aim was to assess the relationship between the anti-proliferative activity of annexin A2-S100A10 inhibitors in PANC-1 cells with LogP and LogS.

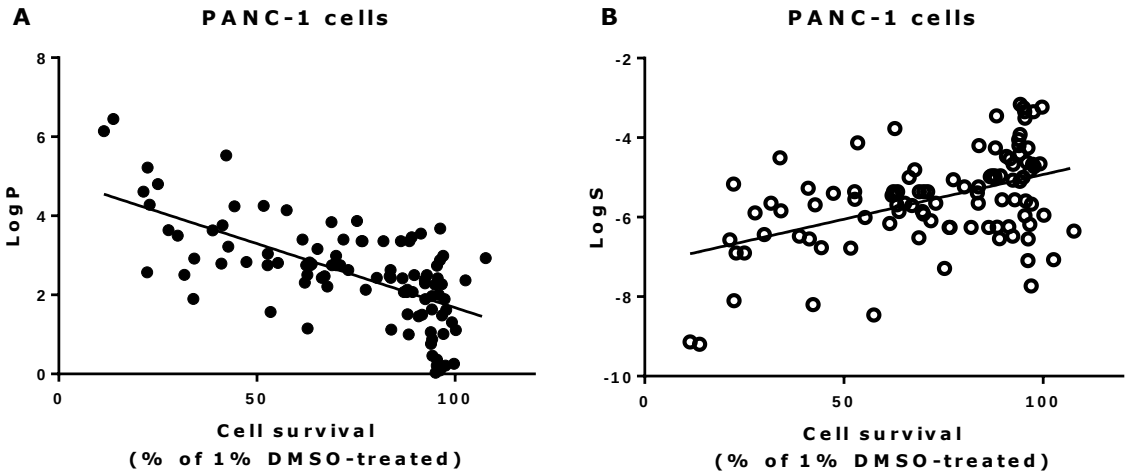


Figure 2.13: The relationship between lipophilicity (A) and aqueous solubility (B) of annexin A2-S100A10 inhibitors and their anti-proliferative activity in PANC-1 cells. The lipophilicity (LogP) and aqueous solubility (LogS) were calculated using ChemBioDraw Ultra software available at Nottingham University.

In Figure 2.13A, linear regression analysis showed a significant relation between the anti-proliferative activity and LogP of annexin A2-S100A10 inhibitors ($P < 0.0001$) (the slop of the linear regression was significantly deviated from zero). The strength and the direction of this correlation were strong and negative with Pearson r of -0.70. Thus as the lipophilicity of annexin A2-S100A10 inhibitors decreases their anti-proliferative activity appears to decrease. This may be related to a decreased ability to pass through the cell membrane and inhibit intracellular annexin A2-S100A10 complex as discussed in section 2.3.3.2 and showed in Figure 2.11.

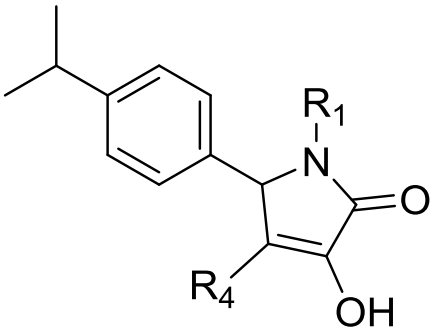
Similarly in Figure 2.13B, linear regression analysis showed a significant relation between the anti-proliferative activity and LogS of annexin A2-S100A10 inhibitors ($P < 0.0001$) (the slop of the linear regression was significantly deviated from zero). The strength and the direction of this relation were moderate to strong and positive with Pearson r of 0.50. Thus as the aqueous solubility of annexin A2-S100A10 inhibitors increases their anti-proliferative activity appears to decrease. This may be also related to a decreased ability of these inhibitors to pass through the cell membrane and inhibit intracellular annexin A2-S100A10 complex.

These observations indicated involvement of lipophilicity and aqueous solubility of annexin A2-S100A10 inhibitors in their target inhibitory activity and anti-proliferative activity reflecting intracellular availability.

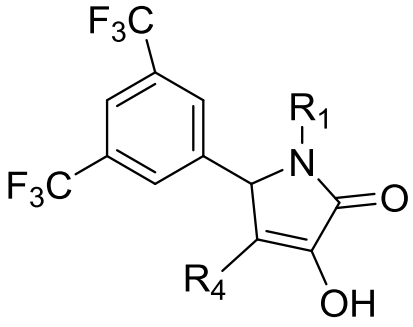
Taken together all these analyses, annexin A2-S100A10 inhibitors may be classified according to their target inhibitory activity and anti-proliferative activity both in relation to lipophilicity as shown in the next section.

2.5. Classification of annexin A2-S100A10 inhibitors

According to the initial chemical template used to synthesize the molecules (1-substituted 4-aroyl-3-hydroxy-5-phenyl-1H-pyrrol-2(5H)-one), their target inhibitory activity, anti-proliferative activity and lipophilicity the annexin A2-S100A10 inhibitors have been categorized as follows.



II



I

Figure 2.14: Chemical structures of 1, 4-Substituted-3-hydroxy-5-(4-isopropylphenyl)-1Hpyrrol-2(5H)-ones (II) and 1, 4-Substituted-3-hydroxy-5-(3,5-bis(trifluoromethyl)phenyl)-1Hpyrrol-2(5H)-ones (I). The structures of the compounds have been drawn by ChemBioDraw Ultra 12.0 available at Nottingham University.

2.5.1. Target-potent intracellular active inhibitors

These annexin A2-S100A10 inhibitors showed a potent target inhibitory activity and very significant intracellular activity (anti-proliferative activity) toward PANC-1 cells. A list of these inhibitors is presented in Table 2.3.

Table 2.3: List of target-potent intracellular active annexin A2-S100A10 inhibitors with their chemical structures. P.IC_{50} = Potency of the inhibitory activity expressed in IC_{50} µM, C.V% = Cell survival (%).

ID	P. IC_{50} (µM)	C.V %	R1	R4
(TRK347) I	3.7	11.41	4-(trifluoromethyl)phenyl	4-methylbenzoyl
(TRK348) I	3.1	13.75	4-isopropylphenyl	4-methylbenzoyl
(TRK354) II	6.8	21.56	phenyl	4-methylbenzoyl
(TRK106) II	3	22.28	3-methoxypropyl	4-methylbenzoyl
(TRK345) I	6.3	22.39	phenyl	4-methylbenzoyl
(TRK394) I	6.8	22.96	cyclopropylmethy	4-methylbenzoyl
(TRK406) I	3.5	25.01	butyl	4-methylbenzoyl
(TRK100) II	6	27.71	allyl	4-methylbenzoyl
(TRK384) I	12	30.02	3-methoxypropyl	4-methylbenzoyl
(TRK412) I	3	34.19	butyl	furan-2-carbonyl
(TRK372) I	4.6	38.85	allyl	4-methoxybenzoyl
(TRK369) I	5	41.33	propyl	4-methoxybenzoyl
(TRK103) II	8	41.06	2-methoxyethyl	4-methylbenzoyl

(TRK355) II	2.6	42.26	4-(trifluoromethyl)phenyl	4-methylbenzoyl
(TRK402) I	8.1	44.34	2-hydroxy-3-methylbutyl	4-methylbenzoyl

Table 2.3 shows that substitution at R1 with lipophilic bulky phenyl groups (TRK347 LogP = 2.96), (TRK348 LogP = 3.27), (TRK345 LogP = 2), (TRK354 LogP = 2) and (TRK355 LogP = 2.96) improved the target inhibitory activity and the anti-proliferative activity. The improvement in target inhibitory activity might be attributed to the phenyl group being able to make π-π stacking and lipophilic interaction with S100A10 at H2 (Figure 1.14A). The improvement in anti-proliferative activity might be also related to the lipophilicity of phenyl ring which may have increased the total LogP of the inhibitor and enhanced its permeability to block the intracellular annexin A2-S100A10 complex and decrease the cell survival. Substitution on the same position with lipophilic aliphatic saturated (TRK106, TRK406, TRK384, TRK4412 and TRK369) or non-saturated (TRK100 and TRK372) groups may also increase the availability of the inhibitors inside the cell to inhibit the intracellular complex and decrease the cell survival.

2.5.2. Target-potent intracellular inactive inhibitors

These annexin A2-S100A10 inhibitors showed a potent target inhibitory activity but insignificant intracellular activity (insignificant anti-proliferative activity) toward PANC-1 cells. A list of these inhibitors is showed in Table 2.4.

Table 2.4: List of target-potent intracellular inactive annexin A2-S100A10 inhibitors with their chemical structures. P.IC_{50} = Potency of the inhibitory activity expressed in IC_{50} µM. C.V% = Cell survival (%).

ID	P. IC_{50} (µM)	C.V %	R1	R4
(TRK389) II	11	92.37	3-(1H-imidazol-1-yl)propyl	4-methylbenzoy
(TRK330) II	2.4	92.5	2,3-dihydroxypropyl	4-methylbenzoyl
(TRK340) I	5	92.89	2,3-dihydroxypropyl	4-methylbenzoyl
(TRK416) II	2.8	94.21	2-hydroxypropyl	furan-2-carbonyl
(AA16) II	14	94.95	2-hydroxypropyl	benzoyl
(TRK373) I	21	95.63	2-hydroxyethyl	4-methoxybenzoyl
(TRK380) I	3	95.44	2-hydroxypropyl	4-methoxybenzoyl
(TRK388) I	6.5	96.17	2-(1H-imidazol-1-yl)ethyl	4-methylbenzoyl
(TRK405) I	10	96.24	2-methylpropanoic acid	4-methylbenzoyl
(TRK407) I	2.5	96.73	2-hydroxypropyl	furan-2-carbonyl
(TRK342) I	1.2	97.01	3-(1H-imidazol-1-yl)propyl	4-methylbenzoyl

(TRK330) II	2.4	97.38	2,3-dihydroxypropyl	4-methylbenzoyl
(TRK381) I	3.9	102.63	3-(1H-imidazol-1-yl)propyl	4-methoxybenzoyl
(TRK343) I	5.7	107.74	2-(piperazin-1-yl)ethyl	4-methylbenzoyl

Table 2.4 shows that substitution at R1 position by a side chained imidazole group (TRK342, TRK388, TRK381 and TRK389) retains the target activity but abolishes the anti-proliferative activity. This might be caused by the hydrophilic nature of imidazole substituted group (LogP = 0.39) which would be expected to reduce the cell permeability. Also substitution with 2-hydroxypropyl group (LogP = 0.38) (TRK416, AA16, TRK373, TRK380 and TRK407), retains the target activity with insignificant anti-proliferative activity.

Most of these inhibitors are able to form hydrogen bonds with S100A10 at H2 (Figure 1.14A) that makes them target active however they would be ionized (polar) at pH 7.4 which could be a reason that they cannot pass through the cell membrane easily. Indeed, the pKa has been found to be a factor in absorption and distribution characteristics of a molecule (Manallack, 2008). Therefore, these inhibitors might be useful probes to differentiate between extracellular and intracellular annexin A2-S100A10 interaction (see chapter 4).

2.5.3. Target-potent intracellular moderately active inhibitors

These annexin A2-S100A10 inhibitors showed a potent target inhibitory activity but only moderate anti-proliferative activity toward PANC-1 cells. A list of these inhibitors is seen in Table 2.5.

Table 2.5: List of target-potent intracellular moderately active annexin A2-S100A10 inhibitors with their chemical structures. P.IC_{50} = Potency of the inhibitory activity expressed in IC_{50} µM. C.V% = Cell survival (%).

ID	P. IC_{50} (µM)	C.V %	R1	R4
(TRK370) I	2	69.71	2-methoxyethyl	4-methoxybenzoyl
(TRK337R) I	4	86.34	(R)-2-hydroxypropyl	4-methylbenzoyl
(TRK336S) I	4	81.92	(S)-2-hydroxypropyl	4-methylbenzoyl
(TRK60) I	4	76.64	2-hydroxypropyl	4-methylbenzoyl
(TRK317) I	4	76.39	2-hydroxypropyl	4-methylbenzoyl
(TRK397) I	5.5	68.8	2-hydroxybutyl	4-methylbenzoyl
(AA50) II	7	87.93	2-hydroxypropyl	3-methoxybenzoyl
(TRK86) II	7	83.48	2-hydroxypropyl	2-ethoxybenzoyl
(TRK404) I	7.8	75.28	2-hydroxypropyl	1-naphthoyl
(TRK395) I	8.3	89.08	3-hydroxybutyl	4-methylbenzoyl
(TRK97) II	12	66.37	2-hydroxyethyl	4-methylbenzoyl
(TRK325R) II	14	70.02	(R)-2-hydroxypropyl	4-methylbenzoyl
(TRK324S) II	14	68.95	(S)-2-hydroxypropyl	4-methylbenzoyl

(TRK368) II	**6.4**	**65.25**	**propyl**	**4-methoxybenzoyl**
(TRK322SR) II	**14**	**63.48**	**2-hydroxypropyl**	**4-methylbenzoyl**
(TRK385) I	**17**	**61.52**	**2-methoxyethyl**	**4-methylbenzoyl**
(TRK399) I	**11**	**57.48**	**3-acetyl-4-hydroxyphenyl**	**4-methylbenzoyl**
(TRK5) II	**14**	**52.76**	**2-hydroxypropyl**	**4-methylbenzoyl**

Table 2.5 reveals that a 2-hydroxypropyl substitution at R1 is crucial for target inhibitory activity, which might be due to the ability to form hydrogen bonds with S100A10. However, in terms of anti-proliferative activity, the 2-hydroxypropyl might be ionised at pH 7.4 and may therefore affect the ability of an inhibitor to pass through the cell membrane. However, a change in the pH of the media (Tannock and Rotin, 1989) may affect the concentration of this inhibitor in an un-ionized form and its ability to pass through the cell membrane to inhibit the intracellular annexin A2-S100A10 interaction.

2.5.4. Target-impotent intracellular inactive inhibitors

These annexin A2-S100A10 inhibitors were neither target inhibitory active nor intracellular active (insignificant anti-proliferative activity) toward PANC-1 cells. A list of these inhibitors is exhibited in Table 2.6.

Table 2.6: List of target-impotent intracellular inactive annexin A2-S100A10 inhibitors with their chemical structures. P.IC_{50} = Potency of the inhibitory activity expressed in IC_{50} µM. C.V% = Cell survival (%).

ID	P. IC_{50} (µM)	C.V %	R1	R4
(TRK415) I	1000	100.18	3-(1H-imidazol-1-yl)propyl	furan-2-carbonyl
(TRK338) I	1000	97.6	2,3-dihydroxypropyl	acetyl
(TRK414) I	1000	97.04	2-(1H-imidazol-1-yl)ethyl	furan-2-carbonyl
(TRK334) II	1000	95.45	3-morpholinopropyl	acetyl
(TRK341) I	1000	95.39	2,3-dihydroxypropyl	acetyl
(TRK319) I	1000	93.85	2-hydroxypropyl	acetyl
(TRK413) I	1000	94.15	2-hydroxybutyl	furan-2-carbonyl
(TRK392) I	1000	91.38	2-(dimethylamino)ethyl	4-methylbenzoyl
(LW37) II	794	94.19	2-hydroxypropyl	6-methylnicotinoyl
(TRK333) II	111	99.72	2-morpholinoethyl	acetyl
(TRK339) II	93	96.18	3-(1H-imidazol-1-yl)propyl	acetyl
(TRK335) II	75	95.09	2-(piperazin-1-yl)ethyl	acetyl

Table 2.6, shows that 4-methylbenzoyl (positioned at H3 Figure 1.14A) is essential for target activity and a substitution at R4 with more hydrophilic groups than 4-methylbenzoyl (LogP = 2.27) resulted in a marked decrease in target activity and in parallel the anti-proliferative activity. Acetyl group (LogP = -0.57) (TRK333, TRK339, TRK335, TRK334, TRK341, TRK319, TRK338) is poorly tolerated in terms of target inhibitory activity. Similar outcome occurs with furan-2-carbonyl group (LogP = 0.4) (TRK415, TRK414 and TRK413). Substitution with more lipophilic 6-methylnicotinoyl (LogP = 1.15) (LW37) resulted in a very little activity (794 μM) and the inhibitor is considered to be inactive.

A diagram to explain the action of the different annexin A2-S100A10 inhibitors on the annexin A2-S100A10 complex formation and the cell activity is shown in Figure 2.15.

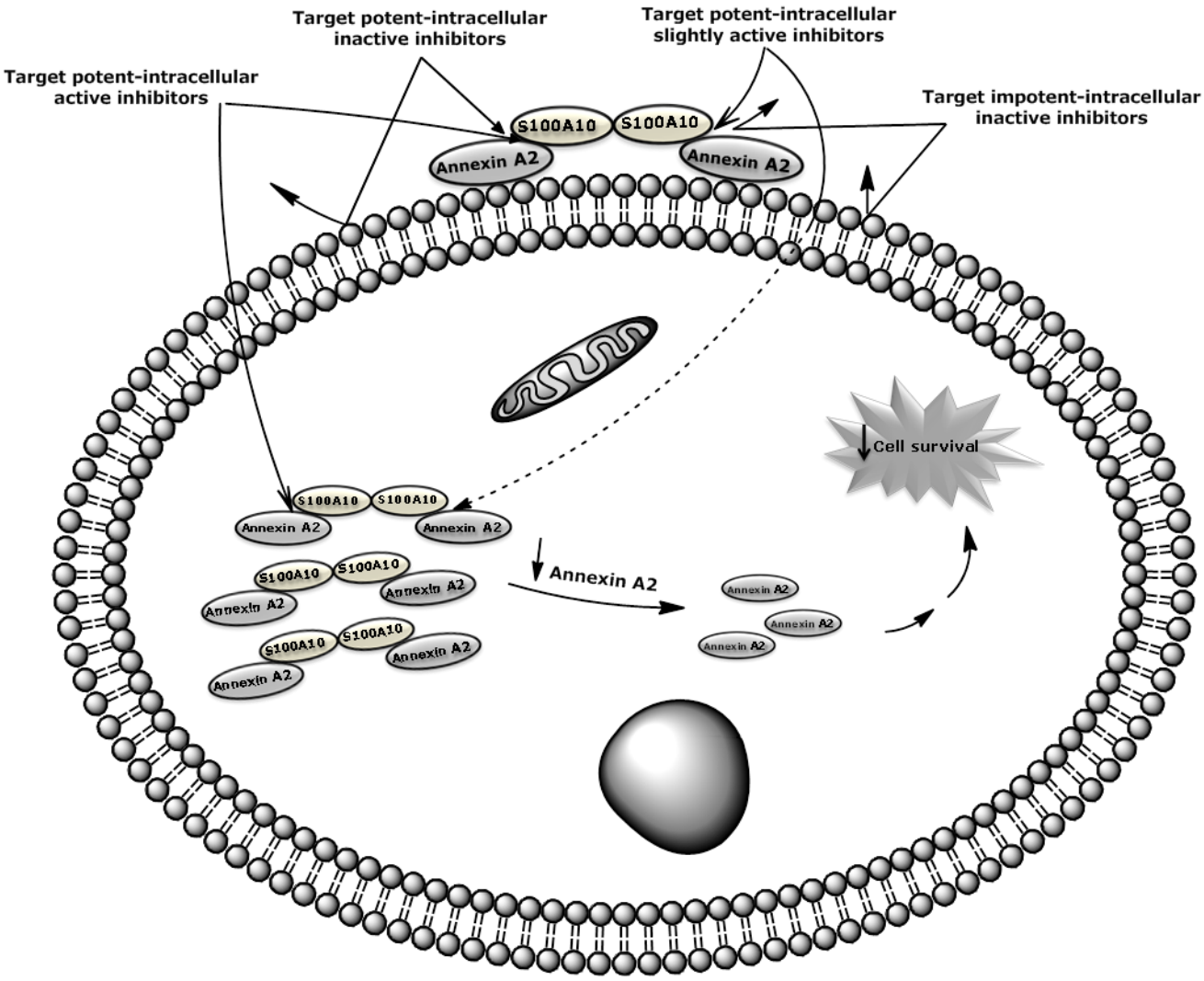


Figure 2.15: Diagrammatic representation of annexin A2-S100A10 inhibitors targeting extracellular and intracellular annexin A2-S100A10 complex formation in PANC-1 cells.

2.6. Conclusion and future plans

In this chapter, measurement of the anti-proliferative activity of annexin A2-S100A10 inhibitors against pancreatic cancer cell lines (PANC-1 and MIA PACA-2) and HMEC-1 cells has been made. Annexin A2-S100A10 inhibitors do have a wide range of cellular activity and correlating the target inhibitory activity with the anti-proliferative activity and annexin A2 expression suggested an involvement of annexin A2 levels in the survival of pancreatic cancer cells.

According to the viability assay, western blotting and SAR analysis, these inhibitors have been classified according to their target inhibitory activity and anti-proliferative activity. It was hypothesized that the lipophilicity (reflecting intracellular availability) of these inhibitors was a factor in their inhibition of annexin A2-S100A10 complex inside the cell and anti-proliferative activity. According to this classification pre-selected candidate annexin A2-S100A10 inhibitors have been chosen for further analysis on other cell biological parameters.

CHAPTER 3

3. INHIBITION OF ANNEXIN A2-S100A10 INTERACTION IMPROVES THE ANTI-PROLIFERATIVE ACTIVITY OF GEMCITABINE IN RESISTANT PANCREATIC CANCER CELLS

3.1. Introduction

The latest advances in pancreatic cancer treatment have improved the prognosis of the disease. However, these improvements have not achieved a satisfactory result for patients with pancreatic cancer, in which the 5-year survival is still less than 10% (Kagawa et al., 2012). Recurrence and resistance to chemotherapy have been reported. Gemcitabine, a pyrimidine analogue, has been shown to be an efficient chemotherapeutic reagent for pancreatic cancer (Burris et al., 1997). Since then, it has become the first line therapy for patients with unresectable pancreatic cancer. However, because of limited response and chemo-resistance, a combination with other cytotoxic agent or molecular targeting agent is required to improve efficacy and overcome resistance (Kagawa et al., 2012). It has been suggested that resistance to gemcitabine could be inherited or acquired during treatment.

The resistance of pancreatic cancer cells to gemcitabine has been attributed to various mechanisms as summarized in the next paragraphs.

Upregulation of the principal gemcitabine cellular transporter, hENT1, has been linked with longer survival of pancreatic cancer patients, whereas downregulation was linked with shorter survival (Giovannetti et al., 2006). However, some of gemcitabine-resistant pancreatic cancer cells did not show a change in the expression of hENT1 as demonstrated by Nakano and colleagues (Nakano et al., 2007), suggesting that hENT1 expression alone is not sufficient to predict gemcitabine resistance. Downregulation of gemcitabine activator deoxycytidine kinase, dCK, has been linked to gemcitabine-resistant in some pancreatic cancer cell lines (Ohhashi et al., 2008). Moreover, high dCK levels have been shown to improve gemcitabine efficacy in certain tumour xenografts in mice (de Sousa Cavalcante and Monteiro, 2014). Upregulation of the enzyme responsible for gemcitabine inactivation, cytidine deaminase, CDA, has been found to mediate gemcitabine resistance in pancreatic cancer cells (Weizman et al., 2014).

Kong et al. showed that siRNA downregulation of NF-κB p65 subunit synergized with gemcitabine and increased the apoptosis in different pancreatic cancer cell lines (Kong et al., 2010). BNIP3 a proapoptotic protein has been reported to be downregulated in gemcitabine resistant pancreatic cancer cells (Akada et al., 2005). Inhibition of the phosphatidylinositide 3-kinase (PI3K)-protein kinase B (PKB)/Akt cell survival pathway has been

found to increase gemcitabine-induced apoptosis in human pancreatic cancer cells (Ng et al., 2000).

Several reports have correlated the resistance to gemcitabine with upregulation of annexin A2 (Jung et al., 2015, Kagawa et al., 2012, Gong et al., 2010). Overexpression of annexin A2 in pancreatic cancer cells resistant to gemcitabine has been shown by Takano et al 2008. The investigators restored the chemo-sensitivity of gemcitabine by silencing annexin A2 expression (Takano et al., 2008).

Gemcitabine resistance has also been correlated with S100 proteins. Mahon et al reported that silencing of the S100A4 gene in pancreatic cancer cells markedly increased cells sensitivity to gemcitabine by enhancement of BNIP3 expression (Mahon et al., 2007). S100A10 expression may also involve in resistance to chemotherapy and has been used as a prognostic factor in the recurrent colon cancer after treatment with 5-FU (Bresnick et al., 2015). Pardo et al. have specifically correlated the expression of S100A10 with pancreatic cancer cell resistance to gemcitabine (Pardo et al., 2010).

Combining these observations, it might be predicted that resistance to gemcitabine may be due to the interaction of annexin A2 and S100A10 rather than the individual proteins.

Taken these observations together with the conclusion from chapter 2 regarding the possible involvement of the annexin A2-S100A10 interaction in the survival of pancreatic cancer cells, it might be hypothesized that inhibiting annexin A2-S100A10 interaction would lead to a change in the annexin A2 and S100A10 expression levels that might result in interference with the resistance to gemcitabine.

3.2. Aim and Objectives

In this chapter the aim was to get some insight into the mechanism of gemcitabine resistance developed during pancreatic cancer treatment. On the basis that gemcitabine resistance was correlated with upregulation of annexin A2 (Takano et al., 2008), and the finding from chapter 2 that annexin A2-S100A10 inhibitors might decrease intracellular annexin A2 expression (Figure 2.8) that would lead eventually to a decrease in cell survival. A hypothesis was made that, treating gemcitabine-resistant pancreatic cancer cells with a combination of gemcitabine and annexin A2-S100A10 inhibitor would restore chemo-sensitivity to the drug by interfering with annexin A2 and S100A10 protein expression.

The main purpose of this chapter is to investigate the consequence of annexin A2-S100A10 inhibition on gemcitabine-resistant pancreatic cancer cells in combination with gemcitabine.

The specific objectives were as following:

1. Develop gemcitabine-resistant (G-R) cells (drug resistant cell line model) to clarify the mechanism of gemcitabine resistance and confirm that upregulation of annexin A2 is associated with gemcitabine resistance.
2. Measure the effect of annexin A2-S100A10 inhibition on the expression level of these proteins.

3. Assess whether there is synergy after treating gemcitabine-resistant cells with gemcitabine and annexin A2-S100A10 inhibitors.
4. Elucidate annexin A2-S100A10 inhibitors mechanism of action when employed to gemcitabine-resistance pancreatic cancer cells.
5. Investigate the mechanisms related to annexin A2 upregulation due to gemcitabine treatment.

3.3. Results and discussion

3.3.1. Development of gemcitabine-resistant pancreatic cancer cells

In order to model gemcitabine resistance it was necessary to develop gemcitabine-resistant (G-R) cells. First, the IC_{50} dose of gemcitabine for wild pancreatic cancer cells was measured and subsequently, this dose was used to develop resistant cells.

3.3.2. Determining the IC_{50} of gemcitabine on pancreatic cancer cells

Pancreatic cancer cells were seeded at a density of 3×10^3 cells per well and the next day were subjected to a treatment with serial concentrations of gemcitabine. After 72 h incubation, cell viability was measured using MTT assay (refer to 6.2.4 for more details) as shown in Figure 3.1.

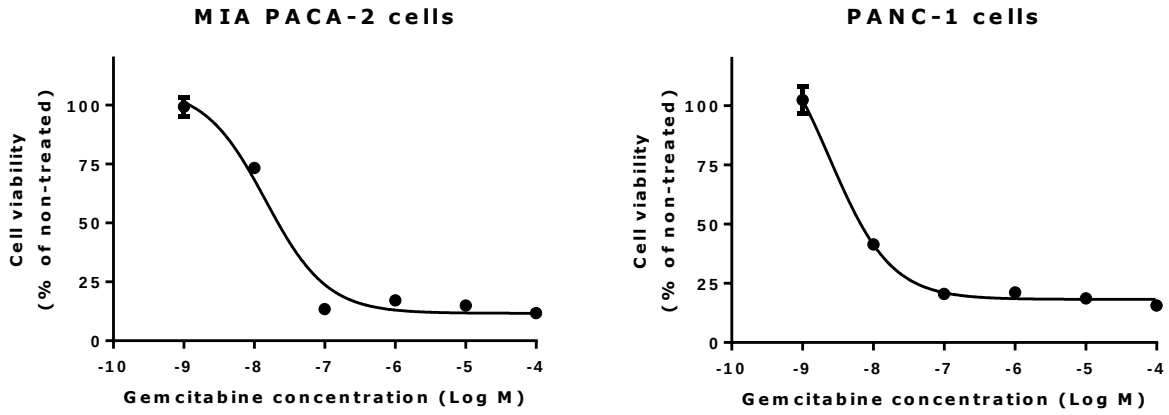


Figure 3.1: The effect of serial gemcitabine concentrations on the viability of MIA PACA-2 cells and PANC-1 cells. Data are expressed as mean ± SEM (n = 3).

As shown in Figure 3.1, gemcitabine has a strong dose dependent anti-proliferative effect on both cell lines. Concentrations of 1 nM or less appear to be tolerated by both MIA PACA-2 and PANC-1 cells. PANC-1 cells showed more sensitivity toward gemcitabine with IC_{50} of 2.4 nM as compared with MIA PACA-2 cells which have IC_{50} of 14.5 nM. Correlating these observations with those findings from chapter 2 (Figure 2.7C) indicating there was higher expression of annexin A2 in MIA PACA-2 cells than PANC-1 cells, it may be suggested that the relative amount of annexin A2 expression is involved in the anti-proliferative effect of gemcitabine. Indeed, annexin A2 expression levels have been found to be associated with gemcitabine resistance in pancreatic cancer cells (Jung et al., 2015).

These results are consistent with published data classified MIA PACA-2 and PANC-1 as moderately sensitive to gemcitabine (Silva et al., 2012). However they are inconsistent with Mahon et al. who reported that PANC-1 was more resistant to gemcitabine with IC_{50} of 262 ng/ml while for MIA PACA-2 the IC_{50} was 98 ng/ml (Mahon et al., 2007). This may be attributed to the difference in seeding densities as they seeded 2×10^4 cells per well which could affect cells growth rate leading to slightly different results.

According to the previous data, a concentration of 1 nM was tolerated by both cell lines and this dose has been used as a starting point to develop resistant cells.

3.3.3. Measuring the IC_{50} of PANC-1 G-R cells

PANC-1 cells have chosen on the basis that they were easier to handle than MIA PACA-2 cells (MIA PACA-2 cells are mainly grown in suspension). They also expressed less annexin A2 (Figure 2.7) therefore, it would be easier to assess if there is an upregulation in annexin A2 after gemcitabine treatment.

PANC-1 G-R cells were developed by continuous exposure of PANC-1 cells to increasing concentrations of gemcitabine over a period of 5-6 months, starting with an initial concentration of 1 nM, with a 1-3 fold increase every 5 to 15 days. After 5 months of continuous exposure, PANC-1 G-R cells were maintained in 1 μM gemcitabine-containing media. A month later, the cells

were seeded at a density of 3×10^3 cells per well and the next day were subjected to a treatment with serial concentrations of gemcitabine ranging from 1 mM to 0.1 nM. After 72 h incubation, viability of the cells was measured using MTT assay (refer to 6.2.4 for more details) and compared with wildtype PANC-1 cells as seen in Figure 3.2.

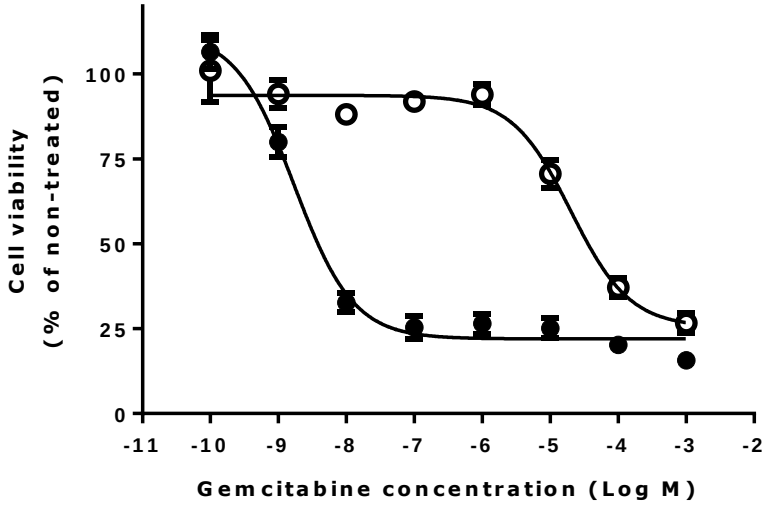


Figure 3.2: Dose response curves of gemcitabine in PANC-1 wildtype cells (close circle) as compared to PANC-1 G-R cells (open circle). Data are expressed as mean ± SEM (n = 4).

The curves in Figure 3.2, show that more than 93.98 ± 3.04% of PANC-1 G-R cells were able to grow in 1 μM gemcitabine containing media while PANC-1 wildtype cells were not. Measuring the IC_{50}s of gemcitabine in PANC-1 G-R cells (20 μM) and PANC-1 wildtype cells (1.7 nM) reveals a developed resistance to gemcitabine after 5 months of continuous treatment with increasing concentrations.

Our results are in a good agreement with Jordheim methods for development of gemcitabine resistant cells (Jordheim et al., 2004). Also the results are in line with Togawa et al. who developed G-R MIA PACA-2 cells after exposure of the cells to increasing gemcitabine concentrations starting from 3.3 nM to 33 μM (Togawa et al., 2003).

3.3.4. Annexin A2 expression is upregulated in PANC-1 G-R cells

The expression of annexin A2 in PANC-1 G-R cells was assessed by western blotting. Briefly, PANC-1 wildtype and G-R cells were seeded in 10 cm^2 dishes. The following day, media was aspirated and fresh media was added to the attached cells. After 2 days, the cells were harvested and the proteins extracted from the cells were subjected to electrophoresis and immunoblotting (refer to 6.2.14 for more details) as seen in Figure 3.3.

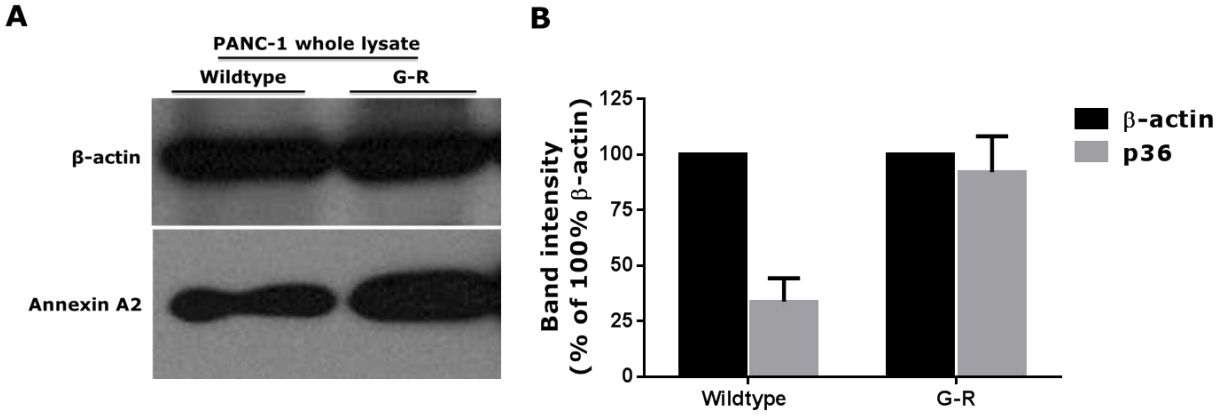


Figure 3.3: (A) Western blot analysis of annexin A2 expression in PANC-1 wildtype and G-R cells. β-actin was used as a loading control. (B) Multiple western blot experiments. Data are expressed as mean ± SEM (n = 3). Band intensity was quantified by ImageJ and the lanes were corrected to 100% β-actin expression.

Figure 3.3 shows that after continuous exposure to gemcitabine treatment for 5 months, there was an upregulation in annexin A2 expression ($P < 0.01$) (two-way ANOVA) in PANC-1 G-R cells as compared with wildtype cells. This result is in line with Takano et al in 2008 who observed annexin A2 upregulation in G-R MIA PACA-2 cells when compared with the wildtype cells (Takano et al., 2008). The result is also in agreement with data indicating annexin A2 upregulation after gemcitabine adjuvant chemotherapy in patients that had undergone pancreatic cancer resection (Kagawa et al., 2012).

It has been known that cellular stresses such as radiations, drugs, temperature change could result in increased level of ROS (reactive oxygen species) (Bharadwaj et al., 2013). Specifically, gemcitabine has been found to promote the invasiveness of pancreatic cancer cells through a ROS dependent mechanism (Arora et al., 2013). In such situations, cysteine in proteins acts as a sensor of change in redox potential and triggers toward signally pathways that activate antioxidant systems (Jones, 2010). Annexin A2 has four cysteine residues Cys8, Cys132, Cys261 and Cys334. The former is considered as redox sensitive cysteine (Bharadwaj et al., 2013). It

has been noted that annexin A2 null mice exhibited increased level of oxidation in liver and lung tissues as compared with wild type. Moreover, annexin A2 depleted tumour cells have shown a marked increase in ROS (Madureira et al., 2011a).

These observations may provide a speculative explanation of the possible chemo-resistance developed to gemcitabine as the cells try to scavenger the ROS resulted from gemcitabine treatment by upregulating annexin A2 expression.

3.3.5. S100A10 expression concomitantly upregulated with annexin A2 expression in PANC-1 G-R cells

The expression of S100A10 in PANC-1 G-R cells was assessed by western blotting. PANC-1 wildtype and G-R cells were seeded in 10 cm^2 dishes. The following day, media was aspirated and fresh media was added to the attached cells. Two days later, the proteins extracted from the cells were subjected to electrophoresis and immunoblotting (refer to 6.2.14 for more details) as seen in Figure 3.4.

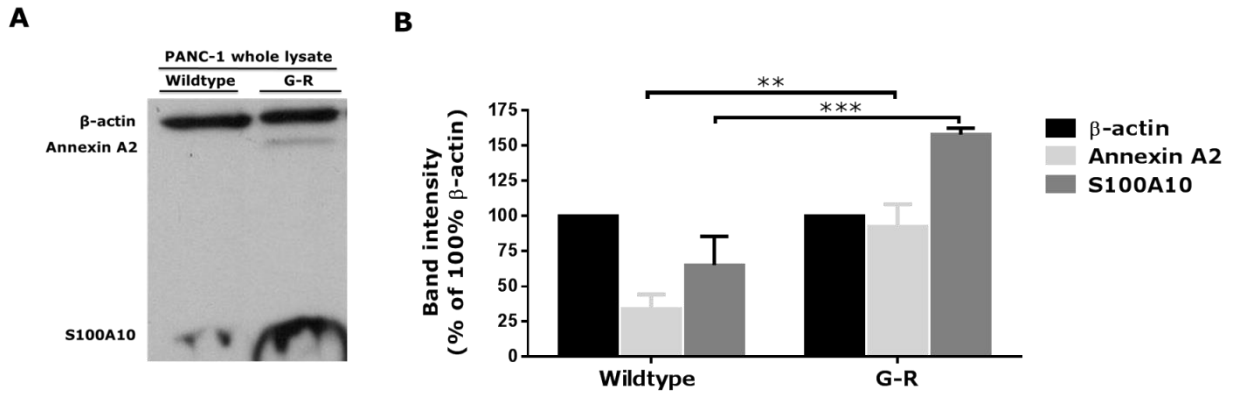


Figure 3.4: (A) Western blot analysis of annexin A2 and S100A10 expressions in PANC-1 wildtype and G-R cells. β-actin was used as a loading control. (B) Multiple western blot experiments. Data are expressed as mean ± SEM (n = 3). Band intensity was quantified by ImageJ and the lanes were corrected to 100% β-actin expression.

As shown in Figure 3.4, there was a marked ($P < 0.0001$) upregulation in S100A10 expression in PANC-1 G-R cells as compared with the wildtype cells. This might be attributed to the significant ($P < 0.01$) upregulation in annexin A2 which has been found to cause upregulation of the cellular levels of S100A10 through a post-translational mechanism (Puisieux et al., 1996). Hajjar group also found in endothelial cells that annexin A2 regulates poly-ubiquitination and degradation of its binding partner S100A10 (He et al., 2008). Thus, there may be a relationship between expression of annexin A2 and S100A10 in pancreatic cancer cells such that as the expression of one protein changes the expression of the other protein also changes.

To further strengthen this hypothesis, the next aim was to assess the expression of annexin A2 and S100A10 in PANC-1 cells after treatment with an inhibitor known to block the interaction between annexin A2 and S100A10 proteins (TRK317).

3.3.6. TRK317 inhibits the interaction of annexin A2 and S100A10 and downregulates their expressions

It has been shown in the previous section that annexin A2 and S100A10 proteins are upregulated in PANC-1 G-R cells.

In this section the aim was to assess whether inhibition of annexin A2-S100A10 interaction would affect the expression of annexin A2 and S100A10 proteins level.

TRK317 has been chosen as a candidate inhibitor to assess on PANC-1 G-R cells because the molecule has a potent in vitro target inhibitory activity of 4 μM (Reddy et al., 2011) and was shown to downregulate annexin A2 expression in PANC-1 wildtype cells (Figure 2.6).

Although TRK317 inhibited the interaction of annexin A2 N-terminus with S100A10 in the low micro-molar range (Reddy et al., 2011) and it is known that the binding of annexin A2 to S100A10 is mediated through annexin A2 N-terminal (Rety et al., 1999), it was necessary to confirm that TRK317

inhibits the native complex of the full length proteins. Therefore, the ability of TRK317 to inhibit annexin A2-S100A10 interaction in a cell lysate extracted from PANC-1 cells was assessed.

Briefly, the complex in protein lysate extracted from PANC-1 cells was immunoprecipitated by S100A10 antibody. Then it was incubated with protein A/G agarose. Protein A/G agarose was then recovered by centrifugation and re-suspended in loading buffer before subjecting to electrophoresis and immunoblotting. TRK317 was pre-incubated with PANC-1 cell lysate prior to the immunoprecipitation (refer to 6.2.15 for more details) as shown in Figure 3.5.

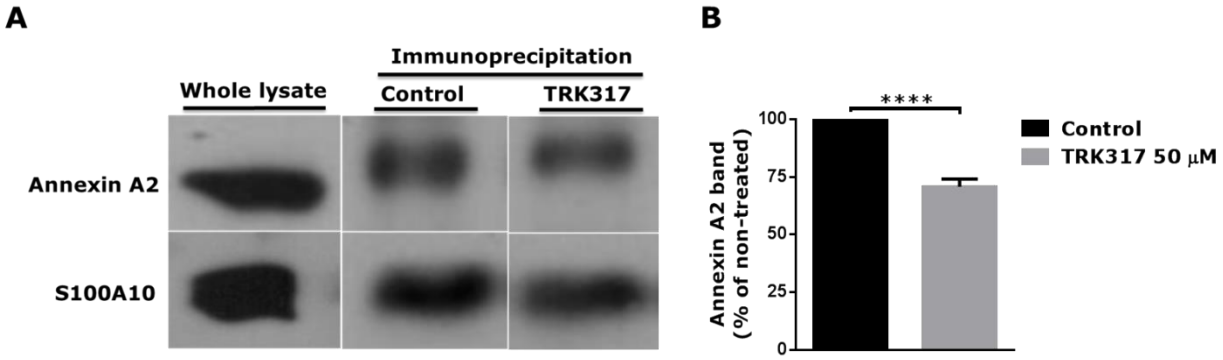


Figure 3.5: Analysis of the interaction between S100A10 and annexin A2. S100A10 was immunoprecipitated then annexin A2 in the immunoprecipitates was analyzed by western blotting using an annexin A2 antibody. (A) annexin A2 bands in TRK317 50 μM pre-treated lysate as compared with non-treated control. (B) Multiple IP experiments (n = 6) with data expressed as mean ± SEM. An unpaired t test

showed that TRK317 50 μM significantly (P < 0.0001) inhibited the complex when compared with non-treated control.

Measuring the expression of annexin A2 and S100A10 after treatment of cells with TRK317 was done by seeding PANC-1 G-R cells in 10 cm^2 dishes. The following day, media was aspirated and fresh media containing TRK317 50 μM was added to the attached cells. Two days later, cells were harvested and proteins extracted from the cells were subjected to electrophoresis and immunoblotting (refer to 6.2.14 for more details) as seen in Figure 3.6.

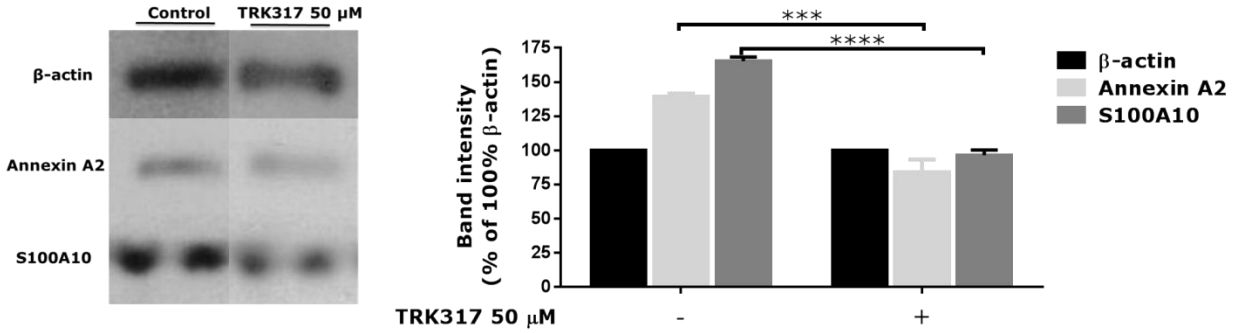


Figure 3.6: Western blot analysis of annexin A2 and S100A10 expressions after TRK317 treatment in PANC-1 G-R cells. (A) Immunoblot shows a decreased expression of annexin A2 and S100A10 in TRK317 50 μM treated cells as compared with PANC-1 G-R non-treated control. β-actin was used as a loading control. (B) Multiple immunoblotting assays show a decreased expression of annexin A2 (P < 0.001) and S100A10 (P < 0.0001) (two-way ANOVA) in TRK317 50 μM treated cells as compared with non-treated control. Data are expressed as mean ± SEM (n = 3).

Band intensity was quantified by ImageJ and the lanes were corrected to 100% β-actin expression.

Figures 3.5 and 3.6 indicate the intimate relation between annexin A2 and S100A10 in PANC-1 cells. In Figure 3.5, treating PANC-1 cell lysate with TRK317 50 μM significantly decreased the band intensity of annexin A2 ($P < 0.0001$) in S100A10 immunoprecipitation which means that TRK317 disrupted the interaction between the annexin A2 and S100A10 proteins in the native complex. This constitutes important validation of the mechanism of action of these inhibitors. Interestingly, in Figure 3.6, when PANC-1 G-R cells were pre-treated with TRK317 50 μM before extraction and the levels of annexin A2 and S100A10 proteins were measured, downregulation of both annexin A2 ($P < 0.001$) and S100A10 ($P < 0.0001$) as compared with non-treated control was observed.

These observations suggest that annexin A2 and S100A10 proteins expressions are closely related and once the interaction between annexin A2 and S100A10 is disrupted by TRK317, their expression is dysregulated.

Most of the S100A10 is tightly associated with annexin A2 dimers, forming a stable heterotetramer (Johnsson et al., 1988). Intracellular S100A10 protein level is regulated post-translationally by annexin A2 expression. Annexin A2 stabilizes S100A10 via binding, which masks the S100A10 poly-ubiquitination signal leading to its proteasomal degradation (He et al.,

2008). Therefore a dysregulated annexin A2 expression leads to a change in S100A10 expression. Indeed, silencing of annexin A2 expression in colorectal cancer cells has led not only to a downregulation of annexin A2 expression but, also to a decrease in S100A10 expression (Suzuki and Tanigawara, 2014).

S100A10 might also affect annexin A2 protein level in some way. Silencing of S100A10 in macrophage cells reduced the total cellular of annexin A2 level by 60% as compared with control cells (O'Connell et al., 2010). Moreover, tissues isolated from S100A10 null mouse showed decreased annexin A2 levels in lung, liver, spleen and kidney (Madureira et al., 2012).

Our results reinforce the suggestion that there might be an auto regulatory mechanism between annexin A2 and S100A10 proteins level. Therefore inhibition of the interaction between annexin A2 and S100A10 leads to a displacement of annexin A2 from binding to S100A10 that might leave both proteins susceptible to cytoplasmic proteolysis.

3.3.7. TRK317 synergizes with gemcitabine in PANC-1 G-R cells

In section 3.3.5, annexin A2 and S100A10 protein levels were shown to be upregulated in PANC-1 G-R cells as compared with PANC-1 wildtype cells. Furthermore it was shown that inhibition of the interaction between annexin A2 and S100A10 by TRK317 downregulates their expressions. Thus, it may be hypothesized that inhibiting annexin A2-S100A10 interaction in PANC-1 G-R cells with TRK317 would restore the chemo-sensitivity and improve the anti-proliferative activity of gemcitabine.

Therefore, in this section the aim was to investigate whether treatment of PANC-1 G-R cells with a combination of annexin A2-S100A10 inhibitor and gemcitabine would improve the anti-proliferative effect of gemcitabine in these cells. There is no single standard method to examine synergy (greater than additive). Here the survival percentage in response to serial concentrations of gemcitabine and TRK317 alone was compared with the response to combination of gemcitabine with TRK317. Synergy was assessed by Chuo`s combination method and data was processed using CompuSyn software (Chou, 2010).

For the synergy testing, PANC-1 G-R cells were seeded at a density of 3×10^3 cell per well and the following day the cells were treated with serial concentrations of gemcitabine and/or TRK317. Three days later, cell viability was measured by MTT assay (refer to 6.2.4 for more details) as presented in Tables 3.1 and 3.2.

Table 3.1: Dose dependent inhibition of PANC-1 G-R survival by gemcitabine or TRK317.

Gemcitabine (μM)	Survival fraction	TRK317 (μM)	Survival fraction
0.1	0.999	1	0.974
1	0.98	5	0.911
10	0.958	10	0.854
100	0.763	30	0.821
500	0.756	50	0.8
		70	0.768
		100	0.699

Next, anti-proliferative effects of gemcitabine and TRK317, alone and in combination were assessed using the MTT assay. Potential synergistic interaction between serial concentrations of gemcitabine and TRK317 at 50 μM was then evaluated in vitro using the combination index (CI) method (Chou and Talalay, 1981, Chou, 2010) as indicated by the following equation,

$$\mathrm{CI} = \frac{(\mathrm{D})_1}{(\mathrm{Dx})_1} + \frac{(\mathrm{D})_2}{(\mathrm{Dx})_2}$$

$(\mathrm{D})_1$ and $(\mathrm{D})_2$ represent the concentrations of two drugs used in combination to achieve x% effect. $(\mathrm{Dx})_1$ and $(\mathrm{Dx})_2$ are the concentrations for single drugs to achieve the same effect. CI > 1 indicated antagonism, CI = 1 indicated additive and CI < 1 indicated synergism.

MTT assays indicated that combination treatment decreased the viability of PANC-1 G-R cells compared to individual treatments as shown in Table 3.2 and Figure 3.7.

Table 3.2: Combination treatment of gemcitabine serial concentrations with TRK317 50 μM in PANC-1 G-R cells show a synergistic effect as indicated by combination index (CI < 1). Experimental data were subjected to automated calculation using CompuSyn software.

Gemcitabine (μM)	TRK317 (μM)	Survival fraction	Combination index (CI)	Evaluation of the effect
0.1	50	0.688	0.438	Synergy
1	50	0.697	0.476	Synergy
10	50	0.65	0.341	Synergy
100	50	0.601	0.381	Synergy
500	50	0.531	0.665	Synergy

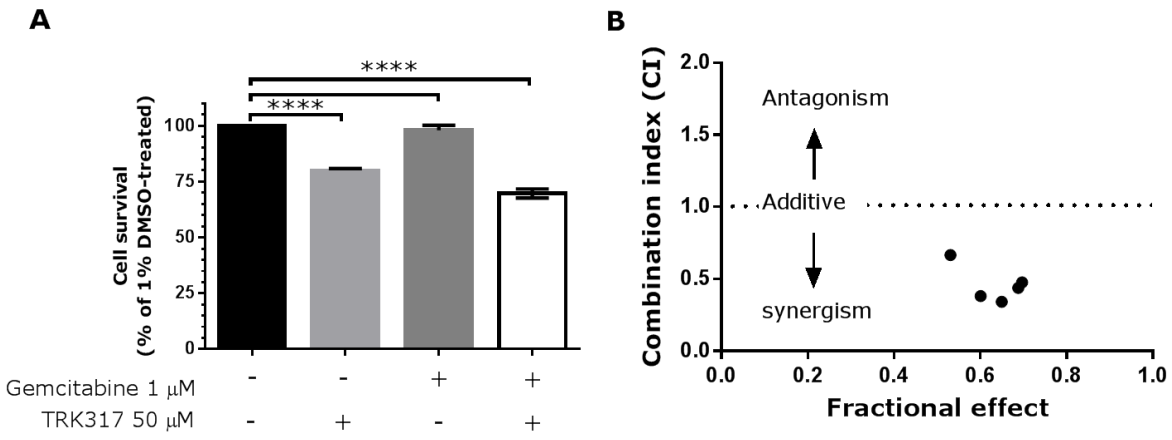


Figure 3.7: (A) TRK317 improves the anti-proliferative effect of gemcitabine in PANC-1 G-R cells. Data are expressed as mean ± SEM (n = 4). (B) Fractional effect-combination index (Fa-CI) plot of combination index analysis in PANC-1 G-R cells.

Figure 3.7A shows that the combination of gemcitabine with TRK317 increased the anti-proliferative activity of gemcitabine in PANC-1 G-R cells. Treatment with 1 μM gemcitabine showed insignificant ($P > 0.05$) effects on PANC-1 G-R cells survival with 98.03 ± 3.58% compared to non-treated control. TRK317 treatment at 50 μM significantly ($P < 0.05$) inhibited the survival of PANC-1 G-R to 80.08 ± 0.86%. Combination of gemcitabine 1 μM and TRK317 50 μM significantly ($P < 0.0001$) inhibited the proliferation of PANC-1 G-R cells by more than 30% with survival of 69.71 ± 2.02%.

According to (Chou, 2006) guidelines for evaluation of synergy based on combination index (CI). Combination of serial concentrations of gemcitabine with TRK317 at 50 μM was found to synergize ($0.3 < CI < 0.7$) with the anti-proliferative activity of gemcitabine in PANC-1 G-R cells as shown in Figure 3.7B. Meaning that, inhibition of annexin A2-S100A10 interaction by TRK317 in PANC-1 G-R cells significantly improved the anti-proliferative activity of gemcitabine.

This significant result is in line with an observation showing that inhibition of the interaction between annexin A2 and S100A10 by DLC1, a tumour suppressor protein, downregulates S100A10 expression and significantly inhibited proliferation of lung cancer cells (Yang et al., 2011). it is also in agreement with data revealing increased sensitivity to gemcitabine due to downregulation of annexin A2 expression (Takano et al., 2008). Very interestingly, an annexin A2-S100A10 inhibitor published by our group (Reddy et al., 2011), (Cluster 3 compound 3 (IC_{50} = 2.1 μM)), was found to improve the sensitivity of acute lymphoblastic leukaemia cells co-cultured with osteoblasts to dexamethasone and vincristine (Gopalakrishnapillai et al., 2015). This observation together with my result validates the importance of disrupting annexin A2-S100A10 complex formation in the sensitivity of cancer cells to chemotherapy.

Taken together all these observations indicate that annexin A2 and S100A10 downregulation may improve the anti-proliferative activity of gemcitabine. However, further investigation is required to get insight into the possible mechanism by which annexin A2 and S100A10 expression levels were involved in gemcitabine resistant.

3.3.8. Altered expression of annexin A2 and S100A10 in PANC-1 cells may affect cell cycle but not apoptotic pathway

It has been shown in the previous sections that annexin A2 and S100A10 were upregulated simultaneously in PANC-1 G-R cells and once their interaction is blocked by TRK317 there was a downregulation in their expression that has led eventually to a decrease in the survival of PANC-1 G-R cells.

This turned our attention to investigate the impact of dysregulated annexin A2 and S100A10 expressions in PANC-1 G-R cells on the cell cycle and apoptosis. In fact, the cell cycle and apoptosis are closely related, as seen by the central role of p53 protein, both in cell cycle arrest and in the induction of apoptosis (Shah and Schwartz, 2001). Moreover, cell cycle has been found to mediate drug resistance and insensitivity to chemotherapeutic treatments because of the cell position in the cell cycle (Shah and Schwartz, 2001). Annexin A2 downregulation has been found to induce G2 cell cycle arrest (Wang et al., 2012a). Recent data indicate that annexin A2 is required for progression of the cell cycle to cytokinesis (where the cell is divided into two daughter cells) (Benaud et al., 2015). Inhibition of annexin A2-S100A10 interaction by TRK317 led to downregulation of annexin A2 expression (Figure 3.6B). Therefore TRK317 may affect the cell cycle of PANC-1 G-R cells.

Irinotecan, a topoisomerase I inhibitor, has been reported to induce G2 cell cycle arrest in lung cancer cells (Tolis et al., 1999). It has also been found to mediate apoptosis through a non-cell cycle dependent mechanism (Morris and Geller, 1996). Therefore it mediates cell survival by two independent mechanisms. Combination of irinotecan and gemcitabine has been used as first-line weekly therapy in locally advanced and metastatic pancreatic cancer. They have shown an improvement in the survival up to 22% (Neri et al., 2009). Thus, comparing irinotecan and TRK317 responses on PANC-1 G-R cells would help understanding the mechanism of dependence of gemcitabine resistance on annexin A2 expression and whether the improvement in gemcitabine anti-proliferative activity after inhibition of annexin A2-S100A10 interaction was cell cycle-dependent or apoptotic pathway dependent.

3.3.8.1. Irinotecan significantly induces apoptosis in PANC-1 wildtype and G-R cells

As mentioned earlier, the next step was to assess whether annexin A2 upregulation could affect gemcitabine resistance via a change in the apoptotic pathway.

The Annexin V assay was used to compare the response of PANC-1 wildtype and G-R cells to gemcitabine or irinotecan treatment. Briefly, cells were seeded at a density of 1-2 x 10^5 cells per well. The next day, the cells (wildtype and G-R) were treated with gemcitabine 10 μM or irinotecan 10 μM concentrations. 72 h later, cells were harvested and subjected to annexin V apoptosis assay (refer to 6.2.12 for more details) as shown in Figure 3.8.

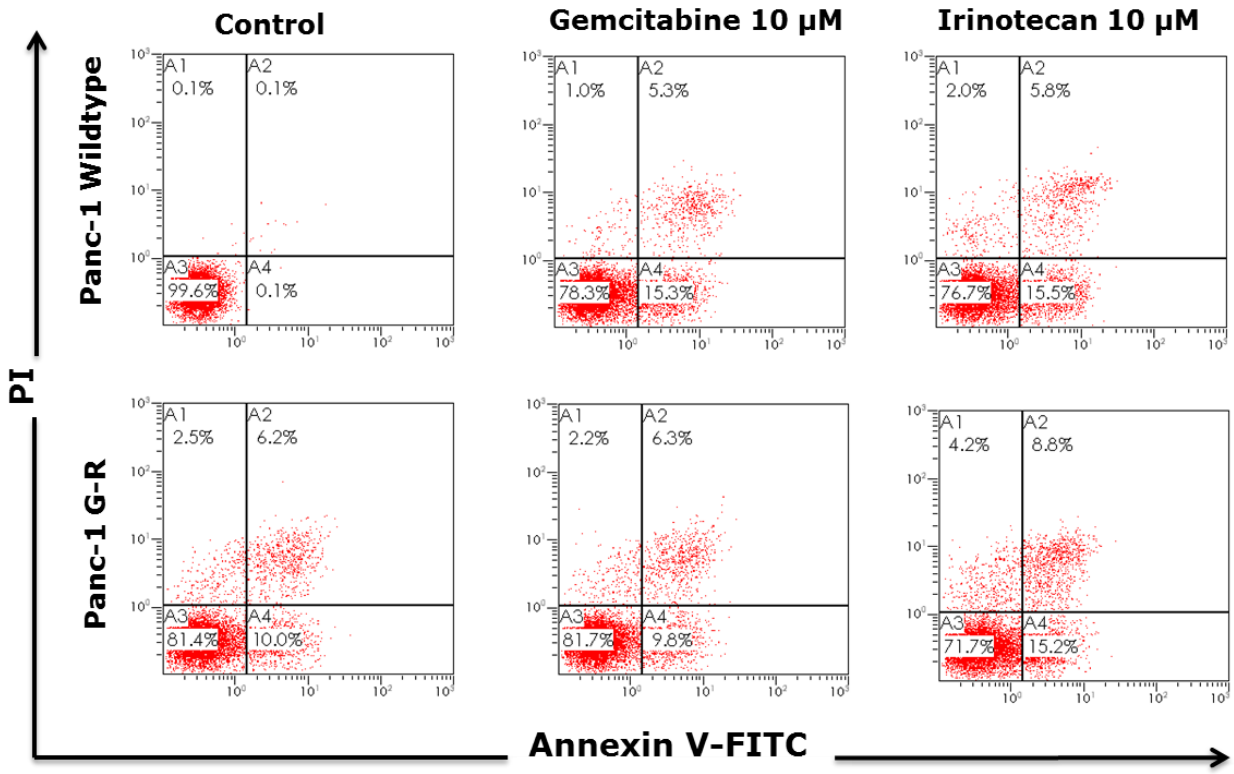


Figure 3.8: Annexin V assay showing a comparison between PANC-1 wildtype and G-R cells treated with gemcitabine 10 µM or irinotecan 10 µM.

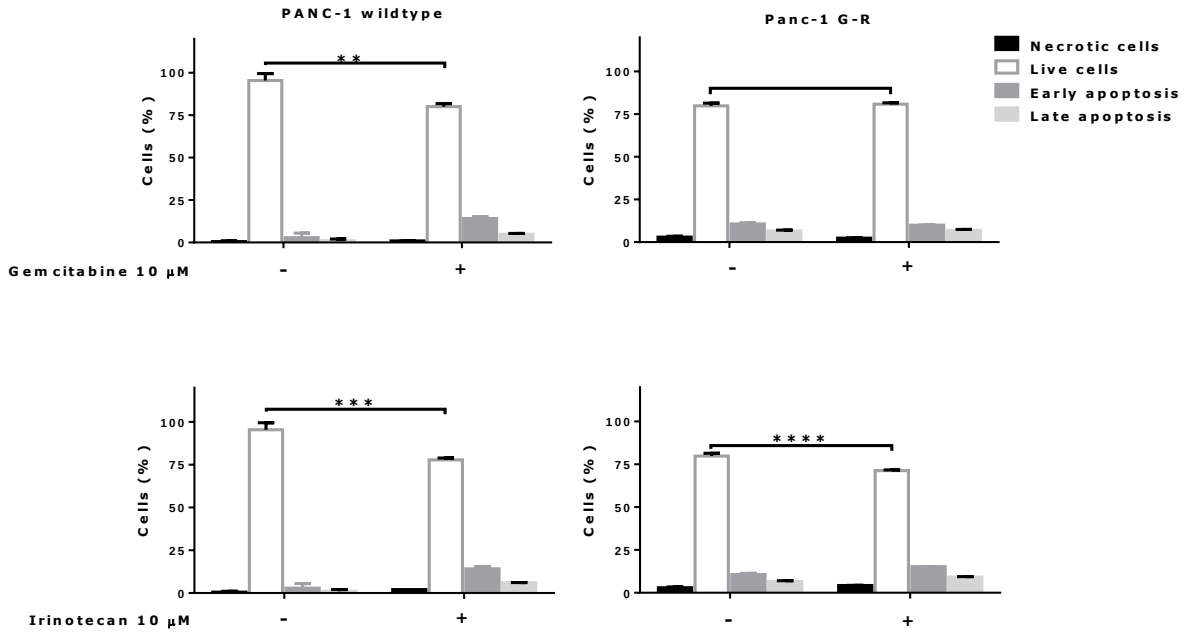


Figure 3.9: A comparison between PANC-1 wildtype and G-R cells treated with gemcitabine 10 µM or irinotecan 10 µM. Data are expressed as mean ± SEM (n = 2).

Figure 3.9 shows that treatment of PANC-1 wildtype cells with gemcitabine 10 µM causes a significant decrease in the number of live cells and increase in the number of apoptotic cells ($P < 0.05$) as compared with non-treated control. PANC-1 G-R cells treatment with gemcitabine 10 µM showed no significant effect on live or apoptotic cells ($P > 0.05$) when compared with non-treated control.

Surprisingly treatment with irinotecan 10 µM causes a significant decrease in live cells and increase in apoptotic cells both in wildtype and G-R PANC-1 cells ($P < 0.05$).

This data indicates that PANC-1 G-R cells were able to survive 10 μM gemcitabine but not 10 μM irinotecan. Thus gemcitabine resistance did not alter the response of PANC-1 cells to irinotecan and change the apoptotic pathway.

Measuring of the pIC_{50} (- Log IC_{50}) of irinotecan by MTT assay (refer to 6.2.4 for more details) in both wildtype and G-R PANC-1 cells indicated that there was no significant difference ($P > 0.05$) between wildtype (5.2 μM) and G-R (4.9 μM) cells as shown in Figure 3.10.

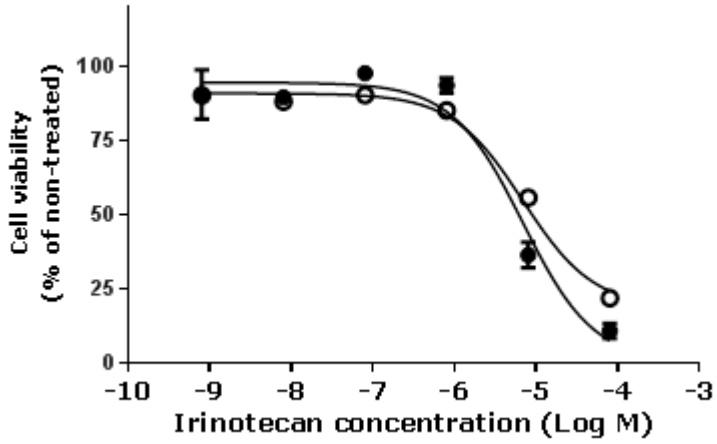


Figure 3.10: A dose response curve of PANC-1 wildtype (close circle) and G-R (open circle) cells treated with serial concentrations of irinotecan. Data are expressed as mean ± SEM (n = 4).

These results indicate that there was no marked change in the apoptotic pathway between PANC-1 wildtype and G-R cells since both responded to irinotecan treatment. It is therefore unlikely that involvement of annexin A2 in gemcitabine resistance can be attributed to actions in the apoptotic pathway.

Irinotecan has been found in colorectal cancer cells to induce G2 cell cycle arrest through p53 independent mechanism (Kaku et al., 2015). Therefore, the next aim was to assess its effect together with gemcitabine and TRK317 on the cell cycle of PANC-1 cells.

3.3.8.2. Upregulation of annexin A2-S100A10 in PANC-1 G-R cells significantly changes cell cycle response to gemcitabine, irinotecan and TRK317

It was shown in the last section that, in PANC-1 G-R cells, increased expression of annexin A2-S100A10 complex did not alter the apoptotic pathways. Annexin A2 expression was found to affect cell cycle of lung cancer cells (Wang et al., 2012a). Thus, a change in the expression of annexin A2 may affect the cell cycle of PANC-1 G-R cells.

Therefore, in this section the aim was to compare the cell cycle of PANC-1 wildtype with G-R (reflecting annexin A2-S100A10 upregulation) cells in relation with their response to gemcitabine, irinotecan and TRK317 treatments.

Cells (wildtype or G-R) were seeded at a density of 1-2 x 10^5 cells per well. The following day, the cells (wildtype or G-R) were treated with gemcitabine 1 μM, irinotecan 50 μM or TRK317 50 μM. 72 h later, DNA content was measured by flow cytometry (refer to 6.2.11 for more details) as seen in Figure 3.11.

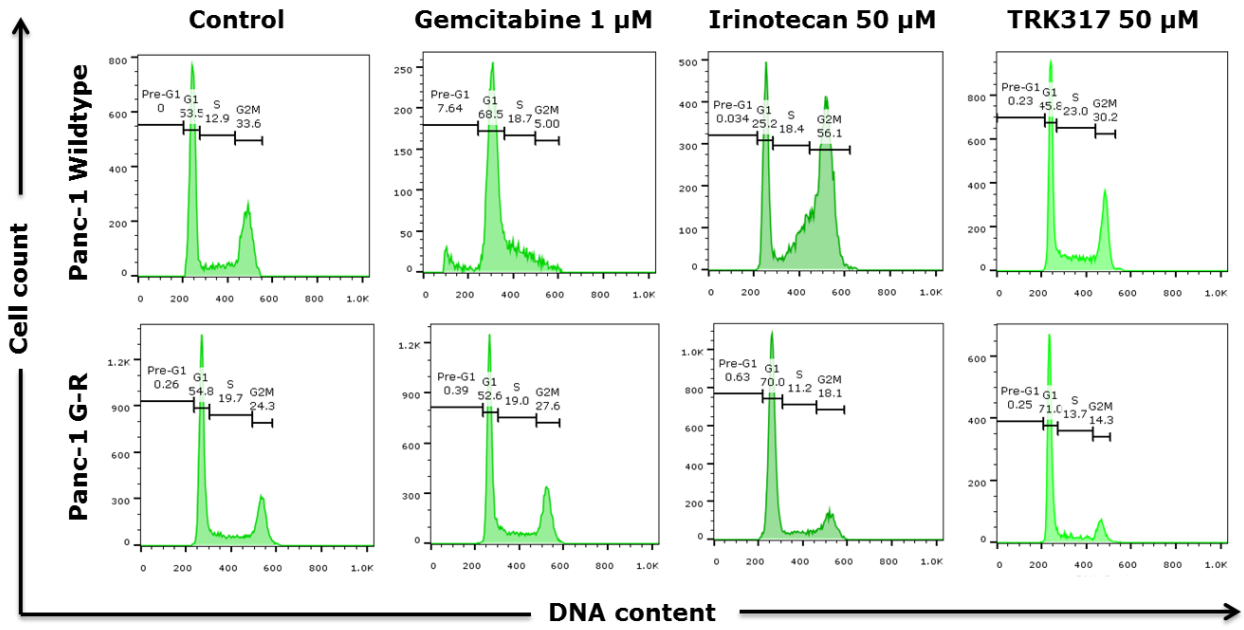


Figure 3.11: Cell cycle phases showing a comparison between PANC-1 wildtype and G-R cells responses to gemcitabine 1 μM, irinotecan 10 μM and TRK317 50 μM.

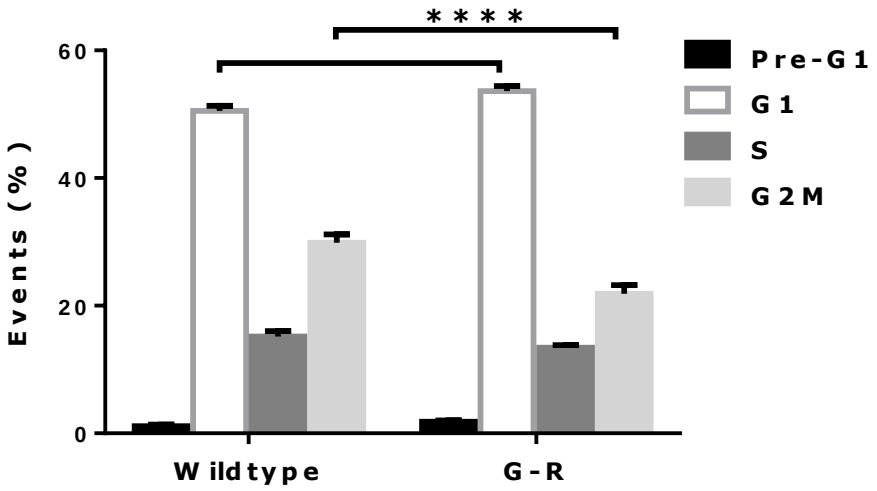


Figure 3.12: A comparison in cell cycle phases between PANC-1 wildtype and G-R cells. Data are expressed as mean ± SEM (n = 4).

Figure 3.12, shows that there was insignificant change ($P > 0.05$) in G1 phases between wildtype and G-R PANC-1 non-treated cells; however, there was a significant decrease ($P < 0.05$) in G2-M phase in PANC-1 G-R cells compared with PANC-1 wildtype cells.

Annexin A2 downregulation was found to mediate an increase in cell cycle G2-M phase of lung cancer cells through p53 independent mechanism (Wang et al., 2012a). By reversed argument it might be predicted that annexin A2 upregulation in PANC-1 G-R cells (Figure 3.3) may cause a decrease in G2-M phase of the cell cycle in p53 independent mechanism.

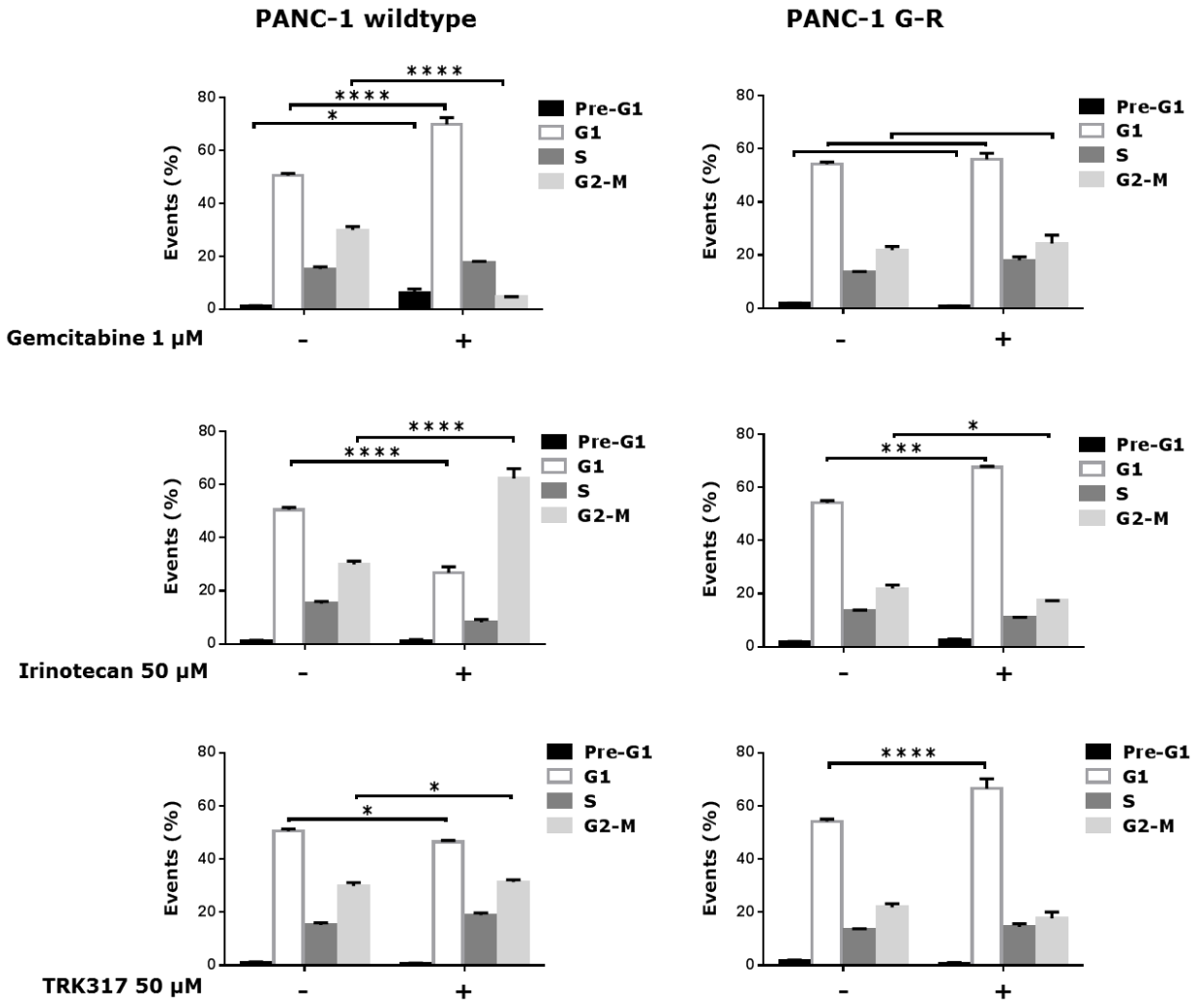


Figure 3.13: A comparison in cell cycle phases between PANC-1 wildtype and G-R cells treated with gemcitabine 1 µM, irinotecan 50 µM and TRK317 50 µM. Data are expressed as mean ± SEM (n = 2).

Figure 3.13 shows marked increase in pre-G1 and G1 phases and a decrease in G2-M phase ($P < 0.05$) in PANC-1 wildtype cells treated with gemcitabine 1 μM as compared with non-treated control. In PANC-1 G-R cells, there was no significant change in cell cycle phases in cells treated with gemcitabine 1 μM as compared with non-treated control ($P > 0.05$). This result confirms a developed resistance to gemcitabine in resistant cells and is in agreement with our previous result (Figure 3.2). Indeed, Tolis et al, observed an increase in G1 and a marked decrease in G2-M phases in H460 lung cancer cells treated with gemcitabine (Tolis et al., 1999).

In PANC-1 wildtype cells, treatment with 50 μM irinotecan causes a significant decrease in G1 phase and increase in G2-M phase ($P < 0.05$) as compared with non-treated control. This is similar to a finding reported a decrease in G1 phase and a marked increase in G2-M phase in HCT116 colon cancer cells treated with irinotecan (Haug et al., 2008). Surprisingly, in PANC-1 G-R cells, treatment with 50 μM irinotecan causes an increase in G1 and a decrease in G2-M phases as compared with non-treated control ($P < 0.05$). This implied that there was a difference in cell cycle response to irinotecan treatment between PANC-1 wildtype and G-R cells.

Treatment with TRK317 also showed distinct results. In PANC-1 wildtype cells, 50 μM TRK317 causes a significant decrease in G1 phase and increase in G2-M phase as compared with non-treated control ($P < 0.05$). However, in PANC-1 G-R cells, 50 μM TRK317 causes a marked increase in G1 phase as compared with non-treated control ($P < 0.05$). This result suggests that alterations in annexin A2 expression (either pharmacologically – using TRK317 – or during acquisition of resistance) may be associated with a change in the cell cycle pattern.

In PANC-1 wildtype cells, TRK317 may have neutralized most of intracellular annexin A2-S100A10 complex leading to a decrease in the expression of the annexin A2. This might have led to a decrease in the transport of annexin A2 as monomer to the nucleus that eventually led to a decrease in G1 phase. In PANC-1 G-R cells, due to upregulation of annexin A2-S100A10 complex, TRK317 was not able to inhibit most of the intracellular annexin A2-S100A10 interaction and some of cytoplasmic annexin A2 might have transported to nucleus as a monomer that has led to an increase in G1 phase. This is in agreement with published data noted, in LNCaP cells, a marked increase in G1 phase due to nuclear accumulation of annexin A2 (Liu et al., 2003a).

An interesting link between cell cycle and annexin A2 expression was established in that, p21, a general regulator of cell cycle, was found to be upregulated after downregulation of annexin A2 expression (Wang et al., 2012a). Moreover, in human lung cancer cells, topotecan (structural analogue of irinotecan) was found to upregulate p21 and induce a G2-M phase arrest without a significant change in p53 expression (Tolis et al., 1999). Guided by these observations, a hypothesis has been made that altered annexin A2 expression in PANC-1 G-R cells may cause a change in cell cycle regulators. Therefore, the next step was to assess the expression of p21 and p53 in PANC-1 G-R cells.

3.3.9. Overexpression of annexin A2-S100A10 complex in PANC-1 G-R may mediate downregulation of p21 expression without significant change in p53

Based on the previous findings, a prediction has been made that PANC-1 G-R cells might have altered p21 (cell cycle inhibitor) expression in a p53 independent mechanism in order to compensate for chronic gemcitabine treatment. Therefore the next aim was to measure the expression of p21, p53 in PANC-1 G-R cells.

Assessing of annexin A2, p53 and p21 expressions was done by seeding PANC-1 wildtype and G-R cells in 10 cm^2 dishes. The following day, the cells were harvested and protein extracts were subjected to electrophoresis and immunoblotting (refer to 6.2.14 for more details) as shown in Figure 3.14.

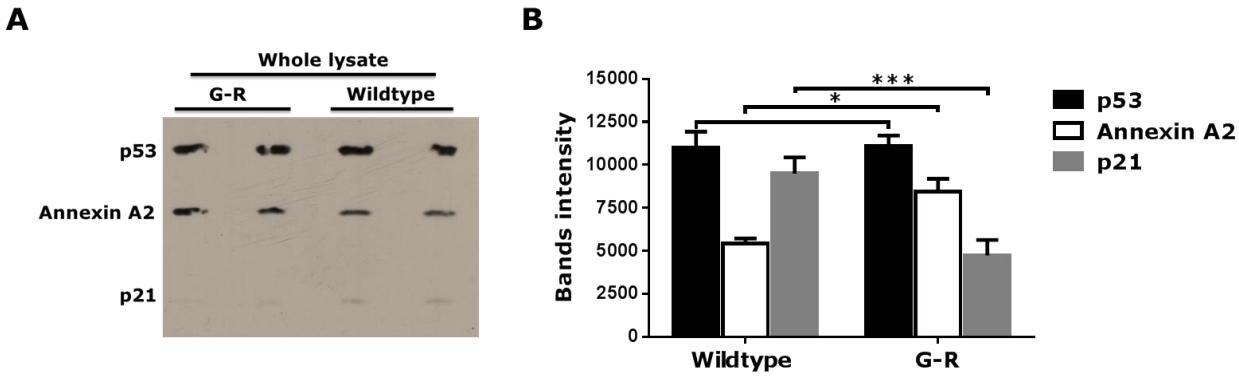


Figure 3.14: (A) Western blot analysis of annexin A2, p21 and p53 in PANC-1 wildtype and G-R cells. (B) Multiple immunoblots show a significant ($P < 0.05$) increase in annexin A2 expression and a decrease in p21 expression without marked change in p53 ($P > 0.05$) in PANC-1 G-R cells as compared with PANC-1

wildtype cells. Data are expressed as mean ± SEM (n = 3). Band intensity was quantified by ImageJ.

Figure 3.14 shows that p21 expression was downregulated in PANC-1 G-R cells ($P < 0.05$) as compared with PANC-1 wildtype cells while at the same time there was upregulation in annexin A2 expression in PANC-1 G-R cells ($P < 0.05$) as compared with PANC-1 wildtype cells. Interestingly, there was no significant change in p53 expression between PANC-1 wildtype and G-R cells ($P > 0.05$). This agrees with our previous result that upregulation of annexin A2-S100A10 complex in PANC-1 G-R cells has not affected their apoptotic pathway (Figures 3.9 and 3.10).

This result reveals a negative correlation between annexin A2 and p21 expressions. Meaning that, as the expression of annexin A2 increases the expression of p21 appears to decrease. An initial experiment revealed upregulation of p21 expression in PANC-1 G-R cells treated with a combination of gemcitabine and TRK317 as compared with non-treated control (Figure 3.15). Although this result is required to be repeated for consistency and statistical analysis, it further enforces the inverse correlation of annexin A2 expression and p21 expression. This might explain the possible mechanism of gemcitabine resistance-dependence on annexin A2 expression. PANC-1 G-R cells exhibited a higher annexin A2 and lower p21 expression than wildtype cells. However, when the PANC-1 G-R cells are treated with TRK317 there was a decrease in annexin A2 expression and

may be a restore in p21 expression (a restore in cell cycle behaviours) and this might have led eventually to improve in gemcitabine chemo-sensitivity.

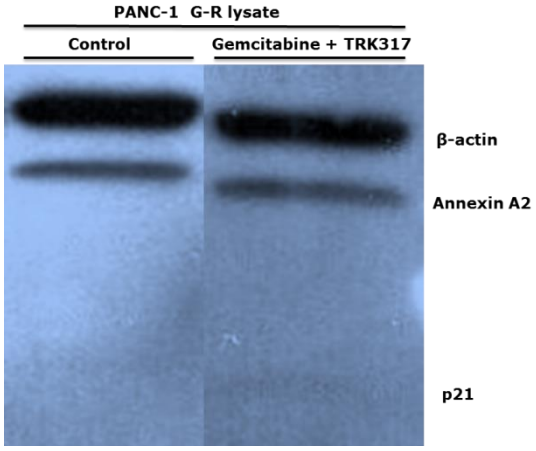


Figure 3.15: Western blot analysis of annexin A2, p21 PANC-1 G-R cells treated with a combination of gemcitabine 10 μM and TRK317 50 μM as compared with non-treated control.

It has been observed in pancreatic cancer cells that, gatifloxacin was able to restore sensitivity to gemcitabine by upregulating p21 expression (Yadav et al., 2012). Indeed, Rathos et al showed an improvement in gemcitabine cytotoxicity after a combination with a cyclin-dependent kinase inhibitor, P276-00, in pancreatic cancer cells (Rathos et al., 2012). Therefore, inhibiting annexin A2-S100A10 interaction appears to restore the chemo-sensitivity to gemcitabine by modulating the expression of p21 through a p53 independent mechanism as summarized in Figure 3.16.

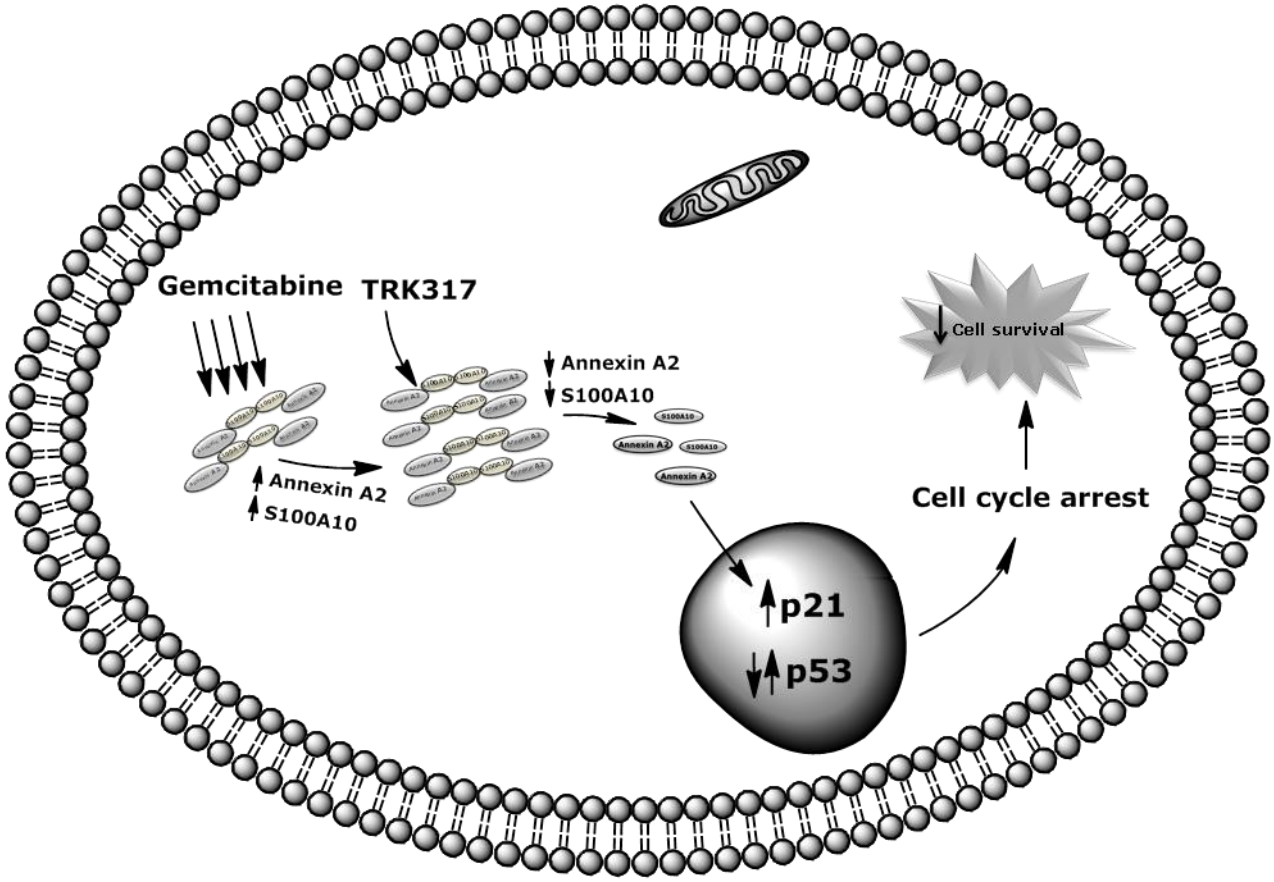


Figure 3.16: Diagrammatic representation of reversion of gemcitabine resistance by TRK317 (An annexin A2-S100A10 inhibitor) in PANC-1 G-R cells.

3.4. Conclusion and Future work

It has been shown in this chapter that, continuous exposure of PANC-1 cells to gemcitabine has led to a development of resistance to the drug and more significantly to upregulation in annexin A2 and S100A10 expressions. Interestingly, inhibiting the interaction between annexin A2 and S100A10 by TRK317 (potent target inhibitor) appears to restore the chemo-sensitivity to gemcitabine by downregulating annexin A2 and S100A10 expressions. Mechanistically, the synergistic effect of TRK317 with gemcitabine revealed an involvement of p21 cell cycle in a p53 independent mechanism. These results have shown convincingly for the first time that blocking of annexin A2-S100A10 interaction might reverse the chemo-resistance of gemcitabine in a p53 independent mechanism. However, involvement of intra-nuclear complex is required to be explored in order to further elucidate the mechanism of action of annexin A2 in gemcitabine treatment. TRK317 inhibited annexin A2-S100A10 complex formation at 50 micro-molar ranges and this concentration appears to synergize with gemcitabine. However, a structural modification might be required to further improve its target potency to Nano-molar ranges.

CHAPTER 4

4. INHIBITION OF ANNEXIN A2-S100A10 INTERACTION REVEALS INVOLVEMENT IN INVASION AND ADHESION OF PANCREATIC CANCER CELLS

4.1. Introduction

The most devastating characteristic of cancer is the appearance of metastases in a site distant from the primary tumour and nearly all deaths from cancer are due to metastases (Keleg et al., 2003). One major hallmark of pancreatic cancer is its ability to disseminate and invade the surrounding tissues. This is contributed for the high mortality rate of pancreatic cancer patients (Keleg et al., 2003). In fact, invasion and metastasis are responsible for almost 90% of pancreatic cancer deaths (DiMagno et al., 1999). How cancer cells detach from the primary tumour, invade and metastasize to distant organs is still required to be fully characterized (Keleg et al., 2003). Thus, understanding molecular mechanism by which cancer cells metastasize is one of the most important issues in cancer research. It has been reported that annexin A2 upregulation is involved in pancreatic cancer invasiveness (Esposito et al., 2006).

In breast cancer cells, MDA-MB231, a high level of annexin A2 expression has been linked to metastatic phenotype of these cells. By contrast, a non-metastatic breast cancer cell line, MCF-7, exhibits very low expression of annexin A2 production (Sharma et al., 2006). Additionally, a study conducted by Wu et al. in 2002 using 2D-gel electrophoresis of two head and neck squamous carcinoma cell line derived from primary and metastatic tumours has reported annexin A2 upregulation in cell line derived from metastatic tumours (Wu et al., 2002). Conversely, silencing of annexin A2 expression resulted in a reduced migration ability of glioma cells (Tatenhorst et al., 2006) and in multiple myeloma cells (Bao et al., 2009). Indeed, Zheng et al, observed a decreased liver metastasis of pancreatic ductal adenocarcinoma in a mouse model as a result of annexin A2 blockade by shRNA or antibodies (Zheng et al., 2011).

S100A10 has also been involved in cell migration and invasion. Waismann group observed a significant decrease in migration and invasion of macrophage cells recovered from S100A10 null mice when compared with wildtype cells (O'Connell et al., 2010). Additionally, transfection of HT1080 cells with S100A10 antisense results in loss of its expression and concomitant decrease in invasion capacity of these cells. By contrast, transfection of HT1080 cells with S100A10 sense results in increased level of the protein and concomitant increase in their invasion capability (Choi et al., 2003). Moreover, inhibition of ubiquitin dependent degradation of S100A10

by DLC1 has led to a decrease in migration and invasion of lung carcinoma cells through a Matrigel extracellular matrix barrier (Yang et al., 2011).

Initially it was suggested that annexin A2 and S100A10 affect cell invasion individually (Hajjar et al., 1994, Cesarman et al., 1994, Kassam et al., 1998b, MacLeod et al., 2003). However, it is more likely now that annexin A2-S100A10 complex has more dominant effect on cancer cell invasion through a plasmin dependent mechanism.

Annexin A2 has been reported as a receptor for tPA and the binding domain of annexin A2 for tPA was within the N-terminal 23-amino acids region of the molecule with a sequence of LCKLSL peptide residues (Hajjar et al., 1998). Indeed, a study conducted by Diaz et al. showed a decrease in plasmin production after inhibition of tPA binding to annexin A2 by LCKLSL peptide leading eventually to a decrease in pancreatic cancer cell invasion (Diaz, 2004). In contrast, Waismann group observed a very significant tPA dependent plasminogen activation by annexin A2-S100A10 complex as compared with annexin A2 alone (Kang et al., 1999). They also noted a marked increase in the rate of tPA dependent plasminogen activation upon addition of a peptide consists of N-terminal 15 amino acids of annexin A2 to a recombinant S100A10 subunit as compared with the stimulation produced by the recombinant S100A10 subunit alone (Kang et al., 1999). Furthermore, the rate of plasmin generation was significantly decreased after annexin A2 and S100A10 silencing in RAW117 cells, a cell line known

to express the complex on the surface (Yeatman et al., 1993), and this dramatic decrease has been reversed by addition of exogenous annexin A2 and S100A10 to the system (Kang et al., 1999). Therefore the contribution of annexin A2-S100A10 complex appears to be more profound in plasmin production.

In order for cancer cells to metastasize, it may initialize angiogenesis which is an essential step for tumour development and provides a route for detached cells to travel through blood vessels (Folkman and Shing, 1992). Then cancer cells have to adhere to endothelial cells in order to penetrate blood vessels and form small metastatic foci that proliferate at secondary site in a process called extravasation (Reymond et al., 2013). Annexin A2 and S100A10 expression on the surface of endothelial cells has been reported by several studies (Konig et al., 1998, Kang et al., 1999, Deora et al., 2004). More significantly their colocalization was reported to be involved in ECM degradation of endothelial cells during in vitro tube formation (Lokman et al., 2011) and activation of plasmin generation (He et al., 2011). Annexin A2 has been also shown to regulate adhesion of prostate cancer cells to osteoblast and endothelial cells (Shiozawa et al., 2008). Interaction between annexin A2 and S100A10 has been found to mediate the adhesion of breast cancer cells to endothelial cells (Myrvang et al., 2013).

Taken together all these observations, it may be predicted that inhibition of the interaction between annexin A2 and S100A10 would affect matrix

invasion, plasmin generation and adhesion of pancreatic cancer cells to the endothelial cells. As mention before our group developed a first generation of the molecules that inhibit interaction between annexin A2 and S100A10 (Reddy et al., 2011). Therefore, a hypothesis has been made that annexin A2-S100A10 inhibitors might attenuate pancreatic cancer progression by interfering with invasion, angiogenesis and adhesion of pancreatic cancer cells.

4.2. Aim and objectives

Little is known about the effect of annexin A2-S100A10 complex on pancreatic cancer cells; the aim of the research described in this chapter was to study and investigate the impact of the surface annexin A2-S100A10 complex in pancreatic cancer cells on invasion and plasminogen activation and endothelial adhesion using peptides and annexin A2-S100A10 inhibitors that have been developed recently.

The objectives of this chapter are as following:

1. Determine the effect of annexin A2-S100A10 inhibitors on the invasion of pancreatic cancer cells.
2. Investigate the mechanistic basis beyond pancreatic cancer cell invasion inhibition (protease cascade assay).
3. Establish the existence of annexin A2 and S100A10 proteins on the surface of pancreatic cancer cells.
4. Assess the colocalization of annexin A2 and S100A10 on the surface of pancreatic cancer cells.
5. Measure the effect of peptide and annexin A2-S100A10 inhibitors on the formation of surface annexin A2-S100A10 complex.
6. Assess the effect of peptides and annexin A2-S100A10 inhibitors on the endothelial cells ability to generate plasmin.

7. Investigate whether surface annexin A2-S100A10 complex expression on pancreatic cancer cells mediates adhesion to endothelial cells.

4.3. Results and discussion

4.3.1. Inhibition of pancreatic cancer cell invasion by peptide and annexin A2-S100A10 inhibitors

The effect of annexin A2-S100A10 inhibitors alongside with annexin A2 (Ac-1–14) peptide which is known to inhibit the interaction between annexin A2 and S100A10 (Li et al., 2010) on the ability of pancreatic cancer cells to invade a Matrigel-coated membrane was assessed. Two inhibitors, TRK342 and TRK389 were selected because they exhibited potent target inhibitory activity and showed insignificant anti-proliferative activity (Table 2.4). Thus any effect would be related to the target inhibitory activity on the surface of PANC-1 cells and not to the anti-proliferative effect of annexin A2-S100A10 inhibitors. In addition, LW37 was used as a negative control (chemotype control) as it exhibits low target inhibitory activity (Table 2.6).

Briefly, overnight-starved cells were loaded into the upper chambers of 96-well permeable plates at a density of 2.5×10^4 cells per well. The upper chambers had been pre coated with Matrigel and kept at 37°C to solidify. The annexin A2-S100A10 inhibitors (TRK342, TRK389 and LW37), N-terminal peptide or scrambled peptide at 50 μM, altogether with plasminogen (Plg) at a concentration of 10 nM were added to the upper chamber. The lower chamber was filled with 10% FBS medium containing

fibronectin at 5 µg/ml. 18 h later, the migrated cells in the lower chamber were quantified using a standard cell survival assay (MTT) as shown in Figure 4.1.

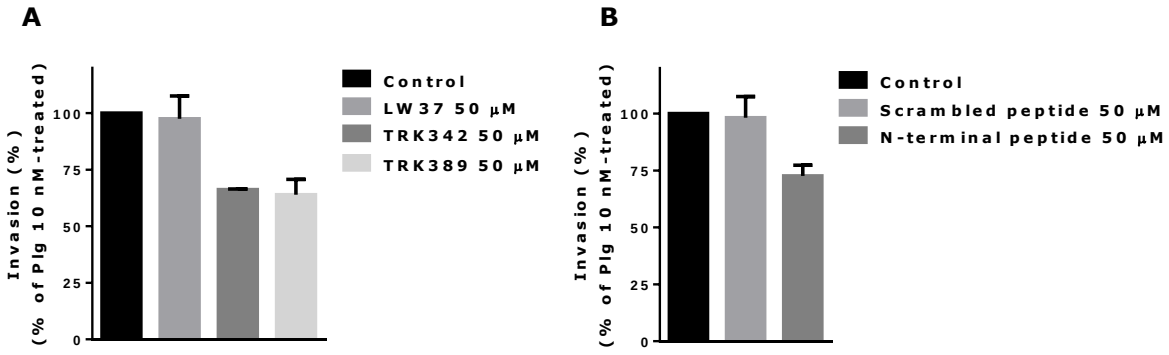


Figure 4.1: The effect of annexin A2-S100A10 inhibitors (A) and peptides (B) on the invasion of PANC-1 cells. Data are expressed as mean ± SEM (n = 3). Non-treated controls were used as a reference for 100% invasion.

As shown in Figure 4.1A, PANC-1 cells invasion was significantly ($P < 0.05$) (one-way ANOVA) reduced after treatment with TRK342 and TRK389 at 50 µM to 66.23 ± 0.28% and 63.94 ± 6.75% of non-treated cells respectively, while at the same time LW37 treatment at 50 µM showed no marked ($P > 0.05$) inhibition with 97.56 ± 10.07% of non-treated cells. Similarly, in Figure 4.1B, the invasion was significantly ($P < 0.05$) reduced after treatment with annexin A2 (Ac-1-14) peptide to 72.68 ± 4.67% of non-treated control, while a scrambled peptide (having same number of residues but different sequence) did not show significant inhibition ($P > 0.05$) with 98.17 ± 9.29% of non-treated control. This indicates that the annexin A2-

S100A10 interaction may be involved in pancreatic cancer cell invasion. The peptide results are in line with a finding showing an 80% decrease in neoangiogenesis of a mouse animal model treated with annexin A2 (Ac-1–14)peptide compared with scrambled peptide (Ling et al., 2004) and with data revealing a decrease in prostate cancer metastasis after treatment with an annexin A2 (1–14) peptide (Shiozawa et al., 2008).

This result turned our attention to address the possible mechanism behind inhibition of pancreatic cancer cell invasion by the above peptide and annexin A2-S100A10 inhibitors.

4.3.2. Protease cascade is involved in pancreatic cancer invasion

Based on the previous results, the next aim was to investigate how peptide and annexin A2-S100A10 inhibitors were able to inhibit pancreatic cancer cell invasion.

4.3.2.1. tPA mediates activation of plasminogen on the surface of pancreatic cancer cells

An important mediator of invasion is the formation of plasmin which is a serine proteinase with a broad proteolytic activity against Extracellular Matrix (ECM), formed from a precursor zymogen plasminogen (Plg) by tPA and uPA. Besides its ability to activate matrix metalloproteinases, facilitating migration and invasion, plasmin itself is also able to degrade some ECM proteins such as laminin and fibronectin leading in the end to metastasis of cancer cells (O'Connell et al., 2010).

Therefore it was assessed whether the invasive ability of pancreatic cancer cells was due to their ability to activate Plg on the surface.

PANC-1 cells were seeded in a 96-well plate at a density of $1x10^5$ cells per well and incubated overnight. The monolayer was then supplemented with tPA 1 nM and incubated for 30 min at room temperature. The unbound tPA was washed away and Plg at 5 nM, and chromogenic plasmin substrate at 100 µM were added consecutively. Plasmin formation was monitored at 405 nm in a PerkinElmer 2104 Multilabel Reader.

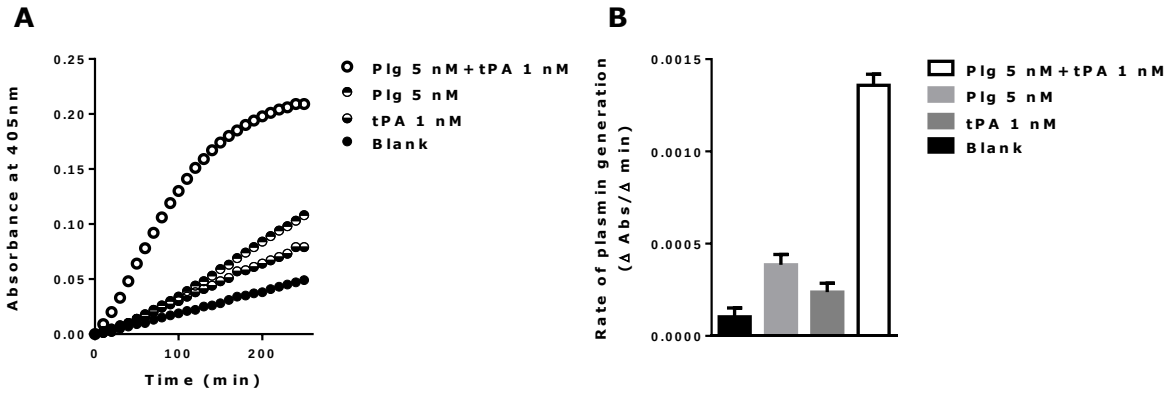


Figure 4.2: (A) Plasmin generation signal. (B) Rate of plasmin generation in PANC-1 cells. Data are expressed as mean ± SEM (n = 3).

Figure 4.2A shows that, additions of Plg 5 nM and tPA 1 nM to PANC-1 cell surface led to a significant increase in the signal, reflecting-plasmin generation. To quantify the activity, the rate of plasmin generation has been determined by the equation Δ Abs/Δ min. Figure 4.2B shows an increase in the rate of plasmin generation upon addition of Plg 5 nM to 3.85×10^{-4} ± 0.56×10^{-4} absorbance units (AU)/time units (min) or tPA 1 nM to 2.37×10^{-4} ± 0.48×10^{-4} absorbance units (AU)/time units (min). Interestingly, the rate

was significantly increased upon addition of both Plg 5 nM and tPA 1 nM to PANC-1 cells to $13.58\times10^{-4} \pm 0.6\times10^{-4}$ absorbance units (AU)/time units (min). This implies that tPA has mediated the conversion of Plg to plasmin due to their binding to the surface of PANC-1 cells rather than in the supernatant solution.

The plasmin generation rate of control was $1.03\times10^{-4} \pm 0.48\times10^{-4}$ absorbance units (AU)/time units (min) which is 7.60% of activity. This may be attributed to auto proteolytic behaviours of PANC-1 cells. However, pre-incubating PANC-1 cells with tPA and benzamidine, a general serine protease inhibitor (Nishimura et al., 1992), followed by addition of Plg and plasmin substrate, has inhibited the percentage rate of the plasmin generation by 84.78% with 15.22 ± 7.97% as shown in Figure 4.3A. This suggested that plasmin substrate may have some auto hydrolysis behaviours.

A significant Plg signal might be attributed to the activation by uPA receptors which have been known to express on the surface of PANC-1 cells (Principe et al., 2015). Pre-incubating PANC-1 cells with tPA and uPA inhibitor II, then addition of Plg and plasmin substrate reduced the plasmin generation by 18.81% to 81.20 ± 3.21% as compared with non-treated control (Figure 4.3B). This indicates a certain contribution of Plg receptors (uPAR) in the activation of Plg to plasmin on the surface of PANC-1 cells as mentioned by (Principe et al., 2015).

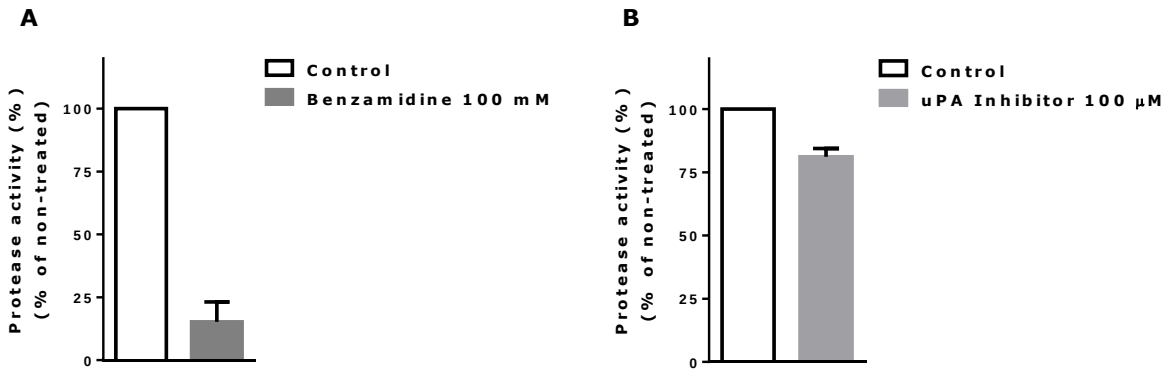


Figure 4.3: Rate percentage of plasmin generation (protease activity percentage) in PANC-1 cells pre-incubated with (A) benzamidine and (B) uPA inhibitor II. Data are expressed as mean ± SEM (n = 3).

Taken together these observations, reveal that PANC-1 cells have significantly activated the conversion of Plg to plasmin on their surface and provide a possible reason for ability of pancreatic cancer cells to digest Matrigel and promote their invasion.

S100A10 and Annexin A2 have been identified as receptors for tPA and Plg; therefore, the next aim was to establish the existence of annexin A2 and S100A10 on the surface of PANC-1 cells and correlate protease activity with their expressions.

4.3.3. Establishment of annexin A2 and S100A10 expression on the surface of pancreatic cancer cells and flow cytometry

It has been shown that pancreatic cancer cells mediate activation of Plg to plasmin on their surfaces that might have led eventually to invasion of these cells. As mentioned in the introduction, several reports correlated in vitro Plg activation with the expression of annexin A2 and/or S100A10 (Kang et al., 1999, Kassam et al., 1998a). Therefore, the next step was to apply the same scenario on PANC-1 cells and assess the relevance of plasmin generation on the surface of these cells with the expression of annexin A2 and S100A10 proteins. Thus, the aim was to determine the presence of annexin A2 and S100A10 on the cell surface of PANC-1 cells using surface biotinylation and flow cytometric technique with specific antibodies.

Briefly, $5x10^5$ cells were gently suspended in ice cold PBS containing 10% FBS and 1% sodium azide. Then a primary antibody to annexin A2 or S100A10 was added to the cells. 30 min later, cells were washed and incubated with secondary fluorescent antibody. Cells were then washed and analyzed by Beckman Coulter Epics XL-MCL flow cytometer (refer to 6.2.13 for more details).

Surface biotinylation was done according the manufacturer instructions. Briefly, confluent cells were incubated with Sulfo-NHS-SS-Biotin solution for 30 min. Then a quenching solution was added before harvesting the cells

and extracting the proteins. Biotinylated proteins were recovered by immobilization on NeutrAvidin beads and eluted in SDS sample buffer. The eluent was analyzed by SDS-PAGE (refer to 6.2.16 for more details).

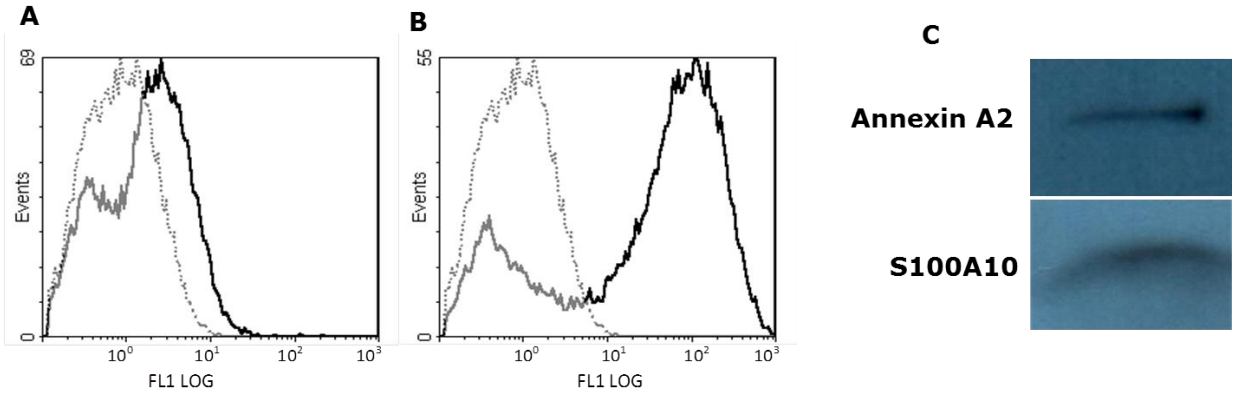


Figure 4.4: Expression of annexin A2 and S100A10 on the surface of PANC-1 cells using flowcytometry and biotinylation techniques. (A) Analysis of annexin A2 antibody binding to PANC-1 cells. Pre-incubation with annexin A2 antibodies then incubation with fluorescent secondary antibodies (solid histogram) or incubation with fluorescent secondary antibodies (dashed histogram). (B) Analysis of S100A10 antibody binding to PANC-1 cells. Pre-incubation with S100A10 antibodies then incubation with fluorescent secondary antibodies (solid histogram) or incubation with fluorescent secondary antibodies (dashed histogram). (C) Expression of annexin A2 and S100A10 on the surface of PANC-1 cells by biotinylation. A representation of single experiment is shown (n = 2).

Figure 4.4A shows a right shift in the signal when the cells were pre-incubated with annexin A2 antibodies then treated with fluorescent secondary antibodies. Figure 4.4B also exhibits a right shift in the signal when cells were pre-incubated with S100A10 antibodies then treated with fluorescent antibodies. To quantify the signal, the geometric mean ± SEM of the histograms has been determined. This revealed a shift from 3.73 ± 1.32 (dashed histograms) to 6.53 ± 1.46 when the cells were pre-incubated with annexin A2 antibody (solid histogram; A) and to 230.53 ± 62.83 when the cells were pre-incubated with S100A10 antibody (solid histogram; B). Figure 4.4C exhibits that annexin A2 and S100A10 were expressed on the surface of PANC-1 cells as measured by surface biotinylation.

Taken together these observations indicate that annexin A2 and S100A10 proteins are expressed on the surface of PANC-1 cells. This implicates that Plg dependent tPA activation on the surface of PANC-1 cells might be due to annexin A2 and or S100A10 expression.

To further strengthen the idea of involvement of S100A10 and annexin A2 in Plg dependent tPA activation on the surface of PANC-1 cells, the next step was to assess the effect of S100A10 and annexin A2 specific antibodies on the PANC-1 cells surface protease activity.

4.3.4. Annexin A2 and S100A10 antibodies inhibit protease cascade on the surface of PANC-1 cells

The aim of the work described in this section was to relate Plg dependent tPA activation on the surface of PANC-1 cells to the expression annexin A2 and/or S100A10 as shown in the previous section. Therefore, the the effect of antibodies targeting annexin A2 and S100A10 proteins on the rate of plasmin generation was determined.

$1x10^5$ cells per well were seeded in a 96-well plate and incubated overnight. The monolayer was exposed to antibodies (annexin A2, S100A10 and isotype IgG1κ control). The monolayer was then supplemented with 2 nM tPA and incubated for 30 min at room temperature. The unbound tPA was washed away and Plg at 5 nM, and chromogenic plasmin substrate at 100 μM were added consecutively. Plasmin formation was monitored at 405 nm in a PerkinElmer 2104 Multilabel Reader as seen in Figure 4.5.

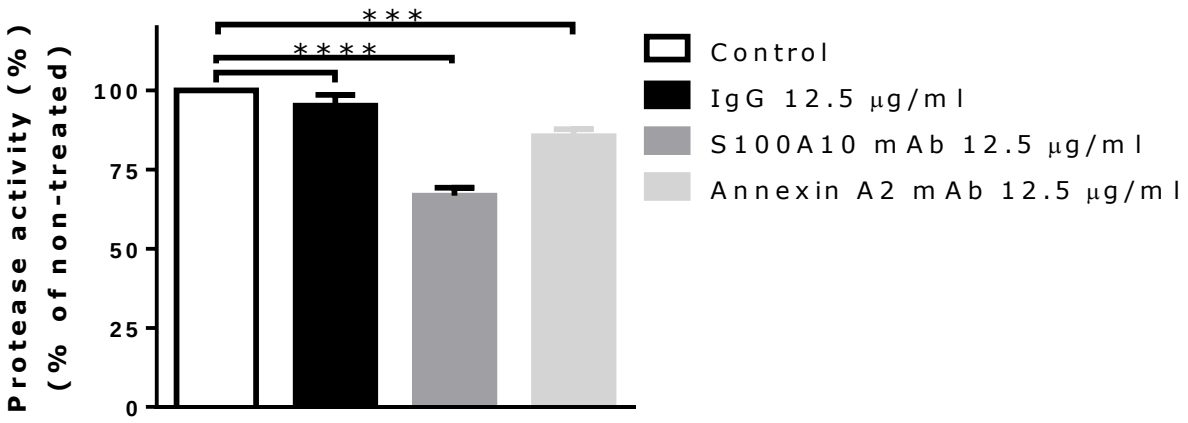


Figure 4.5: Effect of antibodies treatment on the rate of plasmin generation (protease activity percentage) on the surface of PANC-1 cells. Data are expressed as mean ± SEM (n = 3) of unpaired t test.

Figure 4.5 shows a significant ($P < 0.0001$) decrease in plasmin generation in PANC-1 cells pretreated with S100A10 antibodies to 66.83 ± 2.42% protease activity and in cells pretreated with annexin A2 antibodies ($P < 0.0003$) to 85.57 ± 2.20% protease activity both as compared to non-treated control. Pretreatment of PANC-1 cells with isotype IgG showed no significant ($P > 0.05$) inhibition of plasmin generation as compared with non-treated control. This result confirms involvement of S100A10 and annexin A2 in the activation of Plg on the surface of PANC-1 cells.

Annexin A2 antibodies used in this experiment were recognizing the C-terminal portion of the protein (residues 123-328) and since the binding of tPA has been linked to the N-terminal of annexin A2 (Hajjar et al., 1998) therefore it was unlikely to inhibit the plasmin generation by competing with

tPA binding. Thus, this significant inhibition of plasmin generation by annexin A2 antibodies might be related to steric interference of high molecular weight antibodies (150 kDa). Anti-annexin A2 IgG directed to the N-terminal tail of annexin A2 was found to inhibit 55% of plasmin generation on the surface of human monocyte (Brownstein et al., 2004). This might explain why annexin A2 antibodies showed significant inhibition of cell invasion. Indeed, Zheng et al have inhibited the invasion of pancreatic cancer cells using anti annexin A2 antibodies targeting N-terminal (Zheng et al., 2011).

S100A10 antibodies used were recognizing the full length of the protein. This explains the marked significant inhibition of plasmin generation by the antibodies due to the inability of Plg to bind to S100A10. Plg binding to the receptors has been found to be mediated through C-terminal lysine residues (MacLeod et al., 2003) which could not be found in annexin A2 monomer but in the S100A10 C-terminal (Kang et al., 1999). Moreover, S100A10 with the C-terminal lysine deleted retains only 15% of its Plg conversion activity as compared with the wildtype protein (Semov et al., 2005). Indeed, 6-aminocaproic acid, a structural analogue of lysine, inhibited protease activity very significantly ($P < 0.0001$) while at the same time glycine did not ($P > 0.05$) as seen in Figure 4.6.

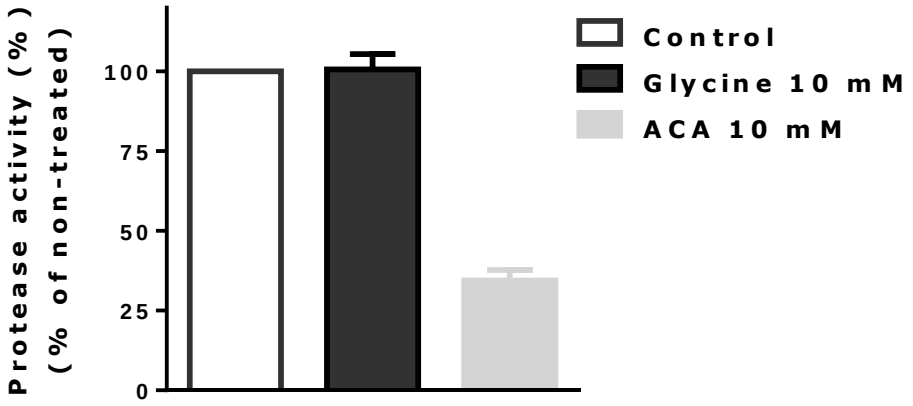


Figure 4.6: Effect of ACA and glycine on the rate percentage of plasmin generation (protease activity percentage). Data are expressed as mean ± SEM (n = 3).

This result reveals the significance of C-terminal lysine residue in the binding of Plg to the cell surface and is in line with data related the anti-angiogenic effect of 6-aminocaproic acid with its ability to suppress plasmin formation (Semov et al., 2005). It also indicates that the S100A10 has a superior role over annexin A2 in regulating plasmin generation on the surface of PANC-1 cells. In fact, a very recent poster showed that S100A10 siRNA knockdown significantly inhibited plasmin dependent PANC-1 cells invasion (Bydoun et al., 2015).

Taken together all these results further confirm that S100A10 and annexin A2 are essential contributors in Plg dependent tPA activation on the surface of PANC-1 cells.

4.3.5. Inhibition of protease cascade by N-terminal peptide and annexin A2-S100A10 inhibitors

It has been shown that pancreatic cancer cells mediated activation of Plg to plasmin on their surfaces through annexin A2 and/or S100A10 dependent mechanism which might have led eventually to invasion of these cells. Therefore, a hypothesis has been made that N-terminal peptide and annexin A2-S100A10 inhibitors might have inhibited the invasion (Figure 4.1) by interfering with annexin A2 and/or S100A10 plasmin generation. Thus the aim was to measure their effect on the surface protease activity of PANC-1 cells.

Besides N-terminal peptide, two target potent cellular active inhibitors (TRK347 and TRK355) (Table 2.3), two target potent cellular inactive inhibitors (TRK381 and TRK342) (Table 2.4), and two target potent moderately cellular active inhibitors (TRK317 and TRK5) (Table 2.5), were chosen for this experiment alongside the inactive LW37 (chemotype) (Table 2.6).

$1x10^5$ cells per well were seeded in a 96-well plate and incubated overnight. The monolayer was then exposed to 50 μM annexin A2-S100A10 inhibitors, 50 μM N-terminal peptide or 50 μM scrambled peptide for 60 min. Each well was then supplemented with 1 nM tPA and incubated for 30 min at room temperature. The cells were washed then 5 nM Plg and chromogenic plasmin

substrate at 100 μM were added consecutively. Plasmin formation was monitored at 405 nm in a PerkinElmer 2104 Multilabel Reader as shown in Figure 4.7.

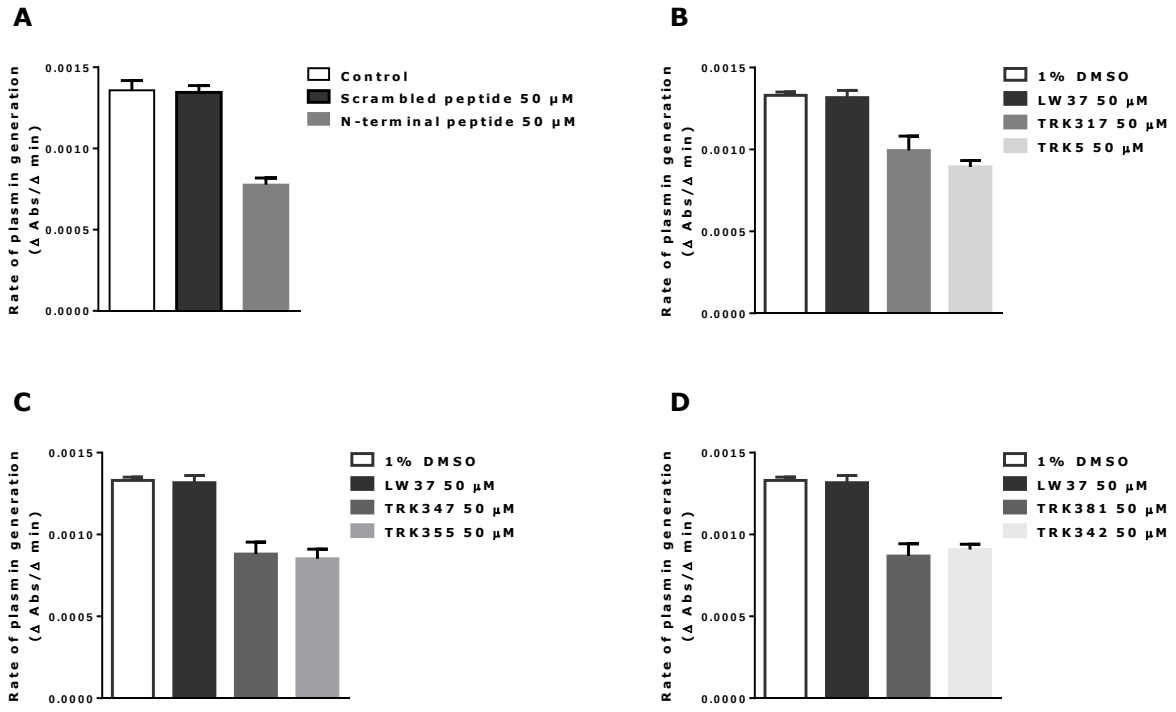


Figure 4.7: Effect of (A) N-terminal peptide, (B), (C) and (D) annexin A2-S100A10 inhibitors on the rate of plasmin generation (protease activity) in PANC-1 cells. Data are expressed as mean ± SEM (n = 3).

As shown in Figure 4.7A the N-terminal annexin (Ac-1-14) peptide at 50 μM significantly ($P < 0.05$) reduced the rate of plasmin generation (Δ Abs/Δ min) to 57.2% form $13.58\times10^{-4} \pm 0.60\times10^{-4}$ absorbance units (AU)/time units (min) of non-treated control to $7.78\times10^{-4} \pm 0.71\times10^{-4}$ absorbance units (AU)/time units (min), while at the same concentration scrambled peptide

has no significant ($P > 0.05$) effect at $13.45\times10^{-4} \pm 0.29\times10^{-4}$ absorbance units (AU)/time units (min) compared to $13.58\times10^{-4} \pm 0.60\times10^{-4}$ absorbance units (AU)/time units (min) in the non-treated control.

Furthermore, in Figures 4.7B-D, all selected annexin A2-S100A10 inhibitors TRK317, TRK5, TRK347, TRK355, TRK381 and TRK342 at 50 μM significantly ($P < 0.05$) decreased the rate of plasmin production (Δ Abs/Δ min) on the surface of PANC-1 cells at a rate of $9.93\times10^{-4} \pm 0.88\times10^{-4}$ absorbance units (AU)/time units (min), $8.93\times10^{-4} \pm 0.39\times10^{-4}$ absorbance units (AU)/time units (min), $8.8\times10^{-4} \pm 0.73\times10^{-4}$ absorbance units (AU)/time units (min), $8.5\times10^{-4} \pm 0.59\times10^{-4}$ absorbance units (AU)/time units (min), $8.6\times10^{-4} \pm 0.75\times10^{-4}$ absorbance units (AU)/time units (min) and $9.0\times10^{-4} \pm 0.31\times10^{-4}$ absorbance units (AU)/time units (min) respectively compared to $13.30\times10^{-4} \pm 0.19\times10^{-4}$ absorbance units (AU)/time units (min) in 1% DMSO-treated control. LW 37 at 50 μM or 1% DMSO showed no significant ($P > 0.05$) inhibitory effect on Plg conversion, with activation rates of $13.16\times10^{-4} \pm 0.44\times10^{-4}$ absorbance units (AU)/time units (min) and $13.30\times10^{-4} \pm 0.19\times10^{-4}$ absorbance units (AU)/time units (min) respectively compared to $13.58\times10^{-4} \pm 0.60\times10^{-4}$ absorbance units (AU)/time units (min) in the non-treated control.

These results indicate that annexin A2-S100A10 inhibitors and N-terminal peptide were able to inhibit surface protease activity of PANC-1 cells and provide an explanation for the ability of these molecules to inhibit PANC-1 cells invasion as shown in Figure 4.1.

These findings appear consistent with the findings reported in biochemical assays that annexin A2-S100A10 complex enhances Plg dependent tPA activation at a higher rate than the annexin A2 monomer (Kassam et al., 1998a). It is also consistent with a finding that N-terminal annexin A2 (Ac-1–14) peptide inhibited metastasis of prostate cancer cells into the bone marrow in mice (Shiozawa et al., 2008) as well as with a previous report that N-terminal annexin A2 (Ac-1–14) peptide inhibits neoangiogenesis into Matrigel plugs in a mouse model system (Ling et al., 2004).

It could be argued that the decrease of the signal (plasmin generation) after treatment with annexin A2-S100A10 inhibitors was due to cell detachment as a consequence of decreased cell viability by annexin A2-S100A10 inhibitors. And as mentioned in chapter 2, cell viability was affected by some inhibitors after 72 h treatment. The protease activation assay described in the previous sections involved incubation for 1 h, which is a lot shorter than 72 h. It is likely that the inhibitors do not affect cell viability over this timeframe. Indeed, 1 h pre-incubation of PANC-1 cells with moderately cellular active or cellular active annexin A2-S100A10 inhibitors then subjecting the cells to MTT assay (refer to 6.2.4 for more details) showed no

significant growth inhibition (*P > 0.05*) on PANC-1 cells as seen in the Figure 4.8. Therefore the decrease in plasmin generation rate was most likely due to inhibition of protease activity on the surface of PANC-1 cells.

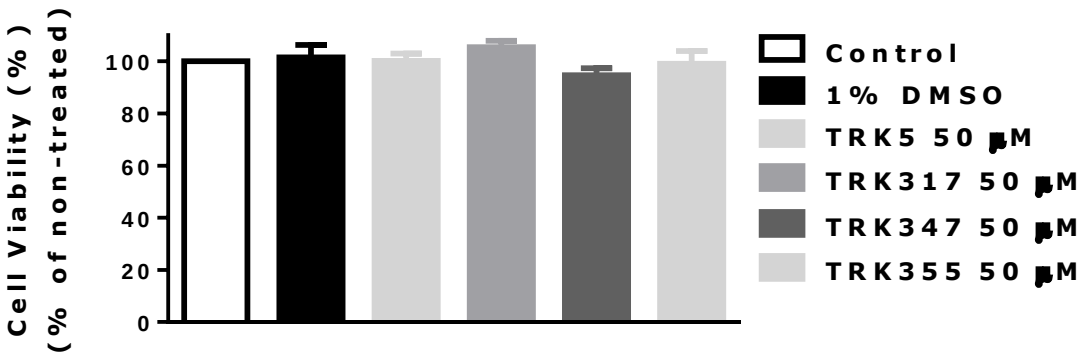


Figure 4.8: Effect of 1 h pre-incubation with moderately cellular active and cellular active annexin A2-S100A10 inhibitors on PANC-1 cells viability. Data are expressed as mean ± SEM (n = 4).

Taken together all these observations indicate that annexin A2-S100A10 inhibitors interfere with protease activity on the surface of PANC-1 cells through Annexin A2 and S100A10 proteins and further confirm the significant role of annexin A2 and S100A10 in the activation of protease cascade on the surface of PANC-1 cells.

At the level of annexin A2-S100A10 complex, S100A10 is likely the major regulator affecting plasmin generation and Plg may bind to S100A10 through C-terminal lysine as shown in Figure 4.6 and mentioned before (MacLeod et al., 2003). On the other hand, tPA binds to annexin A2 N-terminal tail distal to S100A10 binding site (Diaz, 2004). Therefore, the most likely explanation of our results would be that treatment of PANC-1 cells with annexin A2-S100A10 inhibitors releases S100A10 that tethers Plg from the N-terminal annexin A2 that anchors tPA, thereby preventing Plg from being activated by tPA.

Thus, the next step was to assess the colocalization of annexin A2 and S100A10 in PANC-1 cells and whether annexin A2-S100A10 inhibitors would affect the interaction between these proteins.

4.3.6. Annexin A2 and S100A10 are colocalized in PANC-1 cells

It has been shown in the previous sections that annexin A2 and S100A10 individually or in a complex mediated plasmin generation on the surface of PANC-1. It has been also shown that annexin A2-S100A10 inhibitors along with N-terminal peptide inhibited the formation of plasmin on the surface of PANC-1 cells. This inhibition has been related to the ability of annexin A2-S100A10 inhibitors to disrupt a complex formation between annexin A2 and S100A10 proteins.

Therefore, the aim was to assess the colocalization of the annexin A2 and S100A10 in PANC-1 cells and whether annexin A2-S100A10 inhibitors are able to inhibit the complex formation in PANC-1 cell lysate.

Briefly, the complex in PANC-1 cells extract was immunoprecipitated by S100A10 antibody. Then it was incubated with protein A/G agarose. Protein A/G agarose was then recovered by centrifugation and re-suspended in loading buffer before subjecting to electrophoresis and immunoblotting. Annexin A2-S100A10 inhibitors were pre-incubated with PANC-1 cell lysate prior to the immunoprecipitation (refer to 6.2.15 for more details) as shown in Figure 4.9.

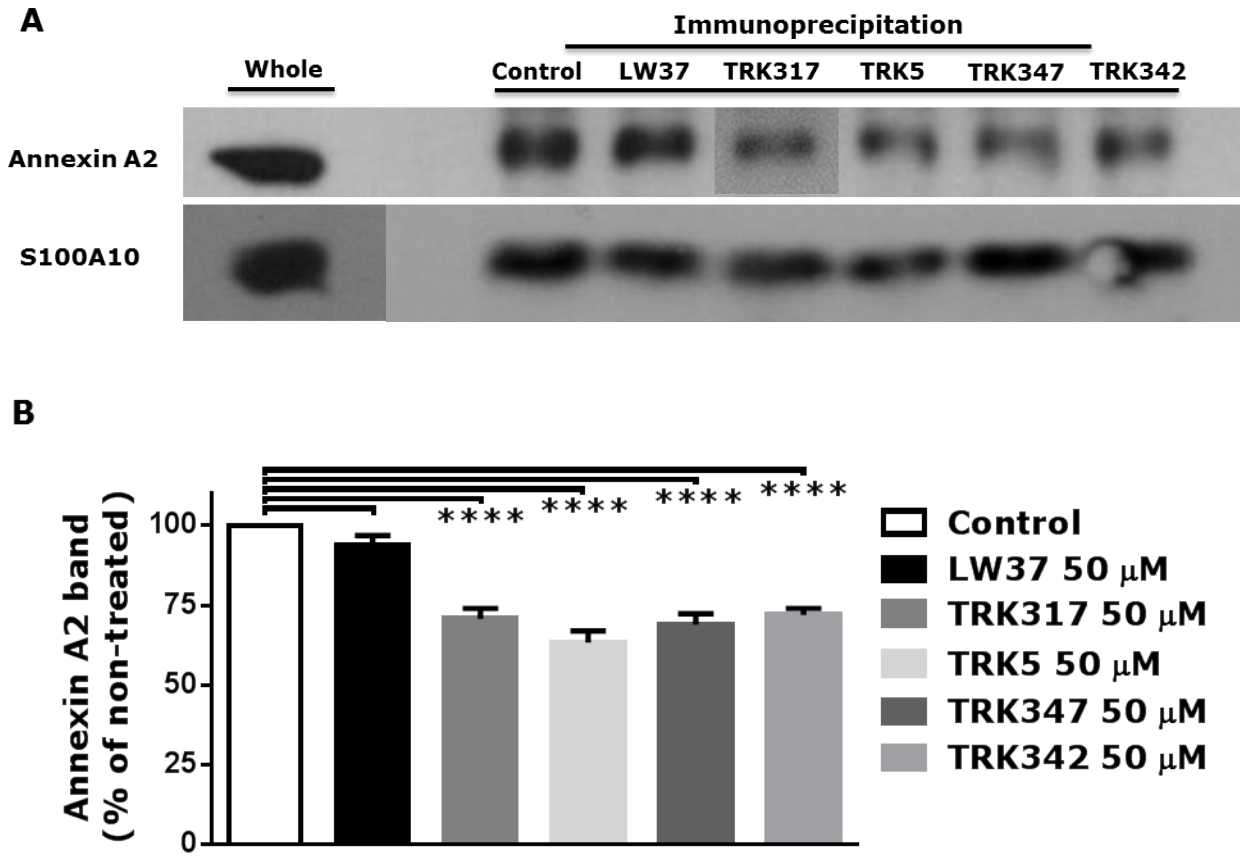


Figure 4.9: Analysis of the interaction between S100A10 and annexin A2. S100A10 was immunoprecipitated then annexin A2 in the immunoprecipitate was analyzed by western blotting using an annexin A2 antibody. (A) Annexin A2 bands in annexin A2-S100A10 inhibitors 50 μM pre-treated lysate as compared with non-treated control. (B) Multiple IP experiments (n = 6) with data expressed as mean ± SEM showed that annexin A2-S100A10 inhibitors at 50 μM significantly ($P < 0.0001$) inhibited annexin A2-S100A10 complex when compared with non-treated control, while at the same time and dose LW37 showed no marked inhibition ($P > 0.05$) (unpaired t test).

Figure 4.9A shows that annexin A2 co-immunoprecipitated with S100A10 in PANC-1 cell lysate. Thus annexin A2 and S100A10 proteins are normally colocalized in PANC-1 cells. Thus annexin A2 and S100A10 proteins may be involved in regulating the protease cascade and invasion of PANC-1 cells in complex form rather than as individual proteins.

Interestingly in Figure 4.9B all selected target active annexin A2-S100A10 inhibitors showed a significant decrease in annexin A2 bands at 50 μM ($P < 0.0001$) when compared to non-treated control, while LW37 at 50 μM showed no marked reduction ($P > 0.05$). Thus all target active annexin A2-S100A10 inhibitors disrupted annexin A2-S100A10 complex in PANC-1 lysate while LW37 (inactive chemotype) did not.

These marked results confirm the idea that annexin A2-S100A10 inhibitors inhibited protease activity and invasion of PANC-1 cells by interfering with annexin A2-S100A10 complex formation. However, since this result showed that these inhibitors targeted annexin A2-S100A10 interaction in PANC-1 cell whole lysate, it might be argued that there is a difference between intracellular and extracellular annexin A2-S100A10 as implied Hajjar group (Deora et al., 2004). Thus it would be more preferable to have direct evidence of disruption of the surface annexin A2-S100A10 complex.

Therefore measuring the effect of annexin A2-S100A10 inhibitors on the surface annexin A2-S100A10 complex of intact PANC-1 cells would reassure

and confirm our hypothesis regarding inhibition of protease activity by disruption of extracellular annexin A2-S100A10 complex.

4.3.7. Annexin A2-S100A10 inhibitors and N-terminal peptide inhibit surface interaction of annexin A2 and S100A10

Deora et al in 2004 mentioned that annexin A2 binds to S100A10 in the cytoplasm, then they migrate together to the inner left of cell membrane where the annexin A2 is phosphorylated by src 60 before they flip out together to the cell surface by mechanism yet to be resolved (Deora et al., 2004). Thus, it could be a possibility that intracellular annexin A2-S100A10 complex has a structural configuration slightly different from the surface complex. Therefore, the aim was to assess the effect of annexin A2-S100A10 inhibitors on the surface complex.

If pretreating PANC-1 cells with annexin A2-S100A10 inhibitors or N-terminal peptide would release S100A10 but not annexin A2 from the cell surface, it would be expected that if cells are subsequently analysed by flow cytometry using an S100A10 antibody for surface detection of S100A10, this would lead to a lower (left shifted) S100A10 signal.

$5x10^5$ cells were suspended in 5% FBS 500 µl PBS then incubated with S100A10 antibody 40 min. Cells were then washed and incubated for 30 min with secondary antibody. Cells were washed and re-suspended in 500 µl

PBS. Whenever indicated, annexin A2-S100A10 inhibitors and N-terminal peptide at 50 μM were incubated with PANC-1 cells for 40 min before surface labelling with the antibodies. Analysis was done by Patrec CyFlow. Data processing as seen in Figures 4.10 and 4.11 was conducted by flowJO.

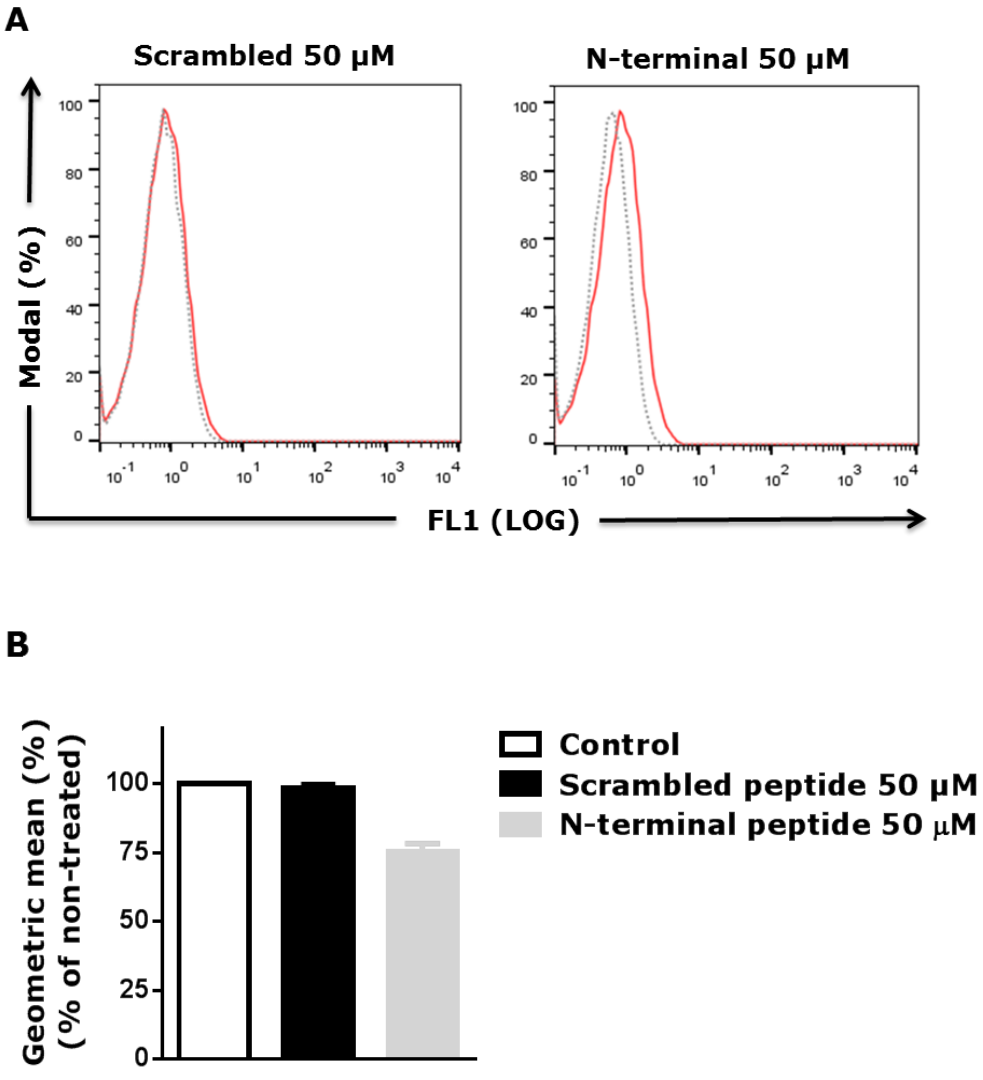


Figure 4.10: Effect of N-terminal peptide treatment on the surface S100A10 signal of PANC-1 cells. (A) Red histograms (incubation with S100A10 antibodies then with secondary fluorescent antibodies); dashed histograms (pre-incubation with

scrambled peptide or N-terminal peptide at 50 μM before incubation with S100A10 antibodies then secondary fluorescent antibodies. (B) Multiple experiments expressed as geometric mean percentage ± SEM (n = 4).

Figure 4.10A reveals a left shift in the S100A10 (dashed) histogram after treatment with N-terminal peptide 50 μM as compared with non-treated control (red) histogram but not after treatment with scrambled peptide at 50 μM. Measuring geometric means of multiple experiments (n = 4) in Figure 4.10B reveals a significant decrease in S100A10 fluorescence of PANC-1 cells pretreated with N-terminal peptides ($P < 0.0001$) but not scrambled peptide ($P > 0.05$) as compared to non-treated controls.

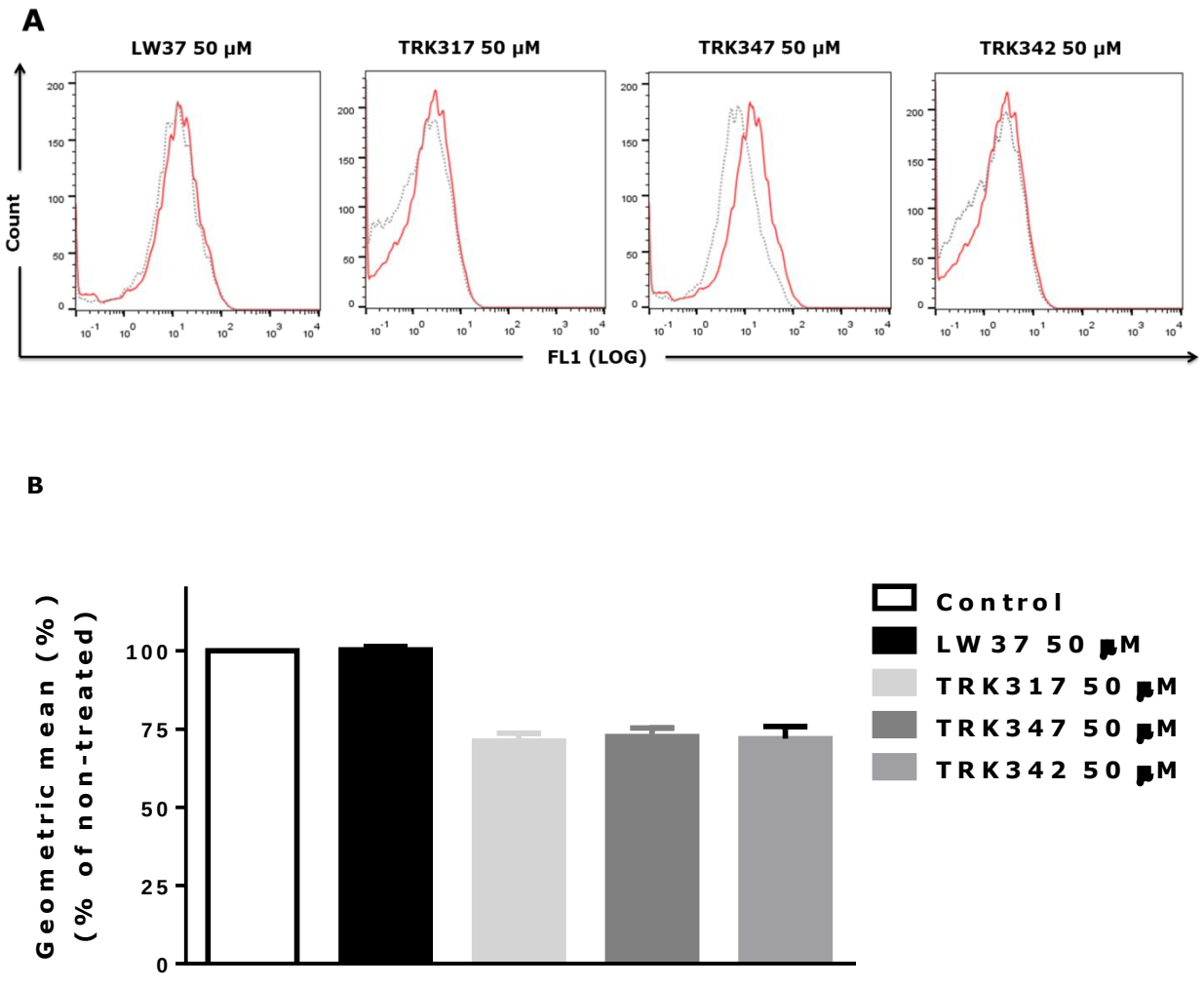


Figure 4.11: Effect of annexin A2-S100A10 inhibitors treatment on the surface S100A10 signal of PANC-1 cells. (A) Red histograms (incubation with S100A10 antibodies then with secondary fluorescent antibodies); dashed histograms (pre-incubation with annexin A2-S100A10 inhibitors at 50 µM before incubation with S100A10 antibodies then secondary fluorescent antibodies. (B) Multiple experiments expressed as geometric mean percentage ± SEM (n = 4).

As per our prediction, in Figure 4.11A pretreating PANC-1 cells with target active annexin A2-S100A10 inhibitors (TRK317, TRK347 and TRK342) at 50 μM but not with LW37 at 50 μM induced a left shift in S100A10 (dashed) histograms as compared with non-treated controls (red) histograms. Measuring geometric means of multiple experiments (n = 4) in Figure 4.11B reveals a significant decrease ($P < 0.0001$) in S100A10 fluorescence of PANC-1 cells pretreated with annexin A2-S100A10 inhibitors (TRK317, TRK347 and TRK342) at 50 μM but not PANC-1 cells pretreated with LW37 at 50 μM ($P > 0.05$) as compared with non-treated controls.

These results indicate that pretreatment of PANC-1 cell surface with N-terminal peptide or annexin A2-S100A10 inhibitors liberates S100A10 from the surface. This would lead to a decreased ability of Plg to attach to the surface in order to be activated by tPA bound annexin A2.

4.3.8. Annexin A2-S100A10 inhibitors increase binding of Cy5-S100A10 to the surface of pancreatic cancer cells

In this section the aim was to strengthen our conclusion in the previous section that S100A10 is released from the PANC-1 cell surface after treatment with annexin A2-S100A10 inhibitors. It was predicted that more freed annexin A2 would exist on the surface PANC-1 cells treated with annexin A2-S100A10 inhibitors than on the non-treated cells. This would lead to more Cy5-S100A10 tracer binding (higher signal) to the treated PANC-1 cells than to the non-treated cells.

4.3.8.1. Preparation of recombinant S100A10

The first aim was to express S100A10 and to label it with Cy5 to use as a tracer on the surface of PANC-1 cells.

S100A10 was expressed using *E.coli*. The bacteria were made competent then transformed using specific DNA. After which a 1 L culture of *E.coli* harboring pET14b-S100A10 was grown then induced by IPTG after which the cells were harvested. The pellet was suspended in binding buffer before protein extraction. The supernatant was then purified by Ni-NTA-agarose beads. S100A10 was then eluted in imidazole elution buffer (refer to 6.2.18 for more details). The purified protein was run on a 15% SDS-PAGE before staining with Coomassie blue (refer to 6.2.18.7 for more details) as shown in Figure 4.12.

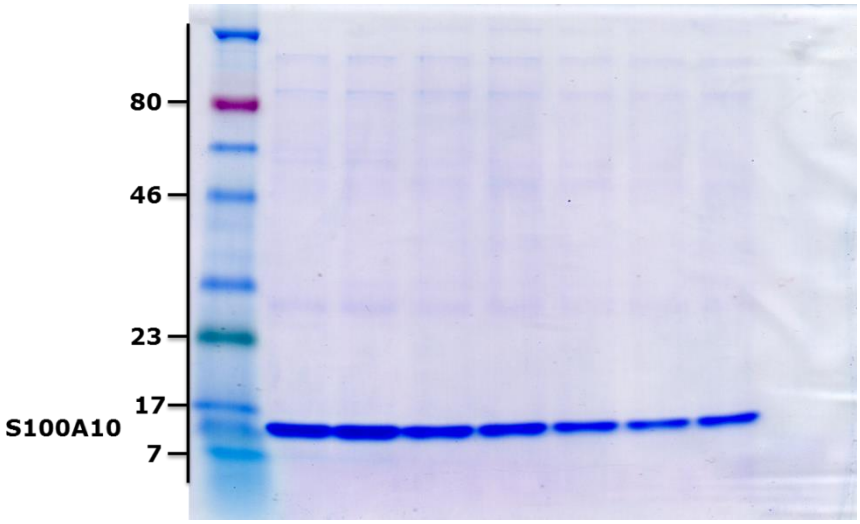


Figure 4.12: Multiple purified S100A10 fractions stained with Coomassie blue.

4.3.8.2. Measuring the concentration of purified S100A10

As shown in the previous section, recombinant S100A10 protein has been expressed and purified. Therefore, the next step was to determine the concentration of S100A10 and use this concentration to assess its binding to the surface of PANC-1 cells.

Protein concentration was measured in a Nano drop available at Nottingham University and calculated using the following equation,

$$\mathbf{C_{protein}(mol \cdot L^{-1}) = \frac{absorbance\ at\ 280\ nm\ (1\ cm)}{extinction\ coefficient}}$$

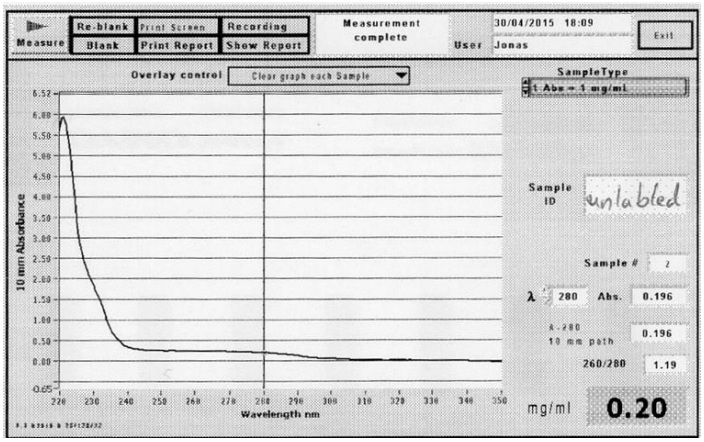


Figure 4.13: Nano drop absorbance of a purified S100A10 at 280 nm with 10 mm path length. The curve shows the absorbance of S100A10 at 280 nm is 0.196.

The extinction coefficient for S100A10 is 2800. Therefore according to the absorbance and equation, the concentration of purified unlabeled S00A10 was 71 µM.

4.3.8.3. S100A10 Cy5-labelling

Purified S100A10 was labelled by incubating with Cy5-monofunctional reactive dye (refer to 6.2.19 for more details). The concentration of labelled S100A10 was also measured by a Nano drop available at Nottingham University.

The concentrations of both Cy5 dye and labelled S100A10 protein were calculated using the GE's Cy5 mono-reactive dye equations as follows:

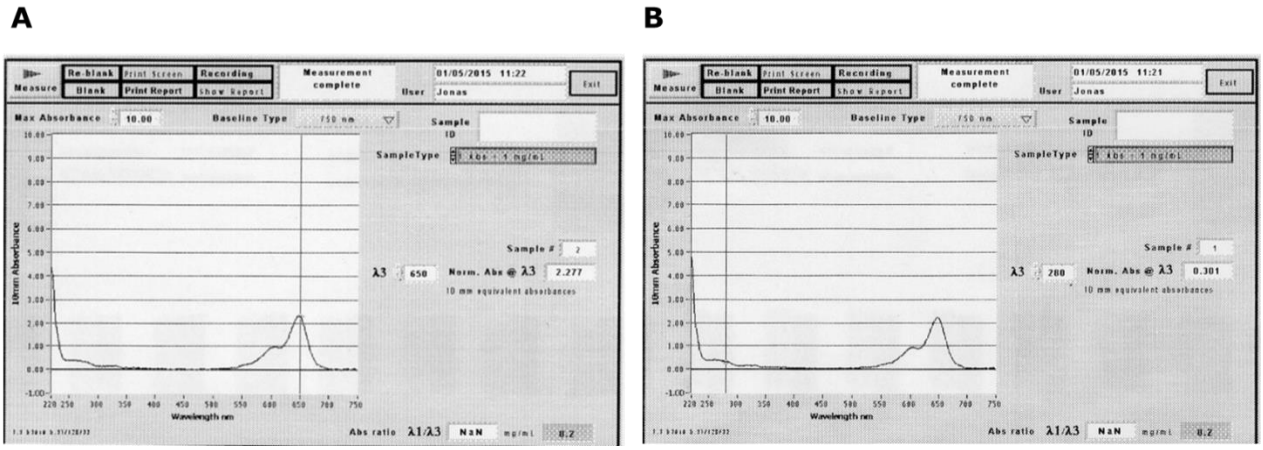


Figure 4.14: Nano drop absorbance of a purified labelled S100A10 at 650 and 280 nm with 10 mm path length. The curve shows the absorbance of S100A10 at 650 and 280 nm is 2.27 and 0.30 respectively.

$$\mathbf{C_{Cy5}(mol \cdot L^{-1}) = \frac{absorbance\ at\ 650\ nm\ (1cm)}{extinction\ coefficient}}$$

$$\mathbf{C_{protein}(mol \cdot L^{-1}) = \frac{[absorbance\ at\ 280\ nm] - 0.05[absorbance\ at\ 650\ nm]}{extinction\ coefficient}}$$

According to the equations the concentration of Cy5 was 9.08 μM and that of labelled S100A10 was 66.9 μM

Calculating the efficiency of labelling indicated that about 13.55% of S100A10 was labelled with Cy5.

Next the ability of Cy5-S100A10 to bind to PANC-1 cell surface and more specifically to the annexin A2 protein was assessed.

4.3.8.4. Cy5-S100A10 binds to the surface of pancreatic cancer cells

The ability of the Cy5-S100A10 tracer to bind to the surface of PANC-1 cells was measured.

PANC-1 cells were seeded in a 96 well plate at $1.5x10^5$ cells per well and incubated overnight. The monolayer was then incubated with serial concentrations of Cy5 labelled S100A10 (5, 0.5, 0.05, 0.005 and 0.0005 μM) alone or with 10 times serial concentrations of unlabeled S100A10 (50, 5, 0.5, 0.05, 0.005 μM) as shown in Figure 4.15.

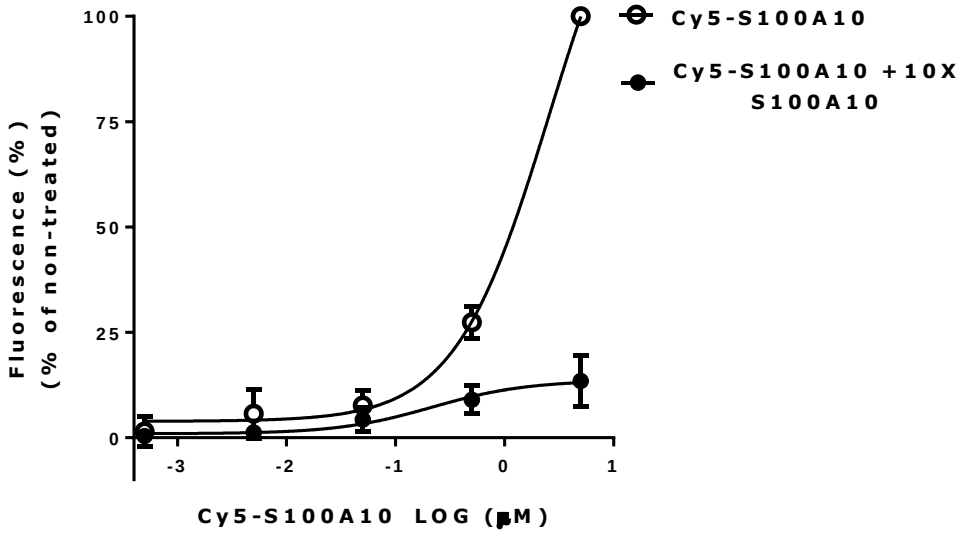


Figure 4.15: Cy5-labelled S100A10 dependent-annexin A2 binding to PANC-1 cells surface. Data are expressed as mean ± SEM (n = 2).

Figure 4.15 shows that Cy5-S100A10 binds to the surface of PANC-1 cells in a dose dependent manner. Incubating PANC-1 cells with Cy5-S100A10 and 10 times unlabeled S100A10 reveals selectivity in binding of Cy5-S100A10 tracer to the cells surface. This might indicate that Cy5-S100A10 was able to

displace the native S100A10 and selectively binds to the freed annexin A2 on the surface of PANC-1 cells.

This result reinforces our previous data of the colocalization of these proteins on the surface of PANC-1 cells and is comparable with Myrvang et al finding who observed a Cy5-S100A10 binding to MDA-MB-231 cells expressing annexin A2 on their surface (Myrvang et al., 2013).

4.3.8.5. Annexin A2-S100A10 inhibitors increase Cy5-S100A10 tracer binding to the surface of PANC-1 cells

The binding of Cy5-labelled S100A10 to PANC-1 cells was used to determine the disruption of the endogenous annexin A2-S100A10 complex on the cell surface of PANC-1 cells. Pretreatment of PANC-1 cells with annexin A2-S100A10 inhibitors would release the native S100A10 from annexin A2 leading to an increase in the binding of the applied Cy5-S100A10 to the annexin A2 on PANC-1 cells surface.

PANC-1 cells were seeded in black 96-well plates at $1.5x10^5$ cells per well and incubated overnight. The monolayer was then incubated with TRK317, TRK347, TRK342 or inactive LW37 at 50 μM. Then cells were incubated with 5 μM Cy5-S100A10 tracer for 20 min. Subsequently, cells were then washed and fluorescence was taken at PerkinElmer 2104 Multilabel Reader with 620 nm excitation and 685 nm emissions as shown in Figure 4.16.

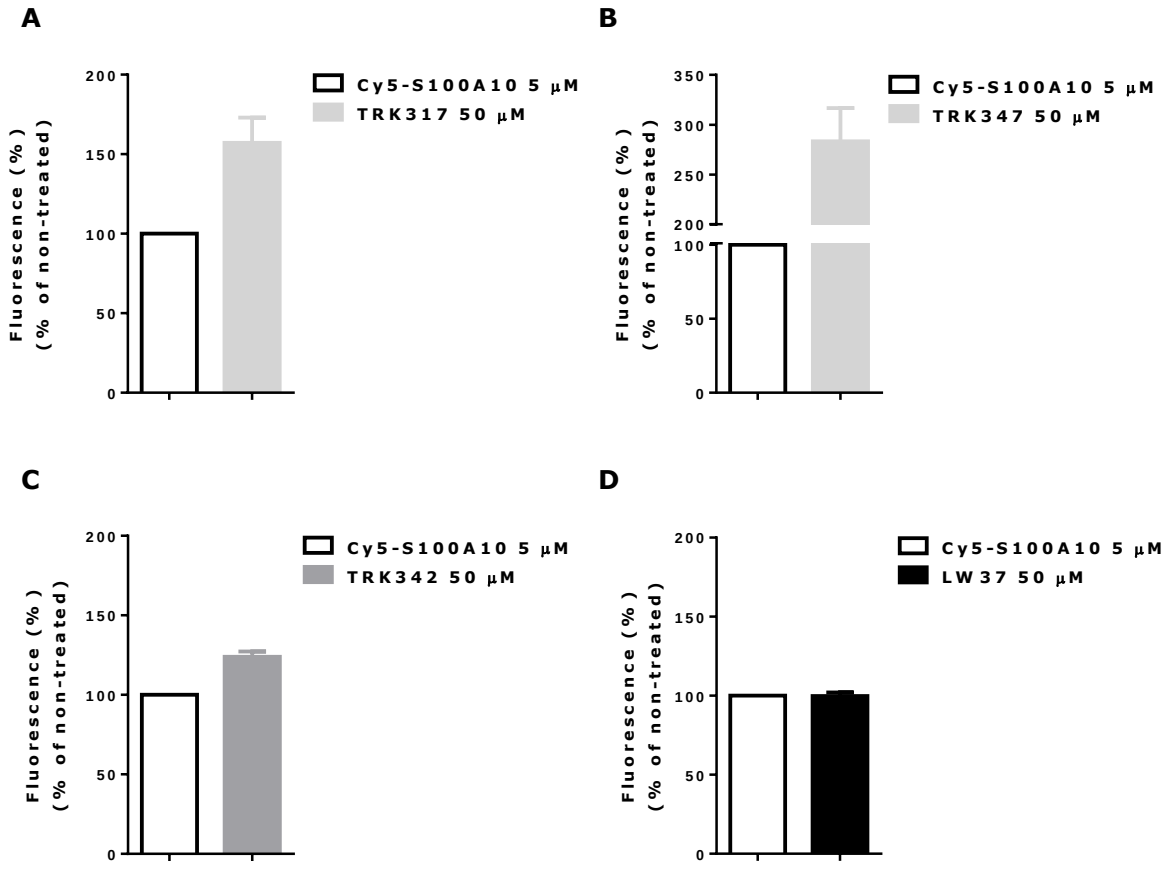
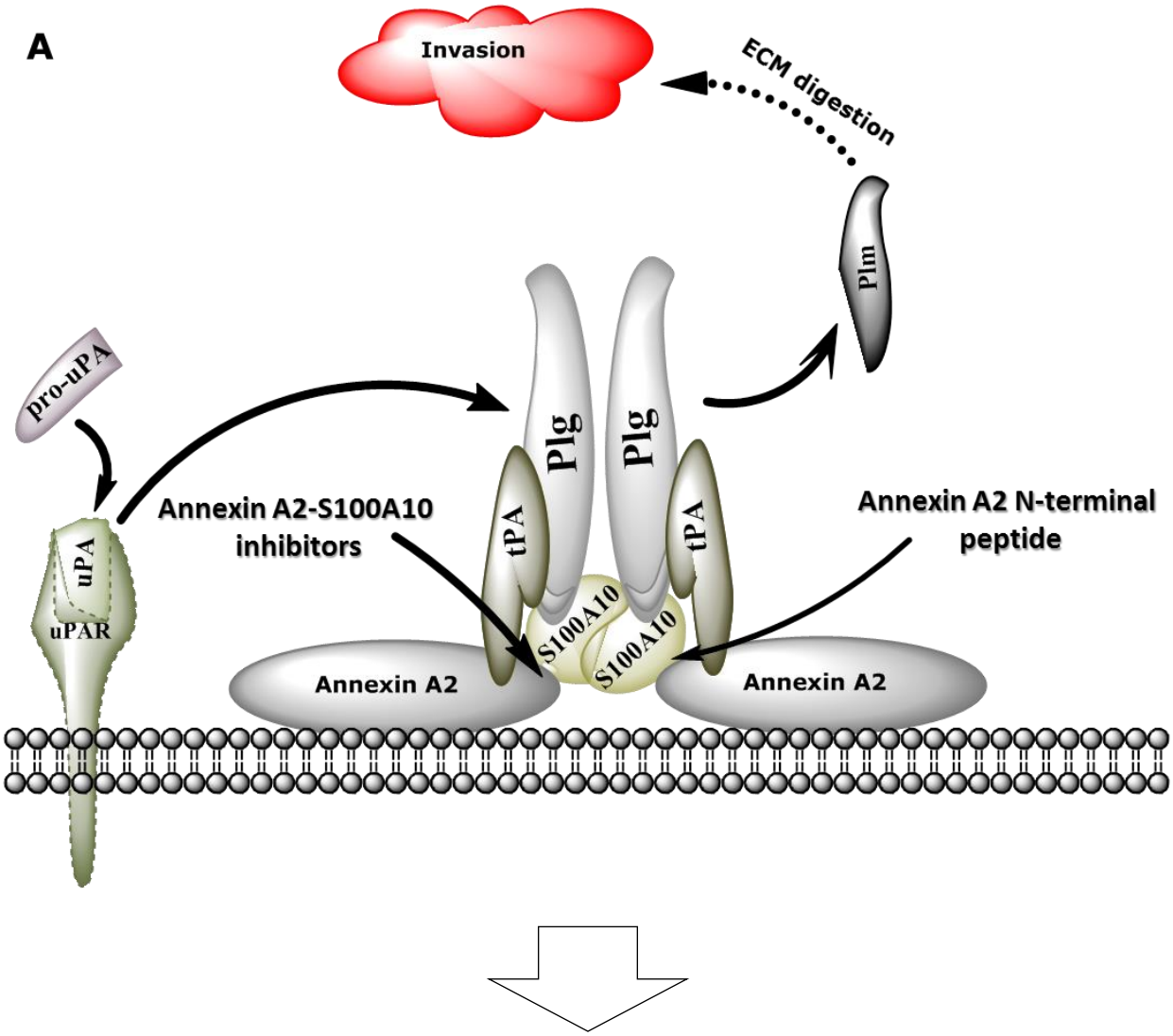


Figure 4.16: Measuring Cy5-S100A10 binding after pre-incubation with annexin A2-S100A10 inhibitors. Data are expressed as mean ± SEM (n = 3).

Figures 4.16A-C show that pretreating PANC-1 cells with annexin A2-S100A10 inhibitors (TRK317, TRK347 and TRK342) at 50 µM significantly increased the fluorescent signal (Cy5-S100A10 binding) as compared with non-treated controls, whereas LW37 at 50 µM did not Figure 4.16D. This suggests that annexin A2-S100A10 inhibitors may be able to release the native S100A10 from its binding partner (annexin A2) and as a consequence more Cy5-S100A10 was able to bind annexin A2.

These results confirm our hypothesis and provide a molecular explanation of protease activity inhibition by annexin A2-S100A10 inhibitors on the surface of PANC-1 cells.

Annexin A2-S100A10 inhibitors release S100A10 from its binding partner annexin A2 on the surface of PANC-1 cells. Therefore the binding of Plg to the surface of PANC-1 cells would be minimized leading to impairment in plasmin generation and consequently a decrease in PANC-1 cells invasion as summarized in Figure 4.17.


A
Invasion
ECM digestion
Plm
pro-uPA
Plg
Plg
tPA
tPA
uPA
uPAR
Annexin A2-S100A10
inhibitors
Annexin A2 N-terminal
peptide
S100A10
S100A10
Annexin A2
Annexin A2

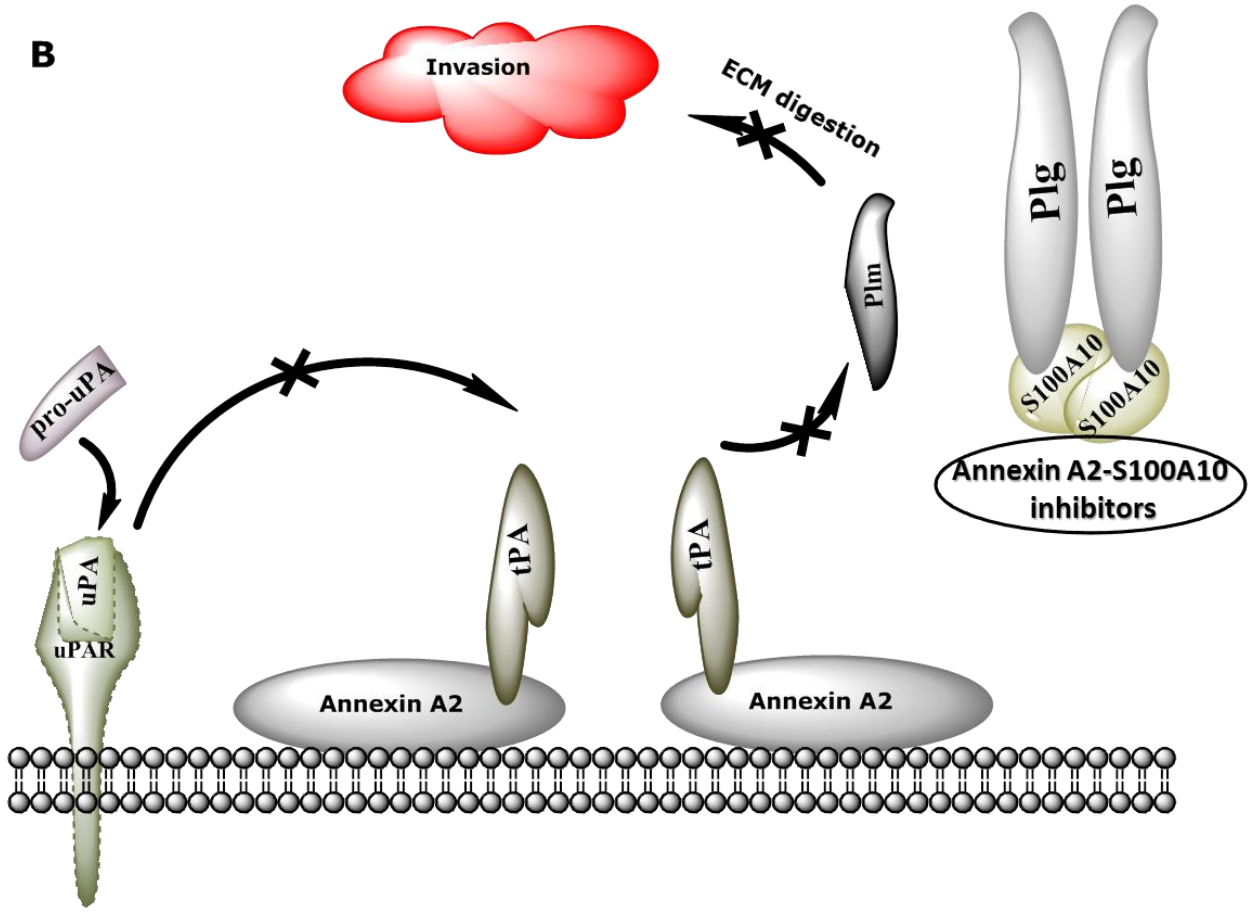


Figure 4.17: Mechanistic representation of annexin A2-S100A10 inhibitors effect on PANC-1 cells invasion. (A) Plg dependent tPA activation on annexin A2-S100A10 complex leads to generation of plasmin (Plm) and PANC-1 cells invasion. (B) Inhibition of annexin A2 and S100A10 interaction by annexin A2-S100A10 inhibitors releases S100A10 with Plg leading to inhibition of plasmin (Plm) generation and PANC-1 cells invasion.

4.3.9. N-terminal peptide and annexin A2-S100A10 inhibitors may be involved in endothelial blood vessel formation

Generation of plasmin is used by endothelial cells to form new vessels. It is thought to be mediated through an annexin A2 dependent mechanism (Ling et al., 2004). In this section the aim was to investigate whether N-terminal peptide and annexin A2-S100A10 inhibitors would inhibit protease cascade on HMEC-1 cells in an annexin A2-S100A10 dependent mechanism. Unpublished data from Dekker group has established the existence and colocalization of annexin A2 and S100A10 on the surface of endothelial cells (HMEC-1 cells). A similar scenario to PANC-1 cells protease activity could hold true if endothelial cells incubated with tPA and Plg. Therefore, the next step was to assess the effect of N-terminal peptide and annexin A2-S100A10 inhibitor on plasmin production that might occur on the surface of endothelial cells after incubation with tPA and Plg.

4.3.9.1. tPA mediates activation of Plg on the surface of endothelial cells

Surface protease activity of HMEC-1 cells was determined as outlined in section 4.3.9.

$1x10^5$ cells per well were seeded in 96-well plates and incubated overnight. The monolayer was then supplemented with 2 nM tPA and incubated for 30 min. The unbound tPA was then washed away and Plg at 5 nM, and chromogenic plasmin substrate at 100 µM were added consecutively. Plasmin formation was monitored at 405 nm in a PerkinElmer 2104 Multilabel Reader as shown in Figure 4.18.

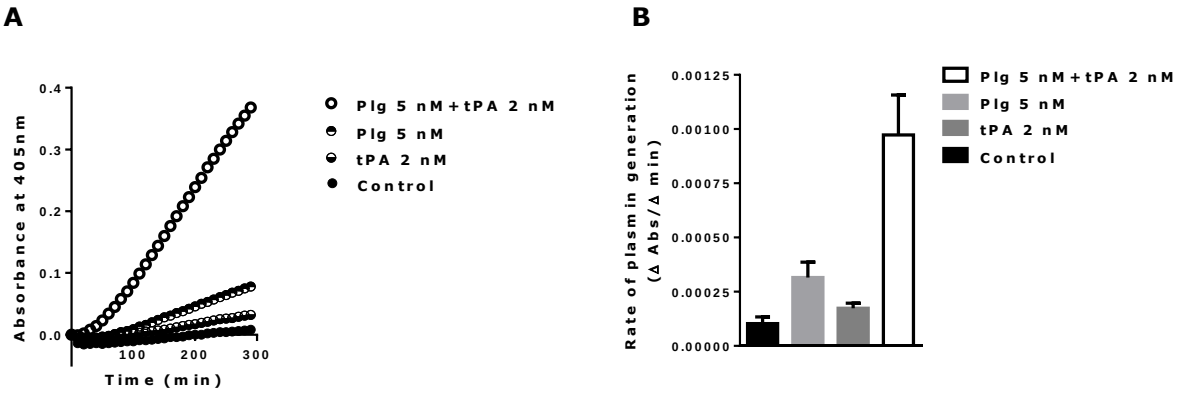


Figure 4.18: (A) Plasmin generation signal. (B) Rate of plasmin generation in HMEC-1 cells. Data are expressed as mean ± SEM (n = 3).

Figure 4.18A shows that, additions of Plg 5 nM and tPA 2 nM to HMEC-1 cell surface has led to a marked increase in the signal reflecting-plasmin

production. To quantify this activity, the rate of plasmin generation has been determined by the equation Δ Abs/Δ min. Figure 4.18B shows an increase in the rate of plasmin generation upon addition of 5 nM Plg to 3.15×10^{-4} ± 0.71×10^{-4} absorbance units (AU)/time units (min) or 2 nM tPA to 1.73×10^{-4} ± 0.22×10^{-4} absorbance units (AU)/time units (min). The rate was raised significantly upon addition of both 5 nM Plg and 2 nM tPA to HMEC-1 cells to 9.72×10^{-4} ± 1.84×10^{-4} absorbance units (AU)/time units (min). This indicates that tPA has mediated the conversion of Plg to plasmin due to their binding to the surface of HMEC-1 cells rather than in the supernatant solution.

These results are in line with Hajjar group finding in 1991 who identified annexin A2 as a receptor for tPA on the surface of endothelial cells (Hajjar, 1991). Also with data mentioning Plg binding to endothelial cells through a C-terminal lysine receptors (Kang et al., 1999).

Loss of endothelial S100A10 results in a significant decrease in Plg activation suggesting the importance of endothelial S100A10 in regulating plasmin generation (Surette and Waisman, 2014). Likewise, release of S100A10 from the surface of HMEC-1 cells would also reduce the plasmin generation on the surface of endothelial cells. Therefore the next aim was to measure the effect of annexin A2-S100A10 inhibitors on the surface protease activity of HMEC-1 cells.

4.3.9.2. Inhibition of protease cascade by N-terminal peptide and annexin A2-S100A10 inhibitors

It has been shown in the previous section that, HMEC-1 cells mediated plasmin generation on their surface. Therefore, a prediction has been made that a similar scenario to PANC-1 cells could happen if HMEC-1 cells were incubated with N-terminal peptide or annexin A2-S100A10 inhibitors. Thus, the next step was to measure their effects on the surface protease activity of HMEC-1 cells.

$1x10^5$ cells per well were seeded in a 96-well plate and incubated overnight. The monolayer was then exposed to 50 μM annexin A2-S100A10 inhibitors, 50 μM N-terminal peptide or 50 μM scrambled peptide for 60 min. The cells were then supplemented with 2 nM tPA and incubated for 30 min. The cells were washed and Plg at 5 nM and chromogenic plasmin substrate at 100 μM were added consecutively. Plasmin formation was monitored at 405 nm in a PerkinElmer 2104 Multilabel Reader as shown in Figure 4.19.

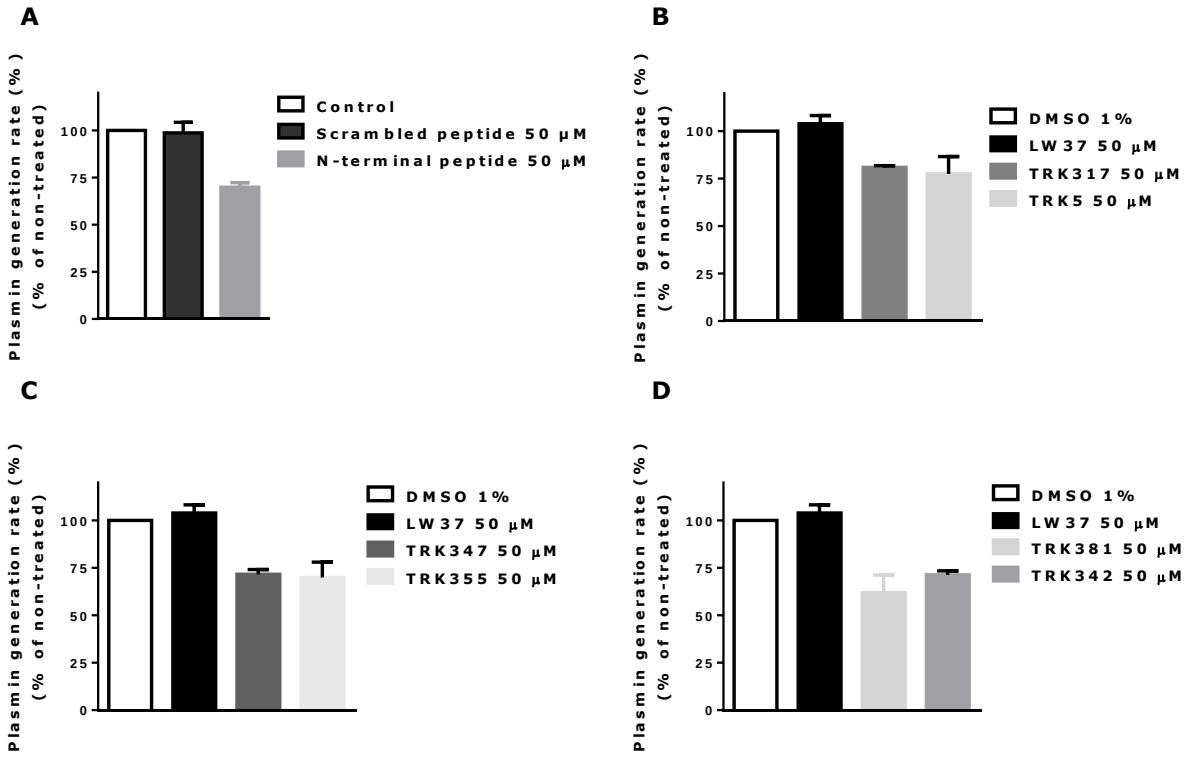


Figure 4.19: Effect of (A) N-terminal peptide, (B), (C) and (D) annexin A2-S100A10 inhibitors on the rate percentage of plasmin generation (protease activity percentage) in HMEC-1 cells. Data are expressed as mean ± SEM (n = 3).

Figure 4.19A shows that N-terminal peptide at 50 µM significantly ($P < 0.05$) reduced the rate percentage of plasmin generation on the surface of HMEC-1 cells to 69.93 ± 2.39% while scrambled peptide at 50 µM did not with 98.73 ± 5.59% compared to non-treated control. Figures 4.19B-D reveal that, all selected active annexin A2-S100A10 inhibitors TRK317, TRK5, TRK347, TRK355, TRK381 and TRK342 at 50 µM significantly ($P < 0.05$) reduced the rate percentage of plasmin generation on the surface of HMEC-1 cells to 80.91 ± 0.90%, 77.53 ± 9.15%, 71.61 ± 2.52%, 69.95 ± 8.10%, 61.93 ±

9.29% and 71.37 ± 2.06% respectively compared to DMSO 1% treated control. LW 37 at 50 μM showed no marked ($P > 0.05$) inhibitory effect with 104 ± 4.26% compared to DMSO 1% treated control.

Since the anti-proliferative activities of TRK317, TRK5, TRK347 and TRK355 reveals, insignificant ($P > 0.05$) cellular activity with survival of 98.06 ± 0.48%, 108 ± 11.89%, 99.15 ± 0.42% and 84.53 ± 6.99% respectively as compared to DMSO 1% as shown in Figure 2.4. Thus, the decrease in plasmin generation by these inhibitors is most likely due to inhibition of the extracellular annexin A2-S100A10 complex rather than inhibition of cells survival.

These results further confirm involvement of annexin A2-S100A10 inhibitors in protease cascade through annexin A2-S100A10 dependent mechanism and implicate that annexin A2-S100A10 inhibitors might inhibit neoangiogenesis by inhibiting plasmin production on the surface of endothelial cells. indeed, a 40% reduction in Plg binding and plasmin generation with impaired neovascularization have been observed in endothelial cells recovered from S100A10-null mice (Surette et al., 2011).

4.3.10. Pancreatic cancer cells adhere to endothelial cells

Given that annexin A2 and S100A10 are colocalized on the surfaces of endothelial and pancreatic cancer cells. And Dekker group has shown that adhesion of breast cancer cells to endothelial cells involved annexin A2 and S100A10 proteins interaction (Myrvang et al., 2013). Furthermore, annexin A2 and S100A10 expressions are involved in the formation of tight junction between Madin-Darby canine kidney cell lines (Lee et al., 2004). It was thought that annexin A2 and S100A10 could be involved in adhesion of pancreatic cancer cells to endothelial cells. A crystal structure of S100A10 reveals a tetramer formation through a disulfide bridge between two dimers of S100A10 (Rety et al., 1999), therefore this could potentially involve an octamer formation (two annexin A2 monomers from each surface linked together by two S100A10 dimers) as a bridge between two cells.

Guided by all these observations, the aim was to measure whether an interaction between these proteins can mediate adhesion of pancreatic cancer cells and endothelial cells.

HMEC-1 cells were seeded at a density of 1.5×10^5 per well in black 96-well plates. The next day, PANC-1 cells were loaded with (BCECF-AM) fluorescent dye and incubated with a monolayer of HMEC-1 cells. 15 min later, the plate was washed and the fluorescence was read on a fluorescence plate reader (PerkinElmer Envision 2104 Multilabel Reader) with excitation at 490 nm and emission at 535 nm as shown in Figure 4.20.

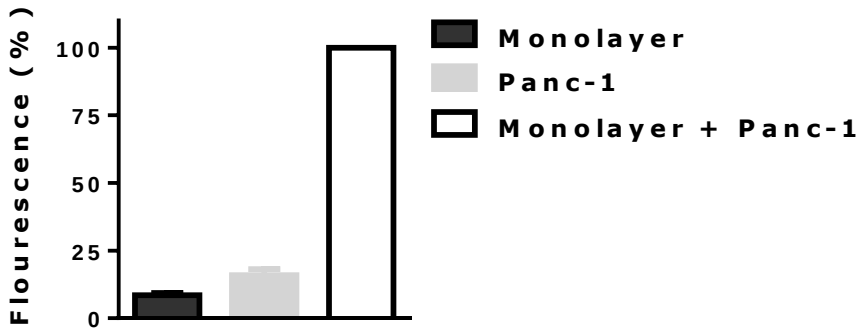


Figure 4.20: Interaction between pancreatic cancer cells and endothelial cells. Data are expressed as mean ± SEM (n = 3).

Figure 4.20 shows that incubation of labelled PANC-1 cells 15.98 ± 2.15% with HMEC-1 monolayer 8.49 ± 0.81% causes a significant increase in the fluorescence to 100%. Meaning that, PANC-1 cells have adhered to HMEC-1 cells through a mutual interaction. This result reveals a cell-cell interaction between pancreatic cancer cells and endothelial cells.

This has turned our attention to assess the contribution of annexin A2 and S100A10 interaction in pancreatic cancer cells adhesion to endothelial cells.

4.3.10.1. N-terminal peptide and annexin A2-S100A10 inhibitors inhibit adhesion of PANC-1 cells to HMEC-1 cells

It has been shown in the previous section that PANC-1 cells adhered to HMEC-1 cells. This adhesion might involve annexin A2 and/or S100A10 proteins on the surfaces of these cells. Therefore, a prediction has been made that; inhibiting annexin A2-S100A10 interaction would inhibit adhesion of PANC-1 cells to HMEC-1 cells.

HMEC-1 cells were seeded at a density of 1.5×10^5 per well in black 96-well plates. The next day N-terminal peptide and annexin A2-S100A10 inhibitors at 50 μM were incubated with HMEC-1 Cells for 30 min. Then BCECF-AM loaded PANC-1 cells were incubated with monolayer for 15 min. The plate was washed and the fluorescence was read on a fluorescence plate reader (PerkinElmer Envision 2104 Multilabel Reader) with excitation at 490 nm and emission at 535 nm as shown in Figure 4.21.

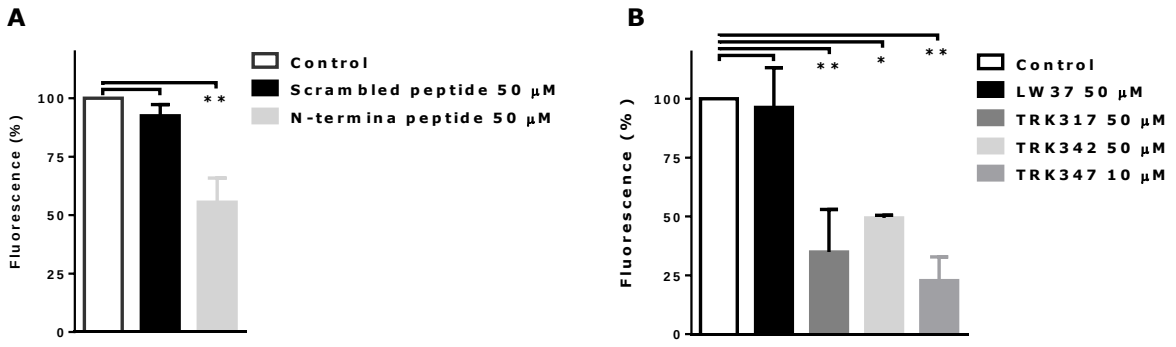


Figure 4.21: Inhibition of pancreatic cancer cells adhesion to endothelial cells by (A) N-terminal peptide and (B) Annexin A2-S100A10 inhibitors. Data are expressed as mean ± SEM (n = 2).

Figure 4.21A shows that, N-terminal peptide at 50 µM significantly (P < 0.05) reduced adhesion of PANC-1 cells to HMEC-1 cells to 55.55 ± 10.33 % while scrambled peptide at 50 µM did not as compared with non-treated control. Interestingly Figure 4.21B reveals that, annexin A2-S100A10 inhibitors TRK317, TRK347, and TRK342 at 50 µM significantly (P < 0.05) inhibited adhesion of PANC-1 cells to HMEC-1 cells with 34.95 ± 18.03%, 22.7 ± 10.12%, and 49.39 ± 1.19% respectively as compared with non-treated control. LW 37 at 50 µM showed no marked (P > 0.05) inhibitory effect with 96.4 ± 16.87% as compared with non-treated control. These results reveal that, N-terminal peptide and annexin A2-S100A10 inhibitors inhibited adhesion of pancreatic cancer cells to endothelial cells.

These findings are consistent with Dekker group observation who showed a significant inhibition of interaction between breast cancer cells and

endothelial cells by N-terminal annexin A2 peptide (Myrvang et al., 2013). Inhibition of annexin A2 and S100A10 interaction by the same peptide has been found to disrupt tight junction formation between kidney cells (Lee et al., 2004). Similarly, an annexin A2-S100A10 inhibitor that has been published by Reddy et al., (Cluster 3 compound 3 (IC_{50} = 2.1 μM)), (Reddy et al., 2011) was able to inhibit adhesion of acute lymphoblastic leukemia to osteoblasts (Gopalakrishnapillai et al., 2015).

Therefore annexin A2-S100A10 expression on the surface of PANC-1 cells mediates the cells adhesion to HMEC-1 cells. This adhesion appears to be inhibited by N-terminal annexin A2 peptide and annexin A2-S100A10 inhibitors as seen in Figure 4.22.

In conclusion, inhibition of pancreatic cancer cells adhesion to endothelial cells by annexin A2-S100A10 inhibitors might lead to a reduction in their penetration through blood vessel to form metastatic foci at a secondary metastatic site.

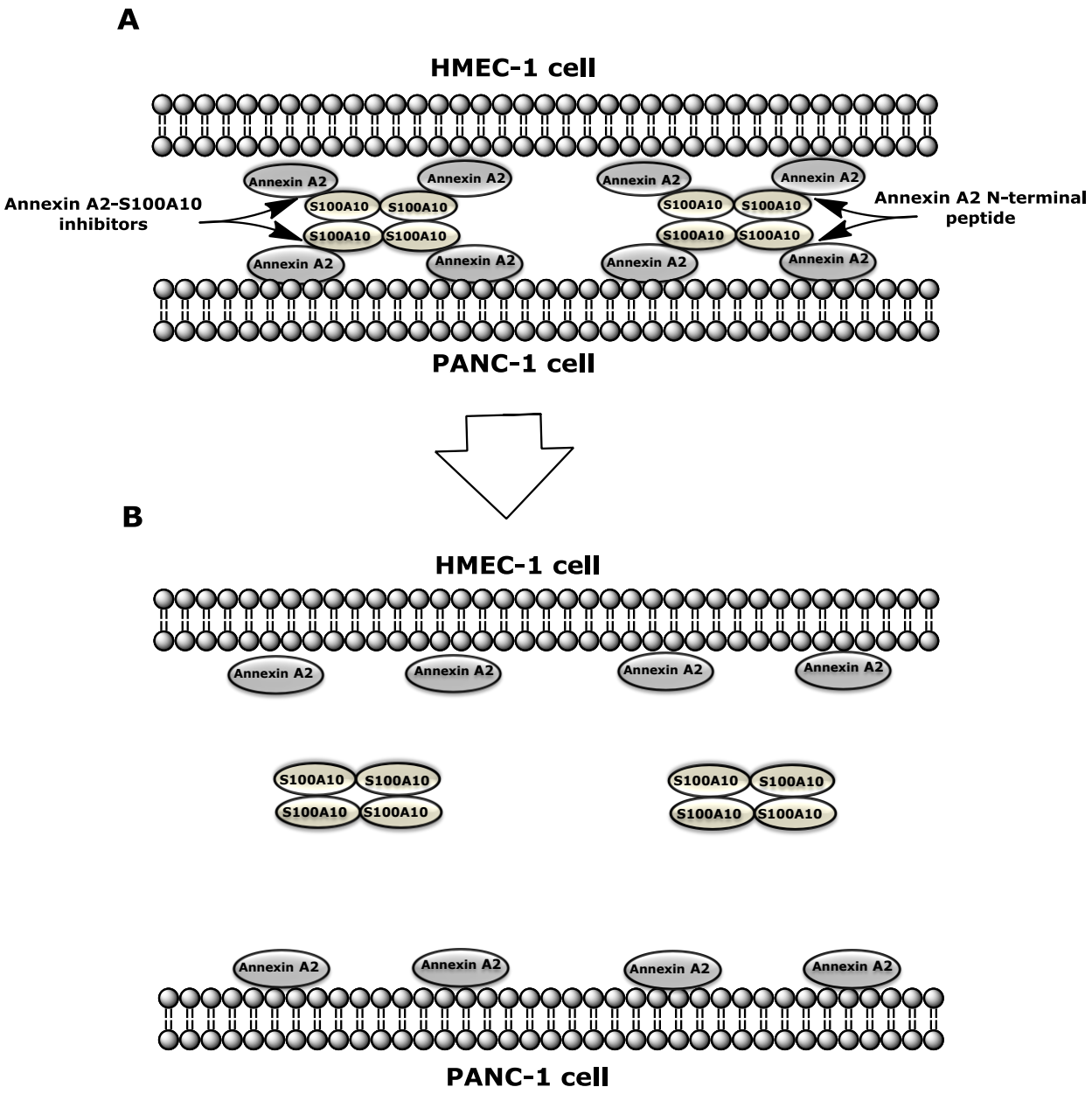


Figure 4.22: Diagrammatic representation showing inhibition of pancreatic cancer cells adhesion to endothelial cells by N-terminal peptide and annexin A2-S100A10 inhibitors.

4.4. Conclusion and Future work

In this chapter an investigation about the effect of annexin A2-S100A10 inhibitors on pancreatic cancer cell invasion has been made. Annexin A2-S100A10 inhibitors and N-terminal annexin A2 peptide inhibited pancreatic cancer cell invasion through a protease dependent mechanism. Linking protease activity with the pancreatic cancer cell surface reveals involvement of annexin A2 and S100A10 expression. With further inspection, it has been shown that, there is a colocalization of these proteins in pancreatic cancer cells. More significantly, molecular evidence has been presented showing that treatment of pancreatic cancer cells with annexin A2-S100A10 inhibitors releases S100A10 from its binding partner Annexin A2 on the cell surface leading to a reduction in Plg binding and less production of plasmin. This has resulted eventually in inhibition of pancreatic cancer cells invasion.

Application of the same scenario on the endothelial cells has shown that, inhibition of extracellular annexin A2-S100A10 interaction reduces protease activity on the surface on HMEC-1 cells that might implicate contributing to neoangiogenesis.

In a further investigation the effect of annexin A2-S100A10 inhibitors on adhesion of pancreatic cancer cells to endothelial cells was determined. N-terminal peptide and annexin A2-S100A10 inhibitors inhibited the adhesion

of the pancreatic cancer cells to the endothelial cells. This inhibition indicated involvement of annexin A2-S100A10 in cell-cell interaction.

In conclusion, these results have shown that annexin A2-S100A10 inhibition would target pancreatic cancer at three different sites; during process of invasion, neoangiogenesis and distant adhesion to endothelial cells (Just before metastasis and invading distant organs).

Collectively this chapter expanded our knowledge and provided us with the essential role of extracellular annexin A2-S100A10 complex in pancreatic cancer cells. Indeed this complex has a pivotal role in pancreatic cancer cells and the annexin A2-S100A10 inhibitors developed recently are good candidates for inhibiting the complex formation and attenuating pancreatic cancer invasiveness. However, although they are useful probes and inhibited the invasion through annexin A2-S100A10 dependent mechanism it might be necessary to chemically modifying these inhibitors to further improves their potency and solubility. Synthesis of a second generation inhibitors with higher potency and better solubility would help for a better understanding of the contribution of these proteins in pancreatic cancer.

CHAPTER 5

5. GENERAL CONCLUSION AND DISCUSSION

In this PhD, the involvement of the function of annexin A2-S100A10 complex in pancreatic cancer has been investigated using chemical inhibitors recently discovered by Dekker group (Reddy et al., 2011).

This approach to interference with the annexin A2-S100A10 complex, relying on disruption of the protein interaction between annexin A2 and S100A10, is different from (and builds upon) earlier functional studies using genetic deletion techniques and knockdown approaches (e.g. shRNA and siRNA). These latter studies focused on interference with the function of individual proteins. These approaches may also cover interference with the protein complex, but not necessarily. Disrupting the protein interaction between annexin A2 and S100A10 is thus a more specific method of interfering with the function of these proteins.

In addition, since it is known that there is significant compartmentalization of the two proteins and their complex (for example a proportion exists inside the cell and a proportion on the cell surface), this compartmentalization will affect the way different functional interference methods act on these proteins. For example, it may be expected that knockout or knockdown methods will deplete the entire population of these proteins (this would depend on their stability in individual compartments) whilst a small molecule

blocker may only target a certain subpopulation (this will depend on the chemical characteristics of the protein).

Thus overall, the small molecule approach used in the current studies is directed at the complex and may affect certain subpopulations of the proteins whilst leaving others unaffected. Using virtual screening, docking studies and fluorescence resonance energy transfer (FRET) between a Cy5 labelled S100A10 and a Cy3 labelled N-terminal annexin A2 peptide, Dekker group has identified and characterized a novel class of molecules (inhibitors) suitable for functional exploration of the annexin A2-S100A10 interaction (Li et al., 2010, Reddy et al., 2011). These molecules would validate the importance of annexin A2-S100A10 interaction and could be used as potential lead molecules for further development as pancreatic cancer drugs.

In Chapter 2, an effort to understand the involvement of the annexin A2-S100A10 complex in cell proliferation was made. It was based on an earlier study that annexin A2 downregulation using siRNA caused a decrease in the proliferation of pancreatic cancer cells (Takano et al., 2008). It was also relying on several reports correlated annexin A2 upregulation with the survival of pancreatic cancer cells (Vishwanatha et al., 1993, Wang and Lin, 2014). Screening of the anti-proliferative activity of these inhibitors using MTT assay revealed an involvement of the annexin A2-S100A10 complex in the cell survival of pancreatic cancer cells. This involvement has been correlated specifically with the level of annexin A2 protein. Annexin A2

expression showed a downregulation after treatment of PANC-1 cells with a target potent and moderately anti-proliferative inhibitor (TRK317). On the other hand, there was no downregulation in annexin A2 expression or a decrease in the cell survival of PANC-1 cells after treatment with an inactive chemotype control (LW37). Based on these results, it was hypothesized that potent annexin A2-S100A10 inhibitors by blocking annexin A2-S100A10 interaction might modulate pancreatic cancer cell survival through an annexin A2 dependent mechanism. This hypothesis was supported by data mentioning an autostability balance between annexin A2 and S100A10 proteins and once this balance is disrupted there would be a decrease in the cell survival (Yang et al., 2011).

Using Crippen fragmentation method (Souza et al., 2011) to predict lipophilicity of these molecules and as a consequence their intracellular availability (Beig et al., 2013). These inhibitors have been classified according to their target inhibitory activity and anti-proliferative activity. The anti-proliferative activity was to some extent dependent on the lipophilicity of annexin A2-S100A10 inhibitors. This physiochemical property has been shown to be involved in the availability of annexin A2-S100A10 inhibitors inside the cell thereafter inhibition of the intracellular complex and modulation of the cell survival. This has increased our understanding of intracellular and extracellular availabilities of these molecules.

Annexin A2 overexpression also has a significant role in gemcitabine resistance developed during pancreatic cancer treatment (Takano et al., 2008). In chapter 3, gemcitabine resistant pancreatic cancer model was developed and characterized. Inhibition of the interaction between annexin A2 and S100A10 by TRK317 revealed downregulation of their expression. The synergistic interaction between gemcitabine and TRK317 on cell survival was evaluated by Chuo combination index (CI) method (Chou, 2010). TRK317 significantly improved the anti-proliferative effect of gemcitabine in PANC-1 G-R cells. This result was in line with a very recent finding related the improvement in the sensitivity of acute lymphoblastic leukemia cells to dexamethasone and vincristine treatment to the inhibition of annexin A2-S100A10 interaction (Gopalakrishnapillai et al., 2015). In the present study, gemcitabine resistant pancreatic cancer model, the synergistic action between gemcitabine and TRK317 has been related to the involvement of annexin A2 in the cell cycle of pancreatic cancer cells. Indeed, nuclear accumulation of annexin A2 has been found to be involved in the cell cycle of cancer cells (Liu et al., 2003a). Further investigation of this involvement revealed a p21 cell cycle protein downregulation in PANC-1 G-R cells as compared with PANC-1 wildtype cells. This may explain the possible mechanism of gemcitabine resistance in pancreatic cancer cells. When the PANC-1 G-R cells are treated with TRK317 there was a decrease in cytoplasmic annexin A2 expression which might be happened as a result of

increased annexin A2 monomer translocation to the nucleus. This might result in a restore in p21 expression that could have led eventually to a restore in the cell cycle regulatory mechanism and improved efficacy of gemcitabine. Interestingly pancreatic cancer cells sensitivity to gemcitabine can be restored by gatifloxacin which induced upregulation of p21 expression (Yadav et al., 2012). Furthermore, combination of gemcitabine with a cyclin-dependent kinase inhibitor, P276-00, improved gemcitabine cytotoxicity in pancreatic cancer cells (Rathos et al., 2012). These results suggest a link between p21 and gemcitabine resistance in pancreatic cancer cells.

Chapter 4 describes the role of extracellular annexin A2-S100A10 complex in pancreatic cancer invasion. Furthermore a comparison was made with the function of the extracellular complex in endothelial cells.

Assays to measure PANC-1 cells invasion through a Matrigel coated membrane were developed and using these assays, it was shown that inhibition of the protein interaction between annexin A2 and S100A10 using a peptide known to inhibit the interaction between annexin A2 and S100A10 and annexin A2-S100A10 inhibitors resulted in inhibition of PANC-1 cells matrix invasion. Inhibition of invasion by the peptides appears to be in line with a report mentioning a reduced pancreatic cancer cells invasion after treatment with the same peptide (Diaz, 2004). Thus it was predicted that annexin A2-S100A10 inhibitors and the peptide inhibited the invasion of PANC-1 cells by a similar mechanism. Measuring surface cellular protease

activity of PANC-1 cells revealed involvement of annexin A2 and/or S100A10 in the pericellular Plg activation pathway. Earlier reports which initiated this study also indicated the binding and activation of Plg to annexin A2 or S100A10 binding (Hajjar et al., 1994, Cesarman et al., 1994, MacLeod et al., 2003).

Plg dependent tPA cascade in PANC-1 cells has been correlated with the ability of PANC-1 cells to invade through a Matrigel coated membrane. Again annexin A2-S100A10 inhibitors together with the peptide showed a significant inhibition of Plg dependent tPA activation cascade. Various techniques have been employed in chapter 4 to investigate the action of annexin A2-S10010 complex inhibitors on the complex itself. This has yielded important data on the validity of the mechanism of action of these inhibitors, in particular versus the endogenous annexin A2-S100A10 protein interaction, which is the key function entity under investigation. Using immunoprecipitation, it was shown that annexin A2 and S100A10 are colocalized at the cell surface of PANC-1 cells and more significantly it was shown that annexin A2-S100A10 inhibitors disrupted the endogenous complex in PANC-1 cell lysate. Further investigation using surface immuno-labeling and employing of an S100A10 fluorescent tracer; annexin A2-S100A10 inhibitors were shown to cause a decrease in the binding of S100A10 to annexin A2 providing a molecular explanation of pancreatic cancer cell invasion inhibition by these inhibitors.

Inhibition of surface protease activity was also observed after employment of these inhibitors to the surface of endothelial cells. This might implicate involvement of annexin A2-S100A10 complex formation in neoangiogenesis. This is in line with data mentioning a decrease in plasmin generation and impairment in the neovascularization in endothelial cells recovered from S100A10-null mice (Surette et al., 2011).

Various models have been proposed to explain the molecular mechanism by which the activation of Plg happens on the cell surface. Annexin A2-S100A10 complex in which annexin A2 contains phospholipid-binding sites that anchor S100A10 to the cell surface membrane, whereas the C-terminal lysine residues of S100A10 dimer bind Plg and tPA. This would provide a colocalization of Plg with its activator tPA (Madureira et al., 2011b). However, according to this model inhibition of the interaction between annexin A2 and S100A10 would not disrupt the colocalization of Plg with tPA and lead to a reduced activation of Plg. Another model has been suggested in which Plg binds to the C-terminal of annexin A2 and tPA binds to its N-terminal. Thus annexin A2 provides a colocalization of Plg with its activator tPA (Cesarman-Maus and Hajjar, 2005). Again according to this model inhibition of the interaction between annexin A2 and S100A10 would not disrupt the colocalization of Plg with tPA and lead to a reduced activation of Plg.

In this study a model has been proposed that Plg binds to the C-terminal S100A10 and tPA binds to the N-terminal annexin A2. This would provide a colocalization of Plg with its activator tPA and inhibition of the interaction between annexin A2 and S100A10 by annexin A2-S100A10 inhibitors would disrupt the colocalization of Plg with tPA and reduce the activation of Plg (see Figure 4.17).

In a final experiment, the relevance of surface expressed annexin A2 and S100A10 for pancreatic cancer cell adhesion was determined. Previously, annexin A2 and S100A10 have been implicated in breast cancer cell adhesion (Myrvang et al., 2013). Using the cell adhesion assay described by Myrvang and colleagues (Myrvang et al., 2013), pancreatic cancer cells adhesion to endothelial cells was measured. Inhibition of the interaction between annexin A2-S100A10 complex using annexin A2-S100A10 inhibitors or the peptide revealed an involvement of annexin A2-S100A10 complex in this cell-cell interaction. The fact that annexin A2-S100A10 inhibitors of the complex affect adhesion is significant since these inhibitors had not previously been tested and the evidence was largely based on peptide interference. Thus, the annexin A2-100A10 complex may be relevant to pancreatic as well as breast (Myrvang et al., 2013) cancer cell intravasation, extravasation and metastasis. Interestingly, adhesion of acute lymphoblastic leukemia to osteoblasts has been also inhibited by another annexin A2-S100A10 inhibitor discovered by Dekker group (Gopalakrishnapillai et al.,

2015) suggesting that the complex may be widely engaged by cancer cells to mediate this functionality.

Annexin A2-S100A10 inhibitors are very useful tools to differentiate between pharmacological functions of extracellular and intracellular annexin A2-S100A10 complexes. The intracellular function of the complex appears to be influenced by annexin A2 and mostly related to cell survival through a cell cycle dependent mechanism. On the other hand, the extracellular function of the complex appears to be influenced by S100A10 and is more related to cell invasion and neoangiogenesis through a Plg dependent tPA activation mechanism.

This study convincingly improved our knowledge and provided us with the essential functions of intracellular and extracellular annexin A2-S100A10 complexes in pancreatic cancer cells. Indeed these complexes have a pivotal role in pancreatic cancer cells gemcitabine-resistance, invasion and adhesion to endothelial cells. Thus inhibition of the annexin A2-S100A10 complexes significantly reverses these phenotypic behaviours.

These inhibitors provide a template to develop a second generation molecules for wider exploration of the function of this complex and though they are useful probes and inhibited the native annexin A2-S100A10 interaction themselves, further potency gains are necessary to allow better understanding of the functional properties of the complex.

6. MATERIALS AND METHODS

6.1. Material list

6.1.1. Cell culture conditions

Product	Ref, No	Supplier	Storage	Recipe
RPMI1640	R8758	Sigma	4°C	A bottle containing 10% FBS
EBM-2	CC-3156	Lonza	4°C	
FBS	044M3397	Sigma	-20°C	A bottle containing 10% FBS, 0.01 µg/ml EGF and 1 µg/ml HC
EGF	1120484B	Invitrogen	-20°C	
HC	H0888-1	Sigma	23°C	
PBS	SLBD8390V	Sigma	23°C	A tablet in 200 ml water
DMSO	D-5879-1L	Sigma-Aldrich	23°C	99.9%
10X Trypsin	T4174-100ML	Sigma	-20°C	1X
IMS	64-17-5	Sigma	23°C	70%

6.1.2. Viability assay (MTT)

Product	Ref, No	Supplier	Storage	Recipe
MTT reagent	M2128-1G OR 298-93-1	Sigma-Aldrich OR Alfa Aesar	4°C in dark	2 mg/ml PBS OR water
DMSO	D-5879-1L	Sigma-Aldrich	23°C	99.9%

6.1.3. Resistant cell line developments

Product	Supplier	Storage	Recipe
Gemcitabine	A kind gift form Dr Dekker	23°C	38 mg/ml

6.1.4. Adhesion assay

Product	Ref, No	Supplier	Storage	Recipe
BCECF-AM	1072761	Invitrogen	-20°C in dark	1.5 µl/1 ml cell suspension

6.1.5. Plasminogen Activation Assay

Product	Ref, No	Supplier	Storage	Recipe
tPA	T5451-1VL OR 612200	Sigma-Aldrich OR Calbiochem	-20°C	1 and 2 nM
Plasminogen	528185	Calbiochem	-20°C	5 and 10 nM
Plasmin substrate	T6140-10MG OR 70314320	Sigma-Aldrich OR Roche Applied Science	-20°C OR 23°C	100 µM
Buffer pH 7.4				
• Tris-HCl	T6066-1KG	Sigma	23°C	50 mM
• NaCl	1498208	Fisher Scientific	23°C	100 mM

• $CaCl_2$	C1016-500G	Sigma	23°C	5 mM
N-terminal peptide	P13611206	Genscript Company USA	-20°C	50 µM
Scrambled peptide	P13601206	Genscript Company USA	-20°C	50 µM
Benzamidine	434760-5G	Sigma-Aldrich	23°C	100 mM
ACA	P500224	Fluka	23°C	10 mM

6.1.6. Invasion assay

Product	Ref, No	Supplier	Storage	Recipe
Matrigel	E1270-5ML	Sigma	-20°C	1 mg/ml
Fibronectin	88088-83-7	Sigma	4°C	5 µg/ml

6.1.7. Cell cycle analysis

Product	Ref, No	Supplier	Storage	Recipe
Fluorochrome solution			4°C	0.3 ml
• Propidium iodide	81845-35MG	Fluka	-20°C	50 µg/ml
• Ribonuclease A	101076	MP Biomedicals	-20°C	0.1 mg/ml
• Triton X-100	10k0192	Sigma	23°C	0.1% v/v

• Sodium citrate	55H0629	Sigma	23°C	0.1% w/v

6.1.8. Apoptosis Assay

Product	Ref, No	Supplier	Storage	Recipe
10X Annexin buffer	51-66121E	BD Pharmingen™	4°C	1 X
Annexin V-FITC	51-65874X	BD Pharmingen™	4°C	5 µl/2×10^5 cells
Propidium iodide	51-66211E	BD Pharmingen™	4°C	10 µl/2×10^5 cells

6.1.9. Surface expression of proteins

Product	Ref, No	Supplier	Storage	Recipe
Working solution			4°C	50 ml
• PBS	SLBD8390V	Sigma	23°C	1 X
• FBS	044M3397	Sigma	-20°C	10%
• Sodium azide	BIS0939	Apollo Scientific	23°C	1%
Annexin A2 antibodies	610068	BD transduction Laboratories	-20°C	2 µl/ml
S100A10 antibodies	610070	BD transduction Laboratories	-20°C	2 µl/ml
AlexaFluor 488 antibodies	1259373	Life technologies	4°C	1 µl/ml

Paraformaldehyde	**28908**	**Thermo Scientific**	**23°C**	**0.1%**

6.1.10. Electrophoresis and immunoblot analysis

6.1.10.1. Protein extraction

Product	Ref, No	Supplier	Storage	Recipe
Lysis buffer pH 8			**4°C**	**10 ml**
• **1M NaCl**	**1498208**	**Fisher Scientific**	**23°C**	**1.5 ml**
• **NP-40**	**74385**	**Fluka**	**23°C**	**100 µl**
• **1M Trizma base**	**T6066-1KG**	**Sigma**	**23°C**	**0.5 ml**
• **Protease inhibitor cocktail tablet**	**04693159001**	**Roche**	**4°C**	**A tablet**
• **Phosphatase inhibitor cocktail tablets**	**04906845001**	**Roche**	**4°C**	**A tablet**

6.1.10.2. Measurement of protein concentration

Product	Ref, No	Supplier	Storage	Recipe
Albumin bovine serum	**A9418-10G**	**Sigma**	**4°C**	**1, 0.8, 0.6, 0.4, 0.2 and zero mg/ml**
Bradford reagent	**B6916-500ML**	**Sigma**	**4°C**	**150 µl/well**

6.1.10.3. Western blotting solutions

Product	Ref, No	Supplier	Storage	Recipe
Resolving buffer pH 8.9			**4°C**	**250 ml**
• **Trizma base**	**T6066-1KG**	**Sigma**	**23°C**	**139.5 g/L**
• **SDS**	**151-21-3**	**MELFORD**	**23°C**	**4 g/L**
Stacking Buffer pH 6.7			**4°C**	**250 ml**
• **Trizma base**	**T6066-1KG**	**Sigma**	**23°C**	**45.36 g/L**
• **SDS**	**151-21-3**	**MELFORD**	**23°C**	**4 g/L**
4X Loading Buffer			**23°C**	**10 ml**
• **99% glycerol**	**G5516-100ML**	**Sigma**	**23°C**	**4 ml**
• **1M Trizma pH 6.8**	**T6066-1KG**	**Sigma**	**23°C**	**2.4 ml**
• **SDS**	**151-21-3**	**MELFORD**	**23°C**	**0.8 g**
Bromophenol blue	**32H3626**	**Sigma**	**23°C**	**4 mg**
β-mercaptoethanol	**M6250-100ML**	**Sigma-Aldrich**	**23°C**	**0.5 ml**
10X Running Buffer			**23°C**	**1 L**
• **Trizma base**	**T6066-1KG**	**Sigma**	**23°C**	**30.3 g**

• SDS	151-21-3	MELFORD	23°C	10 g
• Glycine	PB381-1	Fisher Scientific	23°C	144 g
1X Running Buffer				1 L
• 10X Running Buffer				100 ml
• dH_2O				900 ml
10X Transfer Buffer			4°C	1 L
• Trizma base	T6066-1KG	Sigma	23°C	42.4 g
• Glycine	PB381-1	Fisher Scientific	23°C	144.12 g
1X Transfer Buffer			4°C	1 L
• dH_2O			23°C	700 ml
• 10X Transfer Buffer			4°C	100 ml
• Methanol	32213-2.5L	Sigma	23°C	200 ml
10X TBST buffer pH 7.6			23°C	1 L
• NaCl	1498208	Fisher Scientific	23°C	80 g
• Trizma base	T6066-1KG	Sigma	23°C	24.2 g

• Tween 20	BP337-500	Fisher Scientific	23°C	5 ml
1X TBST buffer			23°C	10 L
• 10X TBST buffer pH 7.6			23°C	1 L
• dH_2O			23°C	9 L
10% Powder milk			4°C	50 ml
• Powder milk		MARVEL	23°C	5 g
• 1X TBST buffer			23°C	50 ml
Acrylamide 30% solution	A3574-100ML	Sigma-Aldrich	4°C	
AMPS	7727-54-0	Sigma	23°C	10%
TEMED	T9281-25ML	Sigma	23°C	

6.1.10.4. Gel preparation

Product	Ref, No	Supplier	Storage	Recipe
Cassettes	1644765	Life technologies	23°C	

Product	Percentage			
10 ml Resolving gel	7.5%	10%	12.5%	15%
• Acrylamide 30% solution	2.5 ml	3.3 ml	4.1 ml	5 ml
• Resolving buffer	2.51 ml	2.5 ml	2.5 ml	2.5 ml
• dH_2O	4.99 ml	4.1 ml	3.3 ml	2.4 ml
• 10% AMPS	45 µl	45 µl	45 µl	45 µl
• TEMED	20 µl	20 µl	20 µl	20 µl
5 ml Stacking gel	5%			
• Acrylamide 30% solution	0.67 ml			
• Stacking buffer	0.63 ml			
• dH_2O	3.7 ml			
• 10% AMPS	30 µl			
• TEMED	15 µl			

6.1.10.5. Immunoblotting and bands detection

Product	Ref, No	Supplier	Storage	Recipe
Nitrocellulose membrane	162-0112	BIO RAD	23°C	....
ColorPlus Protein Marker	0251308	*BioLabs inc.*	-20°C	5 µl
Annexin A2 Antibodies	610068	BD transduction Laboratories	-20°C	1:3000
S100A10 antibodies	610070	BD transduction Laboratories	-20°C	1:4000
p21 antibodies	00061119	Dako	-20°C	1:3000
p53 antibodies	M7001	Dako	-20°C	1:5000
β-actin antibodies	4970	A gift from Dr Dekker and Cell Signaling	-20°C	1:7000
2ry mouse antibodies	00071312	Dako	4°C	1:4000
Amersham ECL Detection Reagents	RPN2106	GE Healthcare	4°C	1 ml
• Reagent 1	RPN2106V1	GE Healthcare	4°C	0.5 ml
• Reagent 2	RPN2106V2	GE Healthcare	4°C	0.5 ml
Developer	P7042	Sigma-Aldrich	23°C	1:4
Fixer	P7167	Sigma-Aldrich	23°C	1:4

6.1.11. Immunoprecipitation Assay

Product	Ref, No	Supplier	Storage	Recipe
protein A/G agarose	PRAG25-AS-2	Alpha Diagnostic International Inc	4°C	30 µl/sample
Annexin A2 Antibodies	610068	BD transduction Laboratories	-20°C	1:3000
S100A10 antibodies	610070	BD transduction Laboratories	-20°C	5 µl/sample

6.1.12. Cell Surface Protein Biotinylation

Pierce® Cell Surface Protein Isolation Kit, (**Thermo** SCIENTIFIC; Cat: 89881)

6.1.13. Cytoplasmic and nuclear proteins extraction

NE-PER™ Nuclear and Cytoplasmic Extraction Reagents, (**Thermo** SCIENTIFIC; Cat: 78833)

6.1.14. Recombinant protein expression and purification

Product	Ref, No	Supplier	Storage	Recipe
Origami 2 cells		A kind gift from Jonas group	-70°C	
Plasmid		Merck-Novagen	-20°C	1 µl
LB	BP-1427-500	Fisher Scientific	23°C	20 mg/ml
LB agar	BP-1425-500	Fisher Scientific	23°C	16 mg/ml
Tetracycline (0.035g/ml)	87128-1006	Sigma	4°C	1:1000
Ampicillin (0.1g/ml)	69-52-3	MELFORD	4°C	1:1000
$CaCl_2$	C1016-500G	Sigma	23°C	50 mM
IPTG	367-93-1	MELFORD	4°C	200 µM
Ni-NTA-agarose beads	130186336	QIAGEN	4°C	2 ml

6.1.14.1. Protein expression buffers

Product	Ref, No	Supplier	Storage	Recipe
Binding Buffers pH 8			**4°C**	**250 ml**
• **NaH_2PO_4**	**Prod 30132**	**BDH GPR™**	**23°C**	**50 mM**
• **NaCl**	**1498208**	**Fisher Scientific**	**23°C**	**300 mM**
• **Imidazole**	**I5513-5G**	**Sigma**	**23°C**	**10, 20 and 40 mM**
Elution buffer pH 8			**4°C**	**250 ml**
• **NaH_2PO_4**	**Prod 30132**	**BDH GPR™**	**23°C**	**50 mM**
• **NaCl**	**1498208**	**Fisher Scientific**	**23°C**	**300 mM**
• **Imidazole**	**I5513-5G**	**Sigma**	**23°C**	**250 mM**
Lysis buffer			**4°C**	**30 ml**
• **Binding buffer 10 mM imidazol**			**4°C**	**30 ml**
• **Lysozyme**	**L6876-5G**	**Sigma**	**-20°C**	**20 mg**
• **Protease inhibitor EDTA free**	**04693159001**	**Roche**	**4°C**	**A tablet**

6.1.14.2. Staining and de staining solutions

Product	Ref, No	Supplier	Storage	Recipe
Staining solution			**23°C**	**250 ml**
• **Coomassie Brilliant Blue R-250**	**038777**	**Fisher Biotech**	**23°C**	**0.1%**
• **Methanol**	**32213-2.5L**	**Sigma**	**23°C**	**50%**
• **Glacial acetic acid**	**2789**	**Fisher Scientific**	**23°C**	**10%**
De-staining solution			**23°C**	**250 ml**
• **Methanol**	**32213-2.5L**	**Sigma**	**23°C**	**40%**
• **Glacial acetic acid**	**2789**	**Fisher Scientific**	**23°C**	**10%**

6.1.14.3. S100A10 Cy5 labelling

Product	Ref, No	Supplier	Storage	Recipe
Cy5 mono-Reactive dye	**PA25001**	**GE Healthcare**	**4°C**	**½ vail/3 mg protein**
PBS labelling buffer			**4°C**	**50 ml**
• **PBS**	**SLBD8390V**	**Sigma**	**23°C**	**50 ml**
• **DTT**	**D0632-25G**	**Sigma**	**23°C**	**2 mM**

6.2. Methods

6.2.1. Cell lines and culture conditions

PANC-1 cells were originally cultured from a 56-year-old male with an adenocarcinoma in the head of the pancreas which has invaded the duodenal wall (Lieber et al., 1975).

MIA PaCa-2 cells were originally derived from a 65-year-old man with an adenocarcinoma in the head and tail of the pancreas which had infiltrated the periaortic area (Yunis et al., 1977).

HMEC-1 cells were originally immortalized with retained morphological, phenotypic and functional characteristics of human microvascular endothelial cells by (Ades et al., 1992).

All cells were obtained from The American Type Culture Collection (ATCC) and maintained in RPMI1640 medium supplemented with 10% heat inactivated foetal bovine serum. Heat inactivation was done by heating the serum at 37°C for 2 h to denature the complement which may provoke cellular immune response. HMEC-1, Human micro-vascular endothelial cells, were maintained in EBM-2 (Endothelial Basal Medium -2 from Lonza Cat CC-3156) supplemented with 10% foetal bovine serum, EGF 0.01 µg/ml and hydrocortisone 1 µg/ml. All cells were incubated at 37°C and 5% CO_2.

6.2.2. Cell passage and freezing

To keep cells healthy and prevent over growth the cells were sub-cultured whenever they become 80-90% confluent.

Briefly mentioned, media were aspirated and cells were washed with PBS 2 ml (25 cm^2 flask) / 4 ml (75 cm^2 flask). The PBS was aspirated and 1X trypsin 0.5 ml (25 cm^2 flask) / 1 ml (75 cm^2 flask) added. The flask was then kept in the incubator for 2-3 min before tapping to detach attached cells and 5 ml (25 cm^2 flask)/ 10 ml (75 cm^2 flask) fresh media was added to form a cell suspension. The suspension was treated in two ways, either a 0.5 ml was added to a new flask with fresh medium 4 ml (25 cm^2 flask)/ 10 ml (75 cm^2 flask) or the number of cells were counted by haemocytometer and used for an experiment. Cell passages used in the experiments were ≤ 30 after which cells were discarded to prevent genotypic drift. A new cell line was picked from the cell bank and grown to passage 3 or 4, and then one flask of the growing cells was trypsinized, washed and centrifuged. The pellet was re-suspended in 1 ml 10% DMSO FBS (a cryoprotectant) and gradually frozen from -20°C freezer to -150 °C liquid nitrogen.

6.2.3. Cell counting

10 µl of cell suspension was taken by pipette and put on haemocytometer for counting under microscope. The density of the cells was expressed as number of cells counted per 0.1 µl.

6.2.4. Viability assay (MTT)

The assay is a simple and useful quantitative technique to measure compounds anti-proliferative activity. It depends on measuring cell viability based on mitochondrial reductase activity. A yellow MTT reagent (3-(4,5-dimethylthiazol-2yl)-2,5-diphenyl tetrazolium bromide) is reduced inside the mitochondria to blue formazan crystals, which then solubilized by 99.9% DMSO giving a blue colour proportional in the intensity to the number of viable cells (Morgan, 1998). Absorbance of the colour was taken at 590 nm in a PerkinElmer 2104 Multilabel Reader.

Drawbacks of the assay are, a damaged mitochondria might still be able to form blue crystals and metabolically inactive cells though still alive, they do not form crystals and considered as dead cells (Mosmann, 1983).

Firstly, cells were seeded in two (96-well plates) at a density of 3×10^3 cells per well in a volume of 180 µl and kept to attach in incubator for an overnight.

Next day, *plate1* was treated with the compounds (Stock concentrations were 5 mM dissolved in 100% DMSO) at concentration of 50 µM 1% DMSO in a volume of 20 µl. *Plate2* (*T0,* estimation of seeding density after 24 h), 20 µl fresh media and 50 µl MTT (2 m/ml) were added consecutively and the plate was incubated at 37°C. 2.5 h later, the media was aspirated carefully

and 150 µl DMSO (99.9%) was added followed by shaking on orbital shaker for 3 min. The absorbance of the solution was taken by plate reader.

After four days *plate1* was treated same as T0 plate except no 20 µl fresh media was added.

The data was expressed according to Singh et al method (Singh et al., 2013).

$$\text{Survival percentage} = \frac{\text{Absorbance of the compound}}{\text{Absorbance of 1\% DMSO}} \times 100$$

6.2.5. Resistant cell line developments

Development of Gemcitabine-resistant cells was done by continuous exposure to increasing concentrations of gemcitabine over a period of 6 months starting with an initial concentration of 1 nM, with an increase 1-3 fold every 5 to 15 days. The cells obtained were viable in a medium containing 1 M gemcitabine and showed no apparent morphological or growth rate differences as compared with the wild cells (Jordheim et al., 2004).

6.2.6. Adhesion assay

The technique is used to measure the ability of cancer cells to make bridges with a monolayer of endothelial cells.

Generally cancer cells loaded with a fluorescent dye then incubated with endothelial monolayer to form adhesion bridges. The measured fluorescence is proportional to the number of adherent cells (Myrvang et al., 2013).

HMEC-1 cells were seeded at a density of 1.5×10^5 per well in black 96-well plates with a clear bottom (Corning Costar, Amsterdam, The Netherlands) and kept in incubator for an overnight to form a confluent monolayer. Compounds at desired concentrations were incubated with HMEC-1 Cells in a volume of 25 µl for 30 min. During this time 80% confluent (75 cm^2 flask) pancreatic cancer cells were trypsinized, counted then incubated at 37°C with 2',7'-bis-(2-carboxyethyl)-5,6-carboxyfluorescein acetoxymethylester (BCECF-AM; Invitrogen) at concentration of 1.5 µl per ml cell suspension. 15 min later, excess dye was washed and 3×10^4 cells in a volume of 25 µl per well were incubated with HMEC-1 cells monolayer at 37°C.

The unbounded cells were aspirated carefully after 20 min and the plate was washed three times by 150 µl PBS before the fluorescence was read on a fluorescence plate reader (PerkinElmer Envision 2104 Multilabel Reader) with excitation at 490 nm and emission at 535 nm.

6.2.7. Plasminogen Activation Assay

Plasminogen activation was determined by measuring the proteolytic activity of plasmin generated by binding of plasminogen and tPA. Plasmin generated from the reaction hydrolyzes a chromogenic substrate forming a yellow colour of p-nitroaniline that absorbs light at 405, thus the change in the colour is a direct measurement of plasmin generation (Sharma et al., 2010). All the experiments were done in a 100 µl volume in 96-well plates. 1 nM tPA (Sigma-Aldrich) was pre-incubated at 25°C for 1 h in a buffer consisting of 50 mM Tris-HCl, pH 7.4, 100 mM NaCl, and 5 mM $CaCl_2$. The reaction was initiated by the addition of Plasminogen (Calbiochem) at 5 nM and chromogenic plasmin substrate (Sigma-Aldrich) at 100 µM. The reaction was monitored at 405 nm in a PerkinElmer 2104 Multilabel Reader.

6.2.8. Plasminogen Activation on the surface of the cells

The cells were seeded in 96-well plates at a density of $1x10^5$ cells per well and incubated overnight for attachment. The monolayer was then rinsed one time with buffer consisting of 50 mM Tris-HCl, pH 7.4, 100 mM NaCl, 5 mM $CaCl_2$, and treated with (Compounds, N-terminal peptide (Ac-STVHEILSKLSLEC) (Genscript Company USA) or scrambled peptide (KIETLSEHVSLSLC) (Genscript Company USA)) at desired concentrations for 45 min. Each well was then supplemented with tPA 1 nM (Sigma-Aldrich) or tPA 2 nM (Calbiochem) and incubated for 30 min at room temperature. The

cells were washed one more time and plasminogen (Calbiochem) at 5 nM, and chromogenic plasmin substrate (Sigma-Aldrich) at 100 μM were added consecutively. Plasmin formation was monitored at 405 nm in a PerkinElmer 2104 Multilabel Reader.

6.2.9. Invasion assay

Invasion of basement membranes by cancer cells is a crucial step in a multistage process which leads eventually to metastasis of cancer cell (Melchiori et al., 1987).

Migration of pancreatic cancer cells through a Matrigel layer (modelling the basement membrane) was quantified according to Imamura et al (Imamura et al., 1994).

A 96-well plate with inserts (Corning® HTS Transwell® 96-well permeable support) was used to assess the invasion potential of pancreatic cancer cells. Briefly, cells were incubated with free serum medium overnight.

The next day a Matrigel (Sigma) at a concentration of 2 mg/ml and a volume of 50 μl was loaded in the upper chambers and kept in the incubator for 3 h. During this time, overnight starved cells were trypsinized, counted and 2.5×10^4 cells per well in 1% FBS medium were then loaded in the upper chamber on the solidified Matrigel. The compounds, N-terminal peptide or scrambled peptide (Genscript Company USA) at 50 μM, altogether with

plasminogen at a concentration of 10 nM were added to the upper chamber as well.

In the Lower chamber, 10% FBS medium and fibronectin 5 µg/ml in a volume of 250 µl were added then the whole plate was incubated at 37°C. After 18 h the Matrigel in the upper chamber was aspirated and a 50 µl MTT solution (2 mg/ml) was added to the lower chamber and the plate was incubated at 37°C. 3 h later, the formazan formed in the migrated cells was solubilised by 200 µL 99.9% DMSO (Sigma). The absorbance was then read out by plate reader at wave length of 590 nm.

6.2.10. Flow Cytometry

Flow cytometry is a technique used to measure optical and fluorescence characteristics of single cells. Size and internal complexity of the cells represented by forward light scatter and side light scatter can be used to resolve cell population. Fluorescent dyes alone or conjugated with antibodies can bind to DNA or cell membrane components. When labelled cells pass through a beam of light, they give a signal proportional in the intensity to the light emitted from the dye (Brown and Wittwer, 2000).

6.2.11. Cell cycle analysis

A technique used to measure DNA contents by flow cytometry. DNA distribution through the cell cycle is measured by addition of Propidium iodide (PI) (a DNA intercalating dye, fluoresces weakly when in solution but strongly when bound to DNA).

According to (Nicoletti et al., 1991), cells were seeded in 6-well plates at a density of 1-2 x 10^5 cells per well in a volume of 2 ml and allowed to attach for an overnight at 37°C. The following day, media was aspirated carefully and fresh media containing compounds at desired concentrations was added to the attached cells. 72 h later, the media containing floating cells was decanted in pre-chilled FACS tubes and the attached cells were trypsinized and added to the FACS tubes as well. The FACS tubes were then centrifuged at 1200 rpm for 5 min, 4°C and the supernatant was discarded carefully then the pellet was re-suspended in 1 ml cold PBS before centrifuging again at 1200 rpm for 5 min, 4°C. The PBS was then aspirated and cell pellet was re-suspended in 500 µl cold hypotonic fluorochrome solution and stored for an overnight in the dark at 4°C. Before sample analysis, the cells were syringed to obtain a single cell suspension. DNA content was measured by a Beckman Coulter EPICS-XL MCL™ flow cytometer, and data was analysed using the EXPO32™ software or FlowJo.

6.2.12. Apoptosis Assay (Annexin V - FITC and propidium iodide)

Annexin V is a small protein that binds to phosphatidylserine (PS), an inner component of the cell membrane, with high affinity during early apoptosis. Propidium iodide (as mentioned previously binds to DNA) is excluded from healthy cells with intact membranes. It can only enter cells with compromised membrane. Thus staining cells with fluorescently labelled annexin V– FITC and PI allows for discrimination as following: healthy cells (annexin V – FITC negative, PI negative), early apoptotic cells (annexin V – FITC positive, PI negative), late apoptotic cells (annexin V – FITC positive, PI positive) and necrotic cells (annexin V – FITC negative, PI positive). The assay was done according to the manufacturer instructions.

Briefly, cells were seeded in 6-well plates at a density of 1-2 x 10^5 cells per well in a volume of 2 ml and allowed to attach for an overnight at 37°C. The next day, media was aspirated carefully and fresh media containing compounds at desired concentrations was added to the attached cells. 72 h later, the media containing floating cells was decanted in pre-chilled FACS tubes and the attached cells were trypsinized and pooled together with floated cells. The FACS tubes were then centrifuged at 1200 rpm for 5 min, 4°C and the supernatant was discarded carefully then the pellet was re-suspended in 1 ml cold PBS before centrifuging again at 1200 rpm for 5 min, 4°C. Cells pellet was then broken up by gentle flicking of the tube and 100 µl 1X annexin binding buffer plus 5 µl annexin V-FITC were added then the

cells were incubated in dark at 4°C. 15 min later, 400 µl 1X annexin binding buffer and 10 µl 50 µg/ml PI solution were added to the cells which then vortexed gently and kept on ice for 10 min in dark. Samples were analysed as soon as possible to prevent deterioration of the cells. Apoptosis was measured by a Beckman Coulter EPICS-XL MCL™ flow cytometer, and data was analysed using the EXPO32™ software or FlowJo.

6.2.13. Surface expression of proteins

Cell surface proteins represent a key regulator of cellular processes. These proteins play major roles in signal transduction, cell adhesion and serve as common pharmacological targets.

Cell surface staining was done indirectly according to ab**cam** procedure.

Briefly, cells were harvested and washed twice with Phosphate-buffered Saline (Sigma). $5x10^5$ cells were gently re-suspended in ice cold PBS, 10% FBS, 1% sodium azide. 10 min later, a primary antibody annexin A2 (BD Bioscience) or S100A10 (BD Bioscience) at concentration of 1.25 µg/ml was incubated for 45 min at room temperature. Cells were then washed two times with Phosphate-buffered Saline and incubated for 30 min at 4°C in dark with secondary antibody (Alexa Fluor 488 antibody) diluted 1:1000 in 10% Foetal Bovine serum in Phosphate-buffered Saline. Cells were washed two times with Phosphate-buffered Saline and re-suspended in 0.5 ml Phosphate-buffered Saline. Whenever indicated, compounds, N-terminal

peptide or scrambled peptide (Genscript Company USA) at a concentration of 50 μM were incubated with the cells for 45 mins then fixation by paraformaldehyde 0.1% for 10 min was done prior to surface labelling with the antibodies.

Analysis was done on a Beckman Coulter Epics XL-MCL flow cytometer and CyFlow Patrec. Data analysis was conducted by Expo32 flow cytometry and flowJO. For each experiment, a minimum of 2 x 10^4 cells were analysed per sample and gated during analysis.

6.2.14. Electrophoresis and immunoblot analysis

A very useful technique used to qualify and quantify proteins expression in the cells. It has been done according to the standards unless specified.

Generally, protein lysates were prepared from pancreatic cancer or HMEC-1 cells. Then concentrations of protein lysates were quantified by Bradford assay. Proteins were then separated by 10-15% SDS-PAGE (sodium dodecyl sulfate-polyacrylamide gel electrophoresis). After electrophoresis, proteins were transferred to a nitrocellulose membrane. The membrane was then blocked in 10% milk in 1X TBST at room temperature. After which the membrane was incubated with primary antibodies at 4°C for an overnight. The following day, the membrane was washed in 1X TBST and incubated with secondary antibody at room temperature for 1 h before washing again in 1X TBST. The Membrane was then developed using ECL plus (Amersham

Pharmacia Biotech, UK) and exposed to films for appropriate amounts of time.

6.2.14.1. Protein extraction

Cells were seeded in 10 cm^2 dishes and kept in the incubator for an overnight attachment. The following day, a fresh media was added after aspiration of the old media and the cells were treated at desired concentrations and time points. Then all cells (floated and attached) were collected and centrifuged at 1200 rpm for 5 min, 4°C. The pellet was washed with ice-cold PBS and re-suspended in a lysis buffer (containing Protease and Phosphatase Inhibitors) for 20 min at 4°C. The proteins were then extracted by centrifugation at 13000 rpm for 10 min, 4°C. The supernatant was separated from debris, stored at -20 °C and used as a cell lysate.

6.2.14.2. Measurement of protein concentration

Measurement of protein concentration was done by Bradford assay.

Firstly, serial concentrations (1, 0.8, 0.6, 0.4, 0.2 mg/ml) of BSA were prepared. 5 µl of each concentration and 150 µl Bradford reagent were added to 96-well plates. The plate was shaken on the orbital shaker for 5 min then the absorbance taken at 595 nm wave length and used to make BSA standard curve. Protein lysate was diluted 10 to 20 times in Demineralised water then 5 µl of the diluted lysate and 150 µl Bradford

reagent were added to 96-well plates consecutively. Absorbance was taken and used to calculate protein concentration.

6.2.14.3. Gel electrophoresis

The proteins in lysate were separated according to their molecular weight. Briefly, SDS polyacrylamide gel was prepared in a concentration of 10 or 15% depending on the molecular size of the protein of interest. 50-75 µg of protein lysate was mixed with 1X loading buffer containing reducing agent and denatured at 95°C for 5-10 min before loading into gel.

Color Plus Prestained Protein Ladder was loaded into the first lane to monitor the progress of the electrophoretic run according to the molecular size. Protein samples were separated at a voltage between 80-140 V in running buffer until the migration of the wanted band reached the desirable level. 1-2 h later, the gel was removed from a cassette for proteins transfer.

6.2.14.4. Immunoblotting and bands detection

Proteins separated by electrophoresis were blotted on a nitrocellulose membrane.

Shortly, membrane and gel were soaked in a transfer buffer for 5 min before layering onto the Semi Dry Transfer Unit from bottom to top as follows: 3 pieces Whatman, nitrocellulose membrane, gel and 3 pieces of Whatman. The unit was run at 25 V for 1.5 h. The membrane was blocked in a 10%

powdered milk dissolved in 1x TBST for 1 h at room temperature. The blot was then washed for 5 min in 1x TBST before incubation with primary antibodies at 4°C for an overnight in a concentration specified by the manufacturer. The next day, the membrane was washed with 1X TBST for 10 min 3X and incubated with horseradish peroxidase conjugated-secondary antibody in a concentration of 1: 4000 at room temperature for 1 h before washing again in 1X TBST. The blot was then developed using ECL plus (Amersham Pharmacia Biotech, UK) and exposed to X-ray films in dark room for appropriate amounts of time. The films were then scanned and bands intensities were quantified by image studio lite.

6.2.15. Immunoprecipitation Assay

Immunoprecipitation (IP) and co-immunoprecipitation (Co-IP) are techniques used to purify a specific protein or group of proteins from a complex mixture using an antibody immobilized on a solid support. It requires a great deal of optimization and troubleshooting.

Briefly, cells were extracted in 50 mM Tris-HCl (pH 8.0) buffer containing 150 mM sodium chloride and 1% (v/v) NP-40. Lysates were then recovered by centrifugation at 13000 rpm for 10 min and incubated at 4°C for 6 h with 5 µL of S100A10 antibody (BD transduction Laboratories). Then 30 µL of protein A/G agarose (Alpha Diagnostic International Inc.) was added and incubated with lysate under rotation for an overnight. Protein A/G agarose

was then recovered by centrifugation at 1500 rpm for 3 min, washed three times with PBS (pH 7.4), re-suspended in 50 µL 2X loading buffer, boiled at 99°C for 10 min, and centrifuged at 13000 rpm for 10 min. The supernatant was then analysed by SDS-PAGE after which the gel was transferred to a nitrocellulose membrane. The membrane was then incubated with an annexin A2 monoclonal antibody (1:3000; BD Transduction Laboratories) followed by incubation with a secondary horseradish peroxidase conjugated antibodies (1:4000; Dako) and then developed using the ECL detection reagent (GE Healthcare). Wherever indicated, compounds were incubated for 45 at 4°C under rotation with cell lysate prior to the immunoprecipitation.

6.2.16. Cell Surface Protein Biotinylation

Biotinylation and isolation of proteins for western blot analysis is a useful technique used to qualify and quantify the expression of certain proteins on the cell membrane.

According the manufacturer instructions and some optimizations, the cells were grown in 10 cm^2 dishes to 80-90% confluence. Prior to biotinylation, media was aspirated, and the cells were washed with chilled PBS. 10 ml EZ-link Sulfo-NHS-LC-Biotin (Thermoscientific) at 0.25 mg/ml was added to cover cell layer surface. The dishes were gently shaken at 4 °C. 30 min later, 500 µl quenching solution was added to stop the reaction. The dishes were then washed with 10 ml TBS three times. A 500 µl lysis buffer

containing protease inhibitor was then added to the cells before scrapping and transferring to pre-chilled 1.5 ml Eppendorf tube. The cells were then vortexed for 5 second every 5 min for 6 times. Then, the cells extract was centrifuged at 10000 rpm for 3 min at 4°C. The supernatant was run on a 500 µl Neutravidin-agarose beads (Thermoscientific) at room temperature for 1 h. the beads were then recovered by centrifuging at 1000 rpm for 1 min. The supernatant was kept in a new tube and used to check for intracellular proteins. The beads were washed 3 times with washing buffer and incubated with 400 µl SDS sample buffer (containing 50 mM DTT) at room temperature for elution of extracellular proteins. 1 h later, the beads were centrifuged at 1300 rpm for 3 min and the supernatant was analysed by western blotting.

6.2.17. Cytoplasmic and nuclear proteins extraction

The technique is used to separate nuclear and cytoplasmic proteins from each other. Following the manufacturer instructions, cells were trypsinized, centrifuged and the pellet was washed with PBS. A 200 µl CER I was added to the pellet and the tube was vortexed vigorously for 10 sec and incubated for 10 min at 4°C.

Ice-cold CER II was added to the tube and vortexed for 5 sec and incubated in ice for 5 min. the tube was then centrifuged at 13000 rpm for 5 min. the supernatant (cytoplasmic extract) was added to new pre-chilled tube. The

insoluble pellet (containing nuclei) was washed 2 times with CER II before incubating with ice-cold NER and vortexed for 10 sec every 10 min for 40 min. The tube was then centrifuged at 13000 rpm for 10 min and supernatant containing nuclear extract was added to new pre-chilled tube. Both extract were analysed by western blotting.

6.2.18. Recombinant protein expression and purification

Recombinant proteins are widely used throughout biological and biomedical science nowadays. They are used in functional assays and protein-protein interaction. *E.coli,* Origami 2 cells tetracycline-resistant, obtained from Jonas Emsley group have been used to express S100A10 protein.

6.2.18.1. Preparation of competent bacterial cells

Competent cells are cells which have the ability to take up a foreign DNA.

The cells were grown in an autoclaved and tetracycline treated (at concentration of 1:1000) 80 ml LB media for an overnight under shaking at 37°C. The next day, a 5 ml of the grown cells was added to a 30 ml fresh LB media and the growth was monitored until the OD600 of the cell suspension was 0.7. The cells were then chilled on ice for 10 min before centrifuging at 4800 rpm for 10 min at 4°C. The supernatant was discarded and the pellet was re-suspended in ice cold sterile 50 mM $CaCl_2$. 15 min later, the cells

were centrifuged again at 4800 rpm for 10 min at 4°C. The pellet (competent cells) was used immediately or stored at -70°C.

6.2.18.2. Bacterial cell transformation

Transformation is a process by which a foreign DNA is introduced into a bacterial cell. The stored competent cells were taken out of -70°C and defrosted in ice for 10 min. 1 µl DNA 10 ng (S100A10 cloned into pET14b containing Ampicillin resistant gene (Merck-Novagen)) was added to 200 µl packed volume Origami cells. The tube was flicked few times before incubating back in ice for 20 min. The cells were then heat shocked for 60 sec at 42°C before incubating back in ice for 5 min. A pre-warmed LB media at a volume of 0.5 ml was added to the cells and incubated for 30 min at 37°C under shaking (220 rpm).

6.2.18.3. Bacterial culturing

A 200 µl of the transformed bacteria was inoculated into LB-agar Ampicillin-Tetracycline plate and incubated for an overnight at 37°C. The colonies should appear next day if the transformation was successful.

A single colony was then picked up and inoculated into 30 ml LB media containing Ampicillin-Tetracycline at concentrations of 1:1000 for both. The cells were then incubated at 37°C under shaking (Speed of 180-220 rpm) for an overnight. The following day, the growing bacteria was transferred into 1

L LB media containing Ampicillin-Tetracycline and incubated at 37°C under shaking (180-220 rpm) until the OD600 = 0.8.

6.2.18.4. Induction of bacteria

Induction of bacteria is the expression of the gene of interests under the control of a lac operon-which could be achieved by IPTG (a sugar that binds to the lac repressor allowing the lac operator to be functional and the gene to be expressed).

When the OD600 of the bacteria was reached 0.8, the temperature of the incubator was lower to 30°C and IPTG added to a final concentration of 200 μM and the cells were kept on incubating for 6 h. Then the cells were harvested by centrifugation (by using 500 ml bottle) at 4800 rpm for 30 min. the supernatant was discarded and the pellet was labelled as induced cells and kept in -20°C.

6.2.18.5. Protein extraction

The frozen cells were thawed and re-suspended in ice cold 30 ml binding buffer containing (20 mg lysozyme and a tablet of protease inhibitor EDTA free) before sonication for 5 times (30 sec on and 30 sec off). The lysate was then transferred to spin tubes and centrifuged at 10000 rpm for 40 min at 4°C. The supernatant was then transferred into new tube for purification.

6.2.18.6. Proteins purification (Ni column affinity chromatography)

The most commonly used tag for purification and detection of recombinant expressed proteins is the polyhistidine tag (Yip et al., 1989). Protein purification using polyhistidine tags relies on the affinity of histidine residues for immobilized nickel, which allows selective protein purification (Hutchens and Yip, 1990). By using the affinity of Ni^{2+} to the histidine tag, the supernatant was incubated with Ni-NTA-agarose beads (QIAGEN) under rotation for 1 h at 4°C. The beads were washed twice in binding buffer containing 10, 20 and 40 mM imidazole pH 8.0, respectively, and proteins were then eluted in elution buffer containing 250 mM imidazole pH 8.0.

6.2.18.7. Checking the purity of the protein

The purified protein was run on a 15% SDS-PAGE. Then, the gel was stained with Coomassie blue and shaken on orbital shaker at room temperature for an overnight. The bands of purified protein were then visualized by incubating the gel in a destaining solution (containing 10% acetic acid and 40% methanol) under shaking at room temperature for 7 h.

After confirming the purity of the protein, a Vivaspin concentrator (membrane: 5000 MWCO PES) was used to make the final volume of the eluent about 1 ml before addition of 10 ml PBS. The final step was repeated 3 times before calculating the concentration of purified protein by Bradford assay and a Nano drop.

6.2.19. S100A10 Cy5 labelling

3 ml S100A10 1 mg/ml in PBS with 2 mM DDT was incubated with the contents of 1/2 vail Cy5-monofunctional reactive dye (GE Healthcare) at 23°C for 2 h. The sample was diluted by 20 ml of PBS containing 2 mM DDT and applied to a Vivaspin concentrator. The tube was centrifuged at 4800 rpm at 4°C until the volume of the solution become 3 ml. the last step was repeated two times before the concentration of labelled S100A10 was measured by a Nano drop available at Nottingham University. The tracer was then stored at 4°C.

6.2.20. S100A10 tracer binding assay

$1.5x10^5$ cells per well were seeded in 96-well and incubated overnight. The monolayer was then rinsed with PBS and then incubated at room temp for 30 min with compounds at 50 μM. Then cells were washed with PBS and incubated with 5 μM S100A10 tracer for 20 min. The cells were then washed and fluorescence was taken at PerkinElmer 2104 Multilabel Reader with 620 excitation and 685 emissions.

6.2.21. Statistical analyses

All experiments were done at least three times unless specified and results were expressed in mean ± standard error of mean (SEM). Analysis was done using Graphpad prism 6 and excel. One-way ANOVA (Dunnett's multiple comparisons), two-way ANOVA (Sidak's multiple comparisons) and student t-test (unpaired) were used to determine statistical significance (*P* value < 0.05). Pearson's correlation coefficient was performed to examine correlation between annexin A2-S100A10 inhibitors anti-proliferative activity and target inhibitory activity. Analysis of synergy was done using Compusyn software.

7. REFERENCES

ADAMS, J. M. & CORY, S. 2007. The Bcl-2 apoptotic switch in cancer development and therapy. *Oncogene,* 26**,** 1324-37.

ADES, E. W., CANDAL, F. J., SWERLICK, R. A., GEORGE, V. G., SUMMERS, S., BOSSE, D. C. & LAWLEY, T. J. 1992. Hmec-1 - Establishment of an Immortalized Human Microvascular Endothelial-Cell Line. *Journal of Investigative Dermatology,* 99**,** 683-690.

AGUILAR, S., COROMINAS, J. M., MALATS, N., PEREIRA, J. A., DUFRESNE, M., REAL, F. X. & NAVARRO, P. 2004. Tissue plasminogen activator in murine exocrine pancreas cancer - Selective expression in ductal tumors and contribution to cancer progression. *American Journal of Pathology,* 165**,** 1129-1139.

AKADA, M., CRNOGORAC-JURCEVIC, T., LATTIMORE, S., MAHON, P., LOPES, R., SUNAMURA, M., MATSUNO, S. & LEMOINE, N. R. 2005. Intrinsic chemoresistance to gemcitabine is associated with decreased expression of BNIP3 in pancreatic cancer. *Clinical Cancer Research,* 11**,** 3094-3101.

ALEEM, E. & ARCECI, R. 2015. Targeting cell cycle regulators in hematologic malignancies. *Frontiers in Cell and Developmental Biology,* 3.

ARORA, S., BHARDWAJ, A., SINGH, S., SRIVASTAVA, S. K., MCCLELLAN, S., NIRODI, C. S., PIAZZA, G. A., GRIZZLE, W. E., OWEN, L. B. & SINGH, A. P.

2013. An undesired effect of chemotherapy: gemcitabine promotes pancreatic cancer cell invasiveness through reactive oxygen species-dependent, nuclear factor kappaB- and hypoxia-inducible factor 1alpha-mediated up-regulation of CXCR4. *J Biol Chem,* 288**,** 21197-207.

ARTANDI, S. E. & DEPINHO, R. A. 2010. Telomeres and telomerase in cancer. *Carcinogenesis,* 31**,** 9-18.

ARUMUGAM, T., RAMACHANDRAN, V., SUN, D., PENG, Z., PAL, A., MAXWELL, D. S., BORNMANN, W. G. & LOGSDON, C. D. 2013. Designing and developing S100P inhibitor 5-methyl cromolyn for pancreatic cancer therapy. *Mol Cancer Ther,* 12**,** 654-62.

BAERISWYL, V. & CHRISTOFORI, G. 2009. The angiogenic switch in carcinogenesis. *Semin Cancer Biol,* 19**,** 329-37.

BAO, H., JIANG, M., ZHU, M., SHENG, F., RUAN, J. & RUAN, C. 2009. Overexpression of Annexin II affects the proliferation, apoptosis, invasion and production of proangiogenic factors in multiple myeloma. *Int J Hematol,* 90**,** 177-85.

BARDEESY, N. & DEPINHO, R. A. 2002. Pancreatic cancer biology and genetics. *Nature Reviews Cancer,* 2**,** 897-909.

BECKER, T., WEBER, K. & JOHNSSON, N. 1990. Protein-protein recognition via short amphiphilic helices; a mutational analysis of the binding site of annexin II for p11. *EMBO J,* 9**,** 4207-13.

BEIG, A., AGBARIA, R. & DAHAN, A. 2013. Oral delivery of lipophilic drugs: the tradeoff between solubility increase and permeability decrease when using cyclodextrin-based formulations. *PLoS One,* 8**,** e68237.

BENAUD, C., LE DEZ, G., MIRONOV, S., GALLI, F., REBOUTIER, D. & PRIGENT, C. 2015. Annexin A2 is required for the early steps of cytokinesis. *EMBO Rep,* 16**,** 481-9.

BENFENATI, E., GINI, G., PICLIN, N., RONCAGLIONI, A. & VARI, M. R. 2003. Predicting logP of pesticides using different software. *Chemosphere,* 53**,** 1155-64.

BHARADWAJ, A., BYDOUN, M., HOLLOWAY, R. & WAISMAN, D. 2013. Annexin A2 heterotetramer: structure and function. *Int J Mol Sci,* 14**,** 6259-305.

BIANKIN, A. V., KENCH, J. G., MOREY, A. L., LEE, C. S., BIANKIN, S. A., HEAD, D. R., HUGH, T. B., HENSHALL, S. M. & SUTHERLAND, R. L. 2001. Overexpression of p21(WAF1/CIP1) is an early event in the development of pancreatic intraepithelial neoplasia. *Cancer Res,* 61**,** 8830-7.

BLASCO, M. A. 2005. Telomeres and human disease: ageing, cancer and beyond. *Nat Rev Genet,* 6**,** 611-22.

BRANDES, N., SCHMITT, S. & JAKOB, U. 2009. Thiol-based redox switches in eukaryotic proteins. *Antioxid Redox Signal,* 11**,** 997-1014.

BRESNICK, A. R., WEBER, D. J. & ZIMMER, D. B. 2015. S100 proteins in cancer. *Nat Rev Cancer,* 15**,** 96-109.

BROWN, M. & WITTWER, C. 2000. Flow cytometry: principles and clinical applications in hematology. *Clin Chem,* 46**,** 1221-9.

BROWNSTEIN, C., DEORA, A. B., JACOVINA, A. T., WEINTRAUB, R., GERTLER, M., KHAN, K. M., FALCONE, D. J. & HAJJAR, K. A. 2004. Annexin II mediates plasminogen-dependent matrix invasion by human monocytes: enhanced expression by macrophages. *Blood,* 103**,** 317-24.

BURKHART, D. L. & SAGE, J. 2008. Cellular mechanisms of tumour suppression by the retinoblastoma gene. *Nat Rev Cancer,* 8**,** 671-82.

BURRIS, H. A., 3RD, MOORE, M. J., ANDERSEN, J., GREEN, M. R., ROTHENBERG, M. L., MODIANO, M. R., CRIPPS, M. C., PORTENOY, R. K., STORNIOLO, A. M., TARASSOFF, P., NELSON, R., DORR, F. A., STEPHENS, C. D. & VON HOFF, D. D. 1997. Improvements in survival and clinical benefit with gemcitabine as first-line therapy for patients with advanced pancreas cancer: a randomized trial. *J Clin Oncol,* 15**,** 2403-13.

BYDOUN, M., HUANG, W. & WAISMAN, D. 2015. The plasminogen receptor P11 contributes to KRAS-driven invasiveness of pancreatic cancer cells and is upregulated in human pancreatic tumors. *Annals of Oncology,* 26.

CANCERCENTER.COM 2015. Pancreatic Cancer Survival Rates & Statistics | CTCA. [online] Available at: http://www.cancercenter.com/pancreatic-cancer/statistics/tab/pancreatic-cancer-survival-statistics/ [Accessed 11 Dec. 2015].

CAVALLARO, U. & CHRISTOFORI, G. 2004. Cell adhesion and signalling by cadherins and Ig-CAMs in cancer. *Nat Rev Cancer,* 4**,** 118-32.

CAVALLO-MEDVED, D., RUDY, D., BLUM, G., BOGYO, M., CAGLIC, D. & SLOANE, B. F. 2009. Live-cell imaging demonstrates extracellular matrix degradation in association with active cathepsin B in caveolae of endothelial cells during tube formation. *Exp Cell Res,* 315**,** 1234-46.

CESARMAN-MAUS, G. & HAJJAR, K. A. 2005. Molecular mechanisms of fibrinolysis. *Br J Haematol,* 129**,** 307-321.

CESARMAN, G. M., GUEVARA, C. A. & HAJJAR, K. A. 1994. An endothelial cell receptor for plasminogen/tissue plasminogen activator (t-PA). II. Annexin II-mediated enhancement of t-PA-dependent plasminogen activation. *J Biol Chem,* 269**,** 21198-203.

CHELLAPPAN, S. P., HIEBERT, S., MUDRYJ, M., HOROWITZ, J. M. & NEVINS, J. R. 1991. The E2F transcription factor is a cellular target for the RB protein. *Cell,* 65**,** 1053-61.

CHEN, H., XU, C., JIN, Q. & LIU, Z. 2014. S100 protein family in human cancer. *Am J Cancer Res,* 4**,** 89-115.

CHEN, J. H., NI, R. Z., XIAO, M. B., GUO, J. G. & ZHOU, J. W. 2009. Comparative proteomic analysis of differentially expressed proteins in human pancreatic cancer tissue. *Hepatobiliary Pancreat Dis Int,* 8**,** 193-200.

CHEN, R., BRENTNALL, T. A., PAN, S., COOKE, K., MOYES, K. W., LANE, Z., CRISPIN, D. A., GOODLETT, D. R., AEBERSOLD, R. & BRONNER, M. P. 2007. Quantitative proteomics analysis reveals that proteins differentially expressed in chronic pancreatitis are also frequently involved in pancreatic cancer. *Molecular & Cellular Proteomics,* 6**,** 1331-1342.

CHEN, R., PAN, S., BRENTNALL, T. A. & AEBERSOLD, R. 2005. Proteomic profiling of pancreatic cancer for biomarker discovery. *Molecular & Cellular Proteomics,* 4**,** 523-533.

CHENG, N., CHYTIL, A., SHYR, Y., JOLY, A. & MOSES, H. L. 2008. Transforming growth factor-beta signaling-deficient fibroblasts enhance hepatocyte growth factor signaling in mammary carcinoma cells to promote scattering and invasion. *Mol Cancer Res,* 6**,** 1521-33.

CHOI, K. S., FOGG, D. K., YOON, C. S. & WAISMAN, D. M. 2003. p11 regulates extracellular plasmin production and invasiveness of HT1080 fibrosarcoma cells. *FASEB J,* 17**,** 235-46.

CHOU, T. C. 2006. Theoretical basis, experimental design, and computerized simulation of synergism and antagonism in drug combination studies. *Pharmacol Rev,* 58**,** 621-81.

CHOU, T. C. 2010. Drug combination studies and their synergy quantification using the Chou-Talalay method. *Cancer Res,* 70**,** 440-6.

CHOU, T. C. & TALALAY, P. 1981. Generalized Equations for the Analysis of Inhibitions of Michaelis-Menten and Higher-Order Kinetic Systems with 2 or More Mutually Exclusive and Non-Exclusive Inhibitors. *European Journal of Biochemistry,* 115**,** 207-216.

CHUNG, C. Y., MURPHY-ULLRICH, J. E. & ERICKSON, H. P. 1996. Mitogenesis, cell migration, and loss of focal adhesions induced by tenascin-C interacting with its cell surface receptor, annexin II. *Mol Biol Cell,* 7**,** 883-92.

COHEN, J. 1992. A Power Primer. *Psychological Bulletin,* 112**,** 155-159.

CRNOGORAC-JURCEVIC, T., GANGESWARAN, R., BHAKTA, V., CAPURSO, G., LATTIMORE, S., AKADA, M., SUNAMURA, M., PRIME, W., CAMPBELL, F., BRENTNALL, T. A., COSTELLO, E., NEOPTOLEMOS, J. & LEMOINE, N. R. 2005.

Proteomic analysis of chronic pancreatitis and pancreatic adenocarcinoma. *Gastroenterology,* 129**,** 1454-1463.

CRNOGORAC-JURCEVIC, T., MISSIAGLIA, E., BLAVERI, E., GANGESWARAN, R., JONES, M., TERRIS, B., COSTELLO, E., NEOPTOLEMOS, J. P. & LEMOINE, N. R. 2003. Molecular alterations in pancreatic carcinoma: expression profiling shows that dysregulated expression of S100 genes is highly prevalent. *J Pathol,* 201**,** 63-74.

CURRAN, S. & MURRAY, G. I. 1999. Matrix metalloproteinases in tumour invasion and metastasis. *Journal of Pathology,* 189**,** 300-308.

DAVIS, R. G. & VISHWANATHA, J. K. 1995. Detection of secreted and intracellular annexin II by a radioimmunoassay. *Journal of Immunological Methods,* 188**,** 91-95.

DE SOUSA CAVALCANTE, L. & MONTEIRO, G. 2014. Gemcitabine: metabolism and molecular mechanisms of action, sensitivity and chemoresistance in pancreatic cancer. *Eur J Pharmacol,* 741**,** 8-16.

DEBERARDINIS, R. J., LUM, J. J., HATZIVASSILIOU, G. & THOMPSON, C. B. 2008. The biology of cancer: metabolic reprogramming fuels cell growth and proliferation. *Cell Metab,* 7**,** 11-20.

DEORA, A. B., KREITZER, G., JACOVINA, A. T. & HAJJAR, K. A. 2004. An annexin 2 phosphorylation switch mediates p11-dependent translocation of annexin 2 to the cell surface. *J Biol Chem,* 279**,** 43411-8.

DIAZ, V. M. 2004. Specific interaction of tissue-type plasminogen activator (t-PA) with annexin II on the membrane of pancreatic cancer cells activates plasminogen and promotes invasion in vitro. *Gut,* 53**,** 993-1000.

DIAZ, V. M., HURTADO, M., THOMSON, T. M., REVENTOS, J. & PACIUCCI, R. 2004. Specific interaction of tissue-type plasminogen activator (t-PA) with annexin II on the membrane of pancreatic cancer cells activates plasminogen and promotes invasion in vitro. *Gut,* 53**,** 993-1000.

DIAZ, V. M., PLANAGUMA, J., THOMSON, T. M., REVENTOS, J. & PACIUCCI, R. 2002. Tissue plasminogen activator is required for the growth, invasion, and angiogenesis of pancreatic tumor cells. *Gastroenterology,* 122**,** 806-19.

DIMAGNO, E. P., REBER, H. A. & TEMPERO, M. A. 1999. AGA technical review on the epidemiology, diagnosis, and treatment of pancreatic ductal adenocarcinoma. American Gastroenterological Association. *Gastroenterology,* 117**,** 1464-84.

DOMOTO, T., MIYAMA, Y., SUZUKI, H., TERATANI, T., ARAI, K., SUGIYAMA, T., TAKAYAMA, T., MUGIYA, S., OZONO, S. & NOZAWA, R. 2007. Evaluation of S100A10, annexin II and B-FABP expression as markers for renal cell carcinoma. *Cancer Sci,* 98**,** 77-82.

DONATO, R., CANNON, B. R., SORCI, G., RIUZZI, F., HSU, K., WEBER, D. J. & GECZY, C. L. 2013. Functions of S100 Proteins. *Current Molecular Medicine,* 13**,** 24-57.

DVORAK, H. F. 1986. Tumors: wounds that do not heal. Similarities between tumor stroma generation and wound healing. *N Engl J Med,* 315**,** 1650-9.

DZIDUSZKO, A. & OZBUN, M. A. 2013. Annexin A2 and S100A10 Regulate Human Papillomavirus Type 16 Entry and Intracellular Trafficking in Human Keratinocytes. *Journal of Virology,* 87**,** 7502-7515.

EBERHARD, D. A., KARNS, L. R., VANDENBERG, S. R. & CREUTZ, C. E. 2001. Control of the nuclear-cytoplasmic partitioning of annexin II by a nuclear export signal and by p11 binding. *J Cell Sci,* 114**,** 3155-66.

ECKERT, R. L., BROOME, A. M., RUSE, M., ROBINSON, N., RYAN, D. & LEE, K. 2004. S100 proteins in the epidermis. *Journal of Investigative Dermatology,* 123**,** 23-33.

EMBERLEY, E. D., NIU, Y., CURTIS, L., TROUP, S., MANDAL, S. K., MYERS, J. N., GIBSON, S. B., MURPHY, L. C. & WATSON, P. H. 2005. The S100A7-c-Jun activation domain binding protein 1 pathway enhances prosurvival pathways in breast cancer. *Cancer Res,* 65**,** 5696-702.

ESPOSITO, I., PENZEL, R., CHAIB-HARRIRECHE, M., BARCENA, U., BERGMANN, F., RIEDL, S., KAYED, H., GIESE, N., KLEEFF, J., FRIESS, H. & SCHIRMACHER,

P. 2006. Tenascin C and annexin II expression in the process of pancreatic carcinogenesis. *Journal of Pathology,* 208**,** 673-685.

FAN, Y. J., DICKMAN, K. G. & ZONG, W. X. 2010. Akt and c-Myc Differentially Activate Cellular Metabolic Programs and Prime Cells to Bioenergetic Inhibition. *Journal of Biological Chemistry,* 285**,** 7324-7333.

FLOOD, E. C. & HAJJAR, K. A. 2011. The annexin A2 system and vascular homeostasis. *Vascul Pharmacol,* 54**,** 59-67.

FOLEY, K., RUCKI, A. A., XIAO, Q., ZHOU, D., LEUBNER, A., MO, G. L., KLEPONIS, J., WU, A. A., SHARMA, R., JIANG, Q. G., ANDERS, R. A., IACOBUZIO-DONAHUE, C. A., HAJJAR, K. A., MAITRA, A., JAFFEE, E. M. & ZHENG, L. 2015. Semaphorin 3D autocrine signaling mediates the metastatic role of annexin A2 in pancreatic cancer. *Science Signaling,* 8.

FOLKMAN, J. & SHING, Y. 1992. Angiogenesis. *J Biol Chem,* 267**,** 10931-4.

FRITZ, G., BOTELHO, H. M., MOROZOVA-ROCHE, L. A. & GOMES, C. M. 2010. Natural and amyloid self-assembly of S100 proteins: structural basis of functional diversity. *FEBS J,* 277**,** 4578-90.

GARRETT, S. C., VARNEY, K. M., WEBER, D. J. & BRESNICK, A. R. 2006. S100A4, a mediator of metastasis. *J Biol Chem,* 281**,** 677-80.

GERKE, V. & MOSS, S. E. 2002. Annexins: From structure to function. *Physiological Reviews,* 82**,** 331-371.

GIOVANNETTI, E., DEL TACCA, M., MEY, V., FUNEL, N., NANNIZZI, S., RICCI, S., ORLANDINI, C., BOGGI, U., CAMPANI, D., DEL CHIARO, M., IANNOPOLLO, M., BEVILACQUA, G., MOSCA, F. & DANESI, R. 2006. Transcription analysis of human equilibrative nucleoside transporter-1 predicts survival in pancreas cancer patients treated with gemcitabine. *Cancer Res,* 66**,** 3928-35.

GONG, X. G., LV, Y. F., LI, X. Q., XU, F. G. & MA, Q. Y. 2010. Gemcitabine resistance induced by interaction between alternatively spliced segment of tenascin-C and annexin A2 in pancreatic cancer cells. *Biol Pharm Bull,* 33**,** 1261-7.

GOPALAKRISHNAPILLAI, A., KOLB, E. A., DHANAN, P., MASON, R. W., NAPPER, A. & BARWE, S. P. 2015. Disruption of Annexin II /p11 Interaction Suppresses Leukemia Cell Binding, Homing and Engraftment, and Sensitizes the Leukemia Cells to Chemotherapy. *Plos One,* 10.

GRIVENNIKOV, S. I., GRETEN, F. R. & KARIN, M. 2010. Immunity, inflammation, and cancer. *Cell,* 140**,** 883-99.

GURTOVENKO, A. A. & ANWAR, J. 2007. Modulating the Structure and Properties of Cell Membranes: The Molecular Mechanism of Action of Dimethyl Sulfoxide. *The Journal of Physical Chemistry B,* 111**,** 10453-10460.

HAJJAR, K. A. 1991. The endothelial cell tissue plasminogen activator receptor. Specific interaction with plasminogen. *J Biol Chem,* 266**,** 21962-70.

HAJJAR, K. A., JACOVINA, A. T. & CHACKO, J. 1994. An endothelial cell receptor for plasminogen/tissue plasminogen activator. I. Identity with annexin II. *J Biol Chem,* 269**,** 21191-7.

HAJJAR, K. A., MAURI, L., JACOVINA, A. T., ZHONG, F., MIRZA, U. A., PADOVAN, J. C. & CHAIT, B. T. 1998. Tissue plasminogen activator binding to the annexin II tail domain. Direct modulation by homocysteine. *J Biol Chem,* 273**,** 9987-93.

HANAHAN, D. & FOLKMAN, J. 1996. Patterns and emerging mechanisms of the angiogenic switch during tumorigenesis. *Cell,* 86**,** 353-64.

HANAHAN, D. & WEINBERG, R. A. 2011. Hallmarks of cancer: the next generation. *Cell,* 144**,** 646-74.

HATA, H., TATEMICHI, M. & NAKADATE, T. 2014. Involvement of annexin A8 in the properties of pancreatic cancer. *Mol Carcinog,* 53**,** 181-91.

HAUG, K., KRAVIK, K. L. & DE ANGELIS, P. M. 2008. Cellular response to irinotecan in colon cancer cell lines showing differential response to 5-fluorouracil. *Anticancer Res,* 28**,** 583-92.

HE, K. L., DEORA, A. B., XIONG, H., LING, Q., WEKSLER, B. B., NIESVIZKY, R. & HAJJAR, K. A. 2008. Endothelial cell annexin A2 regulates polyubiquitination and degradation of its binding partner S100A10/p11. *J Biol Chem,* 283**,** 19192-200.

HE, K. L., SUI, G., XIONG, H., BROEKMAN, M. J., HUANG, B., MARCUS, A. J. & HAJJAR, K. A. 2011. Feedback regulation of endothelial cell surface plasmin generation by PKC-dependent phosphorylation of annexin A2. *J Biol Chem,* 286**,** 15428-39.

HEDHLI, N., FALCONE, D. J., HUANG, B., CESARMAN-MAUS, G., KRAEMER, R., ZHAI, H., TSIRKA, S. E., SANTAMBROGIO, L. & HAJJAR, K. A. 2012. The annexin A2/S100A10 system in health and disease: emerging paradigms. *J Biomed Biotechnol,* 2012**,** 406273.

HEJMADI, M. 2010. *Introduction to cancer biology,* Frederiksberg, Denmark BoonBooks.com.

HIYAMA, E., KODAMA, T., SHINBARA, K., IWAO, T., ITOH, M., HIYAMA, K., SHAY, J. W., MATSUURA, Y. & YOKOYAMA, T. 1997. Telomerase activity is detected in pancreatic cancer but not in benign tumors. *Cancer Res,* 57**,** 326-31.

HOU, T. J., XIA, K., ZHANG, W. & XU, X. J. 2004. ADME evaluation in drug discovery. 4. Prediction of aqueous solubility based on atom contribution approach. *Journal of Chemical Information and Computer Sciences,* 44**,** 266-275.

HRUBAN, R. H., ADSAY, N. V., ALBORES-SAAVEDRA, J., ANVER, M. R., BIANKIN, A. V., BOIVIN, G. P., FURTH, E. E., FURUKAWA, T., KLEIN, A., KLIMSTRA, D. S., KLOPPEL, G., LAUWERS, G. Y., LONGNECKER, D. S., LUTTGES, J., MAITRA, A., OFFERHAUS, G. J., PEREZ-GALLEGO, L., REDSTON, M. & TUVESON, D. A.

2006. Pathology of genetically engineered mouse models of pancreatic exocrine cancer: consensus report and recommendations. *Cancer Res,* 66**,** 95-106.

HRUBAN, R. H., VAN MANSFELD, A. D., OFFERHAUS, G. J., VAN WEERING, D. H., ALLISON, D. C., GOODMAN, S. N., KENSLER, T. W., BOSE, K. K., CAMERON, J. L. & BOS, J. L. 1993. K-ras oncogene activation in adenocarcinoma of the human pancreas. A study of 82 carcinomas using a combination of mutant-enriched polymerase chain reaction analysis and allele-specific oligonucleotide hybridization. *Am J Pathol,* 143**,** 545-54.

HSU, S. Y., KAIPIA, A., ZHU, L. & HSUEH, A. J. 1997. Interference of BAD (Bcl-xL/Bcl-2-associated death promoter)-induced apoptosis in mammalian cells by 14-3-3 isoforms and P11. *Mol Endocrinol,* 11**,** 1858-67.

HUANG, Y., JIN, Y., YAN, C. H., YU, Y., BAI, J., CHEN, F., ZHAO, Y. Z. & FU, S. B. 2008. Involvement of Annexin A2 in p53 induced apoptosis in lung cancer. *Molecular and Cellular Biochemistry,* 309**,** 117-123.

HUTCHENS, T. W. & YIP, T. T. 1990. Differential interaction of peptides and protein surface structures with free metal ions and surface-immobilized metal ions. *J Chromatogr,* 500**,** 531-42.

IMAMURA, H., TAKAO, S. & AIKOU, T. 1994. A modified invasion-3-(4,5-dimethylthiazole-2-yl)-2,5-diphenyltetrazolium bromide assay for quantitating tumor cell invasion. *Cancer Res,* 54**,** 3620-4.

JACKSON, S. P. & BARTEK, J. 2009. The DNA-damage response in human biology and disease. *Nature,* 461**,** 1071-8.

JIANG, B. H. & LIU, L. Z. 2009. PI3K/PTEN Signaling in Angiogenesis and Tumorigenesis. *Advances in Cancer Research, Vol 102,* 102**,** 19-65.

JOHNSSON, N., MARRIOTT, G. & WEBER, K. 1988. p36, the major cytoplasmic substrate of src tyrosine protein kinase, binds to its p11 regulatory subunit via a short amino-terminal amphiphatic helix. *EMBO J,* 7**,** 2435-42.

JONES, D. P. 2010. Redox sensing: orthogonal control in cell cycle and apoptosis signalling. *J Intern Med,* 268**,** 432-48.

JORDHEIM, L. P., CROS, E., GOUY, M. H., GALMARINI, C. M., PEYROTTES, S., MACKEY, J., PERIGAUD, C. & DUMONTET, C. 2004. Characterization of a gemcitabine-resistant murine leukemic cell line: reversion of in vitro resistance by a mononucleotide prodrug. *Clin Cancer Res,* 10**,** 5614-21.

JUNG, H., KIM, J. S., KIM, W. K., OH, K. J., KIM, J. M., LEE, H. J., HAN, B. S., KIM, D. S., SEO, Y. S., LEE, S. C., PARK, S. G. & BAE, K. H. 2015. Intracellular annexin A2 regulates NF-kappaB signaling by binding to the p50 subunit: implications for gemcitabine resistance in pancreatic cancer. *Cell Death Dis,* 6**,** e1606.

JUNG, Y., WANG, J., SONG, J., SHIOZAWA, Y., WANG, J., HAVENS, A., WANG, Z., SUN, Y.-X., EMERSON, S. G., KREBSBACH, P. H. & TAICHMAN, R. S. 2007.

Annexin II expressed by osteoblasts and endothelial cells regulates stem cell adhesion, homing, and engraftment following transplantation. *Blood,* 110**,** 82-90.

KAGAWA, S., TAKANO, S., YOSHITOMI, H., KIMURA, F., SATOH, M., SHIMIZU, H., YOSHIDOME, H., OHTSUKA, M., KATO, A., FURUKAWA, K., MATSUSHITA, K., NOMURA, F. & MIYAZAKI, M. 2012. Akt/mTOR signaling pathway is crucial for gemcitabine resistance induced by Annexin II in pancreatic cancer cells. *J Surg Res,* 178**,** 758-67.

KAKU, Y., TSUCHIYA, A., KANNO, T. & NISHIZAKI, T. 2015. Irinotecan Induces Cell Cycle Arrest, but Not Apoptosis or Necrosis, in Caco-2 and CW2 Colorectal Cancer Cell Lines. *Pharmacology,* 95**,** 154-159.

KANG, H. M., CHOI, K. S., KASSAM, G., FITZPATRICK, S. L., KWON, M. & WAISMAN, D. M. 1999. Role of annexin II tetramer in plasminogen activation. *Trends Cardiovasc Med,* 9**,** 92-102.

KASSAM, G., CHOI, K. S., GHUMAN, J., KANG, H. M., FITZPATRICK, S. L., ZACKSON, T., ZACKSON, S., TOBA, M., SHINOMIYA, A. & WAISMAN, D. M. 1998a. The role of annexin II tetramer in the activation of plasminogen. *Journal of Biological Chemistry,* 273**,** 4790-4799.

KASSAM, G., LE, B. H., CHOI, K. S., KANG, H. M., FITZPATRICK, S. L., LOUIE, P. & WAISMAN, D. M. 1998b. The p11 subunit of the annexin II tetramer plays a

key role in the stimulation of t-PA-dependent plasminogen activation. *Biochemistry,* 37**,** 16958-66.

KAWESHA, A., GHANEH, P., ANDREN-SANDBERG, A., OGRAED, D., SKAR, R., DAWISKIBA, S., EVANS, J. D., CAMPBELL, F., LEMOINE, N. & NEOPTOLEMOS, J. P. 2000. K-ras oncogene subtype mutations are associated with survival but not expression of p53, p16(INK4A), p21(WAF-1), cyclin D1, erbB-2 and erbB-3 in resected pancreatic ductal adenocarcinoma. *Int J Cancer,* 89**,** 469-74.

KELEG, S., BUCHLER, P., LUDWIG, R., BUCHLER, M. W. & FRIESS, H. 2003. Invasion and metastasis in pancreatic cancer. *Mol Cancer,* 2**,** 14.

KONG, R., SUN, B., JIANG, H., PAN, S., CHEN, H., WANG, S., KRISSANSEN, G. W. & SUN, X. 2010. Downregulation of nuclear factor-kappaB p65 subunit by small interfering RNA synergizes with gemcitabine to inhibit the growth of pancreatic cancer. *Cancer Lett,* 291**,** 90-8.

KONIG, J., PRENEN, J., NILIUS, B. & GERKE, V. 1998. The annexin II-p11 complex is involved in regulated exocytosis in bovine pulmonary artery endothelial cells. *J Biol Chem,* 273**,** 19679-84.

KUMBLE, K. D., HIROTA, M., POUR, P. M. & VISHWANATHA, J. K. 1992. Enhanced Levels of Annexins in Pancreatic-Carcinoma Cells of Syrian-Hamsters and Their Intrapancreatic Allografts. *Cancer Research,* 52**,** 163-167.

LAZNICEK, M., KVETINA, J., MAZAK, J. & KRCH, V. 1987. Plasma protein binding-lipophilicity relationships: interspecies comparison of some organic acids. *J Pharm Pharmacol,* 39**,** 79-83.

LAZNICEK, M. & LAZNICKOVA, A. 1995. The effect of lipophilicity on the protein binding and blood cell uptake of some acidic drugs. *J Pharm Biomed Anal,* 13**,** 823-8.

LEE, D. B. N., JAMGOTCHIAN, N., ALLEN, S. G., KAN, F. W. K. & HALE, I. L. 2004. Annexin A2 heterotetramer: role in tight junction assembly. *American Journal of Physiology-Renal Physiology,* 287**,** F481-F491.

LESNIAK, W., SLOMNICKI, L. P. & FILIPEK, A. 2009. S100A6 - new facts and features. *Biochem Biophys Res Commun,* 390**,** 1087-92.

LI, C., REDDY, T. R., FISCHER, P. M. & DEKKER, L. V. 2010. A Cy5-labeled S100A10 tracer used to identify inhibitors of the protein interaction with annexin A2. *Assay Drug Dev Technol,* 8**,** 85-95.

LIEBER, M., MAZZETTA, J., NELSON-REES, W., KAPLAN, M. & TODARO, G. 1975. Establishment of a continuous tumor-cell line (panc-1) from a human carcinoma of the exocrine pancreas. *Int J Cancer,* 15**,** 741-7.

LING, Q., JACOVINA, A. T., DEORA, A., FEBBRAIO, M., SIMANTOV, R., SILVERSTEIN, R. L., HEMPSTEAD, B., MARK, W. H. & HAJJAR, K. A. 2004.

Annexin II regulates fibrin homeostasis and neoangiogenesis in vivo. *J Clin Invest,* 113**,** 38-48.

LIPINSKI, C. A. 2004. Lead- and drug-like compounds: the rule-of-five revolution. *Drug Discov Today Technol,* 1**,** 337-41.

LIPINSKI, C. A., LOMBARDO, F., DOMINY, B. W. & FEENEY, P. J. 2012. Experimental and computational approaches to estimate solubility and permeability in drug discovery and development settings. *Advanced Drug Delivery Reviews,* 64**,** 4-17.

LIU, J., ROTHERMUND, C. A., AYALA-SANMARTIN, J. & VISHWANATHA, J. K. 2003a. Nuclear annexin II negatively regulates growth of LNCaP cells and substitution of ser 11 and 25 to glu prevents nucleo-cytoplasmic shuttling of annexin II. *BMC Biochem,* 4**,** 10.

LIU, J., YOSHIKAWA, H., NAKAJIMA, Y. & TASAKA, K. 2001. Involvement of mitochondrial permeability transition and caspase-9 activation in dimethyl sulfoxide-induced apoptosis of EL-4 lymphoma cells. *International Immunopharmacology,* 1**,** 63-74.

LIU, J. W., SHEN, J. J., TANZILLO-SWARTS, A., BHATIA, B., MALDONADO, C. M., PERSON, M. D., LAU, S. S. & TANG, D. G. 2003b. Annexin II expression is reduced or lost in prostate cancer cells and its re-expression inhibits prostate cancer cell migration. *Oncogene,* 22**,** 1475-1485.

LIU, Y., MYRVANG, H. K. & DEKKER, L. V. 2015. Annexin A2 complexes with S100 proteins: structure, function and pharmacological manipulation. *Br J Pharmacol,* 172**,** 1664-76.

LIZARBE, M. A., BARRASA, J. I., OLMO, N., GAVILANES, F. & TURNAY, J. 2013. Annexin-phospholipid interactions. Functional implications. *Int J Mol Sci,* 14**,** 2652-83.

LOKMAN, N. A., ELDER, A. S. F., WEEN, M. P., PYRAGIUS, C. E., HOFFMANN, P., OEHLER, M. K. & RICCIARDELLI, C. 2013. Annexin A2 is regulated by ovarian cancer-peritoneal cell interactions and promotes metastasis. *Oncotarget,* 4**,** 1199-1211.

LOKMAN, N. A., WEEN, M. P., OEHLER, M. K. & RICCIARDELLI, C. 2011. The role of annexin A2 in tumorigenesis and cancer progression. *Cancer Microenviron,* 4**,** 199-208.

LU, Z., HU, L., EVERS, S., CHEN, J. & SHEN, Y. 2004. Differential expression profiling of human pancreatic adenocarcinoma and healthy pancreatic tissue. *Proteomics,* 4**,** 3975-88.

MACLEOD, T. J., KWON, M., FILIPENKO, N. R. & WAISMAN, D. M. 2003. Phospholipid-associated annexin A2-S100A10 heterotetramer and its subunits: characterization of the interaction with tissue plasminogen activator, plasminogen, and plasmin. *J Biol Chem,* 278**,** 25577-84.

MADUREIRA, P. A., HILL, R., MILLER, V. A., GIACOMANTONIO, C., LEE, P. W. & WAISMAN, D. M. 2011a. Annexin A2 is a novel cellular redox regulatory protein involved in tumorigenesis. *Oncotarget,* 2**,** 1075-93.

MADUREIRA, P. A., O'CONNELL, P. A., SURETTE, A. P., MILLER, V. A. & WAISMAN, D. M. 2012. The biochemistry and regulation of S100A10: a multifunctional plasminogen receptor involved in oncogenesis. *J Biomed Biotechnol,* 2012**,** 353687.

MADUREIRA, P. A., SURETTE, A. P., PHIPPS, K. D., TABOSKI, M. A., MILLER, V. A. & WAISMAN, D. M. 2011b. The role of the annexin A2 heterotetramer in vascular fibrinolysis. *Blood,* 118**,** 4789-97.

MAHON, P. C., BARIL, P., BHAKTA, V., CHELALA, C., CAULEE, K., HARADA, T. & LEMOINE, N. R. 2007. S100A4 contributes to the suppression of BNIP3 expression, chemoresistance, and inhibition of apoptosis in pancreatic cancer. *Cancer Res,* 67**,** 6786-95.

MAITRA, A., ADSAY, N. V., ARGANI, P., IACOBUZIO-DONAHUE, C., DE MARZO, A., CAMERON, J. L., YEO, C. J. & HRUBAN, R. H. 2003. Multicomponent analysis of the pancreatic adenocarcinoma progression model using a pancreatic intraepithelial neoplasia tissue microarray. *Mod Pathol,* 16**,** 902-12.

MAKAWITA, S., SMITH, C., BATRUCH, I., ZHENG, Y., RUCKERT, F., GRUTZMANN, R., PILARSKY, C., GALLINGER, S. & DIAMANDIS, E. P. 2011. Integrated proteomic profiling of cell line conditioned media and pancreatic juice for the

identification of pancreatic cancer biomarkers. *Mol Cell Proteomics,* 10**,** M111 008599.

MALASHKEVICH, V. N., DULYANINOVA, N. G., RAMAGOPAL, U. A., LIRIANO, M. A., VARNEY, K. M., KNIGHT, D., BRENOWITZ, M., WEBER, D. J., ALMO, S. C. & BRESNICK, A. R. 2010. Phenothiazines inhibit S100A4 function by inducing protein oligomerization. *Proc Natl Acad Sci U S A,* 107**,** 8605-10.

MANALLACK, D. T. 2008. The pK(a) Distribution of Drugs: Application to Drug Discovery. *Perspect Medicin Chem,* 1**,** 25-38.

MASAKI, T., TOKUDA, M., FUJIMURA, T., OHNISHI, M., TAI, Y. J., MIYAMOTO, K., ITANO, T., MATSUI, H., WATANABE, S., SOGAWA, K., YAMADA, T., KONISHI, R., NISHIOKA, M. & HATASE, O. 1994. Involvement of Annexin-I and Annexin-Ii in Hepatocyte Proliferation - Can Annexin-I and Annexin-Ii Be Markers for Proliferative Hepatocytes. *Hepatology,* 20**,** 425-435.

MELCHIORI, A., ALLAVENA, G., BOHM, J., REMY, W., SCHMIDT, J., PARODI, S., SANTI, L. & ALBINI, A. 1987. Interferons inhibit chemotaxis of transformed cells and their invasion of a reconstituted basement membrane. *Anticancer Res,* 7**,** 475-9.

MOORE, B. W. 1965. A soluble protein characteristic of the nervous system. *Biochem Biophys Res Commun,* 19**,** 739-44.

MORGAN, D. M. 1998. Tetrazolium (MTT) assay for cellular viability and activity. *Methods Mol Biol,* 79**,** 179-83.

MORRIS, E. J. & GELLER, H. M. 1996. Induction of neuronal apoptosis by camptothecin, an inhibitor of DNA topoisomerase-I: evidence for cell cycle-independent toxicity. *J Cell Biol,* 134**,** 757-70.

MOSMANN, T. 1983. Rapid colorimetric assay for cellular growth and survival: application to proliferation and cytotoxicity assays. *J Immunol Methods,* 65**,** 55-63.

MOUGIAKAKOS, D., CHOUDHURY, A., LLADSER, A., KIESSLING, R. & JOHANSSON, C. C. 2010. Regulatory T Cells in Cancer. *Advances in Cancer Research, Vol 107,* 107**,** 57-117.

MUNIRAJ, T., JAMIDAR, P. A. & ASLANIAN, H. R. 2013. Pancreatic cancer: A comprehensive review and update. *Dm Disease-a-Month,* 59**,** 368-402.

MYRVANG, H. K., GUO, X. X., LI, C. & DEKKER, L. V. 2013. Protein interactions between surface annexin A2 and S100A10 mediate adhesion of breast cancer cells to microvascular endothelial cells. *FEBS Lett,* 587**,** 3210-3215.

NAKAMORI, S., YASHIMA, K., MURAKAMI, Y., ISHIKAWA, O., OHIGASHI, H., IMAOKA, S., YAEGASHI, S., KONISHI, Y. & SEKIYA, T. 1995. Association of p53 gene mutations with short survival in pancreatic adenocarcinoma. *Jpn J Cancer Res,* 86**,** 174-81.

NAKANO, Y., TANNO, S., KOIZUMI, K., NISHIKAWA, T., NAKAMURA, K., MINOGUCHI, M., IZAWA, T., MIZUKAMI, Y., OKUMURA, T. & KOHGO, Y. 2007. Gemcitabine chemoresistance and molecular markers associated with gemcitabine transport and metabolism in human pancreatic cancer cells. *Br J Cancer,* 96**,** 457-63.

NAZMI, A. R., OZOROWSKI, G., PEJIC, M., WHITELEGGE, J. P., GERKE, V. & LUECKE, H. 2012. N-terminal acetylation of annexin A2 is required for S100A10 binding. *Biological Chemistry,* 393**,** 1141-1150.

NEDJADI, T., KITTERINGHAM, N., CAMPBELL, F., JENKINS, R. E., PARK, B. K., NAVARRO, P., ASHCROFT, F., TEPIKIN, A., NEOPTOLEMOS, J. P. & COSTELLO, E. 2009. S100A6 binds to annexin 2 in pancreatic cancer cells and promotes pancreatic cancer cell motility. *Br J Cancer,* 101**,** 1145-54.

NEGRINI, S., GORGOULIS, V. G. & HALAZONETIS, T. D. 2010. Genomic instability--an evolving hallmark of cancer. *Nat Rev Mol Cell Biol,* 11**,** 220-8.

NERI, B., CIPRIANI, G., GRIFONI, R., MOLINARA, E., PANTALEO, P., RANGAN, S., VANNINI, A., TONELLI, P., VALERI, A., PANTALONE, D., TADDEI, A. & BECHI, P. 2009. Gemcitabine plus irinotecan as first-line weekly therapy in locally advanced and/or metastatic pancreatic cancer. *Oncol Res,* 17**,** 559-64.

NG, S. S. W., TSAO, M. S., CHOW, S. & HEDLEY, D. W. 2000. Inhibition of phosphatidylinositide 3-kinase enhances gemcitabine-induced apoptosis in human pancreatic cancer cells. *Cancer Research,* 60**,** 5451-5455.

NICOLETTI, I., MIGLIORATI, G., PAGLIACCI, M. C., GRIGNANI, F. & RICCARDI, C. 1991. A rapid and simple method for measuring thymocyte apoptosis by propidium iodide staining and flow cytometry. *J Immunol Methods,* 139**,** 271-9.

NISHIMURA, Y., YASUI, W., YOSHIDA, K., MATSUYAMA, T., DOHI, K. & TAHARA, E. 1992. A serine protease-inhibitory benzamidine derivative inhibits the growth of human colon carcinoma cells. *Jpn J Cancer Res,* 83**,** 723-8.

NISHIU, M., YANAGAWA, R., NAKATSUKA, S., YAO, M., TSUNODA, T., NAKAMURA, Y. & AOZASA, K. 2002. Microarray analysis of gene-expression profiles in diffuse large B-cell lymphoma: identification of genes related to disease progression. *Jpn J Cancer Res,* 93**,** 894-901.

O'CONNELL, P. A., MADUREIRA, P. A., BERMAN, J. N., LIWSKI, R. S. & WAISMAN, D. M. 2011. Regulation of S100A10 by the PML-RAR-alpha oncoprotein. *Blood,* 117**,** 4095-105.

O'CONNELL, P. A., SURETTE, A. P., LIWSKI, R. S., SVENNINGSSON, P. & WAISMAN, D. M. 2010. S100A10 regulates plasminogen-dependent macrophage invasion. *Blood,* 116**,** 1136-46.

OHHASHI, S., OHUCHIDA, K., MIZUMOTO, K., FUJITA, H., EGAMI, T., YU, J., TOMA, H., SADATOMI, S., NAGAI, E. & TANAKA, M. 2008. Down-regulation of deoxycytidine kinase enhances acquired resistance to gemcitabine in pancreatic cancer. *Anticancer Res,* 28**,** 2205-12.

OREND, G. & CHIQUET-EHRISMANN, R. 2006. Tenascin-C induced signaling in cancer. *Cancer Lett,* 244**,** 143-63.

ORTIZ-ZAPATER, E., PEIRO, S., RODA, O., COROMINAS, J. M., AGUILAR, S., AMPURDANES, C., REAL, F. X. & NAVARRO, P. 2007. Tissue plasminogen activator induces pancreatic cancer cell proliferation by a non-catalytic mechanism that requires extracellular signal-regulated kinase 1/2 activation through epidermal growth factor receptor and annexin A2. *American Journal of Pathology,* 170**,** 1573-1584.

PAGES, F., GALON, J., DIEU-NOSJEAN, M. C., TARTOUR, E., SAUTES-FRIDMAN, C. & FRIDMAN, W. H. 2010. Immune infiltration in human tumors: a prognostic factor that should not be ignored. *Oncogene,* 29**,** 1093-102.

PARDO, R., GRASSO, D., MOLEJON, M. I., IOVANNA, J. L. & VACCARO, M. I. 2010. S100A10 Increases Pancreatic Cancer Cell Resistance to Gemcitabine Treatment by the Inhibition of VMP1-Mediated Autophagy. *Pancreas,* 39**,** 1338-1338.

PATHURI, P., VOGELEY, L. & LUECKE, H. 2008. Crystal structure of metastasis-associated protein S100A4 in the active calcium-bound form. *J Mol Biol,* 383**,** 62-77.

PHIPPS, K. D., SURETTE, A. P., O'CONNELL, P. A. & WAISMAN, D. M. 2011. Plasminogen Receptor S100A10 Is Essential for the Migration of Tumor-Promoting Macrophages into Tumor Sites. *Cancer Research,* 71**,** 6676-6683.

PRINCIPE, M., CERUTI, P., SHIH, N. Y., CHATTARAGADA, M. S., ROLLA, S., CONTI, L., BESTAGNO, M., ZENTILIN, L., YANG, S. H., MIGLIORINI, P., CAPPELLO, P., BURRONE, O. & NOVELLI, F. 2015. Targeting of surface alpha-enolase inhibits the invasiveness of pancreatic cancer cells. *Oncotarget,* 6**,** 11098-113.

PTAK-BELOWSKA, A., GAWAD, A., BRZOZOWSKI, T. & PAWLIK, W. W. 2009. Increased Level of Cell Surface Annexin II Promotes Pancreatic and Colon Cancer Cells Growth In Vitro. *Gastroenterology,* 136**,** A756-A757.

PUISIEUX, A., JI, J. & OZTURK, M. 1996. Annexin II up-regulates cellular levels of p11 protein by a post-translational mechanisms. *Biochem J,* 313 (Pt 1)**,** 51-5.

QI, T., HAN, J., CUI, Y., ZONG, M., LIU, X. & ZHU, B. 2008. Comparative proteomic analysis for the detection of biomarkers in pancreatic ductal adenocarcinomas. *J Clin Pathol,* 61**,** 49-58.

RANI, S. G., MOHAN, S. K. & YU, C. 2010. Molecular level interactions of S100A13 with amlexanox: inhibitor for formation of the multiprotein complex in the nonclassical pathway of acidic fibroblast growth factor. *Biochemistry,* 49**,** 2585-92.

RATHOS, M. J., JOSHI, K., KHANWALKAR, H., MANOHAR, S. M. & JOSHI, K. S. 2012. Molecular evidence for increased antitumor activity of gemcitabine in

combination with a cyclin-dependent kinase inhibitor, P276-00 in pancreatic cancers. *J Transl Med,* 10**,** 161.

REDDY, T. R., LI, C., FISCHER, P. M. & DEKKER, L. V. 2012. Three-dimensional pharmacophore design and biochemical screening identifies substituted 1,2,4-triazoles as inhibitors of the annexin A2-S100A10 protein interaction. *ChemMedChem,* 7**,** 1435-46.

REDDY, T. R., LI, C., GUO, X., MYRVANG, H. K., FISCHER, P. M. & DEKKER, L. V. 2011. Design, synthesis, and structure-activity relationship exploration of 1-substituted 4-aroyl-3-hydroxy-5-phenyl-1H-pyrrol-2(5H)-one analogues as inhibitors of the annexin A2-S100A10 protein interaction. *Journal of Medicinal Chemistry,* 54**,** 2080-94.

REDDY, T. R. K., LI, C., GUO, X. X., FISCHER, P. M. & DEKKER, L. V. 2014. Design, synthesis and SAR exploration of tri-substituted 1,2,4-triazoles as inhibitors of the annexin A2-S100A10 protein interaction. *Bioorg Med Chem,* 22**,** 5378-5391.

RENGIFO-CAM, W., UMAR, S., SARKAR, S. & SINGH, P. 2007. Antiapoptotic effects of progastrin on pancreatic cancer cells are mediated by sustained activation of nuclear factor-kappa B. *Cancer Research,* 67**,** 7266-7274.

RESCHER, U. & GERKE, V. 2004. Annexins--unique membrane binding proteins with diverse functions. *J Cell Sci,* 117**,** 2631-9.

RESCHER, U. & GERKE, V. 2008. S100A10/p11: family, friends and functions. *Pflugers Arch,* 455**,** 575-82.

RESCHER, U., LUDWIG, C., KONIETZKO, V., KHARITONENKOV, A. & GERKE, V. 2008. Tyrosine phosphorylation of annexin A2 regulates Rho-mediated actin rearrangement and cell adhesion. *J Cell Sci,* 121**,** 2177-85.

RETY, S., SOPKOVA, J., RENOUARD, M., OSTERLOH, D., GERKE, V., TABARIES, S., RUSSO-MARIE, F. & LEWIT-BENTLEY, A. 1999. The crystal structure of a complex of p11 with the annexin II N-terminal peptide. *Nat Struct Biol,* 6**,** 89-95.

REYMOND, N., D'AGUA, B. B. & RIDLEY, A. J. 2013. Crossing the endothelial barrier during metastasis. *Nat Rev Cancer,* 13**,** 858-870.

RODA, O., CHIVA, C., ESPUNA, G., GABIUS, H. J., REAL, F. X., NAVARRO, P. & ANDREU, D. 2006. A proteomic approach to the identification of new tPA receptors in pancreatic cancer cells. *Proteomics,* 6**,** S36-S41.

ROSENGARTH, A. & LUECKE, H. 2004. Experimental Paper Annexin A2. *Annexins,* 1**,** 129-136.

RUST, R., VISSER, L., VAN DER LEIJ, J., HARMS, G., BLOKZIJL, T., DELOULME, J. C., VAN DER VLIES, P., KAMPS, W., KOK, K., LIM, M., POPPEMA, S. & VAN DEN BERG, A. 2005. High expression of calcium-binding proteins, S100A10,

S100A11 and CALM2 in anaplastic large cell lymphoma. *Br J Haematol,* 131**,** 596-608.

RYAN, D. P., HONG, T. S. & BARDEESY, N. 2014. Pancreatic adenocarcinoma. *N Engl J Med,* 371**,** 2140-1.

SAKWE, A. M., KOUMANGOYE, R., GUILLORY, B. & OCHIENG, J. 2011. Annexin A6 contributes to the invasiveness of breast carcinoma cells by influencing the organization and localization of functional focal adhesions. *Exp Cell Res,* 317**,** 823-37.

SATO, T., KITA, K., SUGAYA, S., SUZUKI, T. & SUZUKI, N. 2012. Extracellular Release of Annexin II From Pancreatic Cancer Cells and Resistance to Anticancer Drug-Induced Apoptosis by Supplementation of Recombinant Annexin II. *Pancreas,* 41**,** 1247-1254.

SAYEED, S., ASANO, E., ITO, S., OHNO, K., HAMAGUCHI, M. & SENGA, T. 2013. S100A10 is required for the organization of actin stress fibers and promotion of cell spreading. *Molecular and Cellular Biochemistry,* 374**,** 105-111.

SEKINE, H., CHEN, N., SATO, K., SAIKI, Y., YOSHINO, Y., UMETSU, Y., JIN, G., NAGASE, H., GU, Z., FUKUSHIGE, S., SUNAMURA, M. & HORII, A. 2012. S100A4, frequently overexpressed in various human cancers, accelerates cell motility in pancreatic cancer cells. *Biochem Biophys Res Commun,* 429**,** 214-9.

SEMOV, A., MORENO, M. J., ONICHTCHENKO, A., ABULROB, A., BALL, M., EKIEL, I., PIETRZYNSKI, G., STANIMIROVIC, D. & ALAKHOV, V. 2005. Metastasis-associated protein S100A4 induces angiogenesis through interaction with Annexin II and accelerated plasmin formation. *J Biol Chem,* 280**,** 20833-41.

SERRANO, M., LEE, H., CHIN, L., CORDON-CARDO, C., BEACH, D. & DEPINHO, R. A. 1996. Role of the INK4a locus in tumor suppression and cell mortality. *Cell,* 85**,** 27-37.

SHAH, M. A. & SCHWARTZ, G. K. 2001. Cell cycle-mediated drug resistance: an emerging concept in cancer therapy. *Clin Cancer Res,* 7**,** 2168-81.

SHAN, X. X., MIAO, Y. F., FAN, R. G., QIAN, H. X., CHEN, P., LIU, H. Q., YAN, X. M., LI, J. P. & ZHOU, F. 2013. MiR-590-5P Inhibits Growth of HepG2 Cells via Decrease of S100A10 Expression and Inhibition of the Wnt Pathway. *International Journal of Molecular Sciences,* 14**,** 8556-8569.

SHANG, J., ZHANG, Z., SONG, W., ZHOU, B., ZHANG, Y., LI, G. & QIU, S. 2013. S100A10 as a novel biomarker in colorectal cancer. *Tumour Biol,* 34**,** 3785-90.

SHARMA, M., OWNBEY, R. T. & SHARMA, M. C. 2010. Breast cancer cell surface annexin II induces cell migration and neoangiogenesis via tPA dependent plasmin generation. *Exp Mol Pathol,* 88**,** 278-86.

SHARMA, M. R., KOLTOWSKI, L., OWNBEY, R. T., TUSZYNSKI, G. P. & SHARMA, M. C. 2006. Angiogenesis-associated protein annexin II in breast cancer: selective expression in invasive breast cancer and contribution to tumor invasion and progression. *Exp Mol Pathol,* 81**,** 146-56.

SHIOZAWA, Y., HAVENS, A. M., JUNG, Y., ZIEGLER, A. M., PEDERSEN, E. A., WANG, J., WANG, J., LU, G., ROODMAN, G. D., LOBERG, R. D., PIENTA, K. J. & TAICHMAN, R. S. 2008. Annexin II/annexin II receptor axis regulates adhesion, migration, homing, and growth of prostate cancer. *J Cell Biochem,* 105**,** 370-80.

SILVA, M. M., THELWELL, C., WILLIAMS, S. C. & LONGSTAFF, C. 2012. Regulation of fibrinolysis by C-terminal lysines operates through plasminogen and plasmin but not tissue-type plasminogen activator. *J Thromb Haemost,* 10**,** 2354-60.

SINGH, S., CHITKARA, D., KUMAR, V., BEHRMAN, S. W. & MAHATO, R. I. 2013. miRNA profiling in pancreatic cancer and restoration of chemosensitivity. *Cancer Lett,* 334**,** 211-20.

SITEK, B., SIPOS, B., ALKATOUT, I., POSCHMANN, G., STEPHAN, C., SCHULENBORG, T., MARCUS, K., LUTTGES, J., DITTERT, D. D., BARETTON, G., SCHMIEGEL, W., HAHN, S. A., KLOPPEL, G., MEYER, H. E. & STUHLER, K. 2009. Analysis of the pancreatic tumor progression by a quantitative proteomic approach and immunhistochemical validation. *J Proteome Res,* 8**,** 1647-56.

SOUZA, E. S., ZARAMELLO, L., KUHNEN, C. A., JUNKES BDA, S., YUNES, R. A. & HEINZEN, V. E. 2011. Estimating the octanol/water partition coefficient for aliphatic organic compounds using semi-empirical electrotopological index. *Int J Mol Sci,* 12**,** 7250-64.

STAMENKOVIC, I. 2000. Matrix metalloproteinases in tumor invasion and metastasis. *Seminars in Cancer Biology,* 10**,** 415-433.

SURETTE, A. P., MADUREIRA, P. A., PHIPPS, K. D., MILLER, V. A., SVENNINGSSON, P. & WAISMAN, D. M. 2011. Regulation of fibrinolysis by S100A10 in vivo. *Blood,* 118**,** 3172-3181.

SURETTE, A. P. & WAISMAN, D. M. 2014. S100A10: A Key Regulator of Fibrinolysis.

SURYADINATA, R., SADOWSKI, M. & SARCEVIC, B. 2010. Control of cell cycle progression by phosphorylation of cyclin-dependent kinase (CDK) substrates. *Biosci Rep,* 30**,** 243-55.

SUZUKI, S. & TANIGAWARA, Y. 2014. Forced expression of S100A10 reduces sensitivity to oxaliplatin in colorectal cancer cells. *Proteome Sci,* 12**,** 26.

SVENNINGSSON, P. & GREENGARD, P. 2007. p11 (S100A10)--an inducible adaptor protein that modulates neuronal functions. *Curr Opin Pharmacol,* 7**,** 27-32.

TAKANO, S., TOGAWA, A., YOSHITOMI, H., SHIDA, T., KIMURA, F., SHIMIZU, H., YOSHIDOME, H., OHTSUKA, M., KATO, A., TOMONAGA, T., NOMURA, F. & MIYAZAKI, M. 2008. Annexin II overexpression predicts rapid recurrence

after surgery in pancreatic cancer patients undergoing gemcitabine-adjuvant chemotherapy. *Ann Surg Oncol,* 15**,** 3157-68.

TALMADGE, J. E. & FIDLER, I. J. 2010. AACR centennial series: the biology of cancer metastasis: historical perspective. *Cancer Res,* 70**,** 5649-69.

TANNOCK, I. F. & ROTIN, D. 1989. Acid pH in tumors and its potential for therapeutic exploitation. *Cancer Res,* 49**,** 4373-84.

TATENHORST, L., RESCHER, U., GERKE, V. & PAULUS, W. 2006. Knockdown of annexin 2 decreases migration of human glioma cells in vitro. *Neuropathol Appl Neurobiol,* 32**,** 271-7.

TENG, M. W. L., SWANN, J. B., KOEBEL, C. M., SCHREIBER, R. D. & SMYTH, M. J. 2008. Immune-mediated dormancy: an equilibrium with cancer. *Journal of Leukocyte Biology,* 84**,** 988-993.

TIAN, R., WEI, L. M., QIN, R. Y., LI, Y., DU, Z. Y., XIA, W., SHI, C. J. & JIN, H. 2008. Proteome analysis of human pancreatic ductal adenocarcinoma tissue using two-dimensional gel electrophoresis and tandem mass spectrometry for identification of disease-related proteins. *Digestive Diseases and Sciences,* 53**,** 65-72.

TOGAWA, A., ITO, H., KIMURA, F., SHIMIZU, H., OHTSUKA, M., SHIMAMURA, F., YOSHIDOME, H., KATOH, A. & MIYAZAKI, M. 2003. Establishment of

gemcitabine-resistant human pancreatic cancer cells and effect of brefeldin-a on the resistant cell line. *Pancreas,* 27**,** 220-4.

TOLIS, C., PETERS, G. J., FERREIRA, C. G., PINEDO, H. M. & GIACCONE, G. 1999. Cell cycle disturbances and apoptosis induced by topotecan and gemcitabine on human lung cancer cell lines. *Eur J Cancer,* 35**,** 796-807.

TRESSLER, R. J., UPDYKE, T. V., YEATMAN, T. & NICOLSON, G. L. 1993. Extracellular annexin II is associated with divalent cation-dependent tumor cell-endothelial cell adhesion of metastatic RAW117 large-cell lymphoma cells. *J Cell Biochem,* 53**,** 265-76.

VAJDIC, C. M. & VAN LEEUWEN, M. T. 2009. Cancer incidence and risk factors after solid organ transplantation. *Int J Cancer,* 125**,** 1747-54.

VAN DIECK, J., TEUFEL, D. P., JAULENT, A. M., FERNANDEZ-FERNANDEZ, M. R., RUTHERFORD, T. J., WYSLOUCH-CIESZYNSKA, A. & FERSHT, A. R. 2009. Posttranslational modifications affect the interaction of S100 proteins with tumor suppressor p53. *J Mol Biol,* 394**,** 922-30.

VARNEK, A. 2011. Fragment Descriptors in Structure-Property Modeling and Virtual Screening. *Chemoinformatics and Computational Chemical Biology,* 672**,** 213-243.

VERMEULEN, K., VAN BOCKSTAELE, D. R. & BERNEMAN, Z. N. 2003. The cell cycle: a review of regulation, deregulation and therapeutic targets in cancer. *Cell Prolif,* 36**,** 131-49.

VISHWANATHA, J. K., CHIANG, Y., KUMBLE, K. D., HOLLINGSWORTH, M. A. & POUR, P. M. 1993. Enhanced expression of annexin II in human pancreatic carcinoma cells and primary pancreatic cancers. *Carcinogenesis,* 14**,** 2575-9.

WANG, C. Y., CHEN, C. L., TSENG, Y. L., FANG, Y. T., LIN, Y. S., SU, W. C., CHEN, C. C., CHANG, K. C., WANG, Y. C. & LIN, C. F. 2012a. Annexin A2 silencing induces G2 arrest of non-small cell lung cancer cells through p53-dependent and -independent mechanisms. *J Biol Chem,* 287**,** 32512-24.

WANG, C. Y. & LIN, C. F. 2014. Annexin A2: Its Molecular Regulation and Cellular Expression in Cancer Development. *Dis Markers*.

WANG, C. Y., LIN, Y. S., SU, W. C., CHEN, C. L. & LIN, C. F. 2009. Glycogen Synthase Kinase-3 and Omi/HtrA2 Induce Annexin A2 Cleavage followed by Cell Cycle Inhibition and Apoptosis. *Molecular Biology of the Cell,* 20**,** 4153-4161.

WANG, Y. X., LV, H., LI, Z. X., LI, C. & WU, X. Y. 2012b. Effect of shRNA Mediated Down-Regulation of Annexin A2 on Biological Behavior of Human Lung Adencarcinoma Cells A549. *Pathology & Oncology Research,* 18**,** 183-190.

WARBURG, O. 1956a. On respiratory impairment in cancer cells. *Science,* 124**,** 269-70.

WARBURG, O. 1956b. On the origin of cancer cells. *Science,* 123**,** 309-14.

WEI, B., GUO, C., LIU, S. & SUN, M. Z. 2015. Annexin A4 and cancer. *Clin Chim Acta,* 447**,** 72-8.

WEIZMAN, N., KRELIN, Y., SHABTAY-ORBACH, A., AMIT, M., BINENBAUM, Y., WONG, R. J. & GIL, Z. 2014. Macrophages mediate gemcitabine resistance of pancreatic adenocarcinoma by upregulating cytidine deaminase. *Oncogene,* 33**,** 3812-9.

WILDMAN, S. A. & CRIPPEN, G. M. 1999. Prediction of physicochemical parameters by atomic contributions. *Journal of Chemical Information and Computer Sciences,* 39**,** 868-873.

WOLF, S., HAASE-KOHN, C. & PIETZSCH, J. 2011. S100A2 in cancerogenesis: a friend or a foe? *Amino Acids,* 41**,** 849-61.

WRANA, J. L. 2000. Regulation of Smad activity. *Cell,* 100**,** 189-92.

WU, W., TANG, X., HU, W., LOTAN, R., HONG, W. K. & MAO, L. 2002. Identification and validation of metastasis-associated proteins in head and neck cancer cell lines by two-dimensional electrophoresis and mass spectrometry. *Clin Exp Metastasis,* 19**,** 319-26.

XIONG, Y., HANNON, G. J., ZHANG, H., CASSO, D., KOBAYASHI, R. & BEACH, D. 1993. p21 is a universal inhibitor of cyclin kinases. *Nature,* 366**,** 701-4.

YADAV, V., SULTANA, S., YADAV, J. & SAINI, N. 2012. Gatifloxacin induces S and G2-phase cell cycle arrest in pancreatic cancer cells via p21/p27/p53. *PLoS One,* 7**,** e47796.

YAMADA, A., IRIE, K., HIROTA, T., OOSHIO, T., FUKUHARA, A. & TAKAI, Y. 2005. Involvement of the annexin II-S100A10 complex in the formation of E-cadherin-based adherens junctions in Madin-Darby canine kidney cells. *Journal of Biological Chemistry,* 280**,** 6016-6027.

YANG, L., PANG, Y. L. & MOSES, H. L. 2010. TGF-beta and immune cells: an important regulatory axis in the tumor microenvironment and progression. *Trends in Immunology,* 31**,** 220-227.

YANG, X. Y., POPESCU, N. C. & ZIMONJIC, D. B. 2011. DLC1 Interaction with S100A10 Mediates Inhibition of In Vitro Cell Invasion and Tumorigenicity of Lung Cancer Cells through a RhoGAP-Independent Mechanism. *Cancer Res,* 71**,** 2916-2925.

YAP, K. L., AMES, J. B., SWINDELLS, M. B. & IKURA, M. 1999. Diversity of conformational states and changes within the EF-hand protein superfamily. *Proteins,* 37**,** 499-507.

YEATMAN, T. J., UPDYKE, T. V., KAETZEL, M. A., DEDMAN, J. R. & NICOLSON, G. L. 1993. Expression of annexins on the surfaces of non-metastatic and metastatic human and rodent tumor cells. *Clin Exp Metastasis,* 11**,** 37-44.

YIP, T. T., NAKAGAWA, Y. & PORATH, J. 1989. Evaluation of the interaction of peptides with Cu(II), Ni(II), and Zn(II) by high-performance immobilized metal ion affinity chromatography. *Anal Biochem,* 183**,** 159-71.

YUAN, T. L. & CANTLEY, L. C. 2008. PI3K pathway alterations in cancer: variations on a theme. *Oncogene,* 27**,** 5497-5510.

YUNIS, A. A., ARIMURA, G. K. & RUSSIN, D. J. 1977. Human pancreatic carcinoma (MIA PaCa-2) in continuous culture: sensitivity to asparaginase. *Int J Cancer,* 19**,** 128-35.

ZAVORAL, M., MINARIKOVA, P., ZAVADA, F., SALEK, C. & MINARIK, M. 2011. Molecular biology of pancreatic cancer. *World J Gastroenterol,* 17**,** 2897-908.

ZHANG, F., ZHANG, L., ZHANG, B., WEI, X. Y., YANG, Y., QI, R. Z., YING, G. G., ZHANG, N. & NIU, R. F. 2009. Anxa2 Plays a Critical Role in Enhanced Invasiveness of the Multidrug Resistant Human Breast Cancer Cells. *Journal of Proteome Research,* 8**,** 5041-5047.

ZHANG, H. J., YAO, D. F., YAO, M., HUANG, H., WANG, L., YAN, M. J., YAN, X. D., GU, X., WU, W. & LU, S. L. 2013. Annexin A2 silencing inhibits invasion,

migration, and tumorigenic potential of hepatoma cells. *World Journal of Gastroenterology,* 19**,** 3792-3801.

ZHANG, J., GUO, B., ZHANG, Y., CAO, J. & CHEN, T. 2010a. Silencing of the annexin II gene down-regulates the levels of S100A10, c-Myc, and plasmin and inhibits breast cancer cell proliferation and invasion. *Saudi Med J,* 31**,** 374-81.

ZHANG, L., FOGG, D. K. & WAISMAN, D. M. 2004. RNA interference-mediated silencing of the S100A10 gene attenuates plasmin generation and invasiveness of Colo 222 colorectal cancer cells. *J Biol Chem,* 279**,** 2053-62.

ZHANG, Z., HUANG, L., ZHAO, W. & RIGAS, B. 2010b. Annexin 1 induced by anti-inflammatory drugs binds to NF-kappaB and inhibits its activation: anticancer effects in vitro and in vivo. *Cancer Res,* 70**,** 2379-88.

ZHAO, P., ZHANG, W., TANG, J., MA, X. K., DAI, J. Y., LI, Y., JIANG, J. L., ZHANG, S. H. & CHEN, Z. N. 2010. Annexin II promotes invasion and migration of human hepatocellular carcinoma cells in vitro via its interaction with HAb18G/CD147. *Cancer Sci,* 101**,** 387-95.

ZHENG, L., FOLEY, K., HUANG, L. Q., LEUBNER, A., MO, G. L., OLINO, K., EDIL, B. H., MIZUMA, M., SHARMA, R., LE, D. T., ANDERS, R. A., ILLEI, P. B., VAN EYK, J. E., MAITRA, A., LAHERU, D. & JAFFEE, E. M. 2011. Tyrosine 23 Phosphorylation-Dependent Cell-Surface Localization of Annexin A2 Is Required for Invasion and Metastases of Pancreatic Cancer. *Plos One,* 6.